

André Tenchini da Silva

# SEISMIC PERFORMANCE OF HIGH STRENGTH STEEL BUILDING FRAMES

Tese de Doutoramento em Construção Metálica e Mista, orientada pelos  
Professores Carlos Alberto da Silva Rebelo e pelo Professor Luciano Rodrigues Ornelas de Lima,  
apresentada ao Departamento de Engenharia Civil da Faculdade de Ciências e  
Tecnologia da Universidade de Coimbra

2014



UNIVERSIDADE DE COIMBRA



**FCTUC** DEPARTAMENTO DE ENGENHARIA CIVIL  
FACULDADE DE CIÊNCIAS E TECNOLOGIA  
UNIVERSIDADE DE COIMBRA



Institute for Sustainability and Innovation  
in Structural Engineering



# Seismic Performance of High Strength Steel Building Frames

(Desempenho Sísmico de Pórticos de Edifícios em Aço de Alta  
Resistência)

Autor

André Tenchini da Silva

Orientadores: Professor Doutor Carlos Rebelo  
(Universidade de Coimbra)  
Professor Doutor Luciano Rodrigues de Lima  
(Universidade do Estado do Rio de Janeiro)

Coimbra, 2014



## *Acknowledgements*

The difficulty is not to start walking, but continue it. Move forward requires persistence and perseverance, and this time, I believe I get to the end of this period of great growth, both professionally and personally, but not before thanking the people who were essential to the realization of this work. Thus, first thank God that guided and protected me in this long and hard journey. This Thesis, despite being the result of hard and often lonely work, would not be successful without the contributions that were of utmost importance.

My walk began in 2003 when was initiated my passion for Civil Engineering at the State University of Rio de Janeiro. There I had lessons with teachers from an extraordinary ability to transmit their knowledge, thus determining my future choices. I speak in particular of Prof. Luciano Lima, my gratitude for believing in me when I was still an undergraduate student showing simple ways of improving my skills through research activity in another country, and today, we are beyond professional colleagues, great friends. Also, take this opportunity to thank Prof. Peter Vellasco, coordinator of the *Erasmus Mundus Programme* in Brazil, for the extraordinary opportunity to be part of this International Exchange Program. This program along with the "*Ciências Sem Fronteiras*" were responsible for the financial support for this research.

Not so easy to start a research, especially being in another country, so thank you the way I was received by the University of Coimbra on behalf of the Department of Civil Engineering. For nearly five years, Coimbra - Portugal was my main house, and today I am proud to say I'm Portuguese by heart. My academic experience was deeply enriched by reference teachers who were essential in this my walk. I had the opportunity of working closely with Prof. Carlos Rebelo and Prof. Luis Simões da Silva. Prof. Carlos Rebelo, my supervisor, my sincere gratitude for his patience, esteem and all the teachings transmitted competently without whom I would not reach the end, showing even more in this final stage (at the time I most needed) his great dedication and promptness to complete this work. I have no doubt of how important his contribution in this work. Then, Prof. Carlos Rebelo, my most sincere thanks!

To Prof. Luis Simões da Silva, coordinator of the *Erasmus Mundus Programme* in Portugal, thanks for the opportunity given. Working in a European Research Project (HSS-SERF) was a unique experience and contributed, and much to my professional growth. In particular,



I thank Prof. Mario D'Aniello that although does not know it, drove me in several stages, including the most difficult. He was not only a colleague of this profession, even by Skype, but also an important figure that I will also use as a reference for his competence and his always solicitous behaviour. I found a friend with whom I debated both the professional side as day-to-day. Thanks a lot for everything, Prof. Mario D'Aniello!

I also thank Miguel Sierra, Hugo Augusto, Cécile Haremza, Fernanda Lopes, Andre Moura, Liliana Marques, Tiago Pires, my companions of the Department of Civil Engineering, who shared these years of PhD making lighter and pleasant journey. Special mention in my cabinet colleagues and great Portuguese friends fraternal: Rui Mattos, Alexandre Henriques and Laertes Motta. We share great moments and pleasant conversations, not always about work (thankfully!). You were instrumental in the adaptation process that is living in another country. Go on an Easter in Carapinheira, a dinner with a wonderful Chanfana, go to the beach in Aveiro... are some of the great moments that will be kept on my mind. Thank you very much! I take this moment to speak of the Department of Civil Engineering to thank the staff, always kind, in particular: Ricardo de Oliveira, Luis Gaspar, Cristina Carolino, D. Lucinda and Teresa Cordeiro.

And now as Vinicius de Moraes said: "you do not make friends, you recognize them." Not forgetting them, those who fully know my heart and are aware of my real feelings. To all my friends and friends, thank you from my heart for the moments of joys, advice and care. Not only the smile given, but also the shared tears. I dedicate my thanks not only to childhood friends and I left college in Brazil, but even from afar always supported me, but also to the friends I made in Portugal and who were the major pillar in this my stay where they often become a family of Coimbra: Rachel Cesar, Michel Fernandes and Gabriel Barberes. Do not forget the review always very lively in our kitchen. Thanks to the Sambajah group that restored the my energy at times when the Thesis weighed more. This final stage also can not help but thank the new friends, especially CGA Lawyers (former GHC) which gave me a corner so I could finish writing my Thesis, the conversations with Fernanda Cerqueira and Alexandre together with affectionate look from Cristina, cheering me on and boosting. I also thank Rafael Lucena, Leandro and Vinicius by given support in this end.

Finally, I will write about the hardest part, but emotionally more importantly, my biggest thanks. I dedicate this Thesis to the most important people to me. I thank my dear mother, primary responsibility for my life and to whom I owe my character. My beautiful girlfriend and future wife Cristina by support and care given to this my project. She have been very important in difficult times ... listening ... opining ... but always with the intention to support me. Thanks for her strength, for your dedication, for her trust and patient waiting in

moments of absence. My sisters who supported me all the time with my beautiful nieces. Extending this thanksgiving, Cristina's family for encouraging this final step. With love and longing, I offer this work to a person who has always trusted me and caused it to become possible teaching that I can achieve my dreams, thank Father!

Ending this gloomy moment, I apologize for the size of the text, but I had to seize the moment of excitement as the profession makes the reason is essential. In fact, to say goodbye this stage it is difficult to fill and I intend to continue the journey by sharing the knowledge gained, treading new steps in this direction. The first of these steps? Back to Brazil, leaving half of me and what I learned being in Coimbra. To this city, thanks very much.

*“Momentos que passam, saudades que ficam”*

*To my family and my dear Cristina.  
In special, to my Mother and my Father  
who guided me to that this becomes real.  
I would really like Dad were here!*



# ***Abstract***

In steel building frames under seismic action, the members designed to remain elastic during an earthquake are responsible for the robustness of the structure and prevention of collapse, being characterised by high strength demands. On the other hand, seismic resistant building frames designed as dissipative structures should allow the development of plastic deformations in specific members and locations.

In the present work, the framing solution studied is the one obtained by combining two different steel grades: mild carbon steel (MCS) used in dissipative members and high strength steel (HSS) used in non-dissipative “elastic” members. The current seismic design rules, at least in Europe, do not cover the specific configuration of such ‘Dual-Steel’ structures. Therefore, a comprehensive parametric study devoted to investigate the seismic design and performance of EN1998-1 compliant dual-steel Moment-Resisting Frames (MRF), Centrically Braced Frames (CBF) and Dual-Centrically Braced Frames (D-CBF) is presented and discussed in this dissertation.

The overall seismic performance has been analysed through static and dynamic nonlinear analyses against three limit states: damage limitation (DL), severe damage (SD) and near collapse (NC). The investigated parameters cover both, geometric and mechanical variables, as the type columns, span length, number of storeys and spectral shape. The comparison between dual-steel structures with those entirely made of MCS showed that: i) in order to fulfil the codified drift requirements and to limit the stability coefficients, the same shapes for members should be used for both structures for the MRFs, but there is a reduction in both, weight and cost for the CBFs and D-CBFs using HSS, which proves it is efficient in economic terms, ii) a similar performance can be recognized in both, dual steel and single grade steel structures; iii) In all examined structural typology, the behaviour factors obtained from incremental dynamic analyses for SD limit state were smaller than the used in the seismic design. These results suggest the need to calibrate the behaviour factors given by EN1998-1.

The analyses have shown that the use of HSS in EN1998-1 compliant MRFs is effective in providing overall ductile mechanisms with limited plastic demand, due to the large design overstrength. For the braced frames, the use of the HSS in the non-dissipative members ensured that plastic hinges occurred in the dissipative structural elements with large brace ductility demand, mainly for the braces in compression. In addition, the beams from the

braced bay plays an important role in the seismic performance of these structural systems and is concluded that the use of HSS in beams of braced bays is not advisable.

**Keywords:**

Dual-Steel Frames | High Strength Steel | Seismic Performance Based Design | Nonlinear analysis

## ***Resumo***

Em edifícios metálicos submetidos à acção sísmica, os elementos dimensionados para permanecerem elásticos durante um sismo são responsáveis pela robustez da estrutura e pela prevenção de um colapso, sendo caracterizados por altas exigências de resistência. Por outro lado, edifícios resistentes à acção sísmica dimensionados como estruturas dissipativas devem permitir deformações plásticas em elementos ou zonas específicas.

No presente trabalho, a solução porticada estudada é obtida pela combinação de dois diferentes tipos de aço: Aço Carbono (MCS) usado em elementos dissipativos e Aço de Alta Resistência (HSS) a ser aplicado em elementos não dissipativos. As normas atuais para o dimensionamento sísmico não abordam as estruturas usando o conceito “dual-steel”. Justifica-se, portanto, um estudo paramétrico dedicado a investigar o dimensionamento e desempenho sísmico daquele tipo de estruturas, compatíveis com as regras definidas no eurocódigo EN1998-1. Nesta dissertação são investigados Pórticos Simples (MRF), Pórticos com contraventamento centrado (CBF) e Pórticos “dual-system” com contraventamento centrado (D-CBF).

O desempenho global sísmico é avaliado através de análises não lineares estáticas e dinâmicas tendo em conta três tipos de estados limites: Limitação de Danos (DL), Danos Significativos (SD) e Colapso (NC). Os parâmetros investigados levam em conta a variação geométrica e mecânica, o tipo de pilar misto, o vão, o número de pisos e o tipo de espectro de resposta. A comparação entre uma solução “dual-steel” e soluções correntes utilizando apenas MCS mostrou: (i) um desempenho sísmico semelhante em ambas soluções (ii) que os MRFs apresentaram as mesmas secções transversais para ambas soluções havendo, no entanto, uma redução do peso e do custo para os CBFs e D-CBFs mostrando que o HSS é eficiente em termos económicos, e, ainda, (iii) em todas as tipologias estudadas, os fatores de comportamento obtidos para o estado limite SD foram menores do que utilizado no dimensionamento sísmico. Este resultado sugere a necessidade, aliás já reconhecida por outros investigadores, de uma melhor calibração dos fatores de comportamentos fornecidos pelo EN1998-1.

As análises mostraram que o uso de HSS é eficiente em proporcionar um mecanismo global dúctil para os pórticos simples compatíveis com o EN1998-1 com limitadas exigências plásticas devido à sua grande sobrerresistência. Para os pórticos contraventados, o uso do



HSS nos elementos não dissipativos permitiu que as rótulas plásticas ocorressem nos elementos dissipativos com grandes exigências de deformações nos contraventamentos. Além disso, as vigas do vão contraventado desempenham um importante papel para os CBFs e D-CBFs pelo que se conclui que a utilização do HSS nestes elementos não é recomendável.

**Palavras-Chave:**

Pórticos “Dual-Steel” | Aço de Alta Resistência | Dimensionamento Sísmico Baseado no Desempenho | Análise Não Linear

# ***Contents***

<b>Chapter I – Introduction .....</b>	<b>1</b>
1.1 General considerations .....	1
1.2 Objectives.....	6
1.3 Scope of the Thesis.....	7
<b>Chapter II – Seismic Design Methodologies .....</b>	<b>9</b>
2.1 Introduction .....	9
2.2 Steel buildings in seismic areas.....	10
2.2.1 Moment-resisting Frame.....	10
2.2.2 Concentrically Braced Frame .....	13
2.2.3 Eccentrically Braced Frame.....	19
2.3 The use of High Strength Steel in building frames .....	21
2.3.1 Production methods.....	24
2.3.2 Chemical and physical proprieties .....	26
2.3.3 European standard .....	28
2.3.4 Cost of the use of High Strength Steel.....	30
2.4 Force-based design.....	32
2.4.1 Capacity design.....	33
2.4.2 Behaviour factor (q-factor).....	33
2.5 Performance-based design .....	34
2.5.1 Displacement-based design .....	38
2.6 Seismic design according to European Code.....	42
2.6.1 Lateral force based method.....	46
2.6.2 Modal response based method .....	47
2.6.3 Nonlinear static “Pushover” analysis.....	48
2.6.4 Non-linear dynamic time-history analysis .....	49
<b>Chapter III – Study Cases: Definition, Description and Code Design .....</b>	<b>51</b>
3.1 Definition of the structural typologies .....	51
3.1.1 Investigated parameters .....	54
3.1.2 Description of the structural configuration .....	57
3.2 Code design based on Eurocode 8 and AISC 341 .....	60
3.2.1 Elastic response spectra .....	61

3.2.2 Material properties .....	63
3.2.3 Loads and load combination .....	64
3.2.4 Structural analysis .....	65
3.2.5 Requirements to design the Moment-resisting Frames .....	65
3.2.6 Requirements to design the concentrically braced Frames .....	69
3.2.7 Requirements to design the Dual-Concentrically braced Frames .....	77
3.2.8 Comments on the seismic design.....	84
<b>Chapter IV – Nonlinear Analysis Methodology.....</b>	<b>88</b>
4.1 Performance based evaluation .....	88
4.1.1 Performance criteria.....	89
4.1.2 Performance objectives for the study cases.....	90
4.2 Pushover analyses .....	91
4.2.1 Overstrength factor.....	92
4.3 Incremental dynamic analyses.....	92
4.3.1 Selection of accelerograms.....	93
4.4 Behaviour factors (q-factors) .....	97
4.5 Modelling of study cases.....	98
4.5.1 Restraints and boundary conditions .....	103
4.5.2 P-delta effects.....	104
4.5.3 Material properties .....	105
4.5.4 Calibration of the numerical model for the unbraced frames .....	108
4.5.5 Calibration of the numerical model for the braced frames .....	109
<b>Chapter V – Moment-resisting Dual-Steel Frames.....</b>	<b>112</b>
5.1 Static-nonlinear analysis .....	112
5.1.1 Overall overstrength factor.....	117
5.2 Dynamic performance evaluation .....	120
5.2.1 Peak inter-storey drift ratios .....	120
5.2.2 Residual inter-storey drift ratios .....	121
5.2.3 Peak storey accelerations .....	123
5.2.4 Beam ductility demand .....	125
5.2.5 Beam flexural overstrength.....	126
5.3 Behaviour factors.....	128
5.1 Material consumption .....	130
<b>Chapter VI – Concentrically Braced Dual-Steel Frames .....</b>	<b>134</b>
6.1 Nonlinear static analysis.....	134
6.1.1 Overall overstrength factor.....	142

6.2 Dynamic performance evaluation.....	146
6.2.1 Peak inter-storey drift ratios.....	146
6.2.2 Residual inter-storey drift ratios .....	149
6.2.3 Peak storey accelerations .....	151
6.2.4 Brace ductility demand.....	153
6.3 Behaviour factors .....	156
6.3.1 Influence of soil condition .....	156
6.3.2 Influence of HSS steel grade.....	157
6.3.3 Influence of span length .....	158
6.3.4 Influence of number of storey .....	159
6.4 Material consumption.....	160
<b>Chapter VII – Dual-System Concentrically Braced Dual-Steel Frames .....</b>	<b>164</b>
7.1 Static-nonlinear analysis.....	164
7.1.1 Overall overstrength factor .....	172
7.2 Dynamic performance evaluation.....	176
7.2.1 Peak inter-storey drift ratios.....	176
7.2.2 Residual inter-storey drift ratios .....	179
7.2.3 Peak storey accelerations .....	182
7.2.4 Brace ductility demand.....	184
7.2.5 Beam ductility demand in MRF subsystem.....	187
7.3 Behaviour factors .....	189
7.3.1 Influence of soil condition .....	190
7.3.2 Influence of span length .....	191
7.3.3 Influence of HSS steel grade.....	192
7.3.4 Influence of number of storey .....	193
7.4 Material consumption.....	194
7.5 Comparison between the Dual and Simple Concentrically Braced Dual-Steel Frames.....	197
7.5.1 Analysing of the results from Pushover analyses.....	198
7.5.2 Evaluation of the Dynamic response.....	201
7.5.3 Behaviour factors.....	203
7.5.4 Material consumption .....	205
<b>Chapter VIII – Dual-Steel vs Conventional Frames: Economic and Technical comparative evaluation.....</b>	<b>207</b>
8.1 Selection of the study cases .....	207
8.2 Comparison in terms of seismic performance .....	208

8.2.1 Moment-resisting Frames.....	208
8.2.2 Concentrically Braced Frames .....	211
8.2.3 Dual-Concentrically Braced Frames .....	213
8.3 Economic evaluation.....	216
8.3.1 Concentrically Braced Frames .....	218
8.3.2 Dual-Concentrically Braced Frames .....	221
<b>Chapter IX – Conclusions .....</b>	<b>224</b>
9.1 Moment-resisting Frames .....	225
9.2 Concentrically Braced Frames.....	226
9.3 Dual-Concentrically Braced Frames .....	228
9.4 Dual versus simple concentrically braced Frames .....	230
9.5 Comparing the conventional with HSS solution.....	232
9.6 Design recommendations .....	233
9.6.1 Seismic performance expected.....	235
9.6.2 Design checks for Moment-resisting Dual-steel Frames.....	236
9.6.3 Design checks for Concentrically Braced Dual-steel Frames .....	237
9.6.4 Design checks for Dual-Concentrically Braced Dual-steel Frames .....	238
9.7 Future research.....	239
9.8 Published articles and dissemination of results .....	240
<b>References .....</b>	<b>241</b>

## *List of Figures*

FIGURE 1.1 – MAFPRE TOWER (1992).....	2
FIGURE 1.2 – EUROPA TOWER – MADRID (1996) .....	3
FIGURE 1.3 – OVERVIEW OF THE ROOF STRUCTURE (SEDLACEK ET AL., 2005) .....	3
FIGURE 1.4 – YOKOHAMA LANDMARK TOWER (1993).....	4
FIGURE 1.5 – WORLD FINANCIAL CENTER (2008) .....	4
FIGURE 2.1 – POSSIBLE PLASTIC MECHANISMS IN MOMENT-RESISTING FRAMES (ELGHAZOULI, 2009A) .....	11
FIGURE 2.2 – FRACTURE AT THE WELDED BEAM-TO-COLUMN CONNECTION (ADAN AND HAMBURGER, 2010).....	12
FIGURE 2.3 – EXAMPLES OF CONNECTIONS FOR FRAMES LOCATED IN SEISMIC ZONES (ELGHAZOULI, 2009A) .....	12
FIGURE 2.4 – EXAMPLES OF CONCENTRICALLY BRACED FRAMES .....	14
FIGURE 2.5 – TYPICAL RESPONSE OF A BRACE UNDER CYCLIC AXIAL LOADING (MARINO AND NAKASHIMA, 2006) .....	15
FIGURE 2.6 – EARTHQUAKE DAMAGES IN CONCENTRICALLY BRACED FRAMES (SABELLI ET AL., 2013) .....	16
FIGURE 2.7 – LOCAL FAILURE OF HSS BRACE (SABELLI ET AL., 2013).....	17
FIGURE 2.8 – VARIOUS CONCENTRICALLY BRACED SYSTEM CONFIGURATIONS .....	18
FIGURE 2.9 – ECCENTRICALLY BRACED FRAMES CONFIGURATIONS .....	19
FIGURE 2.10 – A EXAMPLE OF THE USE OF EBF IN ISTANBUL BILGI UNIVERSITY (TURKEY) (D'ANIELLO, 2007).....	19
FIGURE 2.11 – HYSTERETIC RESPONSE OF A LINK (D'ANIELLO, 2007).....	20
FIGURE 2.12 – INFLUENCE OF THE LINK LENGTH ( $E/L$ ) (POPOV AND ENGELHARDT, 1988) .....	20
FIGURE 2.13 – HISTORIC EVOLUTION OF YIELD STRESS FOR HOT ROLLED STEEL COMPONENTS(SAMUELSSON AND SCHROTER, 2005).....	22
FIGURE 2.14 – REDUCTION OF PLATE THICKNESS AND WEIGHT VERSUS THE STRENGTH STEEL INCREASING (SAMUELSSON AND SCHROTER, 2005) .....	23
FIGURE 2.15 – COMPARING THE MICROSTRUCTURES AMONG THE PRODUCTION METHODS (WILLMS, 2009) .....	25
FIGURE 2.16 – CHEMICAL COMPOSITION FOR A HSS WITH 50 MM THICK (SAMUELSSON AND SCHROTER, 2005) .....	<b>ERRO! INDICADOR NÃO DEFINIDO.</b>

FIGURE 2.17 – ENGINEERING STRESS-STRAIN CURVES FOR MCS AND HSS (GESCHWINDNER ET AL., 1994).....	27
FIGURE 2.18 – CHARPY V-TEMPERATURE TRANSITION CURVES FOR S460ML AND S690QL IN COMPARISON WITH S355J2 (SAMUELSSON AND SCHROTER, 2005).....	28
FIGURE 2.19 – DUCTILITY COMPARISON (SEDLACEK ET AL., 2005) .....	28
FIGURE 2.20 – CURVES MORE FAVOURABLE FOR THE ELEMENTS MADE UP WITH HSS (SEDLACEK ET AL., 2005).....	30
FIGURE 2.21 – COMPARING THE PRICES AND MATERIAL COSTS WITH THE INCREASING OF STEEL STRENGTH ASSUMING THE S235 AS REFERENCE (COLLINS AND JOHANSSON, 2006).....	31
FIGURE 2.22 – MATERIAL AND FABRICATION COSTS FOR WELDING (DUBINA, 2008) .	31
FIGURE 2.23 – RELATIONSHIPS FOR ELASTIC AND INELASTIC BEHAVIOURS – EQUAL DISPLACEMENT RULE (LESTUZZI AND BADOUX, 2003) s .....	33
FIGURE 2.24 – DEPARTMENT STORE FAÇADE DURING LOMA PIETRA EARTHQUAKE (EERC) .....	35
FIGURE 2.25 – PERFORMANCE OBJECTIVES FOR BUILDING DEFINED IN SEOC-VISION-2000 (1995).....	36
FIGURE 2.26 – PHILOSOPHY OF DIRECT DISPLACEMENT-BASED DESIGN (PRIESTLEY, 2000).....	40
FIGURE 2.27 – ELASTIC SPECTRUMS RECOMMENDED BY (EN1998-1-1, 2004) .....	43
FIGURE 3.1 – DUAL STRUCTURAL SYSTEM STUDIED BY (IYAMA AND KUWAMURA, 1999).....	54
FIGURE 3.2 – COMPOSITE STEEL-CONCRETE CROSS-SECTIONS INVESTIGATED .....	55
FIGURE 3.3 – COMPOSITE STEEL-CONCRETE CROSS-SECTIONS INVESTIGATED .....	55
FIGURE 3.4 – OVERVIEW OF THE 72 STUDY CASES.....	56
FIGURE 3.5 – PLAN VIEW.....	57
FIGURE 3.6 – MOMENT-RESISTING FRAMES.....	58
FIGURE 3.7 – CONCENTRICALLY BRACED FRAMES.....	59
FIGURE 3.8 – DUAL-CONCENTRICALLY BRACED FRAMES.....	60
FIGURE 3.9 – RESPONSE SPECTRA AND RANGE OF FUNDAMENTAL PERIOD FOR THE MRFs.....	62
FIGURE 3.10 – RESPONSE SPECTRA AND RANGE OF FUNDAMENTAL PERIOD FOR THE CBFs.....	63
FIGURE 3.11 – RESPONSE SPECTRA AND RANGE OF FUNDAMENTAL PERIOD FOR THE D-CBFs.....	63
FIGURE 3.12 – UNBALANCED FORCE DUE TO BUCKLING OF COMPRESSION BRACE ....	70



FIGURE 3.13 – OVERSTRENGTH FACTORS DERIVED FROM SEISMIC DESIGN (MRFs)...	84
FIGURE 3.14 – OVERSTRENGTH FACTORS DERIVED FROM SEISMIC DESIGN (CBFs)...	86
FIGURE 3.15 – OVERSTRENGTH FACTORS DERIVED FROM SEISMIC DESIGN (D-CBFs).....	87
FIGURE 4.1 – DETERMINATION OF RESIDUAL DISPLACEMENTS.....	91
FIGURE 4.2 – CAPACITY CURVE FROM PUSHOVER ANALYSES.....	92
FIGURE 4.3 – RESPONSE SPECTRA OF ALL SELECTED ACCELEROGRAMS AND CODE SPECTRUM.....	94
FIGURE 4.4 – EARTHQUAKE RECORDS ADOPTED IN THE ANALYSIS FOR STIFF SOIL....	95
FIGURE 4.5 – EARTHQUAKE RECORDS ADOPTED IN THE ANALYSIS FOR SOFT SOIL.....	96
FIGURE 4.6 – MAXIMUM BASE SHEAR VERSUS ACCELERATION.....	97
FIGURE 4.7 – LUMPED PLASTICITY FORMATION (FRAGIADAKIS AND PAPADRAKAKIS, 2008) .....	99
FIGURE 4.8 – FIBRE APPROACH (SEISMOSTRUCT, 2011) .....	99
FIGURE 4.9 – DISCRETISATION OF THE FRAME FOR A DISPLACEMENT-BASED AND FORCE-BASED FORMULATIONS (FRAGIADAKIS AND PAPADRAKAKIS, 2008) .....	101
FIGURE 4.10 – RESPONSE OF BOTH DISPLACEMENT-BASED AND FORCE-BASED FORMULATIONS (FRAGIADAKIS AND PAPADRAKAKIS, 2008) .....	101
FIGURE 4.11 – INTEGRATION SECTIONS (SEISMOSTRUCT, 2011) .....	102
FIGURE 4.12 – PERFORMANCE OF FORCE-BASED ELEMENT FOR VARIOUS INTEGRATION SCHEMES (PAPAIOANNOU ET AL., 2005) .....	102
FIGURE 4.13 – ROTATIONAL SPRING TO SIMULATE THE PINNED CONNECTIONS.....	104
FIGURE 4.14 – THE BASIC DISPLACEMENT DEGREES-OF-FREEDOM AND FORCES OF BEAM-COLUMN ELEMENT (SEISMOSTRUCT, 2011) .....	104
FIGURE 4.15 – LEARNING COLUMN .....	105
FIGURE 4.16 – CONCRETE STRESS-STRAIN CURVE (MARTLNEZ-RUEDA AND ELNASHAI, 1997) .....	106
FIGURE 4.17 – MATERIAL PROPRIETIES AND STRESS-STRAIN CURVE FOR THE S355 ..	107
FIGURE 2.18 – MATERIAL PROPRIETIES AND STRESS-STRAIN CURVE FOR THE S460 ..	107
FIGURE 4.19 – MATERIAL PROPRIETIES AND STRESS-STRAIN CURVE FOR THE S690 ..	107
FIGURE 4.20 – CHARACTERIZATION OF THE CONFINED REGIONS ON THE COMPOSITE COLUMN SECTIONS .....	108
FIGURE 4.21 – STRUCTURAL SCHEME OF THE SINGLE FRAME (WAKABAYASHI ET AL., 1974) .....	109

FIGURE 4.22 – COMPARISON BETWEEN NUMERICAL AND EXPERIMENTAL CURVES: A) CYCLIC TESTS ON BEAMS BY D'ANIELLO ET AL. (2012); B) CYCLIC TESTS ON SINGLE STOREY MRF BY WAKABAYASHI ET AL. (1974).....	109
FIGURE 4.23 – EXAMPLE OF BRACES WITH OUT-OF-STRAIGHTNESS ( $\epsilon$ ) (DICLELI AND MEHTA, 2007) .....	110
FIGURE 4.24 – COMPARISON BETWEEN THE EXPERIMENTAL AND NUMERICAL RESPONSES.....	111
FIGURE 4.25 – COMPARISON BETWEEN THE EXPERIMENTAL AND NUMERICAL RESPONSES.....	111
FIGURE 5.1 – NORMALIZED PUSHOVER RESPONSE CURVES.....	114
FIGURE 5.2 – 1 <sup>ST</sup> MODE PUSHOVER: DAMAGE DISTRIBUTION FOR FRAMES WITH 7.5M OF SPAN.....	115
FIGURE 5.3 – 1 <sup>ST</sup> MODE PUSHOVER: DAMAGE DISTRIBUTION FOR FRAMES WITH 5.0M OF SPAN.....	116
FIGURE 5.4 – INTER-STOREY DRIFT DEMAND FOR THE THREE LIMIT STATES .....	121
FIGURE 5.5 – RESIDUAL INTER-STOREY DRIFT RATIOS.....	123
FIGURE 5.6 – STOREY ACCELERATION FOR DL, SD AND NC LIMIT STATES.....	124
FIGURE 5.7 – DUCTILITY DEMAND RATIOS .....	126
FIGURE 5.8 – OVERSTRENGTH DEMAND RATIOS .....	127
FIGURE 5.9 – BEHAVIOUR FACTORS USING EUROPEAN APPROACH .....	129
FIGURE 5.10 – BEHAVIOUR FACTORS USING SALVITTI & ELNASHAI APPROACH.....	130
FIGURE 5.11 – AVERAGE OF AMOUNT OF STEEL AND CONCRETE.....	132
FIGURE 5.12 – COMPARISON OF MATERIAL CONSUMPTION TO SPAN LENGTH.....	132
FIGURE 5.13 – COMPARISON OF MATERIAL CONSUMPTION TO NUMBER OF STOREY .....	133
FIGURE 6.1 – NORMALIZED PUSHOVER RESPONSE CURVES FROM EIGHT-STOREY FRAMES.....	135
FIGURE 6.2 – NORMALIZED PUSHOVER RESPONSE CURVES FROM SIXTEEN-STOREY FRAMES.....	136
FIGURE 6.3 – 1 <sup>ST</sup> MODE PUSHOVER: DAMAGE DISTRIBUTION FOR EIGHT-STOREY FRAMES WITH S690 .....	138
FIGURE 6.4 – 1 <sup>ST</sup> MODE PUSHOVER: DAMAGE DISTRIBUTION FOR EIGHT-STOREY FRAMES WITH S460 .....	139
FIGURE 6.5 – 1 <sup>ST</sup> MODE PUSHOVER: DAMAGE DISTRIBUTION FOR SIXTEEN-STOREY FRAMES WITH S460 .....	140
FIGURE 6.6 – 1 <sup>ST</sup> MODE PUSHOVER: DAMAGE DISTRIBUTION FOR SIXTEEN-STOREY FRAMES WITH S690 .....	141

FIGURE 6.7 – INFLUENCE OF STUDIED PARAMETERS IN INTER-STOREY MEDIAN DRIFT DEMAND FOR THE THREE LIMIT STATES ( <i>VALUES IN %</i> ) .....	148
FIGURE 6.8 – INFLUENCE OF STUDIED PARAMETERS IN RESIDUAL DRIFT RATIO FOR THE THREE LIMIT STATES ( <i>VALUES IN %</i> ) .....	150
FIGURE 6.9 – PROFILES OF THE PEAK STOREY ACCELERATION.....	152
FIGURE 6.10 – BRACE DUCTILITY DEMAND FOR THE THREE LIMIT STATES .....	155
FIGURE 6.11 – COMPARISON OF BEHAVIOUR FACTORS FOR SOIL TYPE.....	157
FIGURE 6.12 – COMPARISON OF BEHAVIOUR FACTORS ACCORDING TO STEEL GRADE .....	158
FIGURE 6.13 – COMPARISON OF BEHAVIOUR FACTORS ACCORDING TO SPAN LENGTH.....	159
FIGURE 6.14 – COMPARING THE BEHAVIOUR FACTORS CONCERNING TO NUMBER OF STOREY .....	160
FIGURE 6.15 – AVERAGE OF AMOUNT OF STEEL, CONCRETE AND REINFORCEMENT.....	161
FIGURE 6.16 – COMPARISON BETWEEN THE HSS STEEL GRADES.....	162
FIGURE 6.17 – COMPARISON OF MATERIAL CONSUMPTION TO NUMBER OF STOREY.....	162
FIGURE 6.18 – INFLUENCE OF THE COMPOSITE STEEL-CONCRETE COLUMN .....	163
FIGURE 6.19 – INFLUENCE OF THE LENGTH SPAN ON THE STEEL DENSITY.....	163
FIGURE 7.1 – NORMALIZED PUSHOVER RESPONSE CURVES FROM EIGHT-STOREY FRAMES .....	166
FIGURE 7.2 – NORMALIZED PUSHOVER RESPONSE CURVES FROM SIXTEEN-STOREY FRAMES .....	167
FIGURE 7.3 – 1 <sup>ST</sup> MODE PUSHOVER: DAMAGE DISTRIBUTION FOR FRAMES WITH EIGHT-STOREY FRAMES WITH S690.....	168
FIGURE 7.4 – 1 <sup>ST</sup> MODE PUSHOVER: DAMAGE DISTRIBUTION FOR EIGHT-STOREY FRAMES WITH S460 .....	169
FIGURE 7.5 – 1 <sup>ST</sup> MODE PUSHOVER: DAMAGE DISTRIBUTION FOR FRAMES WITH SIXTEEN-STOREY FRAMES WITH S460 .....	170
FIGURE 7.6 – 1 <sup>ST</sup> MODE PUSHOVER: DAMAGE DISTRIBUTION FOR FRAMES WITH SIXTEEN-STOREY FRAMES WITH S690 .....	171
FIGURE 7.7 – INFLUENCE OF STUDIED PARAMETERS IN INTER-STOREY DRIFT DEMAND FOR THE THREE LIMIT STATES.....	178
FIGURE 7.8 – INFLUENCE OF STUDIED PARAMETERS IN RESIDUAL DRIFT RATIO FOR THE THREE LIMIT STATES.....	181
FIGURE 7.9 – PROFILES OF THE PEAK STOREY ACCELERATION FOR THE D-CBFs.....	183

FIGURE 7.10 – BRACE DUCTILITY DEMAND FROM D-CBFs FOR THE THREE LIMIT STATES.....	186
FIGURE 7.11 – BEAM DUCTILITY DEMAND FROM MRF PART OF THE D-CBFs FOR THE THREE STATES.....	188
FIGURE 7.12 – COMPARISON OF BEHAVIOUR FACTORS FOR SOIL TYPE .....	191
FIGURE 7.13 – COMPARISON OF BEHAVIOUR FACTORS FOR PAN LENGTH .....	192
FIGURE 7.14 – COMPARISON OF BEHAVIOUR FACTORS FOR STEEL GRADE.....	193
FIGURE 7.15 – COMPARING THE BEHAVIOUR FACTORS CONCERNING TO NUMBER OF STOREY.....	194
FIGURE 7.16 – AVERAGE OF AMOUNT OF STEEL, CONCRETE AND REINFORCEMENT.....	195
FIGURE 7.17 – COMPARISON BETWEEN THE HSS STEEL GRADES .....	196
FIGURE 7.18 – COMPARISON OF MATERIAL CONSUMPTION AND NUMBER OF STOREY.....	196
FIGURE 7.19 – INFLUENCE OF THE COMPOSITE STEEL-CONCRETE COLUMN.....	197
FIGURE 7.20 – INFLUENCE OF THE LENGTH SPAN ON THE STEEL DENSITY .....	197
FIGURE 7.21 – COMPARING THE NORMALIZED PUSHOVER RESPONSE CURVES.....	198
FIGURE 7.22 – COMPARING THE OVERSTRENGTH FACTORS FOR STIFF SOIL CONDITION.....	199
FIGURE 7.23 – COMPARING THE OVERSTRENGTH FACTORS FOR SOFT SOIL CONDITION.....	200
FIGURE 7.24 – EXAMPLES OF DAMAGE DISTRIBUTION FOR THE TWO SYSTEMS .....	201
FIGURE 7.25 – SEISMIC PERFORMANCE OF BOTH CBFs AND D-CBFs.....	202
FIGURE 7.26 – BEHAVIOUR FACTOR FOR BOTH CBFs AND D-CBFs USING THE EUROPEAN APPROACH .....	203
FIGURE 7.27 – BEHAVIOUR FACTOR FOR BOTH CBFs AND D-CBFs USING THE SALVITTI AND ELNASHAI APPROACH .....	204
FIGURE 7.28 – COMPARISON TAKING INTO ACCOUNT THE STEEL CONSUMPTION ....	206
FIGURE 8.1 – DESCRIPTION OF THE STUDY CASES COMPARING THE CONVENTIONAL STRUCTURES WITH DUAL-STEEL ONES.....	209
FIGURE 8.2 – DUAL-STEEL <i>VERSUS</i> SINGLE STEEL MRFs: TRANSIENT INTER-STOREY DRIFT RATIOS .....	210
FIGURE 8.3 – DUAL-STEEL <i>VERSUS</i> SINGLE STEEL MRFs: RESIDUAL INTER-STOREY DRIFT RATIOS .....	210
FIGURE 8.4 – DUAL-STEEL <i>VERSUS</i> SINGLE STEEL CBFs: INTER-STOREY DRIFT DEMAND .....	211

FIGURE 8.5 – DUAL-STEEL <i>VERSUS</i> SINGLE STEEL CBFs: RESIDUAL INTER-STOREY DRIFT DEMAND .....	212
FIGURE 8.6 – DUAL-STEEL <i>VERSUS</i> SINGLE STEEL CBFs: BRACE DUCTILITY DEMAND .....	212
FIGURE 8.7 – DUAL-STEEL <i>VERSUS</i> SINGLE STEEL CBFs: STOREY ACCELERATION...	213
FIGURE 8.8 – DUAL-STEEL <i>VERSUS</i> SINGLE STEEL D-CBFs: INTER-STOREY DRIFT DEMAND .....	214
FIGURE 8.9 – DUAL-STEEL <i>VERSUS</i> SINGLE STEEL D-CBFs: RESIDUAL INTER-STOREY DRIFT DEMAND .....	214
FIGURE 8.10 – DUAL-STEEL <i>VERSUS</i> SINGLE STEEL D-CBFs: BRACE DUCTILITY DEMAND .....	215
FIGURE 8.11 – DUAL-STEEL <i>VERSUS</i> SINGLE STEEL D-CBFs: STOREY ACCELERATION .....	215
FIGURE 8.12 – TOTAL COSTS OF THE CBFs COMPARING THE S355, S460 AND S690 STRUCTURES .....	220
FIGURE 8.13 – TOTAL COSTS OF THE D-CBFs COMPARING THE S355, S460 AND S690 STRUCTURES .....	223
FIGURE 9.1 – THE USE OF HSS (THICKER LINES)AND MCS (THINNER LIES) IN THE STUDIED TYPOLOGIES .....	234

## *List of Tables*

TABLE 2.1 – CHEMICAL COMPOSITION FOR A HSS WITH 50 MM THICK (SAMUELSSON AND SCHROTER, 2005).....	26
TABLE 2.2 – KNOWLEDGE LEVELS AND CORRESPONDING METHODS OF ANALYSIS (LF: LATERAL FORCE PROCEDURE, MRS: MODAL RESPONSE SPECTRUM ANALYSIS) AND CONFIDENCE FACTORS (CF) (EN1998-1-3, 2005) .....	38
TABLE 2.3 – CONSEQUENCES OF STRUCTURAL REGULARITY ON SEISMIC ANALYSIS AND DESIGN (EN1998-1-1, 2004).....	45
TABLE 3.1 – CHARACTERISTICS OF THE ELASTIC SPECTRUM FOR THE SEISMIC DESIGN.....	62
TABLE 3.2 – STEEL TYPES EMPLOYED IN THE SEISMIC DESIGN.....	64
TABLE 3.3 – LOAD CASES.....	64
TABLE 3.4 – LOAD COMBINATIONS.....	65
TABLE 3.5 – SECTIONAL PROPERTIES OF COLUMNS AND BEAMS FOR MRFs.....	67
TABLE 3.6 – SECTIONAL PROPERTIES OF COLUMNS AND BEAMS FOR CBFs.....	71
TABLE 3.7 – FUNDAMENTAL PERIODS OF THE CBFs.....	73
TABLE 3.8 – SECTIONAL PROPERTIES OF BRACES.....	74
TABLE 3.9 – SECTIONAL PROPERTIES OF COLUMNS AND BEAMS FOR D-CBFs.....	78
TABLE 3.10 – FUNDAMENTAL PERIODS OF THE D-CBFs.....	80
TABLE 3.11 – SECTIONAL PROPERTIES OF BRACES FOR D-CBFs .....	81
TABLE 3.12 – SECTIONAL PROPERTIES OF BRACES FOR D-CBFs .....	82
TABLE 3.13 – SECTIONAL PROPERTIES OF BRACES FOR D-CBFs .....	83
TABLE 4.1 – PERFORMANCE LEVELS .....	90
TABLE 4.2 – BASIC DATA OF THE EARTHQUAKES SELECTED .....	94
TABLE 5.1 – OVERSTRENGTH FACTORS .....	118
TABLE 5.2 – DISPERSION OF INTER-STOREY DRIFT RATIO DEMAND ( <i>VALUES IN %</i> )	122
TABLE 5.3 – DISPERSION OF RESIDUAL INTER-STOREY DRIFT RATIO DEMAND ( <i>VALUES IN %</i> ).....	123
TABLE 5.4 – MAXIMUM RATIOS OBTAINED FOR PSAs .....	125
TABLE 5.5 – AVERAGE WEIGHT (KG) OF STEEL FOR EACH STRUCTURAL ELEMENT ..	131
TABLE 6.1 – OVERSTRENGTH FACTOR FOR THE CBFs.....	144
TABLE 6.2 – MAXIMUM MEDIAN OF INTER-STOREY DRIFT RATIO DEMAND ( <i>VALUE IN %</i> ).....	147

TABLE 6.3 – MAXIMUM MEDIAN OF RESIDUAL INTER-STOREY DRIFT RATIO DEMAND (VALUES IN %) .....	149
TABLE 6.4 – MAXIMUM VALUES FOUND FOR THE PSAs (VALUES IN %).....	153
TABLE 6.5 – MAXIMUM VALUE OF BRACE DUCTILITY DEMAND .....	154
TABLE 6.6 – THE STEEL WEIGHT (KG) FOR THE FRAMES WITH 5.0M AND 7.5M OF SPAN .....	163
TABLE 7.1 – OVERSTRENGTH FACTOR FOR THE D-CBFs .....	174
TABLE 7.2 – MAXIMUM MEDIAN OF INTER-STOREY DRIFT RATIO DEMAND FOR.....	179
TABLE 7.3 – MAXIMUM MEDIAN OF RESIDUAL INTER-STOREY DRIFT RATIO DEMAND (VALUES IN %) .....	182
TABLE 7.4 – MAXIMUM VALUES FOUND FOR THE PSAs FOR THE D-CBFs .....	184
TABLE 7.5 – MAXIMUM VALUE OF BRACE DUCTILITY DEMAND .....	185
TABLE 7.6 – MAXIMUM VALUE OF BEAM DUCTILITY DEMAND FROM MRF PART OF THE D-CBFs .....	189
TABLE 7.7 – THE STEEL WEIGHT (KG) FOR THE FRAMES WITH 5.0M AND 7.5M OF SPAN .....	197
TABLE 8.1 – PRICES FROM EACH TASK TO BE CONSIDERED IN THE ECONOMIC EVALUATION.....	217
TABLE 8.2 – DIFFERENCES OF PRICES DEPENDING OF THE STEEL GRADE.....	217
TABLE 8.3 – THE STEEL WEIGHT (KG) FOR THE COLUMNS AND BEAMS OF THE CBF WITH S355 .....	218
TABLE 8.4 – THE STEEL WEIGHT (KG) FOR THE COLUMNS AND BEAMS OF THE CBF WITH S355 .....	218
TABLE 8.5 – THE STEEL WEIGHT (KG) FOR THE COLUMNS AND BEAMS OF THE CBF WITH S460 .....	219
TABLE 8.6 – THE STEEL WEIGHT (KG) FOR THE COLUMNS AND BEAMS OF THE CBF WITH S460 .....	219
TABLE 8.7 – THE STEEL WEIGHT (KG) FOR THE COLUMNS AND BEAMS OF THE CBF WITH S690 .....	219
TABLE 8.8 – THE STEEL WEIGHT (KG) FOR THE COLUMNS AND BEAMS OF THE CBF WITH S690 .....	220
TABLE 8.9 – THE STEEL WEIGHT (KG) FOR THE COLUMNS AND BEAMS OF THE D-CBF WITH S355 .....	221
TABLE 8.10 – THE STEEL WEIGHT (KG) FOR THE COLUMNS AND BEAMS OF THE D-CBF WITH S355 .....	221



TABLE 8.11 – THE STEEL WEIGHT (KG) FOR THE COLUMNS AND BEAMS OF THE D-CBF  
WITH S460..... 222

TABLE 8.12 – THE STEEL WEIGHT (KG) FOR THE COLUMNS AND BEAMS OF THE D-CBF  
WITH S460..... 222

TABLE 8.13 – THE STEEL WEIGHT (KG) FOR THE COLUMNS AND BEAMS OF THE D-CBF  
WITH S690..... 223

TABLE 8.14 – THE STEEL WEIGHT (KG) FOR THE COLUMNS AND BEAMS OF THE D-CBF  
WITH S690..... 223

# ***Nomenclature***

## ***Lowercases***

$a_{gR}$	reference peak ground acceleration
$a_g$	seismic action
$a_{g(\text{collapse})}$	acceleration related to the failure
$a_{g(\text{design})}$	acceleration corresponding to limit state
$d_r$	design inter-storey drift
$e$	length links from the eccentrically braced frames
$f_y$	yield strength steel
$f_u$	ultimate strength steel
$f_{ck}$	uniaxial cylinder compressive
$f_{ctk}$	uniaxial cylinder tensile
$h$	storey height
$h_b$	steel beam depth
$l_b$	beam span
$k$	number of modes taken into account
$m$	mass locations
$n$	number of storeys above the foundation or the top of a rigid basement
$q$	behaviour factor
$s$	beam flexural overstrength
$t$	nominal thickness of the element
$\tilde{z}_i$	height of the mass

## ***Uppercases***

$A$	acceleration from IDA
$A_{net}$	net cross-sectional area
$A_d$	design acceleration
$A_y$	acceleration corresponding to the yielding of the frame
$A_\theta$	acceleration corresponding to the maximum permitted inter-storey drift ratio
$A_c$	acceleration corresponding to the column plastification
$A_R$	acceleration corresponding to the maximum permitted local rotation
$A_u$	acceleration related to the failure

$A^{+/-}$	areas of the horizontal projections of the cross-sections of the tension diagonals
$C_t$	factor to calculate the fundamental period of building
$F$	design base shear force
$F_{el}$	elastic base shear force
$F_y$	yield base shear force
$G$	maximum mode response
$H$	height of building
$H_e$	effective height of building
$K_e$	secant stiffness
$K_f$	initial stiffness
$K_e$	effective stiffness
$L$	bay length
$\Sigma M_b$	sum of design values of moments of resistance of the beams framing into a joint in the direction of interest
$\Sigma M_C$	sum of design values of the moments of resistance of the columns framing into a joint in the direction of interest
$M_{Ed}$	bending moment from the analysis for the seismic design situation
$M_{max}$	maximum bending moment on the beam
$M_{pl,Rd}$	design resistant moment
$M_{j,bi,Ed}$	bending moment in the beam at the intersection of the member centrelines into the joints on the side “i”.
$N_{Ed}$	axial force from the analysis for the seismic design situation
$N_{pl,Rd}$	design resistance axial
$N_{plt}$	design resistance axial of the braces in tension
$N_{plc}$	design resistance axial of the braces in compression
$N_{t,Rd}$	design resistance of net section in tension
$R$	reduction factor (similar to behaviour factor)
$T_1$	fundamental period of buildings
$T_e$	effective period
$T_B$	initial period of the constant spectral acceleration
$T_C$	final period of the constant spectral acceleration
$T_D$	Period of the constant displacement spectral acceleration
$T_L$	return period
$T_{LR}$	reference return period for which the reference seismic action may be computed
$T_k$	period of vibration of mode k

$V_{Ed}$	shear force from the analysis for the seismic design situation
$V_y$	base shear from of the yield strength of the structure
$V_{Iy}$	base shear at the formation of the first plastic hinge
$V_d$	design base shear
$V_{pl,Rd}$	design resistance shear
$V_{Rd,i}$	base shear resistance at the i-th storey

### ***Lowercase Greek letters***

$\alpha_i$	angle that the braces make with the horizontal direction
$\alpha_u$	multiplier of horizontal seismic design action at formation of global plastic hinge in the system
$\alpha_1$	multiplier of horizontal seismic design action at formation of first plastic hinge in the system
$\beta$	transformation factor according to EN1993:1-8
$\beta_{dr}$	limitation of inter-storey drift depending of the non-structural elements
$\gamma_I$	importance factor
$\gamma_{ov}$	material overstrength factor
$\gamma_{M12}$	partial factor for bolted connection
$\gamma_{material}$	density of material total mount
$\delta_y$	yield displacement from the N2 method
$\delta_{Iy}$	displacements corresponding to the formation of the first plastic hinge
$\delta_{max}$	roof displacement corresponding to the achievement of an inter-storey drift ratio
$\theta$	inter-storey drift sensitivity coefficient
$\theta_y$	beam yield rotation
$\lambda$	correction factor
$\mu$	displacement ductility demand
$\mu_{el}$	elastic peak displacement
$\mu_p$	inelastic peak displacement
$\mu_\Delta$	ductility factor
$\nu$	reduction effect accounting the lower return period of the seismic action
$\xi$	viscous damping
$\xi_{eq}$	equivalent viscous damping
$\rho_{in}$	correlation coefficient for CQC

### ***Uppercases Greek letters***

$\Delta_c$	axial deformation of the brace at buckling load
$\Delta_t$	axial deformation of the brace at tensile yielding load
$\Delta_d$	design displacement
$\Delta_y$	yield displacement
$\Delta^*$	axial capacity of the braces according to EN1998-1-3
$\Omega$	overstrength factor
$\Omega_1$	overstrength factor associated to EN1998-1-1
$\Omega_2$	overstrength factor related to designed decisions
$\Omega_{\text{design}}$	overstrength factor from seismic design depending of the structural system
$\Omega_{\text{MRF}}$	overstrength factor from seismic design of the MRF beams
$\Omega_{\text{CBF}}$	overstrength factor from seismic design of the CBF braces

### ***Abraviations***

<i>CBF</i>	Concentrically Braced Frames
<i>CFT</i>	Concrete Tube Composite Column
<i>CQC</i>	Complete Quadratic Combination method
<i>DB</i>	Displacement-Based distributed inelasticity frame element
<i>DL</i>	Damage Limitation limit state from EN1998-1-3
<i>DBD</i>	Displacement Based Design
<i>DCH</i>	Ductility Class High
<i>DCM</i>	Ductility Class Medium
<i>DDBD</i>	Direct Displacement Based Design
<i>D-CBF</i>	Dual-Concentrically Braced Frames
<i>EBF</i>	Eccentrically Braced Frames
<i>ERS</i>	Elastic Response Spectra
<i>FB</i>	Force-Based distributed inelasticity frame element
<i>FE</i>	Fully Encased Composite Column
<i>FBD</i>	Force Base Design approach
<i>FEMA</i>	Federal Emergency Management Agency
<i>HR</i>	Hot Rolling cross-section
<i>HPS</i>	High Performance Steel
<i>HSS</i>	High Strength Steel
<i>IDR</i>	Inter-storey Drift Ratio

<i>KL</i>	Level of knowledge from EN1998-1-3
<i>MCS</i>	Mild Carbon Steel
<i>MRF</i>	Moment-resisting Frames
<i>NC</i>	Near Collapse limit state from EN1998-1-3
<i>PE</i>	Partially Encased Composite Column
<i>PBD</i>	Performance Base Design approach
<i>PGA</i>	Peak Ground Acceleration
<i>PSA</i>	Peak Storey Acceleration
<i>PRS</i>	Steel profile custom made by welding
<i>RBS</i>	Reduced Beam Section
<i>RIDR</i>	Residual Inter-storey Drift Ratio
<i>SD</i>	Significant Damage limit state from EN1998-1-3
<i>SRSS</i>	Square Root of the Sum of the Squares

## *Chapter I*

# Introduction

### **1.1 General considerations**

In recent years, there have been significant developments in steel processing. Indeed, the improvements in industrial processes by the combination of rolling practices and cooling rates allowed the achievement of High Strength Steel (HSS) with very attractive properties. Owing to the high performance, the use of HSS has a number of benefits in terms of economic, architectural, environmental, and safety aspects in which the increase of strength allows a size reduction of the structural members, enabling potential benefits in terms of environments impact through energy saving and reduction of gas emissions.

The use of HSS in structural elements has been expanded to civil engineering structures. The HSS has been successfully implemented in the automotive and ship industry due to the limitation of professional experience, standard with adequate information about the design and to a limited number of researches performed in order to investigate the use of HSS in civil structures. However, the increase in the use of HSSs for building construction allowed the creation of research programs aiming at in order the investigation of the structural behaviour of these steels.

An European project has recently been started with the aim of investigating and evaluating the seismic performance of building frames using the dual-steel concept called HSS-SERF (High Strength Steel in Seismic Resistant Building Frames). The research group is composed by steel producers, design and consulting company, research institutions and universities with large and recognized experience in the field of proposed research.

The limited number of HSS applications in civil construction is also related to some lack of information regarding the behaviour and design rules in the codes. A working group within



CEN/TC250/SC3 has recently developed a proposal for Part 1-12 of Eurocode 3 (EN1998-1-12, 2007) to cover the design of steel structures using yield strengths between 460 MPa (S460) to 700MPa (S700). A new European standard with additional rules for the delivery condition of structural steel was also established in 2004 (part 6 of EN 10025:2004). EN10025-6 states the technical delivery conditions for flat products of HSS in the quenched and tempered condition in which they are widely used in structural applications.

Concerning to costs, it is recognized that the price of HSS is superior in comparison with the MCS, especially in Europe. For instance, the S690 steel grade, which it is produced in the Netherlands, is around 70-75 % more expensive than S355 per kg (Mercon Steel).

On the other hand, the cost of material represents only 25-30% of total costs of framed steel structures. The cost of fabrication and erection complete the overall costs. Therefore, an increasing of 20% of material cost would increase in about 5% the cost of the final structure (AISC, 2010).

Nevertheless, the market demands are still quite limited, and only a few fabricators are producing HSS. The trend, however, is that this scenario will change, and the increasing of market demand will result in decreasing of prices for HSS in the near future.

In Europe the use of HSS in bridges is already considered state-of-art, but the applications in buildings are few, especially in seismic zones. Some illustrative examples of its use in building application are following:

- Mafpre Tower in Barcelona, with 42 floors and a height of 150 m, where the columns of H-shaped steel grade S460M were used, resulting in a reduction of 24% of the weight of steel, compared to the S355 solution (see Figure 1.1);



Figure 1.1 – Mafpre Tower (1992)

- Europe Tower in Madrid, in which there is an inclination of 14°, in all structural elements using steel grade S460M (see Figure 1.2);



Figure 1.2 – Europa Tower – Madrid (1996)

- Tower Pleiades Brussels with the steel columns of S460N and a saving of 20% compared to a project using steel S355J0;
- Conference Center "Espace Leopold" in the European Parliament in Brussels with composite columns of steel grade S420M and S355 in steel beams;
- The steel grade S460 was also used in the structure of Commerzt Bank in Frankfurt;
- In the Sony Center in Berlin, the S690 steel grade was used in structures elements and connections (see Figure 1.3);

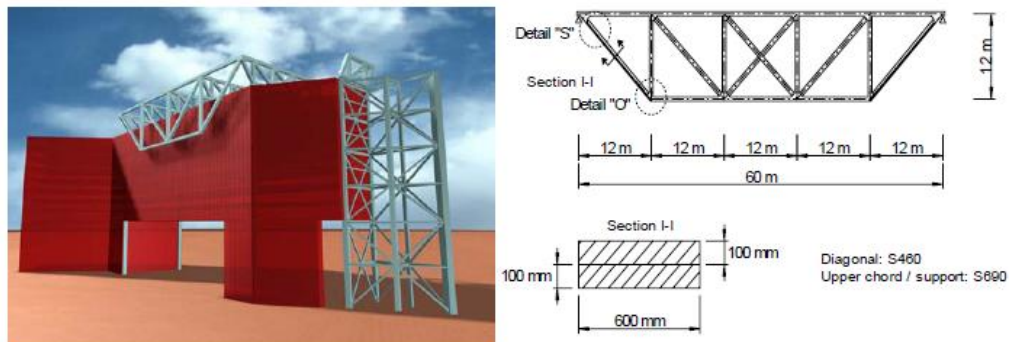


Figure 1.3 – Overview of the roof structure (Sedlacek et al., 2005)

- The Airbus Hangar in Frankfurt is an example of application of steel TM S460ML constant yield up to 120mm thick;

Japan is more advanced in the use of high strength steel to seismic resistant buildings, and some notable buildings can be presented, all based on the concept of dual-steel, i.e., columns with HSS, and, beams together with bracing made with MCS (Dubina et al., 2006).

- In Figure 1.4, Yokohama Landmark Tower located in Yokohama (with 70 floors) is an example of the use of HSS. The SA440 steel was used in the columns;



Figure 1.4 – Yokohama Landmark Tower (1993)

- JR EAST Head Office Building and Roppongi Hills Mori Tower Building located in Tokyo. Both used the SA440 steel in structural elements;
- Triton Square, also located in Tokyo, with 39 floors, used the SA440 steel in the columns.

In China, it can mention the World Financial Center as an example of the use of high strength steel, S460M class (see Figure 1.5).



Figure 1.5 – World Financial Center (2008)

In the USA, there are two examples of buildings that are composed of HSS: Hudson Colgate Center in Jersey, and Fremont building in San Francisco, in which the columns are steel type A919 grade 65 (equivalent to S460 steel) while other elements are formed by steel A919 grade 50 (similar to S355). In both cases, a reduction in weight of steel was approximately 20% when compared to a steel composed exclusively of class A919 grade 50 solution.

Based on the issued stated before, the seismic applications potentially represent the rational field to exploit the high performance of HSS. Indeed, according to modern codes the seismic

design of steel or composite buildings are based on the concept of dissipative structures, in which specific zones of the structures should be able to develop plastic deformation, mainly on ductile member, in order to dissipate the seismic energy. On the contrary, the non-dissipative zones and members should behave elastically under seismic action in order to avoid the brittle collapse of the building. For this reason, these zones should be designed to resist the full plastic strength of the dissipative members. Consequently, the large overstrength demands to non-dissipative zones lead to high material consumption, and sometimes, huge size of members to fulfil this design requirement.

Recent studies (Dubina et al., 2006; Dubina, 2008; Dubina, 2010) have highlighted the advantages of dual-steel concept, especially for what concerns the control of seismic response of multi-storey buildings to achieve overall ductility mechanism. Some studies have also been conducted in Japan using MCS in dissipative elements and HSS in non-dissipative elements that must remain elastic especially during strong earthquakes – dual-steel concept (Takanashi et al., 2005). In particular, Dubina (2010) showed the potential benefits of using HSS in full strength moment-resisting steel beam-to-column connections in order to guarantee the formation of plastic hinge in the beam and preserving both the connection and the column in MRFs.

This Thesis presents the results of a parametric study analysing the seismic behaviour of three structural systems using the dual-steel concept. In detail, the Moment-resisting Frame (MRF), Concentrically Braced Frame (CBF) and Dual-Concentrically Braced Frame (D-CBF) have been investigated. Relevant parameters that can influence the seismic response have been assessed, such as: the soil condition, type of composite steel-concrete column, length span, type of HSS employed in non-dissipative structural elements and the number of storey.

The examined frames have been designed in accordance with requirement preconized by EN1998-1-1 (2004). This code uses the capacity design approach, in which specific zones are responsible for energy dissipation under earthquake. Moreover, due to the absence of adequate information about the seismic design of the dual-system structures. In this Thesis, the AISC-341 (2005) code has also been used in order to design the study cases with dual-system. According to this code, the MRF subsystem should be provided with a minimum of 25% of the total lateral strength of the structures.

Furthermore, a Performance Based Seismic Design has been used in order to investigate the benefits of dual-steel concept. In fact, the lessons learned from recent earthquakes regarding the costs of structural repair and disruptions of the functions of the buildings have evidenced a potential improvement of the current methodologies employed in actual codes. The

earthquake engineering community was able to observe that the control of damage caused by ground motion achieved its goal of life protection. However, the economic impact of excessive structural damage that disable the functionality of the building revealed to be quite high.

In this research, therefore, the seismic performance of study cases has been analysed through static and dynamic nonlinear analyses compared with three limit states as defined in EN1998-1-3 (2005): Damage Limitation (DL), Severe Damage (SL) and Near Collapse (NC). After describing the results of numerical analyses, the discussion look for insights in the following issues: (i) quantification of performance parameters for each limit states, (ii) characterization of the behaviour factors in each limit states, (iii) comparison between dual-steel and single grade steel, (iv) assessment of economic efficiency.

A numerical model has been implemented in order to perform both, nonlinear static and dynamic analyses. The models were developed using the Force-based (FB) distributed inelasticity elements. These elements account for distributed inelasticity through integration of material response over the cross-section and integration of the section response along the length of the elements. The cross-section behaviour is reproduced by means of the fibre approach, assigning a uniaxial stress-strain relationship in each fibre. In order to model the study cases, the SeismoStruct (2011) software has been utilized in this Thesis. The model is validated in comparison with experimental tests results. In addition, a comparison in economic and technical terms between a solution using MCS in the non-dissipative elements and HSS in these is carried out. Moreover, some guidance to design buildings using the dual-steel concept located in seismic zones have been proposed.

## 1.2 Objectives

This dissertation has the purpose of investigating the seismic behaviour of buildings using the dual-steel concept in Moment-resisting Frames, Concentrically Braced Frames and Dual-Concentrically Braced Frames focusing on the following topics:

- Validation of the proposed typologies for high/moderate seismicity zones, by advanced numerical simulations and consideration of different types of seismograms;
- Development of design criteria and performance based design methodology for dual-steel structures using HSS. Criteria for assessment of ultimate building and prediction of the collapse mechanism;

- Recommendation of relevant design parameters (behaviour factor –  $q$ , overstrength factor  $\Omega$ ) to be implemented in further versions of EN1998-1-1 (2004) in order to apply capacity design approach for dual steel framing typologies.

### 1.3 Scope of the Thesis

This Thesis is divided in the following chapters:

**Chapter 1** presents the introduction to the problem and the necessity to study the seismic behaviour of structures using the dual-steel concept. In addition, the objectives and an overview of this research are also presented in this chapter.

**Chapter 2** presents an overview of the use of HSS showing the advantages and limitation due to poor number of application seen for seismic application in Europe. A description of the seismic behaviour of the three structural system based on the studied performer is also addressed in this chapter. Moreover, a brief state-of-the art of the methodology employed on current codes is provided, as well as the actual stage of the Performance Based Design approach.

**Chapter 3** is based on the selection, definition and seismic design of the study cases. In this chapter, the parametrical study is defined in order to investigate and evaluate the seismic performance of the dual-steel structures. In addition, information regarding the assumption assumed in the seismic design stage is provided.

**Chapter 4** is devoted to numerical model and methodology used in order to carry out the nonlinear static and dynamic analyses. In detail, the assumption adopted and implemented is shown. The results are presented in a comparison with the experimental tests in order to validate the model.

**Chapter 5, Chapter 6** and **Chapter 7** present the nonlinear analyses results for the MRFs, CBF and D-CBFs, respectively. In addition, in Chapter 7 a comparison between the use of simple and dual typologies revealing the possible advantages and limitation of the use in seismic-prone areas.

**Chapter 8** is addressed to both, technical and economic evaluation comparing a solution with MCS with another in HSS. The technical evaluation is based on the dynamic performance of the three structural system, in which each typology is designed by S355,

S460 and S690. The economic assessment is considered analysing the total cost of each study case using the three steel grades, taking into account the design, drawings, material, and production costs among others.

**Chapter 9** presents the general conclusions of this research, and also the prospects of future studies. Furthermore, this chapter provides design recommendation for MRF, CBF and D-CBF using the dual-steel concept. The assumption are based on the nonlinear outcomes from the previous chapters and have been introduced in the reports from the HSS-SERF project.

## *Chapter II*

# Seismic Design Methodologies

### 2.1 Introduction

In this chapter, a brief account of the reviewing and discussing concerning the current seismic design codes for steel building located in seismic zones is presented. The current methods that have been employed to design buildings are herein described and discussed showing their advantages and limitation. In detail, the methodology used to design buildings located on seismic zones on the actual codes are based on capacity design criteria using the Force-based Design. However, the structures designed and built considering the requirements incorporated in these codes suffered severe damage under last seismic event even though the global collapse has been prevented.

Therefore, the current codes based on Force-based Design are in a changing process of its philosophy. A new viewpoint has been studied in order to reduce the costs associated to damage caused by earthquakes as well as possible interruption of the activities. The structures should fulfil specify criteria being based on deformation-based criteria and this methodology to design is denominated as Performance Based Design (PBD). This section also states the principles and concepts adopted by PBD.

A description of the main structural typologies used on seismic zones is also presented. Traditionally, two types of structural systems have been used in multi-storey buildings in seismic zones: Moment-resisting Frames and Braced Frames. The braced frames are divided into two structural system: Centrally Braced Frames and Eccentrically Braced Frames. A given structure can suffer severe damage if the choice due to the lack of knowledge of structural system is not adequate.



Therefore, it is performed an approach about characteristics of each system addressing their qualities and deficiencies depending of the seismic application

As the study object of this Thesis is also devoted to the use of the High-Strength Steel (HSS) in non-dissipative elements. A general view of the types of HSS preconized in the European standard are shown. Furthermore, a general review of the production methods is exposed to understand the mechanical and chemical proprieties of the HSSs.

## **2.2 Steel buildings in seismic areas**

To withstand a given earthquake the buildings designer must have in mind the factors that can influence the selection of an adequate structural solution and must obey technical, financial and architectural issues. The structure, its elements and connections must be strong enough to withstand moderate earthquakes and must be sufficiently robust to avoid precocity collapse under strong earthquakes, which endangers the people life. Furthermore, it is necessary to achieve minimum overall cost limiting the damages caused by the earthquake. A given structure can suffer severe damage if the choice due to the lack of knowledge of structural system is not adequate. Although there is no global or local structural collapse, the building may have their functions interrupted due to excessive damage leading to the need for retrofiting.

These considerations are needed to find a balance between the technical, architectural and financial questions that it will influence the decision of designer. Traditionally, two types of structural systems have been used in multi-storey buildings in seismic zones: Moment-resisting Frames and Braced Frames. The braced frames are divided into two structural system: Concentrically Braced Frames and Eccentrically Braced Frames. In next sections, a brief description of these three structural systems is presented.

### *2.2.1 Moment-resisting Frame*

Among the structural systems used in seismic zones, the Moment-resisting Frames (MRFs) stand out for their high level of ductility reflected in the high behaviour factor used in design according to EN1998-1-1 (2004). MRFs are often preferred instead of braced frames because of architectonic reasons.

The seismic design is based on “weak-beam/strong-column” philosophy where the plastic hinges are located in the beam end. Consequently, the column must be designed to remain elastic. This approach allows an overall ductile behaviour because it is ensured that a premature collapse due to storey mechanism is avoided (see Figure 2.1). As can be observed, the exception for this requirement is on the base of columns where plastic hinges may be formed to allow the desired collapse mechanism (Figure 2.1a).

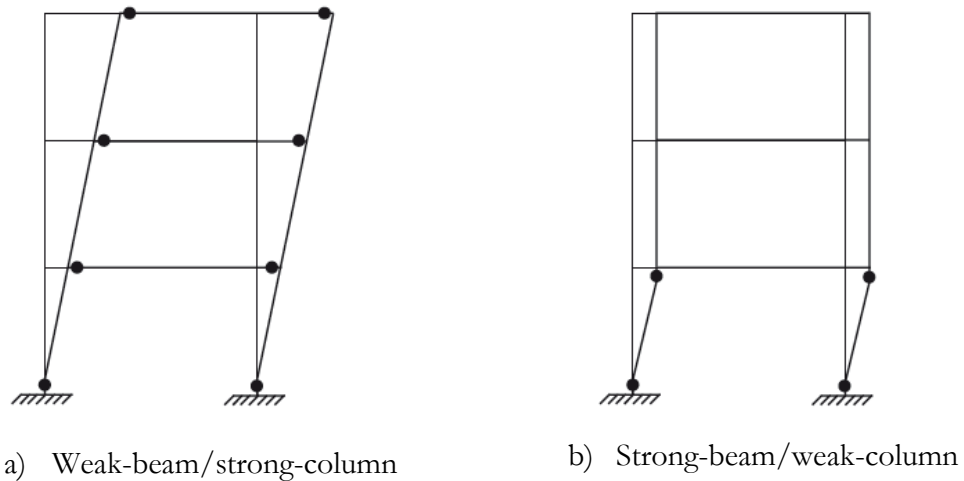


Figure 2.1 – Possible plastic mechanisms in Moment-resisting Frames (Elghazouli, 2009a)

Therefore, taking advantage of a design based on a dissipative behaviour, the beams are the dissipative elements being responsible for the energy dissipation. On the other hand, the columns are the non-dissipative members and they should be designed to resist to seismic action and probable overstrength from dissipative elements.

With the desirable collapse mechanism defined, the key role on the seismic verifications is related to definition of the forces to be applied and resisted by structure. The columns need to have adequate overstrength in order to maintain the structural integrity. It is extremely important to know the possible variations of the yield strength of the material to be used in dissipative elements in order that the maximum forces from these elements are not underestimated. The EN1998-1-1 (2004), therefore, during the design process establish factors to be applied to increase the bending moments, shear forces and axial forces for the non-dissipative members (columns) in order to take into account both the hardening effect and the real yield strength of material.

In the past MRFs have been designed considering that, the connections are rigid full-strength corresponding to fully welded or hybrid welded/bolted typologies. The capacity design assumptions were applied in order to have connections with high degree of overstrength to keep the plastic hinges in the beams. However, after the Northridge in 1994 and Cobe 1995 earthquakes, severe damages in beam-to-column connections in steel MRFs have been reported showing a poor performance of these types of connections (see Figure 2.2).

In order to improve the connection performance a consortium of professional associations and researchers, known as the SAC Join Venture together with agencies in US was created. They showed that the fractures have been related to basic connection geometry, lack of

control of base material properties, use of weld filler metals with low toughness, uncontrolled deposition rates, inadequate quality control and other factors.



Figure 2.2 – Fracture at the welded beam-to-column connection (Adan and Hamburger, 2010)

In EN1998-1-3 (2005) and FEMA-350 (2000), new alternatives were given involving the design and construction of the connection located in seismic zones (see Figure 2.3). The performance improvement is based on the strengthening of the connection using haunches and cover or side plates or on weakening of the beam by reduction of the cross-sections reduced beam section (RBS or “dog-bone” connections), perforation of the flanges, or by enlarged access holes, among others.

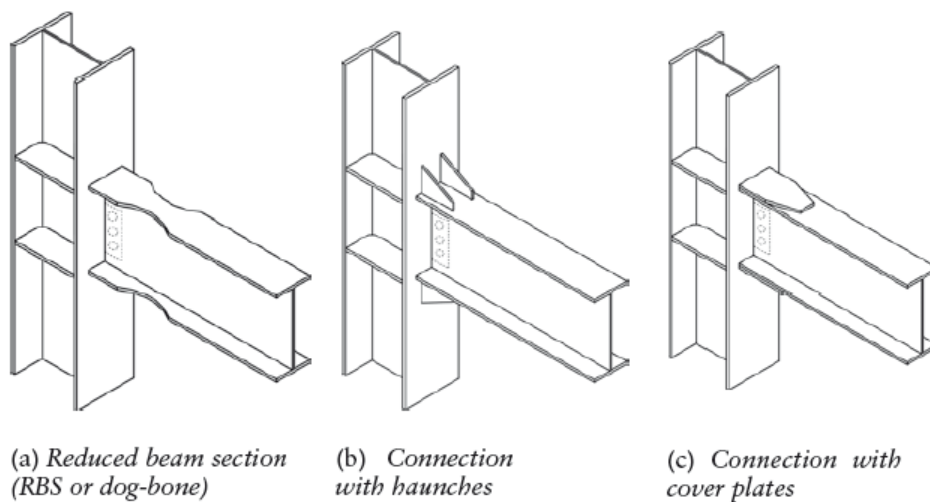


Figure 2.3 – Examples of connections for frames located in seismic zones (Elghazouli, 2009a)

The actual version of European code allows that the energy dissipation be carried out in the connections being provided with adequate behaviour is assured. The connections should be able to have a rotation capacity consistent with the global deformations; members framing into the connections are demonstrated to be stable at the ultimate limit state and taking into

account the effects of connection deformation on global drift using the both static and dynamic non-linear analysis. When partial strength connection are used as dissipative elements, the columns capacity design need to be verified on basis of the plastic resistance of connection excluding the verification concerning to the beams.

The column panel zone is also a component with decisive influence on the behaviour of MRFs. It is recognized that in the last seismic events, the severe damage presented by beam-to-column connections is also associated to excessive deformation in the panel zone regions leading to design rules in the USA. In Dávila-Arbona et al. (2008), a numerical study was carried out to investigate the influence of the parameters on the inelastic response of the panel zone. In detail, it was observed that a weak panel zone could result in very high distortional demands causing an unreliable behaviour, especially in welds.

In Europe, the current code determines that the panel zone should evidence adequate capacity in order to limit its contribution to the energy dissipation under seismic event. The web panel plastic shear resistance should be higher than the design shear and the buckling phenomena should be avoided.

Due to their low lateral stiffness compared to Braced Frames, the seismic design of the MRFs is often governed by deformation criteria. The EN1998-1-1 (2004) determines that the MRFs (although all the other cases should fulfil these criteria) should have adequate lateral stiffness limiting the inter-storey drift and influence of second-order effects. The inter-storey drift is related to damage limitation while the second-order effects are associated to ultimate limit state.

The application of the rules in the EN1998-1-1 (2004) for the deformation criteria is quite stringent in comparison with USA practice. The buildings designed in accordance with the European code present often high lateral capacity showing notable differences between the effective overall lateral capacity, obtained for instance by nonlinear analyses, to the one initially assumed in the seismic design (Elghazouli, 2005). High behaviour factors result in high level of overstrength depending also on the spectral acceleration and gravity design. Therefore, a rational procedure could be used utilizing low behaviour factor permitting relaxation of the local ductility requirements and reducing uncertainties related to capacity design (Elghazouli, 2009b; Castro et al., 2009).

### 2.2.2 *Concentrically Braced Frame*

Concentrically braced Frames (CBFs) are a stiffer lateral force-resisting system in comparison with the MRFs. They are generally an economical system to be used for low-rise building in areas with high seismicity in comparison with the MRFs where the design

often governed by lateral deformation. For mid-rise or high-rise buildings, the CBFs are often used as a core of the structure where MRFs compose the perimeter. On the other hand, their use in the building perimeter is efficient in order to control possible torsional effects. Figure 2.4 show two examples of the use of CBFs.

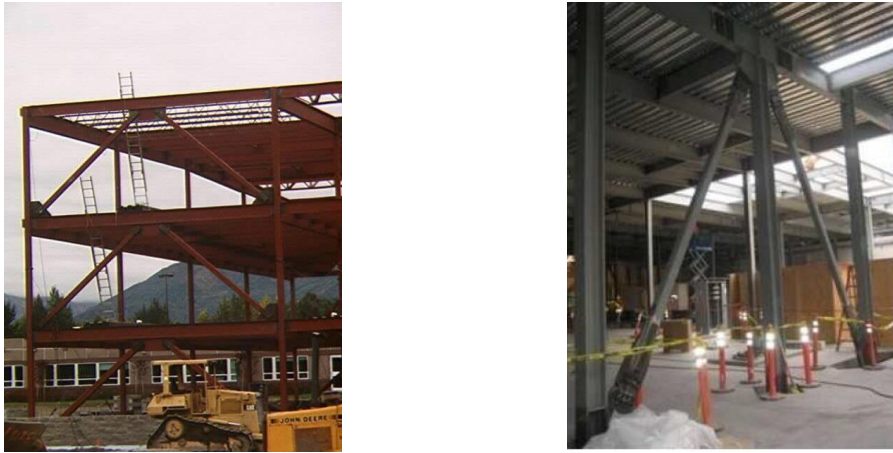


Figure 2.4 – Examples of Concentrically Braced Frames

The truss action is provided by this structural typology with their members subjected to axial force. Most of the inelastic drift is expected to be related to the axial deformation of the braces. Members in elastic bending will also contribute to lateral deformation of the frame.

Initially, the seismic design in codes was based on elastic truss systems where the inelastic effects were simulated by a reduction of the calculated brace strengths. Research showed that this structural system could exhibit a ductile behaviour when an adequate proportion between the members and a careful detailing of connections was carried out.

For moderate earthquakes, the CBFs are adequate to assure serviceable structural performance due to their lateral strength and stiffness. However, in extreme earthquakes the inelastic deformation is dominated by tensile yielding of the brace, brace buckling and post-buckling deformation of the braces reducing considerably CBFs' efficiency. The design procedures follow the philosophy of the capacity design as for the other frame typologies. This means that the seismic performance is achieved considering the use of diagonal bracing members as dissipative elements acting as fuses for the system under seismic event. The other members are provided with adequate overstrength in order to ensure that the yielding occurs in bracing members before yielding or buckling of columns or beams. However, there are notable differences in the design procedures (Elghazouli, 2003) among the codes to design the CBFs. Figure 2.5 shows a typical one cycle axial force-displacement response of the braces under axial loading starting from compression. The first point (point A) corresponds to the buckling load of the braces loaded in compression. The lateral deflection induces an eccentricity of the load, and consequently, bending moment that leads to the

formation of a plastic hinge due to yielding of the cross-section represented by the evolution between points B and C where the axial deformation is increasing as well as the plastic hinge rotation but the axial force is reduced. By load reversal along the CD and DE paths, the plastic hinge disappears with the recovery of the elastic stiffness. In region EF, the brace is stretched near to original straightness although residual deformation and residual stresses will remain in the brace. With another load reversal, imposing axial compression the buckling load will be lower than the initial one due to the residual deflections, the increase in the length as well as the Bauschinger effect. There is an increase of the tensile yielding related to accumulate permanent elongation for the subsequent cycles. In spite of the buckling phenomena that lowers the capability of the braces to dissipate the seismic energy they can still be effective if local buckling and collapse on the connections is controlled.

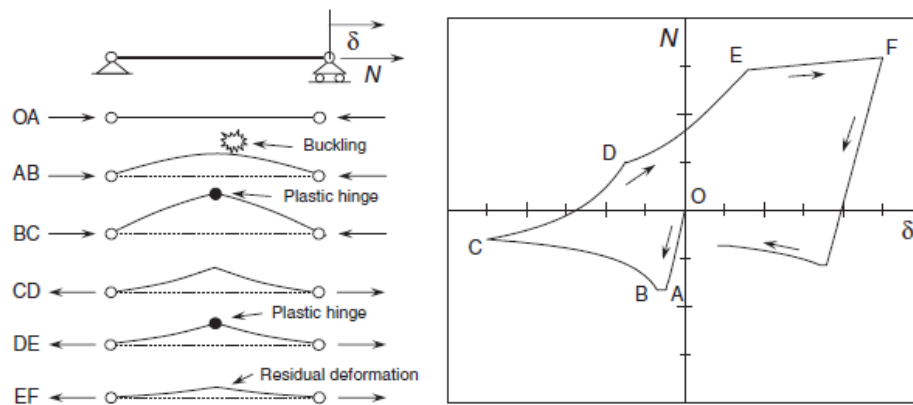


Figure 2.5 – Typical response of a brace under cyclic axial loading (Marino and Nakashima, 2006)

The behaviour of CBFs during earthquakes e.g. Loma Pietra in 1989, Northridge in 1994 and Cobe in 1995, has shown the validity of this analysis. In Figure 2.6a,b the buckling of the braces were noted in many cases as well as fracture at the mid-length plastic hinge is evidenced. Moreover, fracture in the column base plate due to applied loads and deformation can also be observed (Figure 2.6c) as well as the collapse of the gusset connection at the net section (Figure 2.6d).



a) Buckled brace



b) HSS brace fracture at mid-length



c) Base plate fracture



d) HSS brace fracture at net section

Figure 2.6 – Earthquake damages in Concentrically Braced Frames (Sabelli et al., 2013)

After these evidences of damage in the braces, CBFs and more specifically the braces have been the subject of extensive research in order to predict their inelastic behaviour (Tremblay, 2002; Broderick et al., 2008; Lumpkin et al., 2012; Goggins et al., 2005). Experimental tests showed that the slenderness ratio of the brace is the most important factor influencing its hysteretic behaviour.

In general, the available results obtained show that braces with smaller slenderness ratio evidence an improved hysteretic behaviour. The seismic energy dissipated by braces with smaller slenderness is significantly larger than the slender braces. Depending on the typology employed, tensile yielding along the length of the brace or brace buckling in compression is possible. The plastic hinges due to buckling effect can be located at the mid-length and at bar end. In gusset plate, the inelastic deformation is observed in the brace ends although the plastic hinge can occur in the brace adjacent to the connection if the gusset plate is designed with adequate strength and stiffness or the gusset plate has not adequate rotation capacity or the brace is rigidly connected to the adjacent members.

The most of the tensile and plastic strain occurs within the plastic hinge region due to residual stress, imperfections and  $P-\delta$  effects. Consequently, failure can occur due to fracture of the cross-section caused by large strains from cyclic load reversal with the connection



having adequate design and detailing. Figure 2.7 shows the sequence of inelastic deformation under cyclic loading for a HSS cross-section. Initially, there is a localized strain and deformation in the plastic hinge (Figure 2.7a). As results of subsequent cycles, the tearing initiates in the corners of the flange (Figure 2.7b) and, in consequence, fracture of the cross-section is observed (Figure 2.7d).

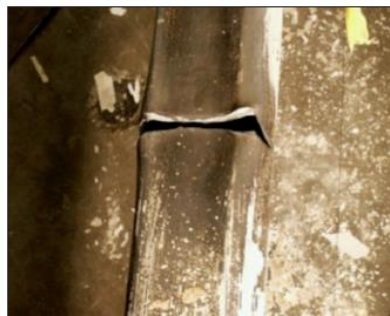
The relation width-to-thickness of the cross-section plays an important role concerning the initiation of local buckling and fracture. Therefore, the current codes recommend maximum values to width-to-thickness ratios of the cross-sections depending of the typology used in order to improve the seismic behaviour preventing or delaying possible local buckling. Moreover, the codes also impose upper limits of the member slenderness to limit the sudden dynamic loading effects and post-buckling deformations.



a) Local strain



b) Initiation of tearing



c) Progression of tearing



d) Collapse

Figure 2.7 – Local failure of HSS brace (Sabelli et al., 2013)

The configuration of the braces also affects the seismic behaviour of the CBF system. The codes allow several different configurations of the bracing that can be used in seismic design (see Figure 2.8). The braces can buckle in compression or yield in tension can occur. It is important to have an adequate lateral resistance in tension and compression in both directions. The diagonal bracing shown in Figure 2.8a can be designed considering only the tension members in the energy dissipation. In order to avoid significant asymmetry in seismic response, the EN1998-1-1 (2004) determines that the difference between opposite areas of cross-section for the braces should be similar.



The systems with X-bracing dissipate the seismic energy by yielding of both tension and compression braces. They are most commonly used with light bracing on low-rise structures. In a recent study (Palmer, 2012), it was noted that the buckling load of the braces can be estimated considering just one half of the length when they are tied together in mid-section. In contrast, the inelastic deformation capacity is reduced because the damage is concentrated in one-half brace length and the remaining half of the brace cannot fully develop its capacity. In the V-bracing, the braces intercept the beam in mid-span. The performance is given by both tension and compression braces. However, the buckling effect provides an unbalanced of forces in beam due to difference between the smaller buckling resistance in comparison with the tensile yield resistance. The EN1998-1-1 (2004) establishes that the seismic design should take into account this unbalanced forces considering that the post-buckling of the brace in compression is equal to 30% of the its tensile yielding resistance. Recent research has shown that the beam deformation associated to unbalanced forces increase the axial deformation of the braces (Tenchini et al., 2013).

In the K-bracing configuration not shown in Figure 2.8 the diagonals intercept the columns in an intermediate point where it is not possible to see a ductile behaviour due to the potential demand for the columns. The unbalanced forces impose bending moments and inelastic deformation in the column a possible failure may occurs. Consequently, the use of the K-bracing in seismic resistant CBFs is not allowed EN1998-1-1 (2004).

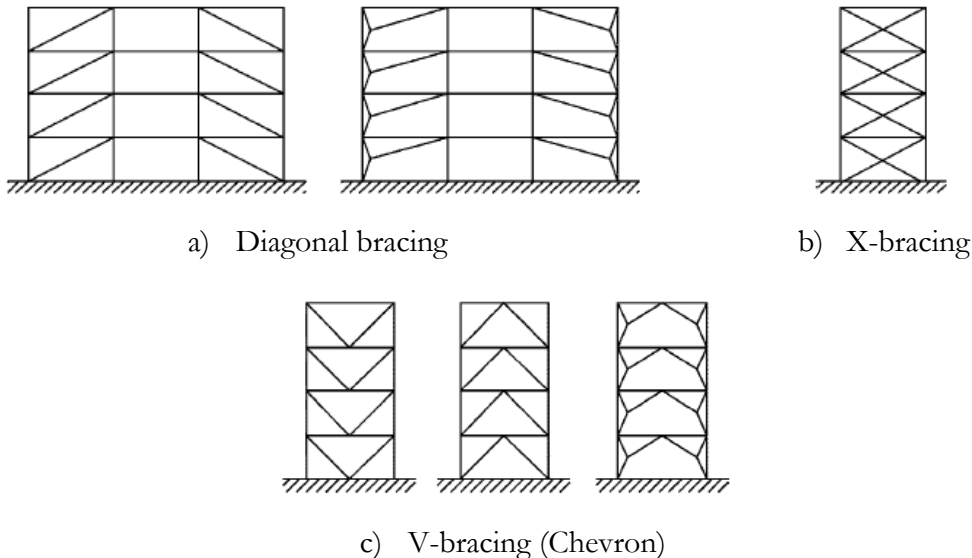


Figure 2.8 – Various Concentrically Braced system configurations

### 2.2.3 Eccentrically Braced Frame

Eccentrically braced Frames (EBFs) can be considered as a hybrid lateral force-resisting system where there is the superposition of the Moment-resisting Frames with the Concentrically braced Frames. This structural system can combine the main advantages and somehow limit the weaknesses of the conventional systems. The bracing members, which give high lateral stiffness to system, intersect the girder at an eccentricity “ $e$ ” transmitting forces by shear and bending (see Figure 2.9). This length “ $e$ ” of the ‘link’ is the dissipative element and therefore responsible for the energy dissipation under ground motion. The specific design requirement is that the yielding occurs in the link before any yielding or collapse of any other members.

Depending on the location of this link, the EBFs may usually exhibit four different arrangements (see Figure 2.9) which are split-K-braced, D-braced, V-braced and inverted-Y-braced frames.

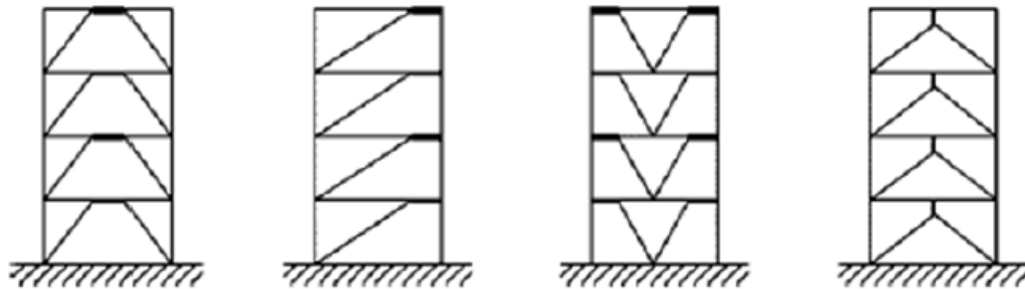


Figure 2.9 – Eccentrically Braced Frames configurations

EBFs are characterized by high elastic stiffness similar to CBFs permitting inter-storey drift requirements to be fulfilled, stable inelastic response under ground motion similar to MRFs allowing for high energy dissipation capacity and ductility. In contrast, EBFs have more practical detailing problems in comparison with the CBFs. Figure 2.10 show an example of building using the EBF system.



Figure 2.10 – A example of the use of EBF in Istanbul Bilgi University (Turkey)  
(D'Aniello, 2007)

The performance of the EBFs is deeply influenced by the link and the inelastic action is located in these elements acting as dissipative element preserving the integrity of the structural system. The links are characterized by providing stable and well-rounded hysteresis loops indicating a high-energy dissipation capacity (see Figure 2.11). Furthermore, the existence of links allows EBFs to allow higher degree of architectural freedom through the flexibility for placement of openings compared to CBFs.

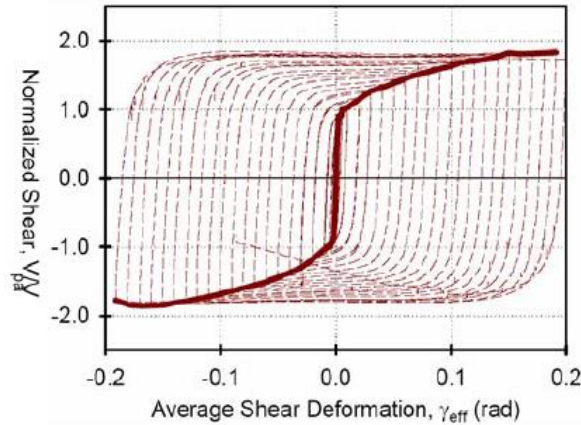


Figure 2.11 – Hysteretic response of a link (D'Aniello, 2007)

The inelastic performance of EBFs depends on the link length. For a given cross-section, the link length influences directly the lateral stiffness. Figure 2.12a illustrates this influence comparing the relation link to span lengths with the lateral stiffness of the frame for different storey height to span length relations. It is possible to see that the short link provides higher lateral stiffness and when the relation  $e/L$  tends to unity, the stiffness of the MRF is obtained. Moreover, the ductility demand on the link is also related to the link length. Figure 2.12b shows the relation between the link length and the ductility demand of the system, that is, for the same level of frame drift the ductility demand increases for shorter links.

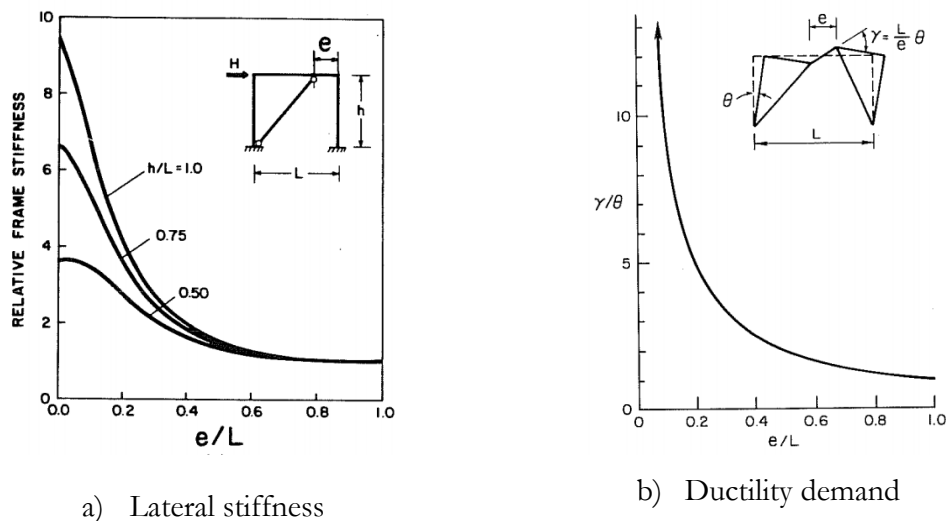


Figure 2.12 – Influence of the link length ( $e/L$ ) (Popov and Engelhardt, 1988)

The approach followed by EN1998-1-1 (2004) to design of the EBFs depends on the classification of the link based its length. The links are able to dissipate the generated energy by seismic event by formation of plastic bending or plastic shear mechanisms. The links can be classified as: short, long or intermediate. Short links are mainly dominated by a shear mechanism while performance of the long links is given by flexure controls. The intermediate links are characterized by interaction between bending and shear. In particular, the experimental tests carried out in 1980s (Hjelmstadt and Popov, 1983; Kasai and Popov, 1986; Engelhardt and Popov, 1989) have showed that shear link behaviour in steel performs better that of flexural plastic hinges.

In general, the EBFs show excellent strength and stiffness in the elastic range and still are capable to ensure sufficient ductile behaviour in order to dissipate the seismic energy avoiding severe non-structural damage.

### **2.3 The use of High Strength Steel in building frames**

The advances on steel production technologies have allowed the improvement of its physical and chemical properties, and hence, new type of steels with attractive characteristics can be produced. In addition to the traditional hot rolling processes, nowadays, another ones such as, controlled rolling, normalizing, and quenching and tempering, various combination of rolling practices and cooling rates have allowed to produce steel with excellent proprieties (Miki et al., 2002).

The steel grade S355 was considered as High Strength Steel (HSS) until 1950, however, at present, this is the predominant class for hot rolled sections in many countries, being an example of technological advances and market needs. Today, the steels are considered to be HSS when the yield strength is greater or equal to 460MPa being possible to find in the market steel for construction with yield strength up to 1100MPa. However, there is no specific rules in seismic Eurocodes for application of these steel grades.

The Figure 2.13 can exemplify this evolution of steel grades and their production process over the last seventy years in Europe. Current steel grade with high yield strength is produced through processes based in quenching and tempering, for instance, S690Q, S890Q, S960Q and S110Q; in addition to these, the thermomechanically rolled steels are provided of moderate yield strength, such as: S355M, S460M and S500M. Nowadays the HSS is produced in Europe (by manufacturers – Arcelor-Mittal, Corus or Ruukki), USA, Japan, Canada and Australia.

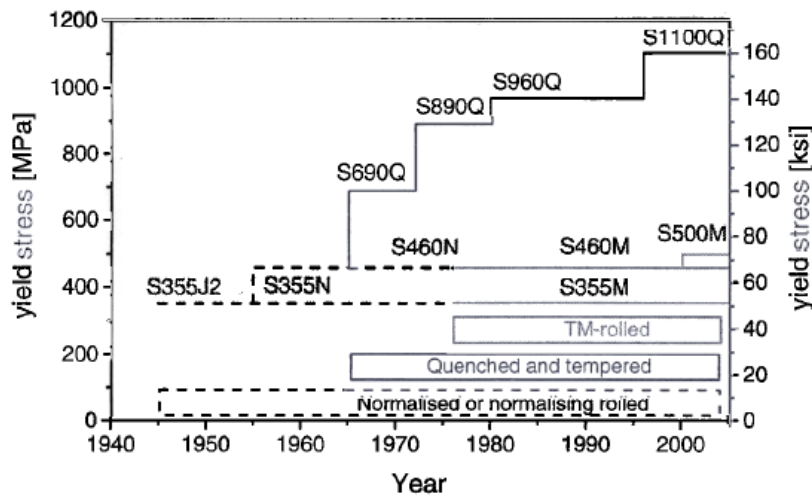


Figure 2.13 – Historic evolution of yield stress for hot rolled steel components (Samuelsson and Schroter, 2005)

After recent earthquakes, some questions raised about the behaviour of steel, especially concerning the determination of mechanical characteristics by uniaxial tensioned specimens. The several collapse modes allowed to have higher and better defined orthogonal strength characteristics appearing the through-thickness strength of the steel. The material properties used on design are calculated in the rolling direction, however, it has long been recognized that commercially available rolled plates and shapes can exhibit anisotropic material properties. In particular, the strength and ductility in the direction can be different in comparison with another direction.

Additionally to resistance other characteristics must be improved such as ductility, fracture toughness, weldability, cold formability, and corrosion. The steel with these characteristics are called of High Performance Steel (HPS) and they have been manufactured most frequently in the USA (Bjorhovde, 2004).

Among their characteristic, the HSSs exhibit some technological advantages for building structures, such as (Galambos et al., 1997; Samuelsson and Schroter, 2005):

- **Economy:** The overall weight of the structure is reduced, so this economy may result in a reduction of cost of transport and assembly; increasing the steel strength, the cross-section size of the elements may be reduced (see Figure 2.14). Hence, this can reduce the structural weight and consequently, the volume of weld metal, and therefore, the manufacturing and assembly costs ;

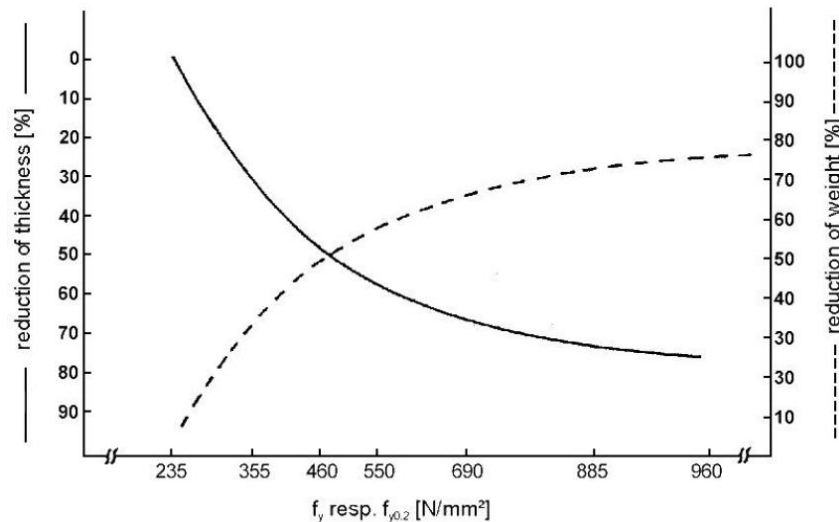


Figure 2.14 – Reduction of plate thickness and weight *versus* the strength steel increasing (Samuelsson and Schroter, 2005)

- Performance: The dynamic forces that are dependent on the mass are reduced; also the structures have a great tensile strength to withstand the dynamic forces due to seismic action; The trend in many applications for metal structures have been thin plates members in the prefabricated industry and cold-formed due to economic reasons. The introduction of HSS for wider use in civil engineering application will extend this trend to a broader spectrum of structural applications;
- Architecture: as the size of the structural elements can be reduced, there is a possibility to have special and elegant structural aesthetics, in which can be inserted into the ambient;
- Environment: the volume of steel produced tends to decrease, therefore, there will also be reducing the consumption of world's resources. Indeed, the steel is considered a material with high recycling potential; however, the consumption of energy in order to recycle is still large and can be reduced by reducing the amount of material.
- Security: the special classes of HSS not only show high values for the resistance, but also combines the strength with excellent toughness properties, for high security, both in manufacture and in their application.

However, it is possible to see that the HSS also have some disadvantages and precautions are necessary (Galambos et al., 1997; Anami and Miki, 2001):

- There is no increase of Young's modulus of steel with the increase of the yield strength, this problem becomes important when deformability criteria is applied; the

serviceability or damage limitation limit states use deflection, inter-storey drifts and vibrations depending directly on the Young's modulus;

- Attention should be given to fatigue phenomenon where the increasing of fatigue performance is not proportional to increase of steel strength of structural welded members. The problem is related to balance between the tensile strength and fatigue performance where it is necessary to find an adequate relation in order to have good weldability;
- Structural members with HSS will not be ductile enough for the cases where it is necessary to have large inelastic deformation such as in seismic applications;
- There is still a limited number of applications and hence, it is still difficult to show statistical evidence of reliability in the structural design. Further testing and research should be carried out to establish new rules for codes with detailed information about the design of structures using HSS.

Besides these, the weldability of HSS can be a problem, especially at low temperatures and in members subjected to cyclic loading. From the point of view of its chemical composition, it is important to limit the Carbon Equivalent (CE) in order to avoid brittle fracture.

For instance, the early steels produced in USA have had carbon content (CE) much higher than current structural steel; moreover, the sulphur and phosphorus tended to be high in comparison with current measures explaining the difficult to weld with any of the traditional methods when older structures are rehabilitated (Bjorhovde, 2004).

Therefore, particular attention should be given to the technology of welding, in which, the welding procedure may be qualified experimentally; being this operation more complex than in the case of Mild Carbon Steel (MCS) (Dubina et al., 2006).

### 2.3.1 *Production methods*

There are different methods for the steel production taking into account the requirement regarding to its use:

- Rolled (R)
- Normalised (N)
- Quenched and Tempered (Q+T)
- Thermomechanical rolling (TM or TMCP)

The rolled condition (R) is achieved when there is a heating of plate at temperatures of about 1100 °C taking place in the austenitic state, and then, the plate cools on calm air.

After this point, it can be performed an additional heating in order to improve homogeneity of the microstructure. The plate is reheated above the temperature for ferrite-austenite transformation with values around 800 – 900 °C depending on the carbon content, and after, is cooled on air again. This process leads to normalised condition (N) with microstructure of ferrite and pearlite producing steel where moderate strength up to S460N may be reached.

The quenching and tempering process (Q+T) is similar to normalised process regarding the heating and cooling sequence. However, the cooling process is faster and carried out using water or another cooling medium that increase cooling speed. In this case, there is no time for formation of ferrite and pearlite resulting in the microstructure that consists mainly martensite being characterized by high strength but with low toughness. Adding a tempering process, the material is relaxed to atomic scale resulting in decreasing strength while the toughness is increased. Steels with yield strength up to 1100MPa can be produced in quenched tempered condition.

Another way to obtain steel with high strength is to create fine grain microstructure. The smaller the grain, the greater the strength and toughness. The thermomechanical rolling (TM or TMCP) is a method that combines rolling steps at particular temperatures in order to obtain fine grained microstructure allowing the reduction of the carbon and alloying content in comparison to normalised steel. This process improves the weldability due to reduction of carbon being a great advantage.

The Figure 2.15 depicts the microstructures of steel produced with the different processes. In detail, it is possible to observe that the microstructure resulting from normalized process shows higher carbon content (black areas) and larger grain size when compared to TM(ACC). The quenched and tempered steel have different appearance due to martensite with acicular microstructure.

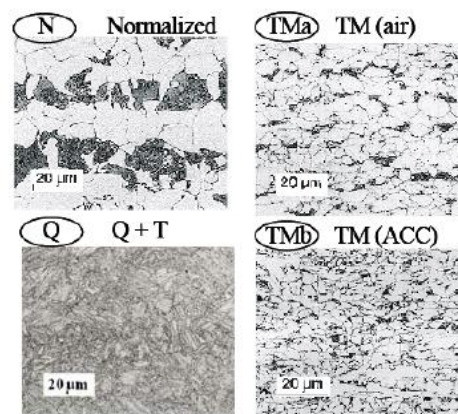


Figure 2.15 – Comparing the microstructures among the production methods (Willms, 2009)



### 2.3.2 Chemical and physical proprieties

The HSS found in market possess chemical composition and quality strictly related to production process, and to fabrication shop (cutting, drilling, welding, etc.) determining its final proprieties. Sometimes, improving a certain characteristic may worsen another. The material properties are oriented towards the specific utilization.

The international organizations, such as, American (ASTM), European (EN) and Japanese (JIS) that control the quality of HSS impose specific criteria to have an adequate quality, for instance the values addressed in Table 2.1. However, it is recognized that these values are conservative where actual tests showed values smaller than upper limits (Samuelsson and Schroter, 2005).

Table 2.1 – Chemical composition for a HSS with 50 mm thick  
(Samuelsson and Schroter, 2005)

	S355J2		S460ML		S460QL		S690QL	
	EN10025 Part 2	Typical analysis*	EN10025 Part 4	Typical Analysis	EN10025 Part 6	Typical analysis	EN10025 Part 6	Typical analysis
<b>C</b>	≤0.22	0.17	≤0.16	0.08	≤0.20	0.15	≤0.20	0.16
<b>Si</b>	≤0.55	0.45	≤0.60	0.45	≤0.80	0.45	≤0.80	0.30
<b>Mn</b>	≤1.60	1.50	≤1.70	1.65	≤1.70	1.50	≤1.70	1.30
<b>P</b>	≤0.025	0.018	≤0.025	0.011	≤0.020	0.012	≤0.020	0.012
<b>S</b>	≤0.025	0.015	≤0.020	0.002	≤0.010	0.005	≤0.010	0.005
<b>Nb</b>			≤0.05	<0.04	≤0.06	0.017	≤0.06	<0.04
<b>V</b>			≤0.12		≤0.12		≤0.12	
<b>Ti</b>			≤0.05		≤0.05		≤0.05	
<b>Mo</b>			≤0.20		≤0.70	0.115	≤0.70	0.37
<b>Ni</b>			≤0.80	0.19	≤2.00		≤2.00	0.15
<b>Cu</b>	≤0.55		≤0.55	0.17	≤0.50		≤0.50	0.08
<b>Cr</b>			≤0.30		≤1.50		≤1.50	0.40
<b>B</b>					≤0.005		≤0.005	<0.003
<b>CE</b>	0.47	0.42	0.47	0.39	0.47	0.39	0.65	0.54
<b>Pcm</b>		0.26		0.19		0.19		0.29
<b>CET</b>		0.32		0.26		0.26		0.35
*Wide variation of the composition is possible due to a variety of possible production routes. Carbon equivalents: $CE = C + Mn/6 + (Cr + Mo + V)/5 + (Ni + Cu)/15$ $Pcm = C + Si/30 + (Mn + Cu + Cr)/20 + Ni/60 + Mo/15 + V/10 + 5B$ $CFT = C + (Mn + Mo)/10 + (Cr + Cu)/20 + Ni/40$								

In general, the HSS for the construction industry with adequate ductility and weldability has a yield strength in the range of 460-690MPa, with elongation in the rupture in the order of 15-20%. These thermo-mechanical steels are generally low-alloy with level of carbon

between 0.06-0.1 percent, not exceeding 0.2%, with  $CE \leq 0.48\%$ . Level of chromium is limited to 0.7%.

Magnesium, molybdenum, vanadium, niobium, copper and nickel are used as well as alloying elements in small quantities. Sulphur and phosphorus are limited in these steels to 0.01% and 0.015%.

The stress-strain curves from MCS and HSS are plotted in Figure 2.16. It is worth to observe that the curves have significant differences reflecting any pre-test treatment for heating and plastic deformation. The MCS curve is characterized by a defined yield level (plateau) while the yield strength of the HSS is determined by the 0.2 percent offset or 0.5 percent total deformations. This method is used for materials without a well-defined yield plateau.

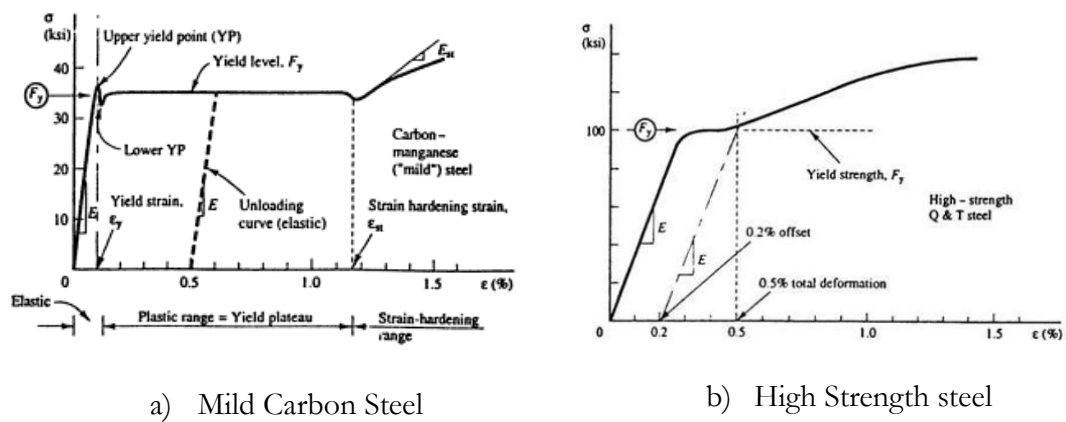


Figure 2.16 – Engineering stress-strain curves for MCS and HSS (Geschwindner et al., 1994)

The structural engineering can also expect better toughness properties for the HSS in comparison with the MCS even at low temperatures. The Figure 2.17 shows the Charpy-V test that is used to measure steel toughness where the temperature and energy absorbed are specified. It is worth mentioning that the S460ML and S690QL show better toughness properties (higher Charpy-V values) in the testing temperatures compared to S355J2. Moreover, in room temperature the behaviour of HSS (S460ML and S690QL) still higher than the MCS (S355J2). These results have also influence on welding properties where the high toughness values provide good steel weldability (Samuelsson and Schroter, 2005).

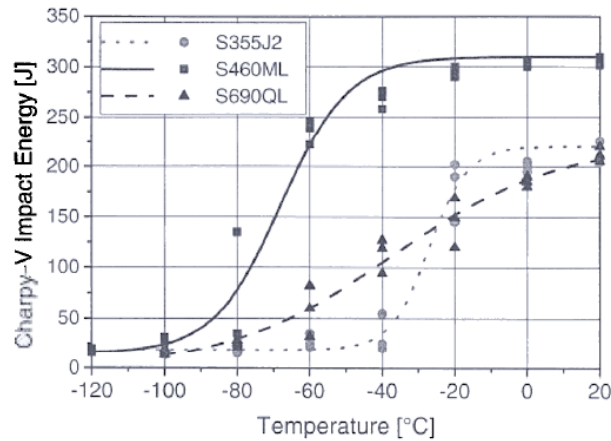


Figure 2.17 – Charpy V-temperature transition curves for S460ML and S690QL in comparison with S355J2 (Samuelsson and Schroter, 2005)

It is recognized that the ductility plays an important role in seismic behaviour of buildings. The requirements impose adequate ductility capacity in order to avoid brittle failure. Thus, the carbon content is an important characteristic. For all structural steels, the carbon content should be between 0.15-0.30 percent. In HSS, it is possible to have high strength with carbon content at very low levels around 0.15%.

Figure 2.18 shows the engineering stress-strain curve for MCS comparing with HSS illustrating the relation between increased steel strength and lower ductility.

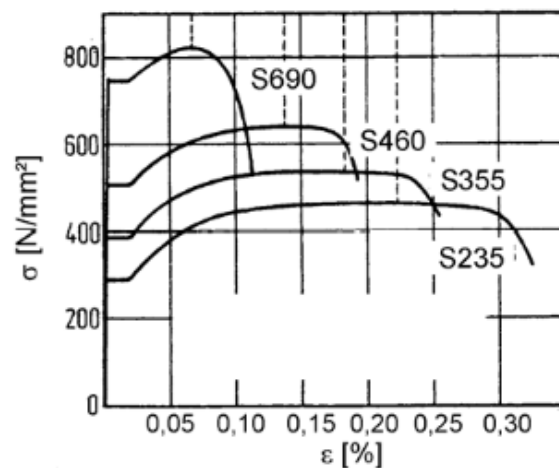


Figure 2.18 – Ductility comparison (Sedlacek et al., 2005)

### 2.3.3 European standard

The limited number HSS applications in civil construction is also related to some lack of information regarding the behaviour and design rules in the codes. A working group within CEN/TC250/SC3 has recently developed a proposal for Part 1-12 of EN1993-1-12 (2007) to cover the design of steel structures using yield strengths between 460 MPa (S460) to 700 MPa (S700). A new European standard with additional rules for the delivery condition

of structural steel was also established in 2004 (part 6 of EN 10025:2004). EN10025-6 states the technical delivery conditions for flat products of HSS in the quenched and tempered condition in which are widely used in structural applications.

Part 1-12 of EN1993-1-12 (2007) gives some differences in comparison with the traditional rules presented in other parts of EN1993-1-1 (2005). The elastic analysis is preferred, although the plastic resistance can also be utilized. The requirements related to material ductility (clause 3.2.2 (1)) are stated as follows:

- Minimum ultimate to yield strength ratio is 1.10,  $\frac{f_u}{f_y} \geq 1.10$
- Elongation at failure not less than 10%

These values differ from the Part 1 of EN1993-1-1 (2005) where these values are given as 1.15 and 15% respectively.

Regarding the welded connections, the EN1993-1-12 (2007) allows the use of undermatched electrodes which makes the welds more ductile and less prone to crack (Collins and Johansson, 2006). Interesting to note is that the undermatched electrodes are not allowed in EN1993-1-8 (2005). The design with undermatched welds should be based on electrode strength and for fillet welds.

For the bolted connection, the evaluation of design resistance of a net section in tension should be taken as:

$$N_{t,Rd} = \frac{0.9 \times A_{net} \times f_u}{\gamma_{M12}} \quad (2.1)$$

The partial factor,  $\gamma_{M12}$ , is the same employed on the EN1993-1 for the steel with yield strength from 460MPa to 700MPa. The national annex may determine this values but the EN1993-1-12 (2007) recommends that factor be equal to 1.

According to EN1993-1-12 (2007), the buckling curves for the HSS are the same as for 460MPa steel grade. However, the resistance to buckling of steel columns with HSS is expected to be higher than normal steels because the residual stresses induced by production is approximately independent of the yield stress of the material. Hence, the residual stresses caused by production affect less for the HSSs in comparison with the MCS (see Figure 2.19).

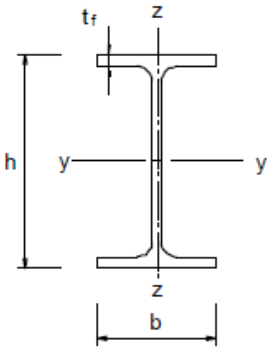
Cross-section	Limits	Buckling about axis	Buckling curve	
			S 235 S 275 S 355 S 420	S 460
	$h/b > 1,2$ $t_f \leq 40\text{mm}$	y - y z - z	a b	$a_0$ $a_0$
	$40\text{mm} < t_f \leq 100\text{mm}$	y - y z - z	b c	a a
	$h/b \leq 1,2$ $t_f \leq 100\text{mm}$	y - y z - z	b c	a a
	$t_f > 100\text{mm}$	y - y z - z	d d	c c

Figure 2.19 – Curves more favourable for the elements made up with HSS (Sedlacek et al., 2005)

#### 2.3.4 Cost of the use of High Strength Steel

Nowadays, the price of HSS is in high levels compared to MCS, especially in Europe. For instance, it is possible to see that the S690, in the Netherlands, is around 70-75 % more expensive than S355 per kg (Mercon Steel).

On the other hand, the cost of material represents only 25-30% of total costs of framed steel structures. The cost of fabrication and erection complete the overall costs. Therefore, an increasing of 20% of cost of material would increase in about 5% the cost of the final structure (AISC, 2010).

Figure 2.20 shows the relation between steel price and resistance. If the yield strength can be fully utilized, that is, the resistance is not limited by buckling, savings in material will be greater the higher the grade of steel which can be seen in the right graph. The relative prices are for heavy plates produced by three European producers of HSS taking as reference value the steel grade S235. The global cost of a structure depends more on costs for fabrication and erection than on the price of the material.

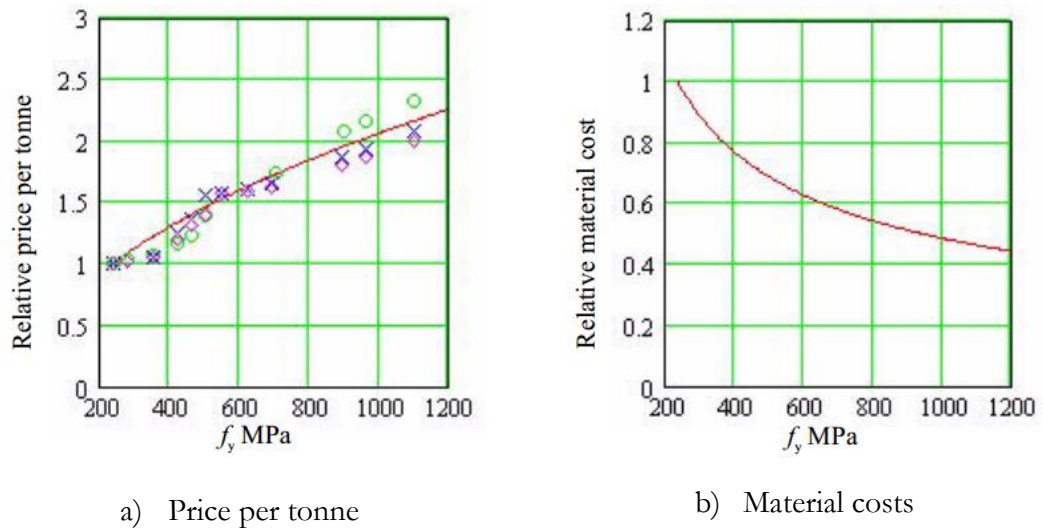


Figure 2.20 – Comparing the prices and material costs with the increasing of steel strength assuming the S235 as reference (Collins and Johansson, 2006)

When using HSS the costs to perform flame cutting, drilling or punching holes are usually the same as for regular steel grades. However, the welding volumes provided by thinner plates are less resulting in cost saving. Also, the preheating in order to avoid cold cracking is left out for plate with thicknesses below 30mm (Dubina, 2008). Figure 2.21 summarizes the costs saving considering S355 as reference

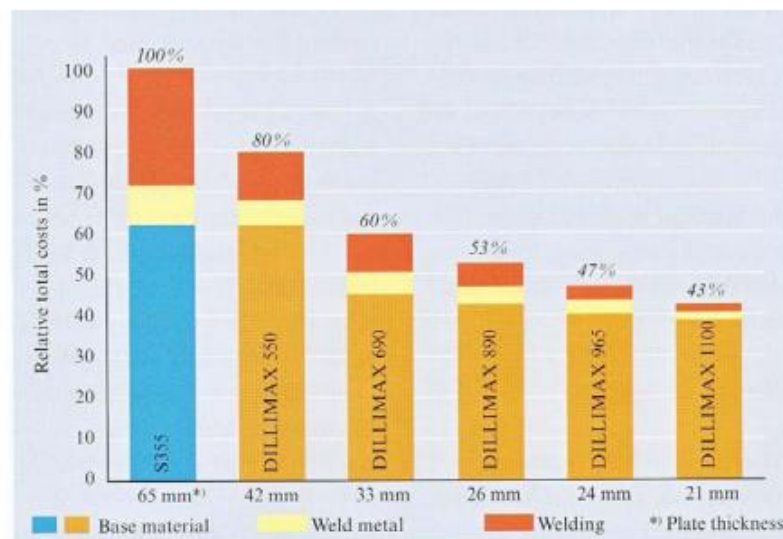


Figure 2.21 – Material and fabrication costs for welding (Dubina, 2008)

Nevertheless, the market demands are still quite limited and only a few fabricators are producing HSS. The trend however is that this scenario is changing and the increasing of market demand will result in decreasing of prices for HSS in the near future.

## 2.4 Force-based design

The force-based design (FBD) methodology has been used in most of the codes as the conventional method used to design structures located in seismic zones. To design the building considering the force (strength) as the key parameter is related to historical questions dating back to the years 1920's and 1930's, when some important earthquakes occurred (Kanto earthquake - Japan in 1925; Long Beach earthquake – USA in 1933, Napier earthquake – New Zealand in 1932). It was noted that the structures initially designed for lateral wind forces obtained good behaviour in comparison with those where this load type was not considered (Elnashai, 2002). Consequently, the structures were designed for earthquake applying horizontal loading corresponding to 10% of the building weight, without taking into account the building modal period. This was corrected some years later and the importance of the ductility was recognized after the finding that the structures could survive to earthquakes inducing inertia forces higher than the structural strength. The “equal displacement” for medium-period and long period structures and “equal energy” for short-period structures were developed as basis of design lateral force levels.

The “equal displacement” approach is an empirical rule for the evaluation of the nonlinear behaviour of buildings. Figure 2.22 shows the relationships between the elastic and inelastic behaviours. In detail, it is considered that the inelastic peak displacement ( $\mu_p$ ) is the same as the elastic peak displacement ( $\mu_{el}$ ) whatever the yield strength of the structure. Since the structural stiffness is not dependent of strength the equal displacement rule lead to strength reduction factor (R in USA) or behaviour factor independent (q in Europe) definition equal to the global ductility ( $\mu_\Delta = \mu_p/\mu_y$ ). This behaviour factor is a key parameter in the current codes in order to quantify the ductility capacity of the structural system and material selected in the seismic design. Furthermore, the seismic design process obeyed to hierarchical criteria based on required strength and ductility capacity. Thus, the “capacity design” concept was introduced where a pattern of inelastic behaviour is desired and specific zones are responsible for the energy dissipation. The current FBD design uses the behaviour factor to reduce the elastic design spectrum to obtain the seismic base shear.

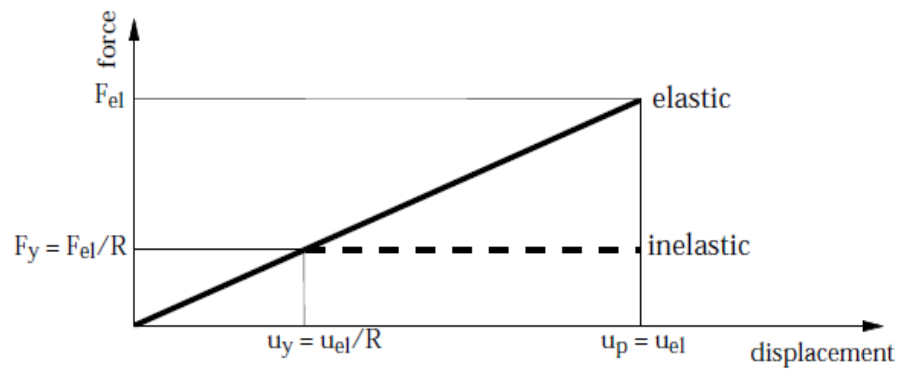


Figure 2.22 – Relationships for elastic and inelastic behaviours – equal displacement rule (Lestuzzi and Badoux, 2003)

#### 2.4.1 Capacity design

The capacity design approach was proposed initially in the 1960's proposed by Hollings (1968). It was recognized that the improvement of structural behaviour under a seismic event was mainly related to the ductile response and maximization of energy dissipation of the collapse mechanism. The main aim of 'capacity design' is to avoid brittle collapse of the structure under strong seismic event. Thus, specific zones of the structure are designed to dissipate the seismic energy by inelastic deformation (dissipative elements). Other zones of structures are responsible for robustness and need to have adequate overstrength to assure the desired collapse mechanism (non-dissipative elements).

The correct application of capacity design requirements is essential to assure the reliability of dissipative zones where the damages are concentrated. The verification of various damage modes is necessary. Moreover, the evaluation of stresses and deformations is very important in order to assure plastic deformation in dissipative members. The underestimation of plastic resistance in dissipative zones may reduce the safety of structure.

In EN1998-1-1 (2004), criteria for 'capacity design' are established including steel and composite structures. In order to assure yielding in dissipative zones the uncertainty of the yield stress and hardening of the material must be taken into account. The overstrength factor  $\gamma_{OV}$  is considered to take into account the ratio real to nominal yield strength. According to EN1998-1-1 (2004) the hardening of material is taken into account multiplying the seismic action for a factor equal to 1.1.

#### 2.4.2 Behaviour factor (*q*-factor)

The structures resisting ground motion are designed to behave inelastic. The aim is to have structures dissipate the seismic energy through plastic deformation located in strategic zones. The magnitude of the inelastic deformation must be compatible with the structural system and material. This degree of yielding must be in accordance with available local and global ductility and the energy dissipation capacity. The measure that gives the ability of the



structure of dissipate the seismic energy is the behaviour factor or q-factor which is an important parameter in the current codes based on force-based design. Its definition in EN1998-1-1 (2004) is “*an approximation of the ratio of the seismic forces that the structure would experience if its response was completely elastic with 5% viscous damping, to the seismic forces that may be used in the design, with a conventional elastic analysis model, still ensuring a satisfactory response of the structure*”. In the code the behaviour factor is a parameter that modify the elastic spectrum based on the energy dissipation capacity of the structure.

Lowering the behaviour factor result in higher seismic loading and may result in uneconomic design. On the other hand, increasing the behaviour factor result in higher ductility demands and larger displacements and may result in increasing damage.

There are several methodologies for computing the behaviour factors which can be grouped into four categories:

- Methods based on the ductility factor theory
- Methods based on an extrapolation of inelastic dynamic response analysis of single-degree-of-freedom systems
- Methods based on energy
- Methods based on the accumulation of damage

## 2.5 Performance-based design

After some intense earthquakes, e.g. the 1994 Northridge and 1989 Loma Prieta, it was acknowledge the excessive structural damage with high economic impact due to disable of the building functionality and need for rehabilitation. Reported damages reached costs of around \$20 billion for Northridge and \$8 billion For Loma Pietra earthquakes (Celikbas, 1999).

In consequence, the limitation of losses became an important issue in the design requirements. The design criteria of current codes impose on one side, the non-collapse in order to protect human life for a strong earthquake and on the other side the limitation of damage using deformation requirements in case of minor or moderate earthquakes. The development of this design philosophy aims at designing economically feasible structures where the damage should be controlled and the structures should fulfil multiple performance objectives. The structure under seismic action should be designed considering specific performance objectives, such as: an inter-storey drift, a displacement, a rotation or a level of stress, when the structure is subjected to different levels of seismic hazard (Ghobarah, 2001). This methodology for the seismic design is known as Performance-based design (PBD).



Figure 2.23 – Department Store Façade during Loma Pietra earthquake (EERC)

The structures can be designed considering various approaches of PBD. A traditional way to design the building is by force-based analysis where the structure is design based on force-based design, and then, the performance objectives may be checked against the values obtained in the analysis. An alternative way to design is based on target displacement or drift associated to specific performance (Priestley et al., 2007; Bachmann and Dazio, 1997).

According to SEOC-Vision-2000 (1995), the PBD is defined as a design methodology *“consisting of the selection of design criteria, appropriate structural systems, layout, proportioning, and detailing for a structure and its non-structural components and contents, and the assurance and control of construction quality and long-term maintenance, such that at specified levels of ground motion and with defined levels of reliability, the structure, will not be damaged beyond certain limiting states or usefulness limits”*.

The degree of damage that a structure could suffer is one of the difficulties in the development of performance-based design approach. Three important documents were released in the mid-1990's with the main purpose to establish performance specifications and associated levels of ground motion, thereby providing a performance design objective: SEOC-Vision-2000 (1995), FEMA-273 (1997) and ATC-40 (1996). These documents incorporated significant developments in seismic design, corresponding to first generation of performance-based frameworks, where the focus was turned from a procedure based on collapse prevention as the main or single objective to a process that took into account the type of use and the damage levels.

The SEOC-Vision-2000 (1995) publication was released one year after the Northridge earthquake and introduced two design levels, namely performance level and earthquake design level, where the first refers to maximum desired structural, non-structural and content

damage observed by a structure, and the second is associated to a specific earthquake design level defined by a certain recurrence period or probability of exceedance. Figure 2.24 illustrates the four recommended performance levels for each earthquake design level depending on building destination. The capacity design principles were adopted in then document in order to keep a desired inelastic performance and the type of analysis can be elastic or inelastic such as force and strength methods, displacement-based design, energy approach and prescriptive design approaches.

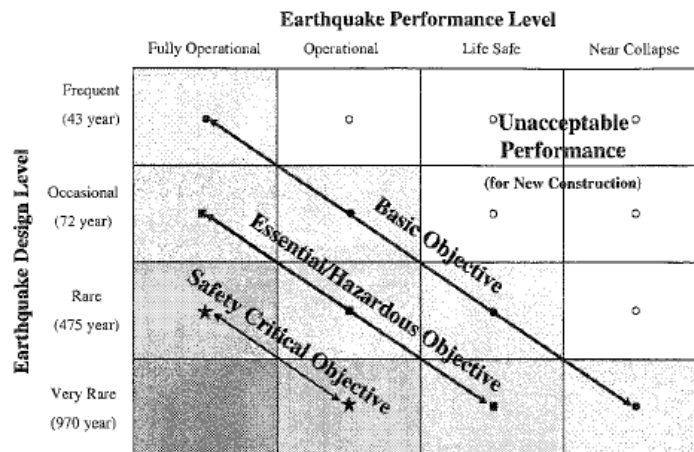


Figure 2.24 – Performance objectives for building defined in SEOC-Vision-2000 (1995)

The USA Federal Emergency Management Agency (FEMA) published, in 1996, a report with guidelines for the seismic rehabilitation of building: FEMA-273 (1997). This was later superseded by FEMA-356 (2000). Both documents present a variety of performance levels for non-structural elements and systems with associated probabilistic ground motions similar to those included in SEOC-Vision-2000 (1995). However, some conceptual differences exist in terms of acceptance criteria.

The ATC-40 (1996) is limited to concrete buildings and is very similar to FEMA-356 (2000), in terms of performance levels although some differences between structural and non-structural performance levels can be found. However, in terms of seismic hazard, the ATC-40 (1996) establishes only three earthquake design levels comparing with four ones in SEOC-Vision-2000 (1995) and FEMA-356 (2000).

In Europe, EN1998-1-3 (2005) has been developed with the aim of evaluating the seismic performance of existing structures by multiple performance objectives. The code is devoted to the evaluation and retrofitting of existing structures and refers to specific aspects concerning knowledge requirements, members and materials, analysis methods and strengthening techniques. Three performance levels (“Limit States”) are considered:

- Near Collapse (NC) – Seismic event with 2475 years return period. The structures are expected to be heavily damaged, with negligible residual lateral strength and stiffness, although vertical elements are still capable of sustaining vertical loads. Large permanent drifts are present. The structures are not able to resist to moderate after-shocks. This limit state is similar to U.S definition of “Collapse prevention”;
- Significant Damage (SD) – Seismic event with 475 years return period. . Corresponds to design condition where the structure shall have no local or global collapse although it may undergo strong damage; residual lateral strength and stiffness and vertical elements are capable of sustaining vertical loads, thus providing the strength to sustain moderate after-shocks;
- Damage Limitation (DL) –. Seismic event with 95 years return period defined in EN1998-1-3 (2005) by the use of a reduction factor  $\nu$  applied to the design earthquake. The structure shall have no occurrence of damage and the associated limitations of use. This limit state is. Members should be verified to remain elastic. This state corresponds to US definition of “Immediate Occupancy”.

Comparing to EN1998-1-1 (2004), the Part 3 of European code introduced an additional limit state (Near Collapse) in order to avoid brittle failure of structures which have not been designed with appropriate ductility provisions to guarantee that the structure will withstand to stronger earthquakes than the design earthquake.

It is recognized that the safety format common to find action and material properties is given by partial factors related to probability on the Eurocodes. In EN1998-1-3 (2005), the introduction of level of knowledge in order to take into account the ordinary material partial factors in which in this code are called “confidence factors” is an important innovative of assessment. The level of knowledge is defined by combination of the knowledge available regarding to geometry, details and materials. The Table 3.4 show the association of the knowledge levels to be considered by seismic assessment in EN1998-1-3 (2005). In detail, three levels of knowledge are defined, denoted by KL1, KL2 and KL3. For each level of knowledge is defined a confidence factor being 1.35, 1.20 and 1.0 for KL1, KL2 and KL3, respectively. It is important to know the level of knowledge defines the method of analysis to be employed. For instance, the KL1 permitting the use of linear methods (see Table 2.2).

Table 2.2 – Knowledge levels and corresponding methods of analysis (LF: Lateral Force procedure, MRS: Modal Response Spectrum analysis) and confidence factors (CF) (EN1998-1-3, 2005)

Knowledge Level	Geometry	Details	Materials	Analysis	CF
KL1	From original outline construction drawings with sample visual survey <i>or</i> from full survey	Simulated design in accordance with relevant practice <i>and</i> from <b>limited in-situ</b> inspection	Default values in accordance with standards of the time of construction <i>and</i> from <b>limited in-situ</b> testing	LF- MRS	CF <sub>KL1</sub>
KL2		From incomplete original detailed construction drawings with <b>limited in-situ</b> inspection <i>or</i> from <b>extended in-situ</b> inspection	From original design specifications with <b>limited in-situ</b> testing <i>or</i> from <b>extended in-situ</b> testing	All	CF <sub>KL2</sub>
KL3		From original detailed construction drawings with <b>limited in-situ</b> inspection <i>or</i> from <b>comprehensive in-situ</b> inspection	From original test reports with <b>limited in-situ</b> testing <i>or</i> from <b>comprehensive in-situ</b> testing	All	CF <sub>KL3</sub>

### 2.5.1 Displacement-based design

As was seen previously, the seismic design in current codes have been based on strength or force considerations which helped to structures to withstand to major earthquake keeping their structural integrity. It was recognized, however, that structural and non-structural damage under seismic event can be directly related to material strain levels, or drift, respectively; and hence both can be integrated to obtain the displacement instead to forces according to FBD. The introduction of PBD raised a series of questions regarding to FBD, though the design process has not had significant changes. The seismic design based in displacement rather than strength is a new way to design structures located on seismic zones called: The displacement-based design (DBD).

The terms PBD and DBD are being used as if they meant the same. This is because there is the idea that the target behaviour may be related to the level of structural damage, which in turn can be related to the displacements. However, this assumption is an oversimplification,

since the level of damage is influenced by several other parameters, such as the accumulation and distribution of structural damage, the failure mode of the elements and connections, the number of cycles and duration of the earthquake and the levels acceleration in the case of secondary systems. In fact the DBD can be seen as a subset of PBD (Ghobarah, 2001).

In Priestley (2000), the main questions associated to FBD are discussed and identified, can be shown following:

- The use of characteristic force-reduction (behaviour factor) or ductility factors – The seismic design according to FBD determines that a behaviour factor be adopted being proportional to the ductility capacity of the structure. However, two different buildings designed in accordance with the same code and employing the same behaviour factor can have different level of damage under a given earthquake.
- The use of the elastic stiffness to predict the force distributions – the distribution of forces in the structures is found applying a design spectrum being reduced by behaviour factor in order to obtain the inelastic design forces. In contrast, the yielding within of the structure does not occur at the same time for all the members. Thus, the elastic force distribution can be very different of the inelastic force distribution.
- The difficult in defining the system ductility for used combined of systems – In codes, the behaviour factor for structures where be combinations of structural systems corresponds to lower of the two systems. However, it is not correct because there is no consideration concern its force distribution and how define the ductility demand.
- The use of the equal-displacement approach – For instance, a given structure with same strength, stiffness and mass is designed considering only steel elements and the other with RC elements. Consequently, the initial period is the same and equal-displacement rule predict the same displacement for the two systems. However, the inelastic displacement is different for both due to high level of energy dissipation of steel. Therefore, the inelastic displacement of structure with steel is less than the one with RC elements. It is possible to conclude that the relationships between elastic and inelastic displacement should takes into account the hysteretic properties of the structure.
- The relationships of strength and stiffness for RC structures – It was observed in Priestley (1998); Priestley and Kowalsky (1998); Paulay (2002) that yield curvature is related to section geometry and yield strain of longitudinal reinforcement. Previously, the structural stiffness is independent of strength, for a given gross

member dimension, and consequently, the yield curvature is directly proportional to strength. Therefore, the yield curvature is not related to strength.

With these issues to be overcome, the DBD have emerged and the methods to design structures located in seismic zones based in displacement have gained importance. In particular, an alternative design method known as “Direct Displacement-based Design (DDBD)” has been developed (Priestley et al., 2007; Priestley, 2007; Sullivan et al., 2003) which to characterise the structure by a SDOF (see Figure 2.25a) representation of performance at peak displacement response. The DDBD was developed by Priestley (1993) where the author used the idea of “substitute structure” conceptualized by Shibata and Sozen (1976). The aim is that the structure should achieve a specified performance level, defined by strain or drift limits, under a specific level of seismic intensity.

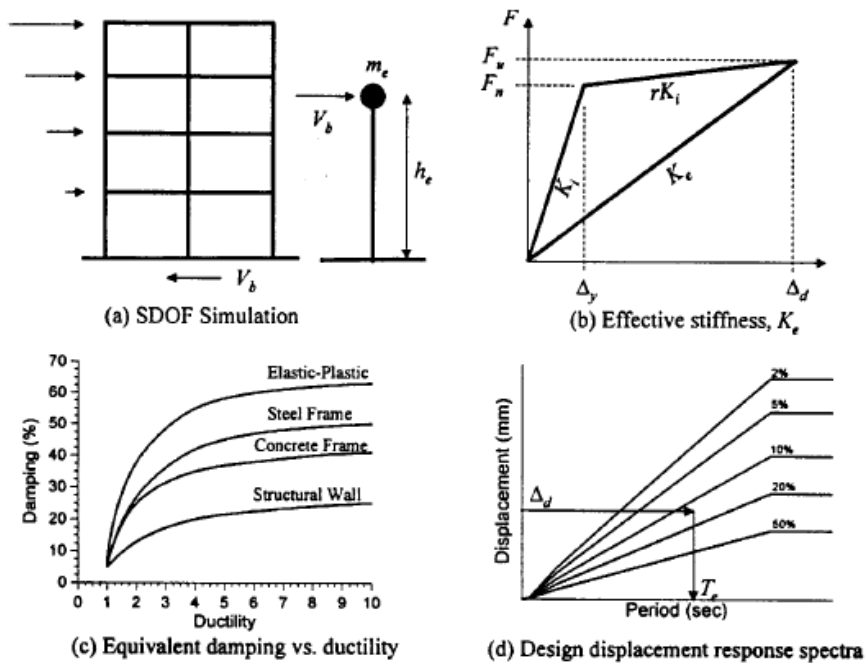


Figure 2.25 – Philosophy of Direct Displacement-based Design (Priestley, 2000)

Unlike of FBD where the structures is characterized in terms of elastic, pre-yield, properties (initial stiffness  $K_i$  elastic damping). The structural characteristics found in DDBD are based on secant stiffness  $K_e$  at design displacement  $\Delta_d$  (see Figure 2.25b) and a level of equivalent viscous damping  $\xi$  that corresponds to use combined of elastic damping and the hysteretic energy absorbed during inelastic response.

In order to obtain the design displacement of the equivalent SDOF structure, the following equation is used:

$$\Delta_d = \sum_{i=1}^n \frac{m_i \Delta_i^2}{m_i \Delta_i} \quad (2.2)$$

where  $m_i$  and  $\Delta_i$  are the masses and displacements of the  $n$  significant mass locations, respectively. In multi-storey buildings, these will normally be at the  $n$  floors of the buildings.

To find the equivalent viscous damping,  $\xi_{eq}$ , depends on the displacement ductility demand (see Figure 2.25c) and is given for steel frames as:

$$\xi_{eq} = 0.05 + 0.577 \left( \frac{\mu - 1}{\mu\pi} \right) \quad (2.3)$$

The displacement ductility demand is given by ratio design displacement at maximum response,  $\Delta_d$ , and yield displacement,  $\Delta_y$ . The yield displacement at the height of the resultant lateral seismic force may be calculated as:

$$\Delta_y = 0.65 \varepsilon_y \left( \frac{l_b}{h_b} \right) (H_e) \quad (2.4)$$

where  $l_b$  is the beam span, and  $h_b$  is the steel beam depth, and  $H_e$  is the effective height of the SDOF system given by:

$$H_e = \sum_{i=1}^n \frac{m_i \Delta_i H_i}{m_i \Delta_i} \quad (2.5)$$

Now, as the design displacement in maximum response determined together with the corresponding damping estimated, the effective period  $T_e$  at maximum displacement response can be read from a set of displacement spectra for different levels of damping (see Figure 2.25d). The effective stiffness,  $K_e$ , of the equivalent SDOF system is found inverting the normal equation for the period of a SDOF oscillator:

$$K_e = \frac{4\pi^2 m_e}{T_e^2} \quad (2.6)$$

where  $m_e$  is the effective mass of the structure participating in the fundamental mode of vibration given by Equation (2.7):

$$m_e = \sum_{i=1}^n \frac{m_i \Delta_i}{\Delta_d} \quad (2.7)$$

With all data properly calculated, the design lateral force, which is also the design base shear force is obtained as:

$$F = V_{base} = K_e \times \Delta_d \quad (2.8)$$

This base shear force is then distributed to the structural masses in accordance with Expression (2.9).

$$F_i = \frac{V_{base} \times (m_i \Delta_i)}{\sum_{i=1}^n (m_i \Delta_i)} \quad (2.9)$$



The DBD is a promising method to design structures located in seismic zones. However, there is some limitation regarding to methods present in literature. In Sullivan et al. (2003), a study have been presented considering eight methods for DBD where their main limitation and probable applications are investigated and discussed.

Recently, two project have been started in order to develop guidelines for DBD considering different structural typologies and materials. The RELUIS (Rete di Laboratorie Universtari Ingegneria Sismica) project aim to produce a model code for the DBD (Calvi and Sullivan, 2009). The DiSTEEL (Displacement Based Seismic Design of STEEL Moment-resisting Frames Structures” have as objectives to define an innovative approach based on DBD that allow to optimise performance for different levels of seismic intensity.

## 2.6 Seismic design according to European Code

The seismic design in Europe is performed according to EN1998-1-1 (2004). This code implements into design rules the set of principles based on capacity design and ductility provisions previously stated. Although structures are allowed to be designed according to either non-dissipative or dissipative behaviour. The design is based on the application of general principles of overall structural behaviour of the buildings and specific detailing of the structural members and components depending on the type of material. Moreover, the standard design procedures are based on modal analysis and the seismic action is defined by suitable response spectra that can be replaced by compatible accelerograms. The structural modelling and analysis can be performed using different levels of complexity concerning static, dynamic, 2D or 3D behaviour with linear-elastic or non-linear post-elastic behaviour of the materials.

Within of the scope from European code, the earthquake motion can be represented by an elastic ground acceleration response spectrum being characterized by two spectral configurations: Type 1 and Type 2. A seismic action Type 1 is considered for strong enough earthquakes (with magnitude higher or equal than 5.5) generating significant accelerations to construction site, while the Type 2 is applied to earthquakes with magnitude lesser than 5.5 contribute most to the seismic hazard. Figure 2.26 illustrates the elastic response spectra for both types of seismic activity.

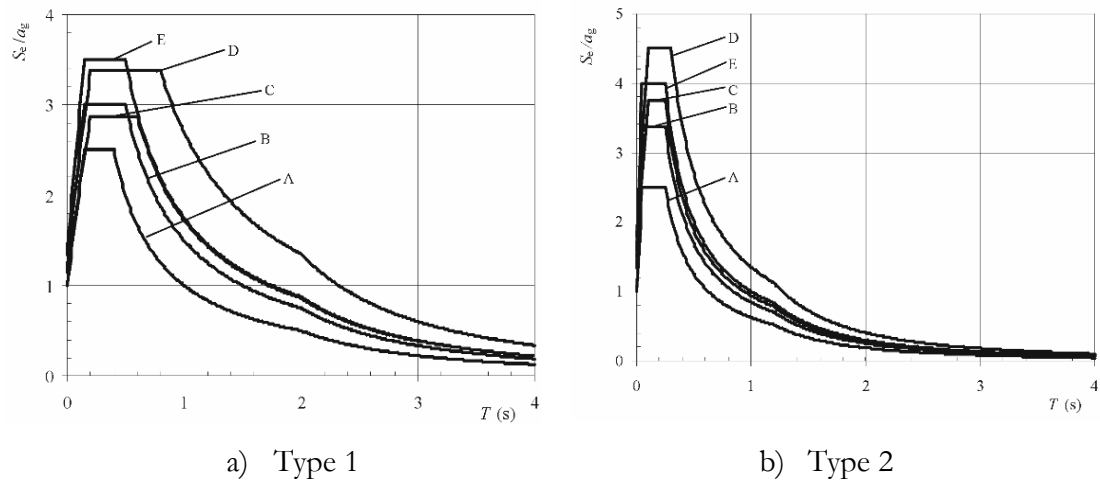


Figure 2.26 – Elastic spectrums recommended by (EN1998-1-1, 2004)

The seismic action can also be represented by accelerograms that present the variation of the acceleration at the ground surface as a function of time and the associated quantities (velocity and displacement). According to EN1998-1-1 (2004), artificial accelerograms should be set to correspond to the elastic response spectra and compatible with the magnitude and other characteristics of the seismic event relevant to establishing the value of  $a_g$  duration. The accelerograms simulated through a numerical simulation of the mechanisms at the source or the path of propagation may be used, if the samples used are properly qualified regarding the characteristics of the source and the ground conditions of the site.

In order to take into account the seismic hazard to have reduced costs, the conceptual design of a building should have some guiding principles for the structure plays a great role when submitted to a seismic event. The part 4.2.1 of EN1998-1-1 (2004) presents some guiding principles for the design due to the seismic casualty, specifically for buildings, which are fundamental to fulfil the requirements of "no-collapse" and "damage limitation":

- Structural simplicity – the simplicity should be an objective in all stages (analysis, design and detailing of structures) in which the structures should provide simple and regular forms either plan or elevation.
- Uniformity, symmetry and redundancy – should be ensured by the configuration and arrangement of structural elements and the distribution of building masses; should as far as possible, maintain, per floor, the constancy of lateral stiffness and mass, or with variations, that the reduction is done gradually, without abrupt changes, from base to top.
- Bi-directional resistance and stiffness – should be secured from the characteristics geometrical and mechanical structural elements arranged according to the structural.

- Torsional resistance and stiffness – the structures should be provided with adequate torsional resistance since compatible with the architectural solution; relationship between the distribution and the mass distribution and stiffness reduces the eccentricity of mass and rigidity while minimizing the effects of torsion.
- Diaphragmatic behaviour at storey level – Non-deformable diaphragms in the horizontal plane at the level of floors to transmit horizontal forces to vertical elements, and also, to help with the strength and stiffness in their plans.
- Adequate foundation – due to uniform excitation of the ground motion, the foundation should be connected by foundation beams. Exceptions are situations where the geotechnical characteristics allow waive this requirement.

The structures designed in accordance with EN1998-1-1 (2004) should verify two criteria:

- Non-collapse requirement
- Damage limitation requirement

The non-collapse requirement is associated with the ultimate limit state, in which requires that the structure be able to withstand the seismic action without local or global collapse ensuring residual capacity and structural stability and other building elements. After the earthquake, there must also have sufficient strength and lateral stiffness to safety life even during strong aftershocks

The damage limitation requirement correspond to serviceability limit state and to have as objectives to avoid high costs associated to occurrence of damage and the limitation of use during a seismic event with a return period equal to 95 years recommended by EN1998-1-1 (2004). In this requirement, the structure should have a maximum inter-storey drift depending of the type non-structural elements of buildings.

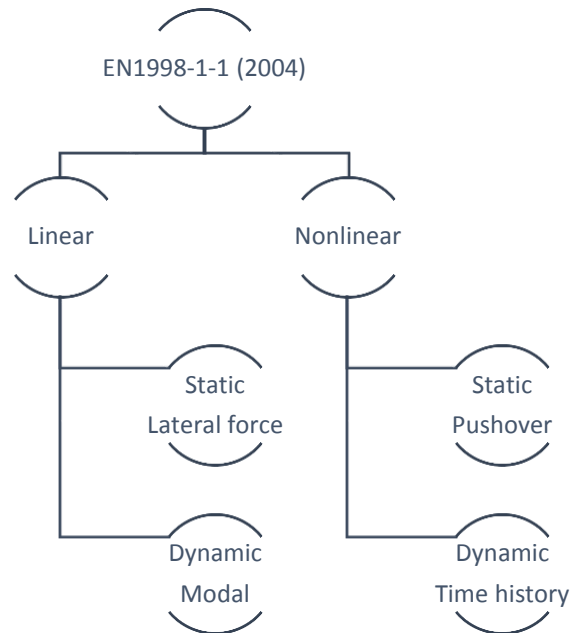
In general, the buildings are classified into four categories of importance, which depend on the size of the building, their level of importance to the public safety and possibility of human losses under a ground motion, for instance, a hospital or office. This classification will affect the seismic action to be considered in seismic design by an importance coefficient,  $\gamma_I$ , multiplying the peak ground acceleration by this factor.

Furthermore, the structures also are classified concerning to their regularity in plan and height in accordance with the requirements from clause 4.2.3 of EN1998-1-1 (2004). This classification will involve the definition of the type of model analysis and the coefficient of behaviour that may be used for each structure (see Table 2.3).

Table 2.3 – Consequences of structural regularity on seismic analysis and design (EN1998-1-1, 2004)

Regularity		Allowed Simplification		Behaviour factor
Plan	Elevation	Model	Linear-elastic Analysis	(for linear analysis)
Yes	Yes	Planar	Lateral force <sup>a</sup>	Reference value
Yes	No	Planar	Modal	Decreased value
No	Yes	Spatial <sup>b</sup>	Lateral force <sup>a</sup>	Reference value
No	No	Spatial	Modal	Decreased value

The seismic design and evaluation of structures can be carried out using static or dynamic methods. Within these two types of methods can still be considered linear or nonlinear behaviour of the material. The diagram below shows the possible paths to be followed by the designer:



In general, there is the possibility to know the seismic response of a given structure by the design on basis the maximum value calculated, or, to assess the seismic response considering the evolution of response by time-history. For the linear analysis, it is usually to use a design spectrum in seismic evaluation.

The linear analyses are based in elastic behaviour of structure. The nonlinear component is typically integrated by using a behaviour factor that varies with the structural type and material. In contrast, the nonlinear analyses are not based on employment of a behaviour factor where the nonlinearities are applied directly. The following is a description of each method is presented.

A structure designed considering that there is no energy dissipation under earthquake is expected to be heavier, and probably cannot ensure a safety level for major earthquakes.

Moreover, the structural behaviour is not assured to be ductile and can lead to brittle collapse.

The seismic design considering a dissipative behaviour of structure is carried out by applying a set of rules to assure the ductile behaviour and maximize the energy dissipated by the collapse mechanism. The advantage is the reduction of the shear base under seismic actions applying a suitable behaviour factor. Those set of rules are based on ‘capacity design’ concept and on imposing that, some members or zones of structural system are responsible for energy dissipation by post-elastic deformation. And some other members/zones have adequate overstrength in order to assure an overall ductile mechanism and avoid a partial collapse.

Concerning to design of non-dissipative members/zones, the yield strength of the steel of dissipative members/zones should be less than its values multiplied by two factor that takes into account the hardening of material and its variability between the nominal and real yield. Thus, the hardening effect is taken into account increasing the yield in 10%. On the other hand, the differences between the nominal and real yield strength is considered multiplying the strength of steel by a factor equal to 1.25. In sense, the seismic load from seismic combination is increased by both hardening and variability of material factors; therefore, it is logical to consider both factor to have non-dissipative members/zones in elastic range.

In fact, a ductile behaviour is generally a great way to structures resist to ground motion. One of the reasons is related to level of uncertainty in determining of seismic action to consider on analyses. In other word, the seismic actions or their damage can be major than the considered in the structural design phase. Ensuring a ductile behaviour, any higher seismic action to those provided are easily absorbed by greater energy dissipation on the plastic deformation of the dissipative members/zones. In addition, a reduction of the base shear means a decreasing of the forces applied to the foundation, resulting in lower costs for the infrastructure of the building.

#### 2.6.1 *Lateral force based method*

This method is commonly used in the seismic design. It is a linear method in which the inelastic behaviour is considered in design through the use of the behaviour factor. It is in general conservative for buildings of small to medium height characterized by regular distribution of mass and stiffness. The structural behaviour is assumed to be governed by the fundamental period of vibration. It applies to building that can be analysed by two planar models and the response is not significantly affected by contributions of higher vibration modes.

The structures need to have fundamental periods of vibration in the two main directions smaller than 2.0s or four times the upper limit of the period of the constant spectral acceleration  $T_C$ . In addition, they must comply with the regularity criteria defined in section 4.2.3.3 of EN1998-1-1 (2004).

The static lateral forces applied at the level of the floors following a distribution close to the shape of the first vibration mode.

The fundamental period of buildings,  $T_1$ , can be assessed using simplified expressions such as Equation (2.10). This expression is suitable for buildings with heights of up to 40m.

$$T_1 = C_t \times H^{3/4} \quad (2.10)$$

where, the  $C_t$  factor is equal to 0.085 or 0.075 for moment resistant space steel frames or concrete frames/eccentrically braced frames, respectively; and 0.050 for all other frames. The height  $H$  of the building in meters is calculated from rigid base or foundation.

The design base shear is obtained for each main horizontal direction in which the building will be analysed according to the following expression:

$$F_b = S_d(T_1) \times m \times \lambda \quad (2.11)$$

where,  $S_d(T_1)$  is obtained from the design spectrum at the fundamental period,  $m$  is the total mass of the building and  $\lambda$  is the correction factor being equal to 0.85 for buildings have more than two storey with  $T_1 \leq T_C$  or 1.0 otherwise.

After obtaining the design base shear, the next step is to distribute it over the height of the building. Although horizontal forces along height are proportional to the displacements in the fundamental mode shape of the structure. The mode can be approximated using linear variation along the height according to Equation (2.12).

$$F_i = F_b \times \frac{z_i \times m_i}{\sum z_j \times m_j} \quad (2.12)$$

where  $z_i$  is the height of the mass  $m_i$  above the level of application of the seismic action.

### 2.6.2 Modal response based method

When the requirements to perform a simple lateral force analysis are not met higher modes have to be included in the analysis. The modal response method is a generalization of the previous method. It is also a linear method in which the inelastic behaviour is considered in design through the use of the behaviour factor. The method of modal response spectrum is used when the effects of higher vibration modes contribute significantly to the structural response. The sum of the effective modal masses should represent at least 90% of the total

mass of the structure or alternatively all modes with effective modal mass greater than 5% of the total mass should be considered.

However, in certain cases where torsion contributes significantly for the response the minimum number  $k$  of modes to be taken into account in a spatial analysis should satisfy both the two following conditions:  $k \geq 3\sqrt{n}$  and  $T_k \leq 0.2sec$

Since the analysis is performed at modal response level, the combination of effects in each vibration mode shall be performed in order to find the total response of structure. The maximum values in each modal response obtained through the application of the response spectrum concept is therefore combined. Although several modal combination strategies can be found in bibliography, the most efficient approach is the Complete Quadratic Combination method (CQC) (Wilson et al., 1981) based on random vibration theory. The maximum response of a certain output parameter can be estimated as:

$$G \approx \sqrt{\sum_{n=1}^m \sum_{i=1}^m \rho_{in} G_i G_n} \quad (2.13)$$

where the correlation coefficient is defined by following equation:

$$\rho_{in} = \frac{8\zeta^2(1 + \beta_{in})\beta_{in}^{3/2}}{(1 - \beta_{in}^2)^2 + 4\zeta^2\beta_{in}(1 + \beta_{in})^2} \quad (2.14)$$

and,

$$\beta_{in} = \frac{p_i}{p_n} \quad (2.15)$$

A simplification of this method is obtained when the correlation coefficient between two different modal responses is zero,  $\rho_{in} = 0$ . This corresponds to the Square Root of the Sum of the Squares (SRSS) where the maximum value of the response is determined by

$$G \approx \sqrt{\sum_{n=1}^m (G_n)^2} \quad (2.16)$$

### 2.6.3 Nonlinear static “Pushover” analysis

Nonlinear analyses are alternative to linear analysis methods. In this type of analysis, the mathematical model used to analyse the structure must include the resistance of the elements as well as their post- yield behaviour.

The static “pushover” nonlinear analysis is an effective tool to assess the inelastic behaviour of building, as well as revealing weaknesses in the linear design performed previously

verifying the relevant aspect in order to ensure the structural integrity. Furthermore, it may also be able to show the plastic mechanisms and potential dissipative regions for specific load pattern applied to floor level evaluating the overall capacity of structure.

This type of analysis have been gaining significance due to applicability in comparison with dynamic analyses because is not necessary to select ground motions records which there is some uncertainties and difficulties regarding to severity, frequency, duration and distances of faults, as well as, in terms of modelling and computational demands and interpretation of results

The pushover analysis is based on constant gravity loads and horizontal forces monotonic growth. It can be applied to verify the structural performance of new buildings and existing buildings for the following purposes:

- Check or revise the values of the overstrength coefficient –  $\alpha_u/\alpha_1$ ;
- Evaluate the plastic mechanisms foreseen and distribution of damage;
- Evaluate the structural performance of existing or rehabilitated buildings;

The method provided by EN1998-1-1 (2004) for this type of analysis is the N2 method started in the mid-1980s (Fajfar and Fischinger, 1987; Fajfar and Fischinger, 1988) in which is based on the lateral capacity curve of the structure. This capacity curve represents the relationship between base shear and its displacement from the top. After determining the capacity curve of the structure is necessary to implement a curve bilinear of an equivalent structure of SDOF.

After meeting the corresponding bilinear configuration of the capacity curve of the system of SDOF, and based on the seismic action considered (defined from the response spectrum), the target displacement of the equivalent structure is determined. The target displacement correspond to roof displacement that the structure will have under a design earthquake.

This analysis should be used at least two distributions of lateral forces: a uniform, based on lateral forces proportional to mass regardless of height and with other modal distribution proportional to the lateral forces in the direction considered, given the elastic analysis.

#### 2.6.4 *Non-linear dynamic time-history analysis*

As an alternative to nonlinear static method, the seismic action can be determined by dynamic time-history analysis on basis in accelerograms to represent the ground motion. According to EN1998-1-1 (2004), it is necessary to use at least three different accelerograms to assess the structural response over time, having as final result, the average of all accelerograms investigated. It is important that the selected accelerograms have



characteristics (duration, number of cycles, intensity) to the appropriate regional seismicity and local soil conditions.

The accelerograms are the most efficient way to represent the action seismic where they have a set of information about the nature of ground motion. However, to obtain a set of records is not a task very easy when there is not a seismic hazard established.

The seismic engineer should find two different criteria in order to select the accelerograms. One is based in terms of strong-motion parameters while the other is associated to the seismological parameters, mainly magnitude, distance and site conditions. The method based on strong-motion parameters consists in to find accelerograms compatible with code-spectrum employed on design, which can be real or artificial. On the other hand, when the site is known and well characterized in seismological terms by either deterministic or probabilistic seismic hazards, the accelerograms are selected from strong-ground database where those seismological parameters are taken into account.

Anyway , this type of analysis is desirable to give results in terms of displacements, strains and efforts that need not be modified by any factor of behaviour and structural response observed through this type of procedure is much more sensitive to the individual characteristics of considered to own shares and type of structure .

### ***Chapter III***

## **Study Cases: Definition, Description and Code Design**

The aim of this chapter is to define the parametrical study in order to investigate and evaluate the seismic performance of dual-steel building frames composed of two different steel grades: Mild Carbon Steel (MCS) and High Strength Steel (HSS). The MCS is used on dissipative elements while the HSS is employed on non-dissipative elements being both elements according to the structural typology.

The seismic design based on current codes applying the force-based design is herein described. The study cases are designed in accordance with the requirements from EN1998-1-1 (2004). However, the information concerning the seismic design of dual-system in this code is scarce. Thus, AISC-341 (2005) has been used in order to design this dual-system. Herein, a dual-system is defined as a structure composed of two structural systems, in this case, composed of CBF and MRF.

### **3.1 Definition of the structural typologies**

Seismic applications potentially represent a rational field to exploit the performance of HSS. Indeed, according to modern codes the seismic design of steel or composite buildings are based on the concept of dissipative structures, in which specific zones of the structures should be able to develop plastic deformation, mainly on ductile member, in order to dissipate the seismic energy. On the contrary, the non-dissipative zones and members should behave elastically under seismic action in order to avoid the brittle collapse of the building. For this reason, these zones should be designed to resist the full plastic strength of the dissipative members. Consequently, the large overstrength demands to non-dissipative zones lead to high material consumption, and sometimes, huge size of members to fulfil this design requirement.

The combined use of HSS for non-dissipative members and of Mild Carbon Steel (MCS) for dissipative members may allow an easier application of capacity design criteria. The expected design improvement would be obtained in terms of smaller member sizes than those obtained when using MCS only. Structures using the combination of HSS and MCS are termed “dual-steel” structures.

Therefore, in this research a parametrical study has been created in order to evaluate the use of HSS in seismic resistant structures. Thus, three structural typologies are selected to assess the seismic behaviour and to fulfil the objectives of this study:

- **Moment-resisting Frames (MRF)** – The beams are the structural members that will dissipate the seismic energy through inelastic deformation while the column should remain in elastic range.

The design of MRFs with HSS columns may lead into structures with lateral stiffness lower than those designs with single steel grade. Hence, some problems may arise such as the nonfulfillment of damage limitation requirements and overall stability problems due to P-Delta effects. These considerations clearly show us the need to investigate the effectiveness of dual-steel concept in the seismic design of MRFs.

- **Concentrically Braced Frames (CBF)** – In this structural system, the braces are responsible for energy dissipation. Therefore, the structures should be designed in order not to have any plastic deformations in the beams and columns. The beams from braced bay are fixed in columns while the un-braced bays have beam-column pinned connections. Braces are inverted V-shape and are considered to be pinned in both ends.

This survey also focuses in the assessment of seismic performance of CBFs with V-inverted bracing using the dual-steel concept. The CBFs are frequently used in regions with high seismicity. This structural system is able to control the lateral displacement due to its larger stiffness compared with MRFs. Their seismic performance is mainly controlled by the braces in which the energy generated by the seismic event is dissipated through post-buckling and yielding hysteric behaviour. Some published research studies (Serra et al., 2010; Broderick et al., 2008; Tremblay, 2002; Roeder et al., 2011) have been devoted to investigate the different parameters that control the seismic performance of CBFs, mainly the ones related not only

to the effect of brace slenderness, but also to lower energy dissipation due to buckling of braces and collapse of connections using gusset plates.

- **Dual-Concentrically Braced Frames (D-CBF)** – The dual-system is characterized by the contribution of two structural systems in the seismic energy induced by ground motion. In this case, one bay is composed of a braced system, CBF, in which the braces will yield either in compression or in tension. The other bay refers to MRFs, in which the beams are responsible for the dissipation of the seismic energy.

As mentioned, dual structural systems are formed by combining two of the basic structural systems: a MRF and a braced frame (here a CBF). The steel shear walls may also be used instead of the braced frames being a typical structural system seen in USA and Japan. Poor design guide in order to design the dual-system is available in the codes (Stratan et al., 2003). According to EN1998-1-1 (2004), a dual-system with both MRFs and braced frames acting in the same direction should be designed using a single behaviour factor and the horizontal forces should be distributed between the different frames according to their elastic stiffness.

The AISC-341 (2005) design code requires a minimum strength (25% of the total one) for the MRF, so that the structure can be defined as “dual”. Iyama and Kuwamura (1999) studied the probabilistic aspect of dual-system obtained by combining the CBF and MRF (see Figure 3.1) with different natural periods of vibrations. According to the authors, this structure is called “fail-safe”, because it provides an alternative load path to earthquake loading (MRF) in case the primary system fails (CBF).

The results of analyses showed that a dual-system has a higher safety factor than a homogeneous system, considering the unknown characteristics of future earthquakes. In addition, the benefits of the dual system are enhanced when the difference between the natural periods of the subsystems is large

Therefore, this research also focuses in the seismic behaviour of dual-system, which is formed by combining the CBF V-inverted bracing with MRF using the dual-steel concept.

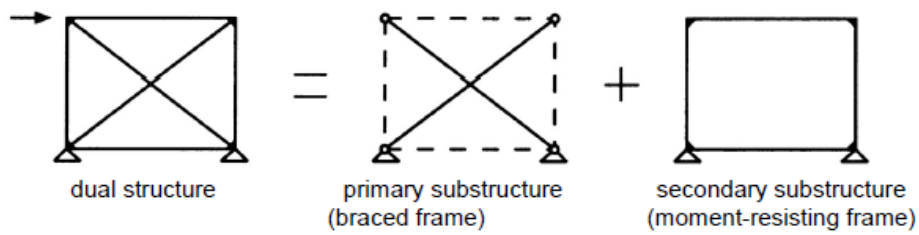


Figure 3.1 – Dual structural system studied by (Iyama and Kuwamura, 1999)

### 3.1.1 Investigated parameters

A wide parametric numerical study has been carried out to evaluate the benefits of dual-steel concept on the Performance Based Seismic Design. A total number of 72 frames has been selected and designed. Each structural typology has a set of 24 frames designed in accordance with EN1998-1-1 (2004) and AISC-341 (2005) varying in specific aspects in order to evaluate their influence on seismic behaviour. The investigated parameters cover both geometric and mechanical variables, such as the column types, the span length, the number of storeys and the spectral shape:

- **Number of storeys:** Two different heights are defined by each structural system. For the MRF, both low-rise and mid-rise buildings, namely four-storey and eight-storey, respectively, have been selected. The braced frames (both Dual and Non-Dual) have eight-storey or sixteen-storey.
- **Span length:** The influence of span length also have been considered. Therefore, frames with 5.0 m and 7.5 m have been designed.

The variation of the number of storey together with the span length is related to overall structural behaviours. The aim is to analyse two different overall structural behaviours: Shear-dominant (racking) and Flexural-dominant (cantilever).

According to Davison and Owens (2000), the flexural behaviour becomes important for relatively slender frames with a height-to-width (aspect) ratio of about 1.5. Hence, the span range 5.00m – 7.0m allows analysing both structural behaviours, the former for flexural-dominant type, the latter for shear dominant type.

- **Composite steel-concrete column typologies:** Three different cross-sections are chosen: Fully Encased (FE), Partially Encased (PE) and Concrete Filled Tube (CFT).

The selection of a composite steel-concrete column is related to enhancing stiffness and strength of these columns type (non-dissipative members), as well as, its fire resistance. The lateral stiffness plays an important role for the design, mainly for the MRFs, which, very often, are governed by design criteria based on lateral displacements and inter-storey drifts.

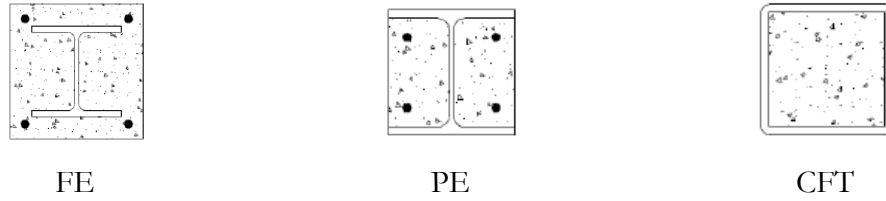


Figure 3.2 – Composite steel-concrete cross-sections investigated

Steel profiles in the columns can be either made up by hot rolling (HR) or custom made by welding (PRS). Reinforcement steel is used to guarantee a proper behaviour of FE and PE columns. CFT columns do not require any reinforcing steel in non-fire conditions. The characterization of welded steel profiles is made as shown below:

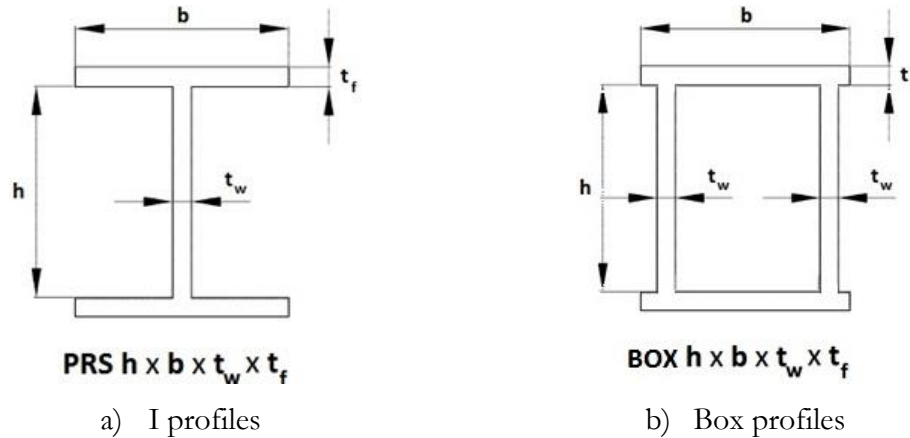


Figure 3.3 – Composite steel-concrete cross-sections investigated

- **Corner period of the design spectra:** two types of soil conditions have been examined. The former representative of soil type C according to EN1998-1-1 (2004) hereinafter identified as “stiff soil” and the latter representative of softer soil conditions with corner period of 1.6s, hereinafter identified as “soft soil”;

Not only the structural configuration and the inelastic characteristics of the structure are important for its seismic response, but also ground motion characteristics influence structural response in a greater extent. Current seismic design codes fail to consider all the influence of ground motion characteristics on ductility demand in dissipative members through adopted behaviour  $q$ -factors. In general, the inelastic response is strongly dependent on the frequency content of the ground motion in comparison with elastic response. The structures located in range of constant spectral accelerations are subjected to considerable

higher ductility demands than the ones with the fundamental period in the range of constant spectral velocities. Thus, the behaviour factors are strongly dependent not only on the structural type, but also on the frequency content of the ground motion. The inclusion in the analysis of ground motions with large corner period enlarges the investigation of the study cases behaviour on such type of soil.

- **Steel grade for non-dissipative members:** two steel grades have been used in this research for the non-dissipative members, S460 and S690. All the elements considered as dissipative have been designed considering steel grade S355, except for the beams from braced bay due to the high demand derived from the design requirements.

Figure 3.4 gives an overview of the 72 study cases. For each of the three structural configurations, 24 frames have been designed in accordance with current codes. In particular, the MRFs are designed only for the lower steel grade S460 and the lower frame heights, four- and eight-storeys, in comparison with braced frames for which additional cases using steel grade, S690, in non-dissipative members were considered and also increasing number: of storeys, eight- and sixteen-storeys.

Span		5.00m						7.50m					
Column		FE		PE		CFT		FE		PE		CFT	
Storeys	Soil type	H	S	H	S	H	S	H	S	H	S	H	S
4	S460												
8													

Legend:

H – Stiff soil

S – Soft Soil

FE – Fully Encased Column

PE – Partially Encased Column

CFT – Concrete Filled Tube

a) Un-braced Frames

Span		5.00m						7.50m					
Column		FE		PE		CFT		FE		PE		CFT	
Storeys	Soil type	H	S	H	S	H	S	H	S	H	S	H	S
8	S460												
	S690												
16	S460												
	S690*												

b) Braced Frames (CBF and D-CBF)

Figure 3.4 – Overview of the 72 study cases

In order to organize the work properly and to be easy to invoke a given frame, a label code has been developed to number the frames. The numbering system obeys the following format:

**(Type of Structural System) – (Storeys).(Steel).(Spans).(Soil).(Column Type)**

Where

- Type of Structural System                      MRF / CBF / D-CBF;
- Storeys    1 → 8 storeys / 2 → 16 storeys / 3 → 4 storeys;
- Steel (non-dissipative members)            1 → S460 / 2 → S690;
- Spans    1 → 5.00m / 2 → 7.50m;
- Soil    1 → Stiff / 2 → Soft;
- Column Type                                      1 → FE / 2 → PE / 3 → CFT;

**Example**

D-CBF	2	1	2	1	2
D-CBF	16 Storeys	S460	7.5m Span	Hard Soil	PE Column

**3.1.2 Description of the structural configuration**

The analysed frames were extracted from a reference building considered to satisfy the plan and elevation uniformity as defined in EN1998-1-1 (2004), assuming an indefinite width, in which the generic braced frame alternates with gravitational loads resisting frames. Therefore, the spacing of braced frames is equal to  $2L$ , being  $L$  the span length in the transverse direction, as shown in Figure 3.5.

Floors are made of composite steel decks simply supported by steel beams (primary and secondary), which are restrained to avoid flexural-torsional buckling.

Beams, in each frame, act like girders. They are indirectly loaded by the slab through the secondary beams. In this way, the forces from the slabs are applied on the girders by point loads.

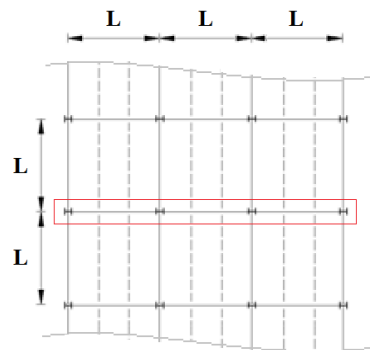


Figure 3.5 – Plan view



**Moment-resisting Frames (MRF)**

The MRFs consist of both four-storey and eight-storey composite steel-concrete as shown in Figure 3.6. The study cases are composed of three-bay frames spaced at length “L”. The buildings are regular in elevation and all beam-to-column connections are assumed to be full strength and full rigid.

The columns are considered to be fixed at the base and continuous through the height. The four-storey has a total height equal to 14.5m while the taller building has 28.5m. For both cases, the first floor is 4.0m high and the rest are 3.5m high.

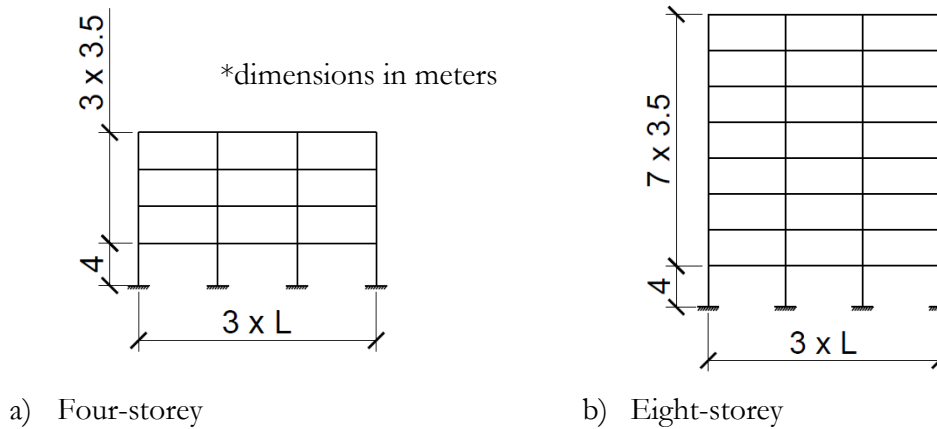


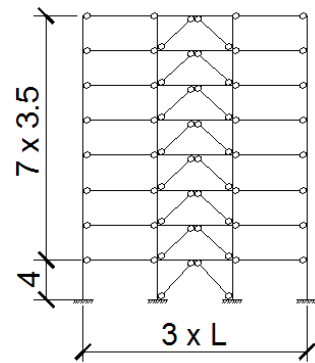
Figure 3.6 – Moment-resisting Frames

**Concentrically braced Frames (CBF)**

The CBFs are composed of three spans and eight or sixteen storeys (see Figure 3.7). As for the MRFs, also the CBFs fulfil the criteria of regularity over the height.

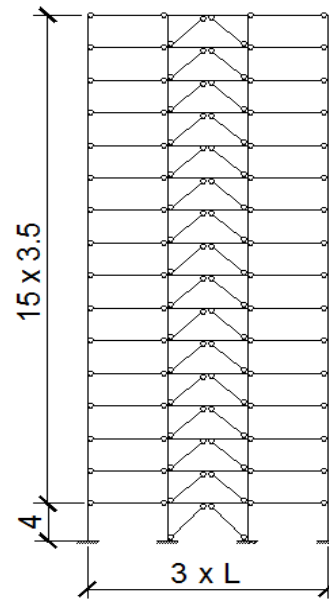
Concerning the boundary conditions, the braces are pinned on both ends due to low out-of-plane stiffness of gusset plate connections. Owing to the high in-plane stiffness and the presence of flange stiffeners, the beam-to-column connections of braced part are assumed to be rigid. On the other hand, the beams in the non-braced bays are assumed to be pinned.

The columns are considered to be fixed at the base and continuous through the height.



\*dimensions in meters

a) Eight-storey



b) Sixteen-storey

Figure 3.7 – Concentrically Braced Frames

### **Dual-Concentrically braced Frames (D-CBF)**

Basically, the D-CBFs have the same geometrical characteristics of the CBFs (see Figure 3.8). However, as the MRF parts are responsible for energy dissipation, the beam-to-column connections from the structural part of the building outside braced span are assumed as full strength and full rigid. Analogous to CBFs, the braces are pinned on both ends and the beam-to-column connections from braced bay are considered to be rigid due to the presence of flange stiffeners.

Again, the composite steel-concrete columns are assumed to be fixed at the base and continuous through the height, which is the same as for the CBFs.

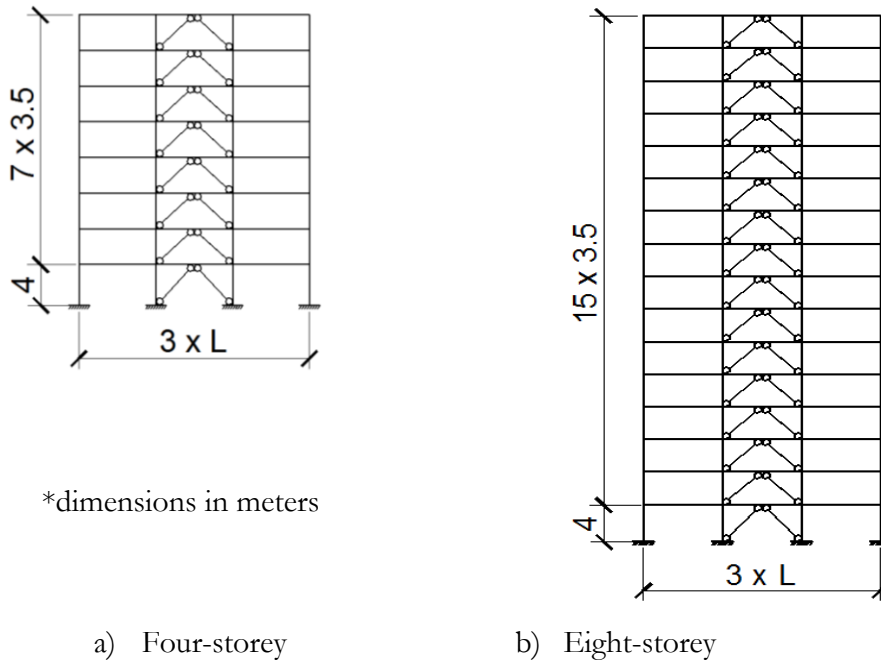


Figure 3.8 – Dual-Concentrically Braced Frames

### 3.2 Code design based on Eurocode 8 and AISC 341

The frames were designed in accordance with EN1998-1-1 (2004), EN1993-1-1 (2005), EN1994-1-1 (2004) and with AISC-341 (2005) regarding dual-system, that is, the frames with the combination of two structural system were designed considering that the MRF system is provided with a minimum of 25% of the total lateral strength of the structures. In the design calculations, first order elastic analyses have been carried out using amplification of relevant action effects to account for P-Delta effects. In addition, the effects of initial sway imperfection have been taken into account using equivalent horizontal forces as indicated by EN1993-1-1 (2005).

Concerning to seismic design, the study cases were designed considering the two limit states defined in EN1998-1-1 (2004): no-collapse and damage limitation.

#### ***No-collapse requirement***

The no-collapse requirement corresponds to seismic action with a return period of 475 years. The aim is to guarantee that, although the structures may suffer severe damage there is no local or global collapse, ensuring therefore people's safety. The structure should be stable under the design seismic action. In addition, EN1998-1-1 (2004) establishes that the structures should have a ratio on all connections, in which the resistance capacity of columns is higher than the sum of resistance capacity of the beams, as shown:

$$\sum M_c \geq 1.3 \times \sum M_b \quad (3.1)$$

$M_c$  is the sum of the plastic moment of the column of the connection;  $M_b$  corresponds to sum of the plastic moment of the beams concerning those same connections.

### ***Damage limitation***

The damage limitation requirement is based on the deformability and the criterion inter-storey drift limitation is used. The following expression is applied:

$$d_r \times \nu \geq \beta_{dr} \times h \quad (3.2)$$

in which,  $d_r$  is the design inter-storey drift being the inter-storey drift obtained through seismic analyses multiplied by behaviour factor employed;  $h$  is the storey height;  $\nu$  is a reduction factor which depends of the importance class of the building. In this research, a maximum inter-storey drift of  $0.0075h$  has been used for all the study cases.

#### ***3.2.1 Elastic response spectra***

According to EN1998-1-1 (2004), the standard method for seismic design is based on Elastic Response Spectra (ERS) defined on the basis of various parameters. The peak ground acceleration (PGA) of the seismic action ( $a_g$ ) incorporates the level of reliability imposed for the structure and is obtained multiplying the reference PGA ( $a_{gR}$ ) by the importance factor of the construction  $\gamma_I$ . Considering that the building is of importance class II (ordinary buildings, not belonging in the other categories), thus  $\gamma_I = 1.0$  and  $a_g = a_{gR}$ .

The MRFs are assumed to be on a location of moderate seismicity. The PGA  $a_g$  was taken as 0.24g and 0.16g, respectively, for Stiff Soil and Soft Soil. The smaller PGA became necessary to limit the drift demands in case of soft soil condition.

Braced Frames are assumed to be on a location of high seismicity. The foundation conditions are similar to MRF but with peak ground accelerations of 0.32g for both soil types.

Table 3.1 presents the relevant characteristics to determine the response spectrum in seismic analysis for the MRFs, CBFs and D-CBFs.

Table 3.1 – Characteristics of the elastic spectrum for the seismic design

	<b>MRF</b>		<b>CBF</b>		<b>D-CBF</b>	
	<i>Stiff Soil</i>	<i>Soft Soil</i>	<i>Stiff Soil</i>	<i>Soft Soil</i>	<i>Stiff Soil</i>	<i>Soft Soil</i>
<b>Spectrum</b>	Type 1		Type 1		Type 1	
<b>Soil Type</b>	C	---	C	---	C	---
<b>P.G.A.</b>	0.24g	0.16g	0.32g		0.32g	
<b><math>\beta</math></b>	0,20		0.20		0,20	
<b>S</b>	1.15	1.00	1.15	1.00	1.15	1.00
<b>T<sub>B</sub></b>	0.20s	0.16s	0,20s	0,16s	0.20s	0.16s
<b>T<sub>C</sub></b>	0.60s	1.60s	0.60s	1.60s	0.60s	1.60s
<b>T<sub>D</sub></b>	2.00s	2.00s	2.00s	2.00s	2.00s	2.00s
<b>A.A.F.</b>	2.50	2.75	2.50	2.75	2.50	2.75
<b>q-factor</b>	4.00		2.50		4.80	

A.A.F. is the acceleration amplification factor that is, by default, 2,50 in EN1998-1-1 (2004) and is changed to 2.75 for Soft Soil spectrum.

The reference behaviour factor was assumed to be  $q = 4.0$  for the MRFs, which corresponds to recommended value for DCM concept in EN1998-1-1 (2004). It should be noted that although higher values for the behaviour factor are possible according to EN1998-1-1 (2004) in order to exploit the potentially large ductility and energy dissipation capabilities of MRFs, the use of lower behaviour factors is generally the more rational design choice as shown by Elghazouli (2005); Elghazouli et al. (2008) particularly to design frames in low-to-moderate seismicity regions. Figure 3.9 illustrates the both elastic and design spectra used on seismic design for MRFs showing the range of the fundamental period of the MRFs.

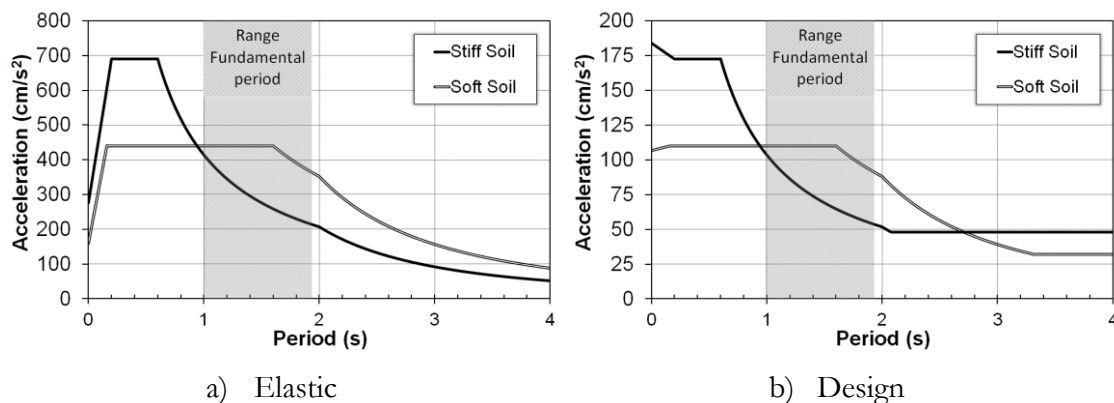


Figure 3.9 – Response Spectra and range of fundamental period for the MRFs

For the CBFs, the reference behaviour factor was assumed to be  $q = 2.5$  corresponding to DCH concept (EN1998-1-1, 2004). In contrast to what was assumed for the MRFs, it was adopted a higher class of ductility to take advantage of using HSS in non-dissipative elements and exploiting the large ductility of the CBFs. Figure 3.10 reveals the both elastic and design response spectra as well as the range of the CBFs fundamental period of vibration.

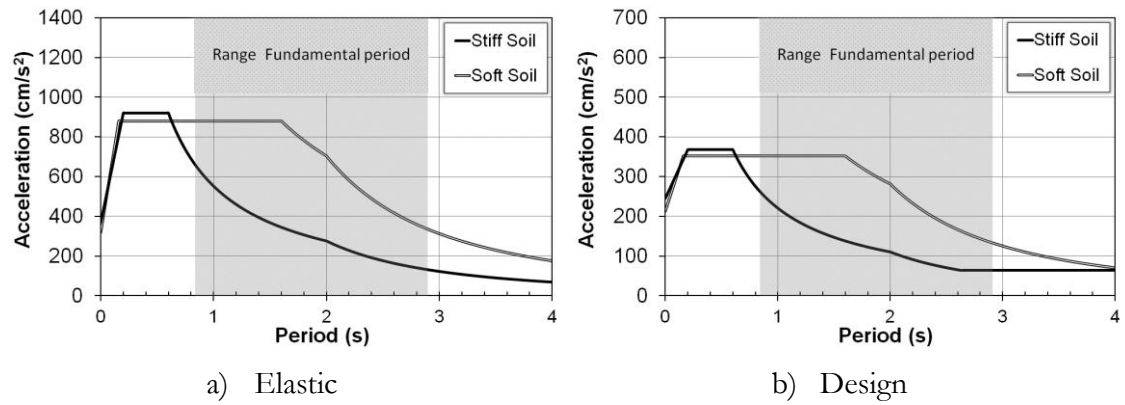


Figure 3.10 – Response Spectra and range of fundamental period for the CBFs

According to EN1998-1-1 (2004), the behaviour factor for a D-CBF formed by MRF+CBF considering a DCH concept is given by  $4\alpha_u/\alpha_1$ . The ratio  $\alpha_u/\alpha_1$  is the overstrength factor obtained from a pushover analysis. Thus, in case of D-CBFs, a behaviour factor equal to 4.8 is adopted using an overstrength factor of 1.2. The elastic and design spectra used on seismic design of the D-CBFs are given in Figure 3.11. In particular, it is possible to see the range of fundamental period of the study cases.

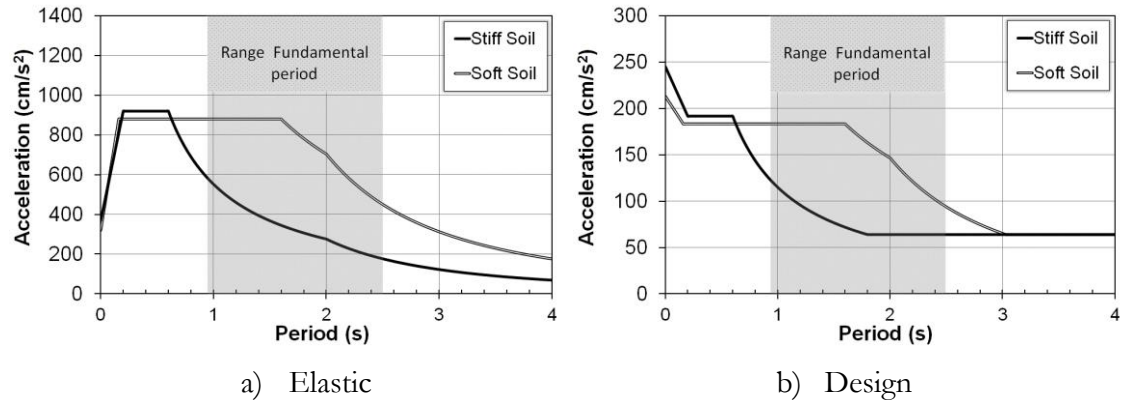


Figure 3.11 – Response Spectra and range of fundamental period for the D-CBFs

### 3.2.2 Material properties

Two different types of materials are used for structural members, namely steel and concrete. Regarding the steel, structural sections are made up of S355, S460 or S690 steel grades whereas reinforcing bars are classified as S500. The yield ( $f_y$ ) and ultimate ( $f_u$ ) nominal strengths of each steel grade are listed in Table 3.2.

Table 3.2 – Steel types employed in the seismic design

Components	Steel Grade	<i>Nominal thickness of the element <math>t</math> (mm)</i>			
		$t \leq 40$ (S355 and S460) or $t \leq 50$ (S690)		$40 < t \leq 80$ (S355 and S460) or $50 < t \leq 100$ (S690)	
		$f_y$ (N/mm <sup>2</sup> )	$f_u$ (N/mm <sup>2</sup> )	$f_y$ (N/mm <sup>2</sup> )	$f_u$ (N/mm <sup>2</sup> )
Steel sections	S355	355	510	335	470
	S460	460	540	430	540
	S690	690	770	650	760
Reinforcing bars	S500	500	Not specified	500	Not specified

Regarding concrete, only class C30/37 is adopted. This concrete grade has a uniaxial cylinder compressive ( $f_{ck}$ ) and tensile ( $f_{ctk}$ ) strengths of 30 N/mm<sup>2</sup> and 2N/mm<sup>2</sup>, respectively. The secant modulus of elasticity is considered as 33kN/mm<sup>2</sup>.

### 3.2.3 Loads and load combination

All loads are quantified according to EN1991-1-1 (2002) and EN1998-1-1 (2004). The combinations were considered applying the requirements imposed by EN1990 (2002).

Regarding to gravity loads, permanent and imposed load on office building floors considered, which are equal to 4.0 kN/m<sup>2</sup> and 3.0 kN/m<sup>2</sup>, respectively (see Table 3.3).

The total mass that can be accounted for inertial effects quantification is given by Clause 3.2.4(2)P of EN1998-1-1 (2004). In this study, the total mass is given by sum of permanent load and imposed load multiplied by a coefficient equal to 0.24.

Table 3.3 – Load Cases

Load Case	Description	Type	Value
<b>G</b>	Self-weight of structural elements	Permanent load	varies
	Permanent load on floor	Permanent load	$g_k = 4.0$ kN/m <sup>2</sup>
<b>Q<sub>1</sub></b>	Imposed load on office buildings (Cat. B)	Variable load	$q_{k1} = 3.0$ kN/m <sup>2</sup>
<b>A</b>	Seismic action	Seismic	varies

Concerning the load combination, the seismic design was based on two possible combinations, non-seismic and seismic (see Table 3.4).

Table 3.4 – Load Combinations

Design	Limit State	Combination	G	Q1	A
Non seismic	ULS	Ed1	1.35	1.5	-
Seismic	ULS and DAMAGE	Ed2	1.00	0.30	1.00

#### 3.2.4 Structural analysis

The analysis was carried out using the finite elements commercial software Autodesk Robot Structural Analysis Professional 2010. This software is well known for its capabilities in analysis of structures, particularly steel structures, offering various types of linear and non-linear analyses, having good import/export data solutions and offering post-processing to various codes.

The analyses used to carry out the study cases were all linear analyses. The modal response spectrum analyses were performed, according to EN1998-1-1 (2004) (clause 4.3.3.3). The responses of all modes of vibration contributing significantly to the global response were taken into account. The combination of modal responses was made using Complete Quadratic Combination (CQC). Moreover, all frames were modelled with 6 degree of freedom beam finite elements, in a 2D analysis.

Elements consisting of hot rolled steel profiles, such as beams and braces, were defined in the software using built-in databases, while welded steel profiles were computed in the software by inputting section geometry and, finally, composite columns were defined directly inputting their properties after being calculated according EN1994-1-1 (2004) and EN1998-1-1 (2004).

#### 3.2.5 Requirements to design the Moment-resisting Frames

The seismic design of MRFs is totally based on EN1998-1-1 (2004) where the philosophy weak-beam/strong-column is applied. The plastic hinges should be formed in the beams except at the base of the frame and at the top level of multi-storey frame. To obtain ductile plastic hinges in the beams, a set of rules for the dissipative and non-dissipative members are employed. The aim is to have beams where the full plastic moment resistance and rotation is not reduced due to compression and shear forces.

EN1998-1-1 (2004) states that moment applied ( $M_{Ed}$ ) on beam should not exceed the its design resistant moment ( $M_{pl,Rd}$ ). In addition, the axial force ( $N_{Ed}$ ) should not be higher than 15 percent of plastic resistance ( $N_{pl,Rd}$ ) and the capacity design establish that design shear ( $V_{Ed}$ ) should not exceed 50 per cent of the design plastic shear resistance ( $V_{pl,Rd}$ ). In addition, the shear force is obtained by the sum of shear forces due to the gravity and moment



components on the beam ( $V_{Ed} = V_{Ed,G} + V_{Ed,M}$ ), respectively. The following expressions apply:

$$\frac{M_{Ed}}{M_{pl,Rd}} \leq 1.0 \quad \frac{N_{Ed}}{N_{pl,Rd}} \leq 0.15 \quad \frac{V_{Ed}}{V_{pl,Rd}} \leq 1.0 \quad (3.3)$$

For the non-dissipative members (columns), the resistance capacity should be verified by unfavourable combination of bending moments, axial or shear forces:

$$X_{Rd} \geq X_{Ed,G} + 1.1 \times \gamma_{ov} \times \Omega_{MRF} \times X_{Ed,E} \quad (3.4)$$

in which, X represents the any member force – axial (N), shear (V) or bending moment (M); the parameter  $\Omega_{MRF}$  corresponds to overstrength of the building. In Equation (3.5), it is considered the minimum overstrength in the connected beams being defined as the overstrength of the most utilized beam:

$$\Omega_{MRF} = \frac{M_{pl,Rd}}{M_{Ed,i}} \quad (3.5)$$

The characters, “Ed,G” and “Ed,E”, correspond to seismic design situation for the gravity loads and lateral earthquake forces, respectively. In addition, the design axial forces on columns should not exceed 30 per cent of resistance capacity.

The designed cross sections for beam and columns and the relevant first and second natural periods per structure are reported in Table 3.5.

Table 3.5 – Sectional properties of columns and beams for MRFs

<i>Frames</i>	<i>Columns</i>		<i>Beams</i>					<i>Periods</i>	
	<i>1<sup>st</sup> to 4<sup>th</sup> floor</i>	<i>5<sup>th</sup> to 8<sup>th</sup> floor</i>	<i>1<sup>st</sup> to 2<sup>th</sup> floor</i>	<i>3<sup>th</sup> floor</i>	<i>4<sup>th</sup> floor</i>	<i>5<sup>th</sup> to 6<sup>th</sup> floor</i>	<i>7<sup>th</sup> to 8<sup>th</sup> floor</i>	<i>First</i>	<i>Second</i>
MRF_1.1.1.1.1	HEB 280	HEB 260	IPE 360	IPE 360	IPE 300	IPE 300	IPE 240	1.91	0.69
MRF_1.1.1.1.2	HEB 300	HEB 280	IPE 360	IPE 360	IPE 300	IPE 300	IPE 240	1.92	0.70
MRF_1.1.1.1.3	SHS 300x16	SHS 300x12	IPE 360	IPE 360	IPE 300	IPE 300	IPE 240	1.84	0.63
MRF_1.1.1.2.1	HEB 340	HEB 300	IPE 400	IPE 400	IPE 360	IPE 360	IPE 240	1.53	0.58
MRF_1.1.1.2.2	HEB 360	HEB 320	IPE 400	IPE 400	IPE 360	IPE 360	IPE 240	1.53	0.58
MRF_1.1.1.2.3	SHS 500x20	SHS 450x16	IPE 400	IPE 400	IPE 360	IPE 360	IPE 240	1.41	0.51
MRF_1.1.2.1.1	HEB 600	HEB 500	IPE 450	IPE 450	IPE 400	IPE 400	IPE 360	1.89	0.60
MRF_1.1.2.1.2	HEB 650	HEB 550	IPE 450	IPE 450	IPE 400	IPE 400	IPE 360	1.86	0.59
MRF_1.1.2.1.3	SHS 550x25	SHS500x25	IPE 450	IPE 450	IPE 400	IPE 400	IPE 360	1.89	0.60
MRF_1.1.2.2.1	HEB 650	HEB 550	IPE 550	IPE 550	IPE 500	IPE 500	IPE 360	1.43	0.51
MRF_1.1.2.2.2	HEB 700	HEB 600	IPE 550	IPE 550	IPE 500	IPE 500	IPE 360	1.42	0.50
MRF_1.1.2.2.3	SHS 600x25	SHS550x25	IPE 550	IPE 550	IPE 500	IPE 500	IPE 360	1.44	0.50

Table 3.5 – Sectional properties of columns and beams for MRFs(*Continued*)

<i>Frames</i>	<i>Columns</i>		<i>Beams</i>					<i>Periods</i>	
	<i>1<sup>st</sup> to 4<sup>th</sup> floor</i>	<i>5<sup>th</sup> to 8<sup>th</sup> floor</i>	<i>1<sup>st</sup> to 2<sup>th</sup> floor</i>	<i>3<sup>th</sup> floor</i>	<i>4<sup>th</sup> floor</i>	<i>5<sup>th</sup> to 6<sup>th</sup> floor</i>	<i>7<sup>th</sup> to 8<sup>th</sup> floor</i>	<i>First</i>	<i>Second</i>
MRF_3.1.1.1.1	HEB 280	-	IPE 300	IPE 270	IPE 270	-	-	1.08	0.32
MRF_3.1.1.1.2	HEB 300	-	IPE 300	IPE 270	IPE 270	-	-	1.10	0.33
MRF_3.1.1.1.3	SHS 300x16	-	IPE 300	IPE 270	IPE 270	-	-	1.11	0.34
MRF_3.1.1.2.1	HEB 320	-	IPE 300	IPE 270	IPE 270	-	-	1.02	0.29
MRF_3.1.1.2.2	HEB 360	-	IPE 300	IPE 270	IPE 270	-	-	1.02	0.29
MRF_3.1.1.2.3	SHS 400x12	-	IPE 300	IPE 270	IPE 270	-	-	1.02	0.28
MRF_3.1.2.1.1	HEB 400	-	IPE 400	IPE 360	IPE 360	-	-	1.10	0.31
MRF_3.1.2.1.2	HEB 450	-	IPE 400	IPE 360	IPE 360	-	-	1.08	0.31
MRF_3.1.2.1.3	SHS 400x20	-	IPE 400	IPE 360	IPE 360	-	-	1.12	0.33
MRF_3.1.2.2.1	HEB 500	-	IPE 400	IPE 360	IPE 360	-	-	1.00	0.26
MRF_3.1.2.2.2	HEB 550	-	IPE 400	IPE 360	IPE 360	-	-	0.99	0.26
MRF_3.1.2.2.3	SHS 500x20	-	IPE 400	IPE 360	IPE 360	-	-	1.01	0.27

### 3.2.6 Requirements to design the concentrically braced Frames

In CBFs in V-inverted, the braces, in tension and compression, are considered to be the main ductile members. The yielding/buckling of braces should occur before yielding or buckling of beams or columns. The diagonal elements of bracings should be placed in such a way that the structure has a similar behaviour under load reversals. To achieve this, the following rule should be applied at every storey:

$$\frac{|A^+ - A^-|}{A^+ + A^-} \leq 0.05 \quad (3.6)$$

in which  $A^+$  and  $A^-$  are the areas of the horizontal projections of the cross-sections of the tension diagonals, when the seismic action may have distinct horizontal directions.

The braces are designed applying the code EN1998-1-1 (2004) and EN1994-1-1 (2004) requirements of concerning the yield or compression resistance of diagonals that should be higher than the design axial force ( $N_{pl,Rd}$  or  $N_{b,Rd} > N_{Ed}$ ). Furthermore, the non-dimensional slenderness plays an important role in the behaviour of concentrically braced. Hence, the EN1998-1-1 (2004) imposes limit in which the concentrically braced frames in V should have braces with maximum non-dimensional slenderness of 2.0.

The non-dissipative elements (beams and columns) should be designed to resist the following condition:

$$N_{pl,Rd}(M_{Ed}) \geq N_{Ed,G} + 1.1 \times \gamma_{ov} \times \Omega_{CBF} \times N_{Ed,E} \quad (3.7)$$

In which  $N_{pl,Rd}(M_{Ed})$  is the design resistance of the beam or column taking into account the influence of the bending moment,  $N_{Ed,G}$  and  $N_{Ed,E}$  are the axial forces in non-dissipative element to seismic design situation for the gravity loads and lateral earthquake forces, respectively. The factor  $\Omega_{CBF}$  is the minimum overstrength; it corresponds to the following ratio from diagonal members:

$$\Omega_{CBF} = \frac{N_{pl,Rd,i}}{N_{Ed,i}} \quad (3.8)$$

In order to obtain a homogenous distribution of ductility, the EN1998-1-1 (2004) determines that maximum and minimum value of  $\Omega_{CBF}$  should not differ by more than 25 percent.

The beams in braced bays need to be designed for gravity loading without considering the intermediate support due to presence of braces, as well as account for an unbalanced vertical action due to brace buckling. According to EN1998-1-1 (2004), the post-buckling resistance should be accounted as 30 per cent of yield resistance. The distribution of forces to be considered on mid-length of the beam from braced bay is illustrated in Figure 3.12.

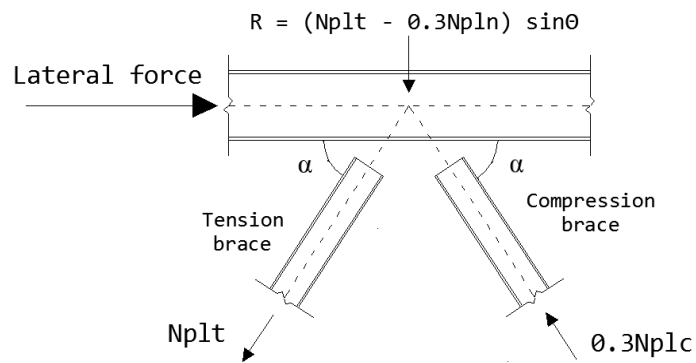


Figure 3.12 – Unbalanced force due to buckling of compression brace

The designed cross sections for beam and columns and the relevant first and second natural periods per structure are reported in Table 3.6.

Table 3.6 – Sectional properties of columns and beams for CBFs

<i>Frames</i>	<i>Columns</i>		<i>Beams (all outer are IPE 450)</i>		
	<i>1<sup>st</sup> to 4<sup>th</sup> floor</i>	<i>5<sup>th</sup> to 8<sup>th</sup> floor</i>	<i>1<sup>st</sup> to 4<sup>th</sup> floor</i>	<i>5<sup>th</sup> to 7<sup>th</sup> floor</i>	<i>8<sup>th</sup> floor</i>
CBF_1.1.1.1.1	HEM 300	HEB 300	HEA 450	HEA 360	HEA 360
CBF_1.1.1.1.2	HEM 360	HEB 300	HEA 450	HEA 360	HEA 300
CBF_1.1.1.1.3	SHS 400x20	SHS 300X8	HEB 450	HEA 360	HEA 300
CBF_1.1.1.2.1	PRS 400x400X21X40	HEB 300	HEB 450	HEA 450	HEA 400
CBF_1.1.1.2.2	PRS 450x400X21X40	HEB 300	HEB 450	HEA 450	HEA 400
CBF_1.1.1.2.3	BOX 400x400x30x20	SHS 300x10	HEB 450	HEA 450	HEA 400
CBF_1.1.2.1.1	HEM 400	HEB 300	HEB 550	HEA 500	HEA 360
CBF_1.1.2.1.2	HEM 700	HEB 300	HEB 500	HEA 500	HEA 360
CBF_1.1.2.1.3	BOX 450x400x20x20	SHS 300X10	HEB 500	HEA 500	HEA 360
CBF_1.1.2.2.1	PRS 620x300x25x40	HEB 300	HEB 550	HEB 500	HEA 360
CBF_1.1.2.2.2	PRS 700x350x25x40	HEB 300	HEB 550	HEA 500	HEA 360
CBF_1.1.2.2.3	BOX 500x450x25x20	SHS 300X12	HEB 550	HEB 500	HEA 360
CBF_1.2.2.1.2	PRS 262x310x21x39	HEB 300	HEA 500	HEA 450	HEA 320
CBF_1.2.2.1.3	BOX 350x380x16x16	SHS 300X10	HEA 500	HEA 450	HEA 320
CBF_1.2.2.2.2	PRS 398x307x21x40	HEB 300	HEA 500	HEA 450	HEA 320
CBF_1.2.2.2.3	BOX 400x400x20x20	SHS 300X12.5	HEB 500	HEA 450	HEA 320

Table 3.6 – Sectional properties of columns and beams for CBFs (*Continued*)

Frames	Columns				Beams (all outer are IPE 450)					
	1 <sup>st</sup> to 4 <sup>th</sup> floor	5 <sup>th</sup> to 8 <sup>th</sup> floor	9 <sup>th</sup> to 12 <sup>th</sup> floor	13 <sup>th</sup> to 16 <sup>th</sup> floor	1 <sup>st</sup> to 4 <sup>th</sup> floor	5 <sup>th</sup> to 7 <sup>th</sup> floor	8 <sup>th</sup> floor	9 <sup>th</sup> to 12 <sup>th</sup> floor	13 <sup>th</sup> to 15 <sup>th</sup> floor	16 <sup>th</sup> floor
CBF_2.1.2.1.1	PRS 700x300x25x60	HEM 500	HEB400	HEB280	HEB 500	HEB 450	HEB 450	HEA 340	HEA 280	HEA 280
CBF_2.1.2.1.2	PRS 750x330x25x70	HEM 700	HEB550	HEB280	HEB 500	HEB 450	HEB 450	HEA 340	HEA 280	HEA 280
CBF_2.1.2.2.1	PRS 600x700x40x100	PRS 700x600x18x40	HEM 700	HEB280	PRS 410x355x25 x45	PRS 400x370x20x 45	PRS 400x370x2 0x45	HEM 280	HEM 220	HEA 300
CBF_2.1.2.2.2	PRS 650x700x50x100	PRS 750x450x30x70	HEM900	HEB300	PRS 410x355x25 x45	PRS 370x400x20x 45	PRS 370x400x2 0x45	HEM 280	HEM 220	HEM 260
CBF_2.2.2.1.2	PRS 550x350x20x40	PRS 400x300x20x35	PRS 315x300x12.5x22.5	PRS 206x240x10x 17	HEB 400	HEA 450	HEA 450	IPE 400	IPE 330	IPE 330
CBF_2.2.2.1.3	BOX 450x500x18x18	BOX 350x410x16x16	BOX 330x360x12x 12	BOX 220x250x8x8	HEB 400	HEB 360	HEB 360	IPE 360	IPE 330	IPE 330
CBF_2.2.2.2.2	PRS 900x400x40x70	PRS 700x350x30x50	HEM 650	HEB 280	HEB 550	HEB 550	HEB 550	IPE 500	IPE 360	IPE 360
CBF_2.2.2.2.3	BOX 600x670x25x30	BOX 520x520x20x20	BOX 400x430x16x 16	BOX 220x220x10x 10	PRS 440x300x15 x30	PRS 440x300x15x 30	PRS 440x300x1 5x30	PRS 450x210x 10x15	PRS 290x160x 8x15	PRS 215x250x 8x12

Table 3.7 – Fundamental periods of the CBFs

<i>Frames</i>	<i>Periods</i>		<i>Frames</i>	<i>Periods</i>	
	<i>First</i>	<i>Second</i>		<i>First</i>	<i>Second</i>
CBF_1.1.1.1.1	0.95	0.34	CBF_1.2.2.1.2	1.06	0.39
CBF_1.1.1.1.2	0.95	0.33	CBF_1.2.2.1.3	1.09	0.39
CBF_1.1.1.1.3	0.95	0.33	CBF_1.2.2.2.2	0.97	0.35
CBF_1.1.1.2.1	0.84	0.32	CBF_1.2.2.2.3	0.98	0.38
CBF_1.1.1.2.2	0.83	0.33	CBF_2.1.2.1.1	2.30	0.72
CBF_1.1.1.2.3	0.89	0.33	CBF_2.1.2.1.2	2.33	0.72
CBF_1.1.2.1.1	0.97	0.38	CBF_2.1.2.2.1	1.55	0.54
CBF_1.1.2.1.2	0.95	0.38	CBF_2.1.2.2.2	1.67	0.57
CBF_1.1.2.1.3	1.02	0.36	CBF_2.2.2.1.2	2.59	0.78
CBF_1.1.2.2.1	0.86	0.37	CBF_2.2.2.1.3	2.86	0.82
CBF_1.1.2.2.2	0.86	0.37	CBF_2.2.2.2.2	1.94	0.62
CBF_1.1.2.2.3	0.90	0.38	CBF_2.2.2.2.3	2.18	0.69



Table 3.8 – Sectional properties of braces

<i>Frames</i>	<i>Braces</i>							
	<i>1<sup>st</sup> floor</i>	<i>2<sup>th</sup> floor</i>	<i>3<sup>th</sup> floor</i>	<i>4<sup>th</sup> floor</i>	<i>5<sup>th</sup> floor</i>	<i>6<sup>th</sup> floor</i>	<i>7<sup>th</sup> floor</i>	<i>8<sup>th</sup> floor</i>
CBF_1.1.1.1.1	CHS 193.7x10	CHS 193.7x10	CHS 193.7x10	CHS 168.3x10	CHS 168.3x10	CHS 168.3x8	CHS 139.7x6.3	CHS 114.3x5
CBF_1.1.1.1.2	CHS 193.7x12	CHS 193.7x10	CHS 193.7x10	CHS 168.3x10	CHS 168.3x10	CHS 168.3x8	CHS 139.7x8	CHS 114.3x6
CBF_1.1.1.1.3	CHS 219.1x10	CHS 219.1x10	CHS 193.7x10	CHS 168.3x10	CHS 168.3x10	CHS 168.3x8	CHS 139.7x8	CHS 114.3x6.3
CBF_1.1.1.2.1	CHS 219.1x10	CHS 244.5x12	CHS 244.5x12	CHS 244.5x10	CHS 244.5x10	CHS 193.7x10	CHS 168.3x8	CHS 139.7x5
CBF_1.1.1.2.2	CHS 244.5x8	CHS 244.5x12	CHS 244.5x12	CHS 244.5x10	CHS 244.5x10	CHS 193.7x10	CHS 193.7x6.3	CHS 139.7x5
CBF_1.1.1.2.3	CHS 244.5x10	CHS 244.5x10	CHS 244.5x10	CHS 219.1x10	CHS 219.1x10	CHS 219.1x8	CHS 193.7x6	CHS 139.7x5
CBF_1.1.2.1.1	CHS 219.1x12.5	CHS 219.1x12.5	CHS 219.1x12.5	CHS 219.1x10	CHS 219.1x10	CHS 193.7x10	CHS 168.3x8	CHS 168.3x6
CBF_1.1.2.1.2	CHS 219.1x12.5	CHS 219.1x12.5	CHS 219.1x12.5	CHS 219.1x10	CHS 219.1x10	CHS 193.7x10	CHS 168.3x8	CHS 168.3x6
CBF_1.1.2.1.3	CHS 219.1x12	CHS 219.1x12	CHS 219.1x12	CHS 193.7x12	CHS 193.7x12	CHS 193.7x10	CHS 168.3x8	CHS 168.3x6
CBF_1.1.2.2.1	CHS 273x12	CHS 273x12	CHS 273x12	CHS 244.5x12	CHS 244.5x12	CHS 244.5x10	CHS 219.1x8	CHS 168.3x6
CBF_1.1.2.2.2	CHS 273x12	CHS 273x12	CHS 273x12	CHS 244.5x12	CHS 244.5x12	CHS 244.5x10	CHS 219.1x8	CHS 168.3x6
CBF_1.1.2.2.3	CHS 273x12	CHS 273x12	CHS 273x12	CHS 244.5x12	CHS 244.5x12	CHS 244.5x10	CHS 219.1x8	CHS 168.3x6
CBF_1.2.2.1.2	CHS 219.1x12.5	CHS 219.1x12	CHS 219.1x12	CHS 219.1x10	CHS 219.1x10	CHS 193.7x10	CHS 168.3x8	CHS 168.3x6
CBF_1.2.2.1.3	CHS 219.1x12.5	CHS 219.1x12	CHS 219.1x12	CHS 219.1x10	CHS 219.1x10	CHS 193.7x10	CHS 168.3x8	CHS 168.3x6
CBF_1.2.2.2.2	CHS 273x12	CHS 273x12	CHS 273x12	CHS 244.5x10	CHS 244.5x10	CHS 219.1x10	CHS 193.7x8	CHS 168.3x6
CBF_1.2.2.2.3	CHS 273x12	CHS 273x12	CHS 273x12	CHS 244.5x10	CHS 244.5x10	CHS 219.1x10	CHS 193.7x8	CHS 168.3x6

Table 3.8 – Sectional properties of braces (*Continued*)

<i>Frames</i>	<i>Braces</i>							
	<i>1<sup>st</sup> floor</i>	<i>2<sup>nd</sup> floor</i>	<i>3<sup>rd</sup> floor</i>	<i>4<sup>th</sup> floor</i>	<i>5<sup>th</sup> floor</i>	<i>6<sup>th</sup> floor</i>	<i>7<sup>th</sup> floor</i>	<i>8<sup>th</sup> floor</i>
CBF_2.1.2.1.1	CHS 244.5x8	CHS 244.5x12	CHS 244.5x12	CHS 244.5x12	CHS 244.5x12	CHS 244.5x10	CHS 219.1x12	CHS 219.1x10
CBF_2.1.2.1.2	CHS 244.5x8	CHS 244.5x12	CHS 244.5x12	CHS 244.5x12	CHS 244.5x12	CHS 244.5x10	CHS 219.1x10	CHS 193.7x10
CBF_2.1.2.2.1	CHS 193.7x10	CHS 406.4x12.5	CHS 406.4x12.5	CHS 406.4x12.5	CHS 244.5x12.5	CHS 406.4x12.5	CHS 323.9x16	CHS 273x16
CBF_2.1.2.2.2	CHS 273x10	CHS 406.4x12.5	CHS 406.4x12.5	CHS 406.4x12.5	CHS 244.5x12.5	CHS 406.4x12.5	CHS 323.9x16	CHS 273x16
CBF_2.2.2.1.2	CHS 244.5x10	CHS 244.5x12	CHS 244.5x12	CHS 244.5x12	CHS 244.5x12	CHS 244.5x10	CHS 219.1x10	CHS 193.7x10
CBF_2.2.2.1.3	CHS 244.5x12	CHS 273x12	CHS 273x10	CHS 273x10	CHS 244.5x10	CHS 244.5x10	CHS 244.5x8	CHS 219.1x8
CBF_2.2.2.2.2	CHS 273x10	CHS 355.6x12.5	CHS 355.6x12.5	CHS 355.6x12.5	CHS 355.6x12.5	CHS 355.6x12	CHS 355.6x12	CHS 355.6x12
CBF_2.2.2.2.3	CHS 323.9x12.5	CHS 323.9x12.5	CHS 323.9x12.5	CHS 323.9x12	CHS 323.9x12	CHS 323.9x12	CHS 273x12.5	CHS 273x12

Table 3.8 – Sectional properties of braces (*Continued*)

<i>Frames</i>	<i>Braces</i>							
	<i>9<sup>th</sup> floor</i>	<i>10<sup>th</sup> floor</i>	<i>11<sup>th</sup> floor</i>	<i>12<sup>th</sup> floor</i>	<i>13<sup>th</sup> floor</i>	<i>14<sup>th</sup> floor</i>	<i>15<sup>th</sup> floor</i>	<i>16<sup>th</sup> floor</i>
CBF_2.1.2.1.1	219,1 x 10,0	219,1 x 10,0	193,7 x 10,0	193,7 x 10,0	193,7 x 10,0	168,3 x 10,0	168,3 x 8,0	168,3 x 6,0
CBF_2.1.2.1.2	193,7 x 10,0	193,7 x 10,0	193,7 x 10,0	193,7 x 10,0	193,7 x 10,0	168,3 x 10,0	168,3 x 8,0	168,3 x 6,0
CBF_2.1.2.2.1	273 x 16	273 x 16	244,5 x 16	219,1 x 16	244,5 x 12	219,1 x 12	219,1 x 8	193,7 x 6
CBF_2.1.2.2.2	273 x 16	273 x 16	244,5 x 16	219,1 x 16	244,5 x 12	219,1 x 12	219,1 x 8	193,7 x 6
CBF_2.2.2.1.2	193,7 x 10,0	193,7 x 10,0	193,7 x 10,0	193,7 x 10,0	193,7 x 10,0	168,3 x 10,0	168,3 x 8,0	168,3 x 6,0
CBF_2.2.2.1.3	193,7 x 8	193,7 x 8	193,7 x 8	193,7 x 8	193,7 x 8	193,7 x 8	168,3 x 8	168,3 x 6
CBF_2.2.2.2.2	323,9 x 12,0	323,9 x 12,0	323,9 x 10,0	273,0 x 10,0	244,5 x 10,0	219,1 x 10,0	193,7 x 8,0	168,3 x 6,3
CBF_2.2.2.2.3	244,5 x 12,5	244,5 x 12	219,1 x 12	219,1 x 12	219,1 x 10	193,7 x 10	193,7 x 8	168,3 x 6

### 3.2.7 Requirements to design the Dual-Concentrically braced Frames

As described previously, the D-CBFs combine the MRF system with CBF one. The design rules in EN1998-1-1 (2004) are scarce and AISC-341 (2005) was used to balance the resistance between both structural systems. The MRF system was imposed a minimum lateral strength equal to 25 per cent. Thus, the following expression was used to determine the lateral strength of MRF part:

$$V_{Rd,i}^{MRF} \geq 0.25 \times V_{Rd,i}^{DUAL} \rightarrow V_{Rd,i}^{DUAL} = \frac{1}{0.75} \times (N_{plt} + 0.3 \times N_{plc})_i \times \cos \alpha_i \quad (3.9)$$

in which,  $V_{Rd,i}$  is the base shear resistance at the  $i$ -th storey and  $\alpha_i$  is the angle that the braces make with the horizontal direction. The minimum resistance of the MRF part is derived from the plastic resistance of the brace for a specify storey. This resistance is considered for both compression and tension braces applying the post-buckling effect according EN1998-1-1 (2004).

The members belonging to each structural system are designed in accordance with the respective rules given in EN1998-1-1 (2004).

It is important to observe that there are two different  $\Omega$  factors according to the structural system. So, the non-dissipative members belonging to MRF part are checked applying the overstrength factor ( $\Omega_{MRF}$ ) from the MRF part and the non-dissipative structural members from CBF system are designed considering the brace overstrength ( $\Omega_{CBF}$ ).

The designed cross sections for beam and columns and the relevant first and second natural periods per structure are reported in Table 3.9.

Table 3.9 – Sectional properties of columns and beams for D-CBFs

<i>Frames</i>	<i>Columns</i>		<i>Beams (Inner/Outer)</i>		
	<i>1<sup>st</sup> to 4<sup>th</sup> floor</i>	<i>5<sup>th</sup> to 8<sup>th</sup> floor</i>	<i>1<sup>st</sup> to 4<sup>th</sup> floor</i>	<i>5<sup>th</sup> to 7<sup>th</sup> floor</i>	<i>8<sup>th</sup> floor</i>
D-CBF_1.1.1.1.1	HEB 300	HEB 180	IPE 500/IPE400	IPE 450/IPE330	IPE 330/IPE240
D-CBF_1.1.1.1.2	HEB 340	HEB 200	IPE 500 / IPE400	IPE 450 / IPE330	IPE 330/IPE/240
D-CBF_1.1.1.1.3	SHS 300x12,5	SHS 220x6,3	IPE 500 / IPE400	IPE 450 / IPE330	IPE 330 / IPE240
D-CBF_1.1.1.2.1	HEB 320	HEB 200	IPE 550 / IPE400	IPE 500 / IPE360	IPE 330 / IPE240
D-CBF_1.1.1.2.2	HEB 400	HEB 220	IPE 550 / IPE400	IPE 500 / IPE360	IPE 330 / IPE240
D-CBF_1.1.1.2.3	SHS 350x12,5	SHS 250x16	IPE 550 / IPE400	IPE 500 / IPE360	IPE 330 / IPE240
D-CBF_1.1.2.1.1	HEM 300	HEB 300	HEB450 /IPE500	HEA450 /IPE450	HEA320 /IPE360
D-CBF_1.1.2.1.2	HEM 300	HEB 300	HEB 450/IPE500	HEA 450/IPE450	HEA320/IPE 360
D-CBF_1.1.2.1.3	SHS 400x16	SHS 300x8	HEB 450/IPE500	HEA 450/IPE450	HEA 320/IPE360
D-CBF_1.1.2.2.1	HEM 300	HEB 300	HEB 500/IPE500	HEA 450/IPE450	HEA 320/IPE360
D-CBF_1.1.2.2.2	HEM 400	HEB 300	HEB 500/IPE500	HEA 450/IPE450	HEA 320/IPE360
D-CBF_1.1.2.2.3	SHS 400x20	SHS 300x10	HEB 500/IPE500	HEA 450/IPE450	HEA 320/IPE360
D-CBF_1.2.2.1.2	PRS 398x300x14x26	HEB 300	PRS 398x300x11,5x21 / IPE 500	PRS 315x300x10x17,5 / IPE 450	PRS 262x300x8,50x14 / IPE360
D-CBF_1.2.2.1.3	BOX 325x380x12,5x12,5	SHS 300x8	PRS 398x300x11,5x21 / IPE500	PRS 315x300x10x17,5 / IPE450	PRS 262x300x8,5x14 / IPE360
D-CBF_1.2.2.2.2	PRS 262x310x21x39	HEB 300	PRS 444x300x12x23 / IPE 500	PRS 352x300x11x19 / IPE 450	PRS 262x300x8,50x14 / IPE 360
D-CBF_1.2.2.2.3	BOX 318x380x16x16	SHS 300x8	PRS 444x300x12x23 / IPE 500	PRS 352x300x11x19 / IPE450	PRS 262x300x8,50x14 / IPE 360

Table 3.9 – Sectional properties of columns and beams for D-CBFs (*Continued*)

Frames	Columns				Beams (Inner/Outer)					
	1 <sup>st</sup> to 4 <sup>th</sup> floor	5 <sup>th</sup> to 8 <sup>th</sup> floor	9 <sup>th</sup> to 12 <sup>th</sup> floor	13 <sup>th</sup> to 16 <sup>th</sup> floor	1 <sup>st</sup> to 4 <sup>th</sup> floor	5 <sup>th</sup> to 7 <sup>th</sup> floor	8 <sup>th</sup> floor	9 <sup>th</sup> to 12 <sup>th</sup> floor	13 <sup>th</sup> to 15 <sup>th</sup> floor	16 <sup>th</sup> floor
D-CBF_2.1.2.1.1	HEM 700	HEB 500	HEB 320	HEB 280	HEB 500 / HEA 400	HEB 450 / IPE 500	HEB 450 / IPE 450	HEA 320 / IPE 450	HEA 280 / IPE 400	HEB 220 / HEB 240
D-CBF_2.1.2.1.2	PRS 700x400x20x 40	HEM 400	HEB 360	HEB280	HEB 500 / HEA 400	HEB 450 / IPE 500	HEB 450 / IPE 450	HEA 320 / IPE 450	HEA 280 / IPE 400	HEA 280 / HEB 240
D-CBF_2.1.2.2.1	PRS 600x450x25x 60	HEM 650	HEB 450	HEB 300	HEM 400 / HEB 500	HEM 360 / HEB 500	HEM 360/ HEA 400	HEA 360 / HEA 400	HEA 280 / IPE 450	HEM 180 / HEB 240
D-CBF_2.1.2.2.2	PRS 900x500x20x 65	PRS 700x400x20x 40	HEB 600	HEB 280	HEM 450 / HEA 500	HEM 400 / HEA 500	HEM 400/ HEA400	HEA 360 /HEA 400	HEA 280 / IPE 450	HEA 280 / HEB 240
D-CBF_2.2.2.1.2	PRS 600x350x20x 40	PRS 444x300x15x 28	PRS 314x300x13x 23	HEB 280	PRS 444x300x14,5x 28/ HEA 400	PRS 398x300x11,5x 21/ IPE 500	PRS 398x300x11,5 x21/ IPE 450	PRS 279x300x9,0x1 5,5/ IPE 450	PRS 280x244x8,0x 13,0/ IPE 400	PRS 280x244x8,0x 13,0/ HEA280
D-CBF_2.2.2.1.3	BOX 360x430x20x 20	BOX 318x380x16x 16	BOX 276x330x12x 12	BOX 204x250x8 x8	PRS 352x300x13,5x 24/ HEA 400	PRS 315x300x12,5x 22,5/ IPE 500	PRS 315x300x12,5 x22,5/ IPE 450	PRS 334x170x8,0x1 2,7/ IPE 450	PRS 307x160xx7,5 x11,5/ IPE 400	PRS 249x135x6,6x 10,2/ IPE 360
D-CBF_2.2.2.2.2	PRS 900x400x20x 50	PRS 750x300x20x 40	PRS 540x300x16x 30	HEB 280	PRS 398x307x21x40 / HEA 500	PRS 352x307x21x4 0/ HEA 500	PRS 352x307x21x4 0/ HEA 400	PRS 315x300x10x17 ,5/ IPE 400	PRS 244x280x8x13 / IPE 450	PRS 244x280x8x13 / HEB 240
D-CBF_2.2.2.2.3	BOX 450x420x30x 25	BOX 360x450x20x 20	SHS 400x16	SHS 250x10	PRS 444x300x14,5x 28/ HEA 500	PRS 350x300x14x2 5/ HEA 450	PRS 350x300x14x2 5/ IPE 500	PRS 371x180x11x14 ,5/ IPE 500	PRS 335x170x8x12 ,7/ IPE 450	PRS 188x220x7x11 / IPE 360

Table 3.10 – Fundamental periods of the D-CBFs

<i>Frames</i>	<i>Periods</i>		<i>Frames</i>	<i>Periods</i>	
	<i>First</i>	<i>Second</i>		<i>First</i>	<i>Second</i>
D-CBF_1.1.1.1.1	1.03	0.38	D-CBF_1.2.2.1.2	1.07	0.38
D-CBF_1.1.1.1.2	1.05	0.38	D-CBF_1.2.2.1.3	1.11	0.39
D-CBF_1.1.1.1.3	1.10	0.39	D-CBF_1.2.2.2.2	1.01	0.37
D-CBF_1.1.1.2.1	0.94	0.35	D-CBF_1.2.2.2.3	1.04	0.37
D-CBF_1.1.1.2.2	0.95	0.35	D-CBF_2.1.2.1.1	2.16	0.73
D-CBF_1.1.1.2.3	0.96	0.35	D-CBF_2.1.2.1.2	2.20	0.73
D-CBF_1.1.2.1.1	1.02	0.37	D-CBF_2.1.2.2.1	1.76	0.63
D-CBF_1.1.2.1.2	1.05	0.38	D-CBF_2.1.2.2.2	1.76	0.62
D-CBF_1.1.2.1.3	1.05	0.38	D-CBF_2.2.2.1.2	2.25	0.73
D-CBF_1.1.2.2.1	0.96	0.36	D-CBF_2.2.2.1.3	2.51	0.81
D-CBF_1.1.2.2.2	0.98	0.36	D-CBF_2.2.2.2.2	1.82	0.62
D-CBF_1.1.2.2.3	1.00	0.37	D-CBF_2.2.2.2.3	2.12	0.68

Table 3.11 – Sectional properties of braces for D-CBFs

<i>Frames</i>	<i>Braces</i>							
	<i>1<sup>st</sup> floor</i>	<i>2<sup>nd</sup> floor</i>	<i>3<sup>rd</sup> floor</i>	<i>4<sup>th</sup> floor</i>	<i>5<sup>th</sup> floor</i>	<i>6<sup>th</sup> floor</i>	<i>7<sup>th</sup> floor</i>	<i>8<sup>th</sup> floor</i>
D-CBF_1.1.1.1.1	CHS 193.7x8	CHS 193.7x6.3	CHS 139.7x8	CHS 139.7x8	CHS 139.7x8	CHS 139.7x6	CHS 114.3x6	CHS 114.3x3.6
D-CBF_1.1.1.1.2	CHS 193.7x8	CHS 193.7x6.3	CHS 168.3x6.3	CHS 139.7x8	CHS 139.7x8	CHS 139.7x6	CHS 114.3x6	CHS 114.3x3.6
D-CBF_1.1.1.1.3	CHS 193.7x8	CHS 193.7x6.3	CHS 168.3x6.3	CHS 139.7x8	CHS 139.7x8	CHS 139.7x6	CHS 114.3x6	CHS 114.3x3.6
D-CBF_1.1.1.2.1	CHS 193.7x10	CHS 193.7x8	CHS 193.7x6.3	CHS 168.3x8	CHS 168.3x8	CHS 139.7x8	CHS 114.3x6	CHS 114.3x3.6
D-CBF_1.1.1.2.2	CHS 193.7x10	CHS 193.7x8	CHS 193.7x8	CHS 193.7x6.3	CHS 193.7x6.3	CHS 168.3x6.3	CHS 114.3x6	CHS 114.3x3.6
D-CBF_1.1.1.2.3	CHS 193.7x10	CHS 193.7x8	CHS 193.7x8	CHS 168.3x8	CHS 168.3x8	CHS 139.7x8	CHS 114.3x6	CHS 114.3x3.6
D-CBF_1.1.2.1.1	CHS 219.1x10	CHS 219.1x10	CHS 219.1x10	CHS 193.7x8	CHS 168.3x10	CHS 168.3x8	CHS 168.3x6	CHS 139.7x5
D-CBF_1.1.2.1.2	CHS 219.1x10	CHS 219.1x10	CHS 193.7x10	CHS 193.7x8	CHS 168.3x10	CHS 168.3x8	CHS 168.3x6	CHS 139.7x5
D-CBF_1.1.2.1.3	CHS 219.1x10	CHS 219.1x10	CHS 193.7x10	CHS 193.7x8	CHS 168.3x10	CHS 168.3x8	CHS 168.3x6	CHS 139.7x5
D-CBF_1.1.2.2.1	CHS 244.5x12	CHS 244.5x10	CHS 219.1x12	CHS 193.7x12	CHS 193.7x10	CHS 193.7x8	CHS 168.3x6	CHS 139.7x5
D-CBF_1.1.2.2.2	CHS 244.5x10	CHS 244.5x10	CHS 219.1x10	CHS 219.1x10	CHS 193.7x10	CHS 193.7x8	CHS 168.3x6.3	CHS 139.7x5
D-CBF_1.1.2.2.3	CHS 244.5x10	CHS 244.5x10	CHS 219.1x10	CHS 193.7x10	CHS 193.7x10	CHS 193.7x8	CHS 168.3x6.3	CHS 139.7x5
D-CBF_1.2.2.1.2	CHS 219.1x10	CHS 219.1x10	CHS 193.7x10	CHS 193.7x8	CHS 168.3x10	CHS 168.3x8	CHS 168.3x6	CHS 139.7x5
D-CBF_1.2.2.1.3	CHS 219.1x10	CHS 219.1x10	CHS 193.7x10	CHS 193.7x8	CHS 168.3x10	CHS 168.3x8	CHS 168.3x6	CHS 139.7x5
D-CBF_1.2.2.2.2	CHS 244.5x12	CHS 244.5x10	CHS 219.1x10	CHS 219.1x10	CHS 193.7x10	CHS 193.7x8	CHS 168.3x6.3	CHS 139.7x5
D-CBF_1.2.2.2.3	CHS 244.5x12	CHS 244.5x10	CHS 219.1x10	CHS 193.7x10	CHS 193.7x10	CHS 193.7x8	CHS 168.3x6.3	CHS 139.7x5



Table 3.12 – Sectional properties of braces for D-CBFs

<i>Frames</i>	<i>Braces</i>							
	<i>1<sup>st</sup> floor</i>	<i>2<sup>th</sup> floor</i>	<i>3<sup>th</sup> floor</i>	<i>4<sup>th</sup> floor</i>	<i>5<sup>th</sup> floor</i>	<i>6<sup>th</sup> floor</i>	<i>7<sup>th</sup> floor</i>	<i>8<sup>th</sup> floor</i>
D-CBF_2.1.2.1.1	CHS 219.1x8	CHS 244.5x12	CHS 244.5x10	CHS 244.5x10	CHS 219.1x10	CHS 219.1x10	CHS 219.1x10	CHS 219.1x8
D-CBF_2.1.2.1.2	CHS 219.1x8	CHS 219.1x12.5	CHS 219.1x12	CHS 219.1x12	CHS 219.1x10	CHS 219.1x10	CHS 219.1x10	CHS 193.7x10
D-CBF_2.1.2.2.1	CHS 273x10	CHS 323.9x12	CHS 323.9x12	CHS 323.9x12	CHS 273x12.5	CHS 273x12	CHS 244.5x12	CHS 244.5x12
D-CBF_2.1.2.2.2	CHS 193.7x8	CHS 323.9x12	CHS 323.9x12	CHS 323.9x12	CHS 323.9x12	CHS 273x12	CHS 273x12	CHS 244.5x12
D-CBF_2.2.2.1.2	CHS 219.1x10	CHS 244.5x12	CHS 219.1x12	CHS 219.1x12	CHS 219.1x12	CHS 219.1x10	CHS 219.1x10	CHS 193.7x10
D-CBF_2.2.2.1.3	CHS 219.1x12.5	CHS 219.1x12.5	CHS 219.1x12	CHS 193.7x12	CHS 193.7x12	CHS 193.7x12	CHS 193.7x10	CHS 193.7x10
D-CBF_2.2.2.2.2	CHS 219.1x10	CHS 323.9x12.5	CHS 323.9x12	CHS 323.9x12	CHS 323.9x12	CHS 273x12	CHS 273x12	CHS 244.5x12
D-CBF_2.2.2.2.3	CHS 323.9x12	CHS 323.9x12	CHS 323.9x12	CHS 273x12	CHS 193.7x12	CHS 193.7x12	CHS 193.7x12	CHS 273x12

Table 3.13 – Sectional properties of braces for D-CBFs

<i>Frames</i>	<i>Braces</i>							
	<i>9<sup>th</sup> floor</i>	<i>10<sup>th</sup> floor</i>	<i>11<sup>th</sup> floor</i>	<i>12<sup>th</sup> floor</i>	<i>13<sup>th</sup> floor</i>	<i>14<sup>th</sup> floor</i>	<i>15<sup>th</sup> floor</i>	<i>16<sup>th</sup> floor</i>
D-CBF_2.1.2.1.1	219,1 x 8	219,1 x 8	193,7 x 8	168,3 x 8	168,3 x 8	168,3 x 8	168,3 x 6	139,7 x 5
D-CBF_2.1.2.1.2	193,7 x 10	193,7 x 10	168,3 x 10	168,3 x 10	139,7 x 10	139,7 x 10	139,7 x 8	139,7 x 5
D-CBF_2.1.2.2.1	244,5 x 12	219,1 x 12,5	219,1 x 12,0	193,7 x 12	168,3 x 12	168,3 x 10	168,3 x 6	139,7 x 5
D-CBF_2.1.2.2.2	244,5 x 12,5	219,1 x 12,5	193,7 x 12,5	193,7 x 10	168,3 x 12,5	168,3 x 10	168,3 x 6,3	139,7 x 5
D-CBF_2.2.2.1.2	193,7 x 10	193,7 x 10	168,3 x 10	168,3 x 10	168,3 x 10	139,7 x 10	139,7 x 8	139,7 x 5
D-CBF_2.2.2.1.3	193,7 x 10	168,3 x 10	168,3 x 10	168,3 x 8	168,3 x 8	168,3 x 8	168,3 x 6	139,7 x 5
D-CBF_2.2.2.2.2	244,5 x 12,0	219,1 x 12,5	193,7 x 12,5	193,7 x 10,0	168,3 x 12,5	168,3 x 10	168,3 x 6,3	139,7 x 5
D-CBF_2.2.2.2.3	244,5 x 10	244,5 x 10	219,1 x 10	193,7 x 10	193,7 x 10	168,3 x 10	168,3 x 6	139,5 x 5

### 3.2.8 Comments on the seismic design

The aim of the seismic design was to find the most economical solution by monitoring the overstrength factor within of the dissipative element in which this factor is associated applying an expression in order to define the actions of the non-dissipative elements. Therefore, the main idea was to find a structural configuration that could provide a minimum overstrength factor (approximately equal to 1.0). This corresponds to the formation of the first plastic hinge for the dissipative elements. Nevertheless, there are some cases in which the seismic design was governed by criteria associated to local or global instability, as well as, limit imposed by serviceability.

#### ***Moment-resisting Frames***

For the MRFs, the strategy adopted was to keep the beam dimensions to the minimum required by the vertical loads and to choose appropriate columns sections, in order to verify the damage limit state under seismic load combination. The idea is to promote a collapse plastic mechanism of the global type.

Figure 3.13 depicts the overstrength factors obtained for MRFs with an overall average of 1.37. The non-seismic combination controlled the design of the beams resulting in larger overstrength factors. The frames located in soft soil present smaller overstrength factors due to larger seismic demand, mainly for the taller frames. The span length has significant influence on the low rise frames. Moreover, increasing the number of storeys is possible to see a reduction of the overstrength factors.

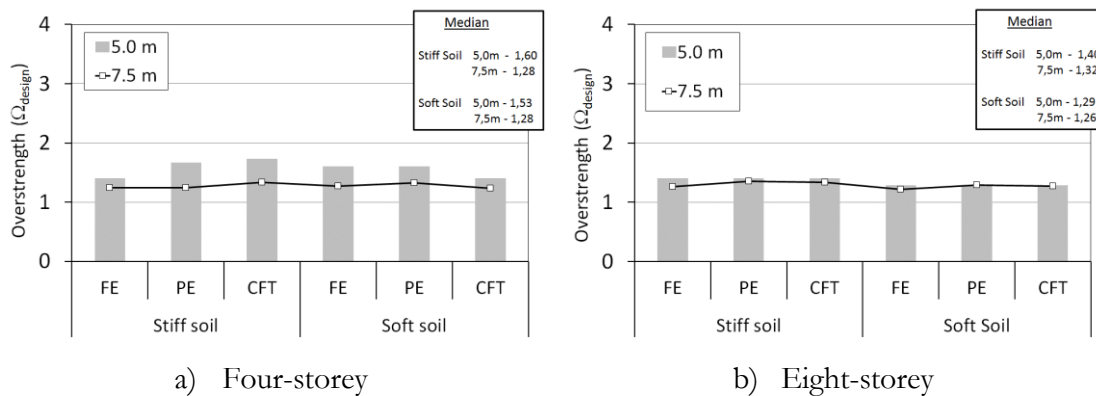


Figure 3.13 – Overstrength factors derived from seismic design (MRFs)

In general, the seismic design of the MRFs was governed by damage limitation requirements. This result, at some point, was expected, due to its inherent flexibility. According to EN1998-1-1 (2004), the second-order effects are evaluated through an inter-storey drift sensitivity coefficient,  $\theta$ . The second-order effects may be ignored for  $\theta \leq 0.1$ , whilst for values between 0.1 and 0.2; the second-order effects may be approximately accounted for

using a multiplier that amplifies the seismic action. This criterion has direct implication on seismic design for the MRFs. In recent study, Castro et al. (2009) showed that the EN1998-1-1 (2004) requirements for the coefficient,  $\theta$ , are quite stringent in comparison with other codes. The consequence is that the use of HSS for the MRFs may not be advantageous since the size of cross-sections is governed by displacement instead of resistance criteria and is chosen to provide adequate lateral stiffness.

### ***Concentrically Braced Frames***

For this structural system, the braces are the responsible for the energy dissipation and the overstrength is given by the ratio between the axial capacity of the braces and the axial force from seismic combination. As before, the aim is to have as small as possible overstrength factors. Figure 3.14 shows the overstrength factors obtained for the CBFs.

In order to achieve satisfactory hysteretic behaviour and avoid shock loading under cyclic conditions, the non-dimensionless slenderness should not exceed 2.0 for CBFs with V-inverted. Fulfilling this clause, the braces need to have adequate dimensions and an increasing of the size of the cross-sections is also necessary. So, together with the clause that determines that the energy dissipation should be homogenous at long the height of the building, which the maximum overstrength should not be greater than 25% of the minimum value, the size of brace cross-section is conditioned by non-dimensionless slenderness criterion instead of the resistance capacity. Furthermore, the overstrength factor is obtained by considering the plastic capacity of the braces instead of the buckling capacity. However, due to the brace length, the capacity of the braces is reduced by the buckling effects also resulting in higher overstrength factors.

Analysing the results in Figure 3.14 it becomes obvious that the frames with 5.0m of span show higher overstrength factor in comparison with the frames with larger span. This is due to difference between the design axial force of the braces and their buckling capacity. The braces from upper floor, where this difference is more pronounced, determined the minimum overstrength due to a large difference between the design load and capacity resistance. On the other hand, when the seismic demand is increased, the overstrength decreases because the difference between the design load and the capacity resistance also decreases (there is an increasing of the axial load on the braces). No noticeable differences are appreciated for the employment of a superior steel grade on the non-dissipative members. Moreover, the taller frames present larger overstrength than other frames, expect for the cases where S460 and stiff soil are considered.

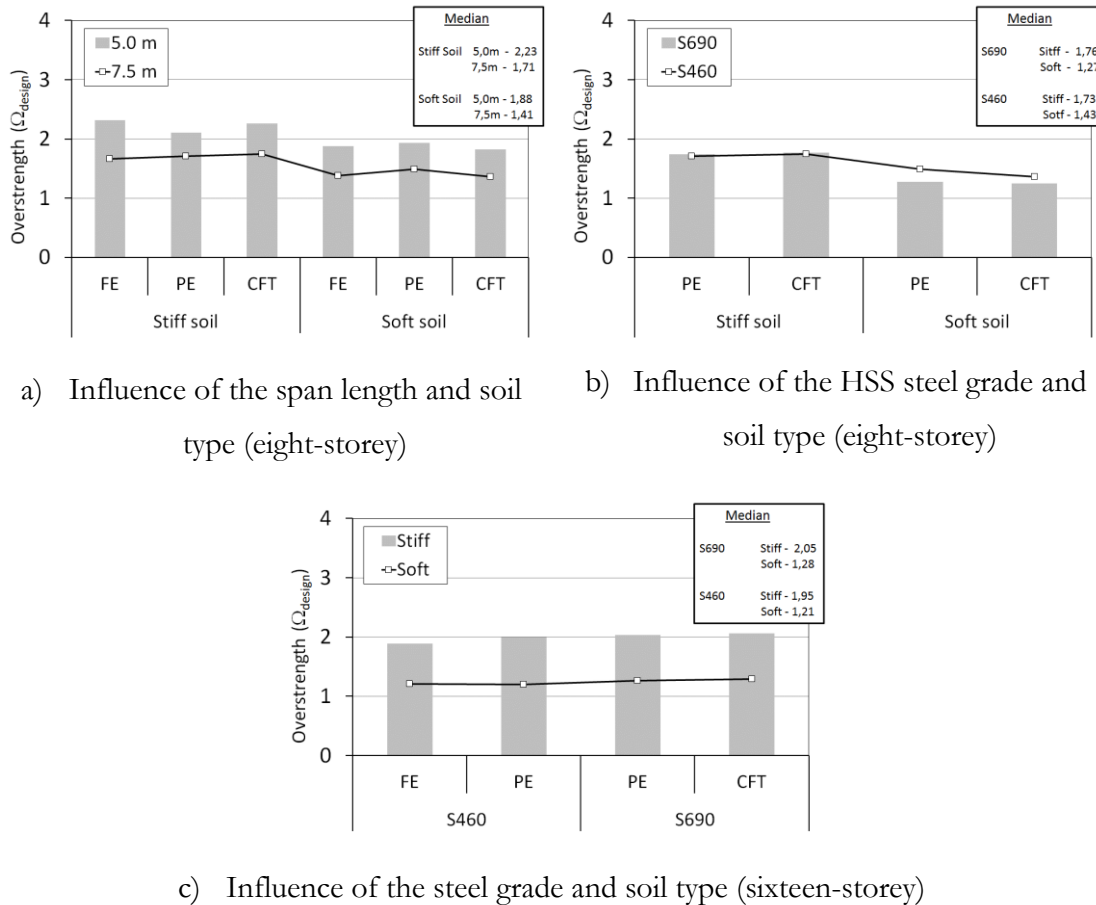


Figure 3.14 – Overstrength factors derived from seismic design (CBFs)

Different from the MRFs, the second-order effects and inter-storey drifts do not govern design, even though these requirements may lead to modification of member sizes in some cases.

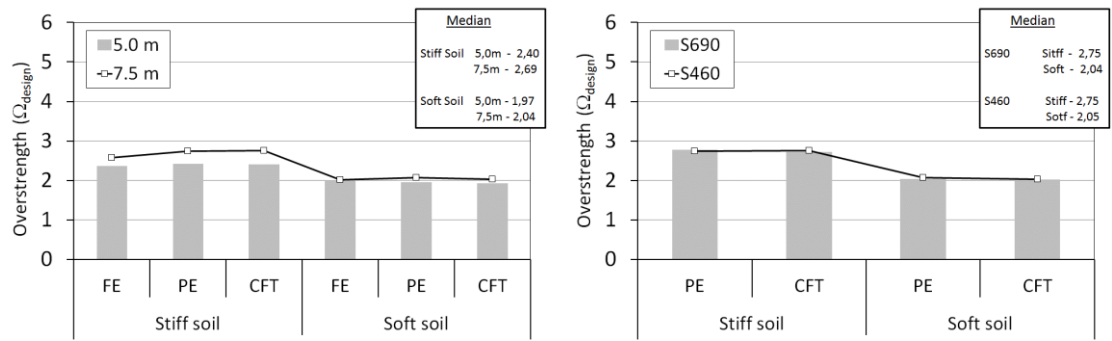
### ***Dual-Concentrically Braced Frames***

For the dual-system, the same comments are valid concerning the non-dimensionless slenderness previously discussed for CBFs as well as the difference between to consider the plastic resistance instead the buckling resistance on the expression of the overstrength. These issues become even more prominent for the dual-system because the beams in the MRF part are designed considering the plastic resistance of the braces. Therefore, the increasing of the braces also resulted in an increasing of the beam size. Moreover, the use of a high behaviour factor increased this influence of the non-dimensionless criterion on seismic design.

Figure 3.15 shows the overstrength factor from the seismic design of the D-CBFs for the braces only. The use of a superior behaviour factor allowed increasing the difference between the demand and capacity of the braces with values for the D-CBFs larger than those obtained for the CBFs. Concerning to soil condition, the increasing of the seismic demand

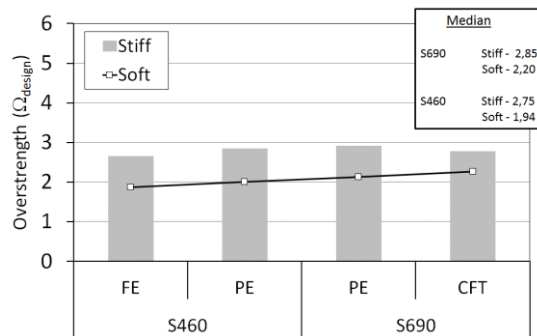
provided smaller overstrength factors. There are no significant differences between the two HSS steel grades. Moreover, the taller frames presented larger overstrength compared to frames with eight-storey.

The design of beam from the MRFs part was governed by criterion concerning the minimum resistance to be defined to consider that a structure is Dual. Thus, the size of beam is established to fulfil this criterion. This scenario resulted in an overstrength average of 1.54 in case of the sixteen-storey frames while a value of 2.36 is found for the frames with eight storey. These high values clearly justify the fact discussed above about the system to be considered Dual or Non-Dual.



a) Influence of the span length and soil type (eight-storey)

b) Influence of the HSS steel grade and soil type (eight-storey)



c) Influence of the steel grade and soil type (sixteen-storey)

Figure 3.15 – Overstrength factors derived from seismic design (D-CBFs)

## *Chapter IV*

# Nonlinear Analysis Methodology

The nonlinear analyses both static and dynamic are standard methods presented in the current seismic design codes. However, it is important to define detailed numerical modelling instructions, since an accurate numerical model plays a key role in the evaluation of building performance.

This Chapter aims at providing the description of the methodology adopted in order to assess the nonlinear behaviour of the study cases. The focus is on the criteria to be assumed to investigate the performance objectives. A part of this Chapter is also addressed to the implementation of numerical model showing the assumptions assumed and comparing it with experimental tests present in literature.

### **4.1 Performance based evaluation**

The structures subjected to recent seismic events obtained a good behaviour concerning the life safety designed by the current codes. However, severe damages on structures, as well as economic loss due to lack of use and repair cost were unexpectedly high. Hence, the codes are in a process of fundamental change, and the goal is to reduce these high losses.

Performance-based design (PBD) is expressed in terms of performance criteria when the structure is subjected to different seismic hazard levels represented by either magnitudes or accelerations. The level of ground motion acceleration for each performance level (limit state) may be determined as a function of the return periods, which are related to a certain probability of exceedance during predefined periods of time. In this research, the seismic performance has been analysed through static and dynamic nonlinear analyses compared with three limit states as defined in EN1998-1-3 (2005): Damage Limitation (DL), Severe Damage (SL) and Near Collapse (NC).

The static nonlinear analyses provide the overstrength factor used to determine the behaviour factor according to European method. The dynamic analyses are used to determine the seismic performance for the three limit states, as well as the behaviour factors. For each limit state, behaviour factors are obtained using the approaches found in the literature.

#### 4.1.1 *Performance criteria*

According to EN1998-1-1 (2004) at the DL state the building is subjected to the frequent earthquake with 95-year-return period, the structure shall have no occurrence of damage and the associated limitations of use. EN1998-1-3 (2005) presents a reduction factor  $v$  taking into account the determination of the frequent earthquake from the design earthquake. In the examined cases,  $v$  is equal to 0.5 and the corresponding structural performance should provide inter-storey drift ratios lesser than 0.75% (EN1998-1-1, 2004).

The SD state corresponds to design condition where the structure shall have no local or global collapse under the design seismic action with 475-year-return period. At this performance level, the structure is strongly damaged but has some residual lateral strength and stiffness; moreover, vertical elements are capable of sustaining vertical loads, thus providing the strength to sustain moderate after-shocks.

At the NC state, the structures are expected to be heavily damaged, with negligible residual lateral strength and stiffness, although vertical elements are still capable of sustaining vertical loads. Large permanent drifts are present. The structures are near collapse and are not able to resist to moderate earthquake after-shocks. This performance level corresponds to a seismic action with 2475-year-return period.

Table 3.4 shows the performance levels together with their seismic intensity, as well as their associated return period. The frames are subjected to accelerograms varying the seismic intensity, namely, the peak ground acceleration. The acceleration of the frame evaluated in the DL limit state corresponds to half of the total design peak ground acceleration ( $A_d$ ). For the SD and NC limit states, the ratio of the acceleration level to be analysed and design peak ground acceleration is 1.0 and 1.72 (EN1998-1-3, 2005), respectively.



Table 4.1 – Performance levels

<i>Limit state</i>	<i>Return period (years)</i>	<i>A/A<sub>d</sub></i>
Damage limitation (DL)	95	0.50
Severe damage (SD)	475	1.00
Near collapse (NC)	2475	1.72

#### 4.1.2 Performance objectives for the study cases

Once the performance level is established, it is necessary to define the performance objectives according to the PBD approach. The performance objectives may be a lateral deflection, an inter-storey drift, an element ductility or an element damage index.

In order to describe the damage state in the performance levels, the values proposed by EN1998-1-3 (2005) have been used to investigate the seismic behaviour of the CBFs or D-CBFs. In the case of the MRFs, the values proposed are based on the study carried out by Grecea et al. (2004) in order to describe the damage scenario in each limit states.

The EN1998-1-3 (2005) determines parameters in each limit state related to capacities of ductile or brittle elements. The evaluation may be based on inelastic capacity of braces, axial/flexural yielding or buckling of the columns, beam capacity in developing deformations without local buckling resulting in full plastic moment capacity or rotation capacity of connections.

For the braces in compression a percentage of the axial deformation at buckling load,  $\Delta_c$  is defined. The limit values for braces cross section Class 1 are  $0.25\Delta_c$ ,  $4.0\Delta_c$  and  $6.0\Delta_c$  for Class 2 are  $0.25\Delta_c$ ,  $1.0\Delta_c$  and  $2.0\Delta_c$ , respectively for the DL, SD and NC limit states. In case of braces in tension, the corresponding limits are  $0.25\Delta_t$ ,  $7.0\Delta_t$  and  $9.0\Delta_t$ .

Based on limits proposed by Grecea et al. (2004), the MRFs are evaluated through both transient or residual inter-storey drift ratios. For the SD limit state, a residual drift of 0.4% is assumed. The residual drift is obtained adding 10 seconds to accelerograms, resulting in a free vibration of the frames (see Figure 4.1). An inter-storey drift of 3.0% has been assumed to characterize the damage scenario of the NC limit state.

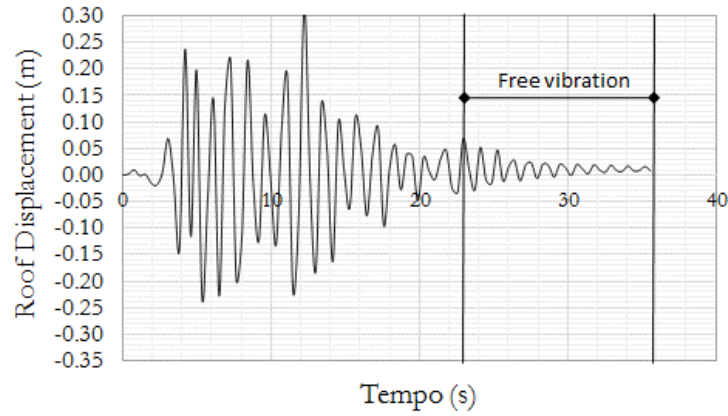


Figure 4.1 – Determination of residual displacements

## 4.2 Pushover analyses

The nonlinear static “pushover” analysis is an effective tool, not only to assess the inelastic behaviour of a building, but also to reveal weaknesses in the linear design performed previously in order to ensure the structural integrity. The plastic mechanisms and potential dissipative regions are obtained for specific load pattern applied to floor level in order to evaluate the overall capacity of structure. The main advantages of this type of analysis in comparison with incremental dynamic analyses are the lower complexity of modelling, lower computational demands, easier interpretation of results (Krawinkler and Seneviratna, 1998) and no need for selecting ground motion records, which can present some uncertainties and difficulties regarding severity, frequency, duration and distances of faults.

The lateral response capacity curve illustrated in Figure 4.2 is obtained through a nonlinear “pushover” analysis. In this figure,  $V_y$  refers to the yield strength of the structure,  $V_{1y}$  is the base shear at the formation of the first plastic hinge and  $V_d$  corresponds to the design base shear;  $\delta_1$ ,  $\delta_y$  and  $\delta_u$  are displacements at formation of the first plastic hinge, yield and ultimate displacement, respectively. In detail, it should be seen a simplification of capacity curve in an idealized bilinear curve which is obtained applying the N2 method incorporated in EN1998-1-1 (2004). The pushover analyses were carried out applying a lateral load distribution proportional to first mode and a uniform pattern. The seismic response of lower modes is estimated employing the first mode pattern. On the other hand, the uniform pattern is important when the seismic response is considerably affected by higher modes or when damage concentration occurs.

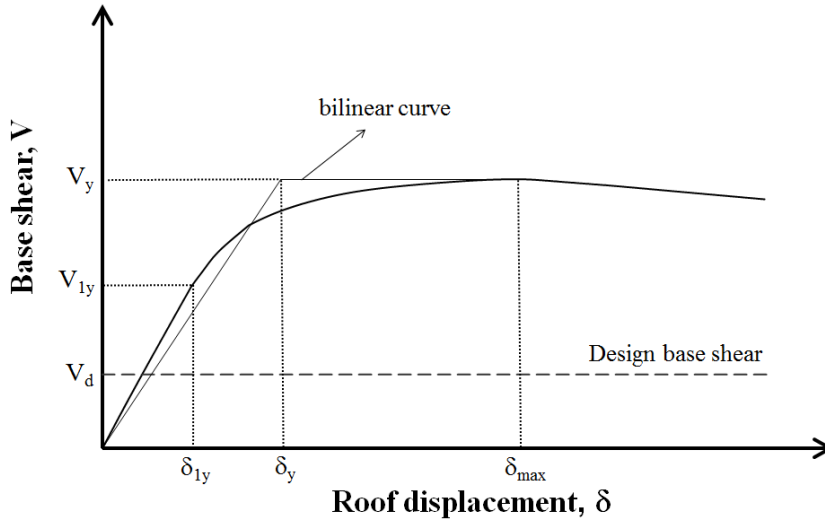


Figure 4.2 – Capacity curve from pushover analyses

#### 4.2.1 Overstrength factor

The overstrength factor of the study case is defined applying the expression (4.1). This formulation corresponds to the overall overstrength factor  $\Omega$ , which is defined as the ratio between the base shear corresponding to the overall yield strength of the frame and the design base shear. This ratio can be decomposed in two terms:

$$\Omega = \frac{V_y}{V_d} = \frac{V_y}{V_{1y}} \times \frac{V_{1y}}{V_d} \quad (4.1)$$

The first term,  $\Omega_1 = V_y/V_{1y}$ , corresponds to  $\alpha_u/\alpha_1$  defined in the EN1998-1-1 (2004). This value depends on the frame configuration, formation of the collapse mechanism, redistribution capacity and gravity loading (Elghazouli, 2005). The second term  $\Omega_2 = (V_{1y}/V_d)$  is related to aspects of the design procedure such as differences between actual and nominal material strength, member oversizing due to choices of commercial cross-section and design governed by deformation and/or non-seismic loading. This term may be associated to the degree of specialization of frame for seismic resistance (Castro et al., 2009).

### 4.3 Incremental dynamic analyses

In addition to static nonlinear analysis, incremental dynamic analyses (IDAs) were carried out in order to evaluate the inelastic behaviour of examined frames. The incremental dynamic analyses are a type of dynamic analyses where the accelerograms are monotonically increased by a non-negative scalar resulting on a set of accelerograms for a given earthquake. In contrast to nonlinear-static analysis, these dynamic analyses are more complex and the computational processing time is longer (Vamvatsikos and Cornell, 2002).

Nonlinear incremental dynamic analyses were performed to obtain the evolution of the inelastic behaviour of the frames for increasing PGA in order to check criteria defined for the three limit states. In particular, the behaviour factors were derived from the results of a set of dynamic analyses, applying in each record the following increments of PGA, assumed as the intensity measure:

- from 0.2 PGA to 1.2 PGA with a scaling step of 0.2
- from 1.2 PGA to 12.0 PGA with a scaling step of 0.4

In addition, nonlinear dynamic analyses were performed at 0.5 PGA in order to assess the DL state.

#### 4.3.1 *Selection of accelerograms*

The accelerograms are the most efficient way to represent the seismic action, where there is a set of information about the nature of ground motion. However, obtaining a set of records is not an easy task, especially when there is not a seismic hazard established. The designer should find two different criteria in order to select the accelerograms. One is based on strong-motion parameters while the other is associated to the seismological parameters, mainly magnitude, distance and site conditions. The method based on strong-motion parameters consists in finding accelerograms that are compatible with code-spectrum employed on design, which can be real or artificial. On the other hand, when the site is known and well characterized in seismological terms by either deterministic or probabilistic seismic hazards, the accelerograms are selected from strong-motion database where those seismological parameters are taken into account.

Two sets of seven records (artificial and real) were selected so that they can have a good fit to code-spectrum assumed on design for both stiff and soft soil. As the seismological scenario is not defined, the records were mixed from this point of view, resulting in records with different frequency contents.

The artificial records were obtained using SIMQKE software, while the natural records were selected from the European Strong-Motion Data - ESMD database. For stiff soil, six artificial records and one natural were selected and for soft soil, the records were based on the ESMD only. All records were scaled based on procedure used by Balling et al. (2009), considering that the pseudo-spectral acceleration for the period interval of interest is assumed as intensity measure. Accordingly, the input motion and their principal characteristics are listed in Table 4.2, particularly, none of the records are from very small events ( $M_s > 5$ ), and the peak ground acceleration has not been smaller than  $PGA_{min} = 0.33 \text{ m/s}^2$  for any of the records.

Table 4.2 – Basic data of the earthquakes selected

Identification	Date	Measurement location	Magnitude (Ms)	Foundation category	Scaled to PGA=1 (AI)
1S_2SR1		Artificial by SIMQKE			0.107
1S_2SR6		Artificial by SIMQKE			0.223
1S_2SR7		Artificial by SIMQKE			0.223
2S-R5-SC1		Artificial by SIMQKE			0.155
2S-R6-SC1		Artificial by SIMQKE			0.173
2S-R7-SC1		Artificial by SIMQKE			0.127
000296YA	1980/11/23	Torre del Greco (Italy)	6.87	Rock	0.284
000155XA	1977/03/04	Bucharest Building Res Inst. (Romania)	7.05	Alluvium	0.205
000184XA	1978/09/16	Kashmar (Iran)	7.33	Stiff soil	0.400
000297YA	1980/11/23	Tricarico (Italy)	6.87	Rock	0.424
000298YA	1980/11/23	Garigliano-NPP 1 (Italy)	6.87	Very soft soil	0.306
000479YA	1990/06/20	Rudsar (Iran)	7.32	Soft soil	0.426
000535XA	1992/03/13	Erzincan-Meteorolog. (Turkey)	6.75	Stiff soil	0.108
000612YA	1997/09/26	Gubbio-Piana (Italy)	5.90	Rock	0.349

The acceleration time-histories with normalized peak ground acceleration are shown in Figure 4.3 as well as the response spectra for all accelerograms with code-spectrum in Figure 4.4 and Figure 4.5 for both, stiff or soft soil, respectively.

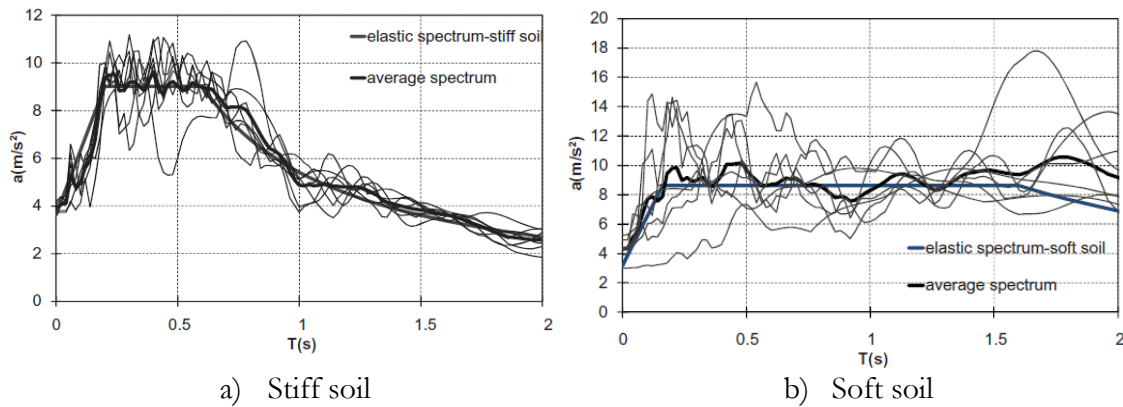


Figure 4.3 – Response spectra of all selected accelerograms and code spectrum

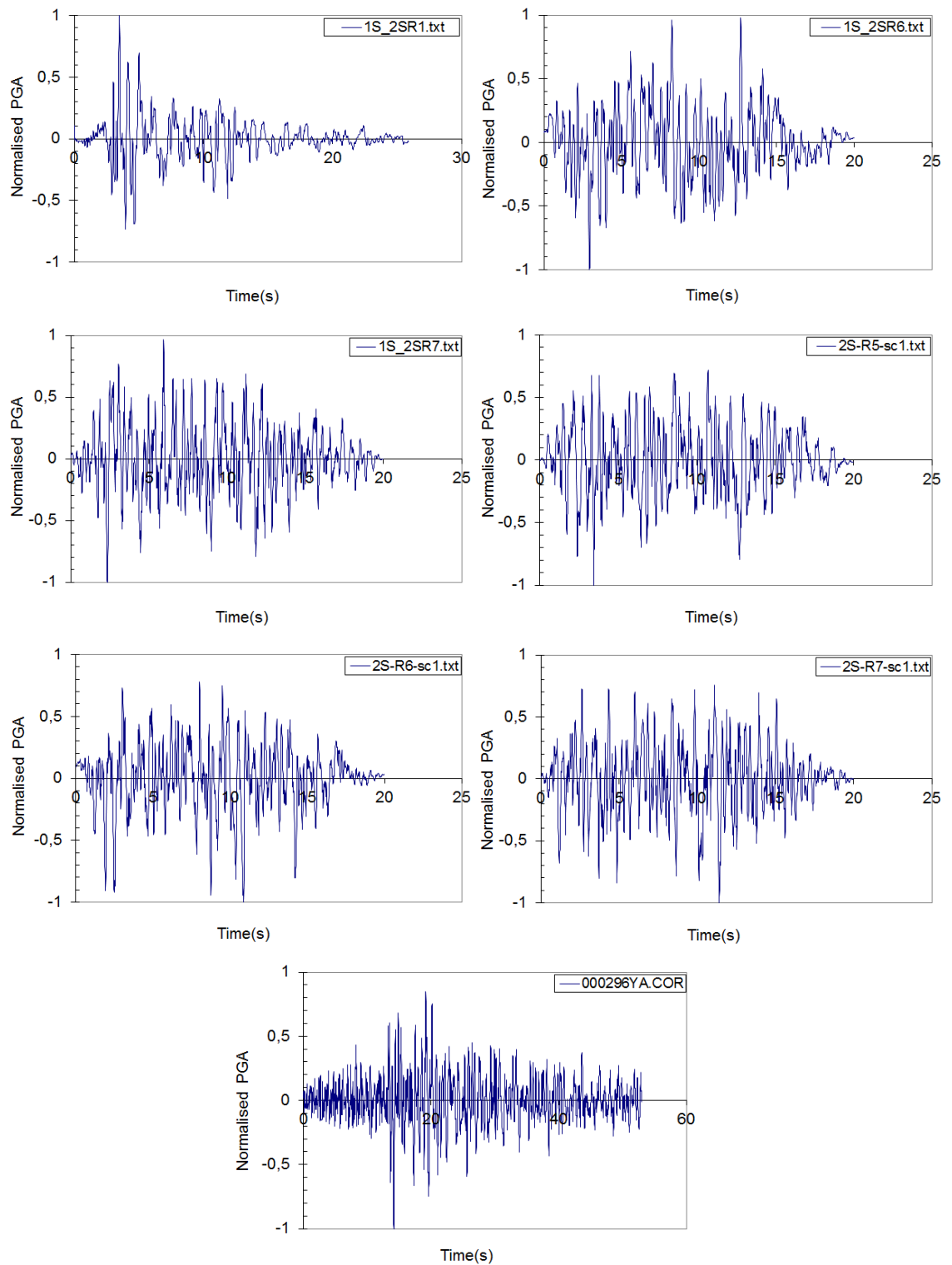


Figure 4.4 – Earthquake records adopted in the analysis for stiff soil

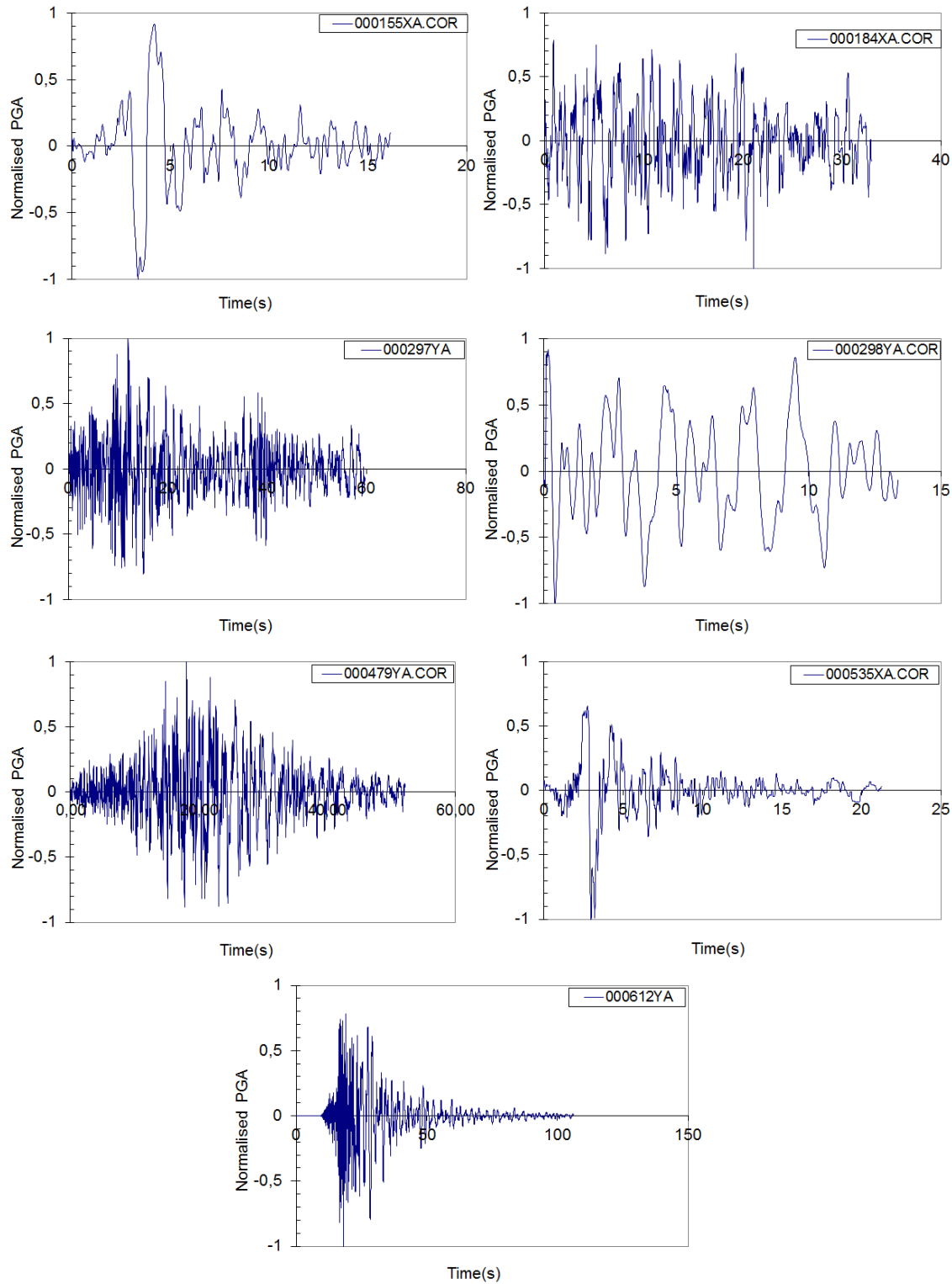


Figure 4.5 – Earthquake records adopted in the analysis for soft soil

#### 4.4 Behaviour factors (q-factors)

In this study, two approaches have been chosen to assess the q-factor, hereafter described in more detail.

In the first approach designated European approach, the behaviour factor is obtained by applying the Equation (4.2):

$$q = \alpha_{push} \times \frac{A_u}{A_y} \quad (4.2)$$

in which,  $A_u$  is the peak ground acceleration leading to accepted failure for the selected performance level  $A_y$  is the peak ground acceleration corresponding to the yielding of the frame and finally,  $\alpha$  is the overstrength factor from pushover analysis corresponding to ratio between maximum base shear ( $\alpha_u$ ) and base shear when the first plastic hinge occurs ( $\alpha_1$ ). In order to obtain the values of  $A_y$  and  $A_u$  it is necessary to perform a set of dynamic incremental non-linear time history analyses, scaling the accelerograms up to the level that leads to collapse. Figure 4.6 shows an example of a curve of maximum base shear versus acceleration.

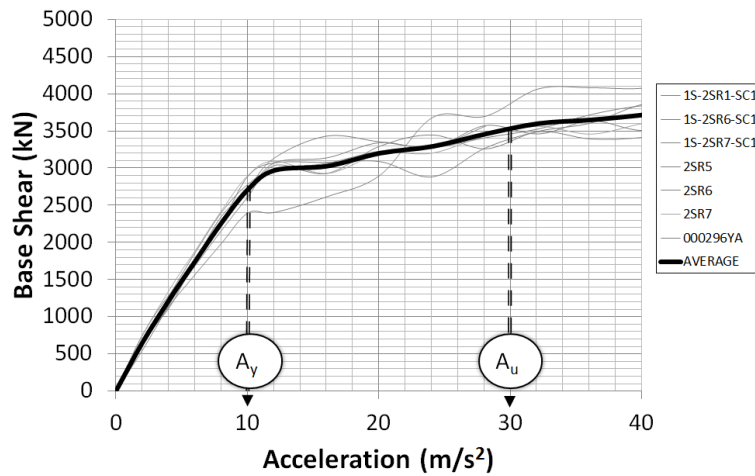


Figure 4.6 – Maximum base shear versus acceleration

In Salvitti and Elnashai (1996) approach, the behaviour factor is obtained applying the same process of previous methods, in which successive scaling of records are applied in order to find the acceleration that corresponds to failure criterion. According to Salvitti and Elnashai (1996), this approach checks the q-factor employed on seismic design considering the overstrength of structures excluding the need to perform pushover analyses as can be seen in Eurocode approach. Equation (4.3) is used to obtain the q-factor using this approach, in which the  $a_{g(collapse)}$  corresponds to acceleration on desired failure criterion,  $a_{g(design)}$  is the acceleration associated to each limit state employed, and finally, the  $q_{code}$  is the behaviour factor used on seismic design according to EN1998-1-1 (2004).



$$\mathbf{q} = \frac{a_{g(\text{collapse})}}{a_{g(\text{design})}} \times q_{code} \quad (4.3)$$

As previously mentioned in the present study, the values of  $A_y$  and  $A_u$  (or  $a_{g(\text{collapse})}$ ) have been derived from IDAs. The amplitude corresponding to the acceleration  $A_u$  (or  $a_{g(\text{collapse})}$ ) is the minimum value corresponding to all possible theoretical states of collapse:

$$A_u = \min(A_\theta, A_c, A_R)$$

In which  $A_\theta$  is the acceleration corresponding to the maximum permitted inter-story drift ratio (either transient and residual, as reported in Section 4.4.1);  $A_c$  corresponds to the buckling of columns;  $A_R$  corresponds to the maximum permitted inelastic demand of structural elements (as given by EN1998-1-3 (2005)).

#### 4.5 Modelling of study cases

In order to assess the nonlinear static and dynamic behaviour of the study cases, numerical models were developed using the nonlinear finite element-based software (SeismoStruct, 2011).

In general, the nonlinear behaviour is related to two sources: material and geometric nonlinearity. The geometric nonlinearity will be presented in next sub-section. Thus, giving focus on the material nonlinearity, the models may be developed on the basis of two categories, concentrated plasticity models and distributed plasticity models.

The first is based on concentrated plasticity models where the linear-elastic behaviour is attributed to elements and the plastic deformations are lumped at the ends and are based on the moment-rotation relationships of the end sections for a given axial force. The behaviour of the members may be monitored by the inclusion of rotational spring. Figure 4.7 reveals an example of single-storey frame where the nonlinear behaviour is given by rotational spring located at the end of the members. The constitutive laws are expressed in terms of moment-rotations, enabling to simulate complicated responses if properly calibrated. On the other hand, finding the spring calibration to be carried out in order to have good results is not an easy task. Models have been developed to introduce the effects of cyclic law through reproducing the stiffness degradation and pinching as well as the development of hysteric models (Song and Pincheira, 2000; Sivaselvan and Reinhorn, 2000; Krawinkler et al., 2006).

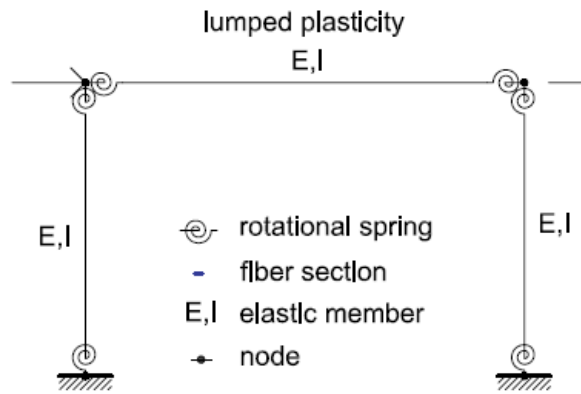


Figure 4.7 – Lumped plasticity formation (Fragiadakis and Papadrakakis, 2008)

The second approach is the distributed plasticity where the plastic hinges may form at any location along the members. This methodology offers a more accurate description of the inelastic behaviour of the building. The cross-section behaviour is reproduced by means of the fibre approach. The cross-section is divided into small regions in both, horizontal and vertical directions, giving rise to “fibre”. In each fibre, a uniaxial stress-strain relationship is assumed, depending on the material used within for cross-section. Thus, the inelasticity is monitored in terms of stresses and strains and accounted through the integration of material response over the cross-section and the integration of the section response along the length of the element. Although the distributed plasticity approach allows the inelastic deformation to occur in any region of the members, the numerical calculations that aims at finding the stresses and strains are carried out in the integration sections. Figure 4.8 shows a typical reinforced discretised concrete cross-section where each material has a specific constitutive law, and it is still possible to see its integration sections.

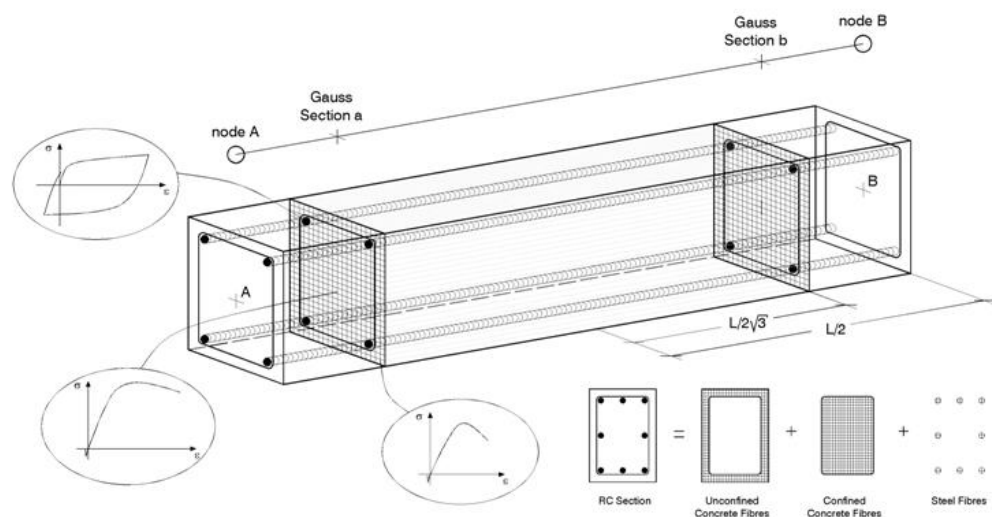


Figure 4.8 – Fibre approach (SeismoStruct, 2011)

In comparison with the concentrated plasticity, the distributed plasticity approach requires more computing resources due to the simplifications present in the concentrated plasticity.

The distributed plasticity does not require experience, since the user needs to introduce the geometrical and material characteristic of structural member by avoiding calibrating the moment-rotation law of a section for a given geometry and axial force. Moreover, there is no requirement for a prior moment-curvature analysis of members, no need to introduce any element of hysteretic response (as it is implicitly defined by the material constitutive models), direct modelling of axial load-bending moment interaction (on both, strength and stiffness), straightforward representation of biaxial loading and interaction between flexural strength in orthogonal directions, are considered other advantages of the distributed plasticity approach (SeismoStruct, 2011).

The distributed inelasticity frame elements can be implemented with two different finite element formulations: the displacement-based (DB) and force-based (FB). In DB formulation, a displacement field is imposed, while for FB elements an equilibrium is strictly satisfied and no restrains are placed for the development of inelastic deformations throughout the member. In relation to DB, displacement shape functions are used, assuming a linear distribution of the curvature along the element, which is not correct when the element end sections have yielded. In contrast, the FB approach produces accurate predictions about post yield deformation path entering a segment with negative slope. This latter approach keeps the equilibrium between the force and the deformation at the integration sections, and the constitutive laws are fulfilled within a specified tolerance. Furthermore, the whole process is adjusted to be compatible with general purpose FE codes based on the direct stiffness method (Fragiadakis and Papadrakakis, 2008).

The two approaches produce the same response when a linear elastic material is employed in the analyses. On the other hand, whenever a displacement field is imposed, it is not possible to capture the real deformed shape in relation to material inelasticity where the curvature can be nonlinear. In order to overcome this problem, a refined discretisation of the structural elements is necessary, mainly where inelastic deformations are expected to be high for the DB formulation. For the FB formulation, only a single beam-column element per member is required to simulate the material nonlinear response, which is contrary to displacement-based elements. Figure 4.9 reveals the discretisation of a non-braced frame using both, displacement-based and force-based formulations. In detail, the end members of the DB formulation require a denser mesh for the regions, probably with inelastic deformations (five elements per each structural member). In contrast, only one force-based element is employed in order to simulate the structural members.

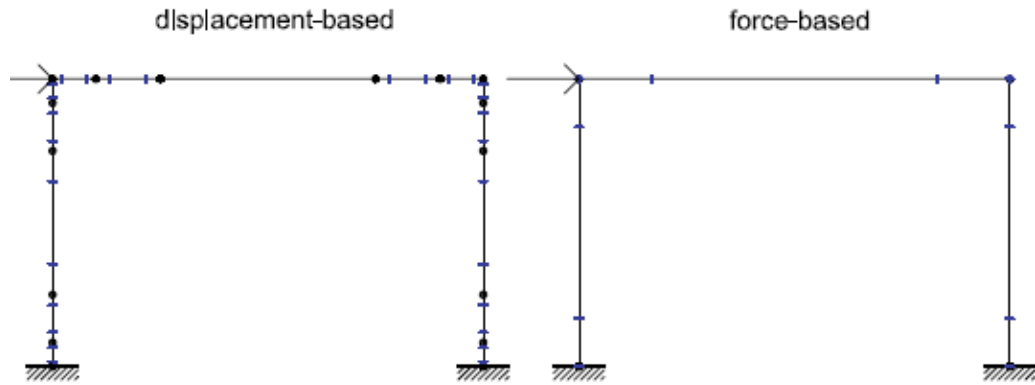


Figure 4.9 – Discretisation of the frame for a displacement-based and force-based formulations (Fragiadakis and Papadrakakis, 2008)

Figure 4.10 compares the response of a same structure being simulated by displacement-based and force-based elements. As it can be observed, the performance of both formulations are very similar, however the DB formulation requires a higher number of elements compared to FB.

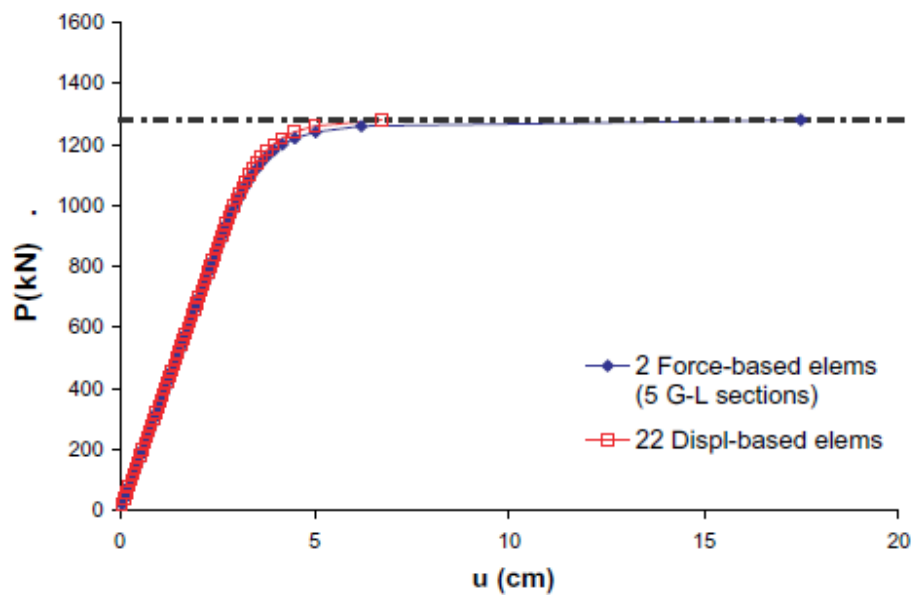


Figure 4.10 – Response of both displacement-based and force-based formulations (Fragiadakis and Papadrakakis, 2008)

The FB formulation has a superior behaviour, since the use of the interpolation functions assumed entails the satisfying equilibrium, as opposed to the displacement-based element that depends on the assumed sectional constitutive behaviour (Neuenhofer and Filippou, 1997). The FB formulation is only an approximation introduced by a discrete number of the controlling sections along with the element used for the numerical integration, producing only numerical errors, while discretization errors caused by the finite element mesh for the DB formulation are also present.

In SeismoStruct (2011), Gauss-Legendre quadrature is employed for the DB elements which make use of two integrations sections. Whilst Gauss-Lobatto quadrature is employed for FB elements that may feature four to ten integration sections (see Figure 4.11), a minimum number of 3 Gauss-Lobatto integration sections can be used to avoid under-integration, however, it is not indicated, since it does not simulate the spread of inelasticity in an acceptable way. Generally speaking, it is suggested to use 4 numbers of Gauss-Lobatto integration sections while increasing the number of sections, but that does not always improve the results because of the influence of different weights assumed for every section of numerical integrations (see Figure 4.12) (Papaioannou et al., 2005). For a refined discretisation, it is necessary that the structural members can be divided typically by 4 or 5 DB elements per each structural members.

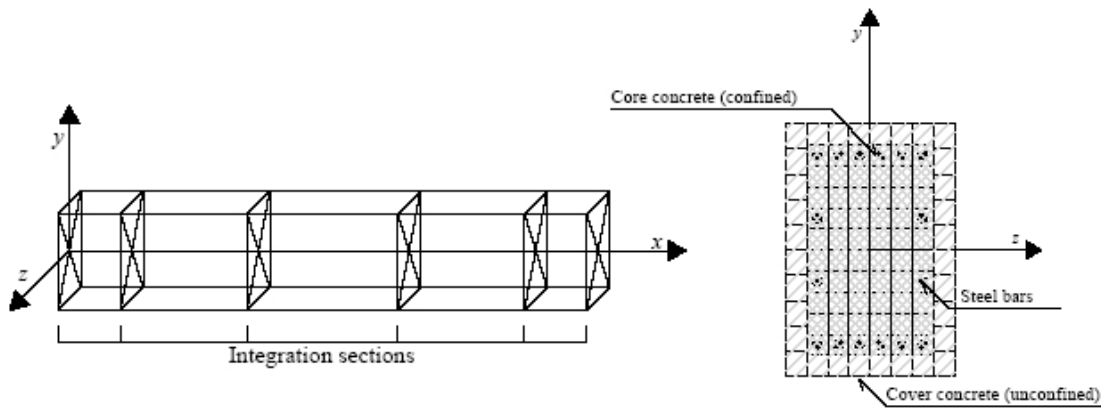


Figure 4.11 – Integration sections (SeismoStruct, 2011)

From the points made above, the numeral models were developed using the distributed inelastic elements. Although the SeismoStruct (2011), both DB and FB formulations can be used, it was decided to use the FB elements for all the structural members.

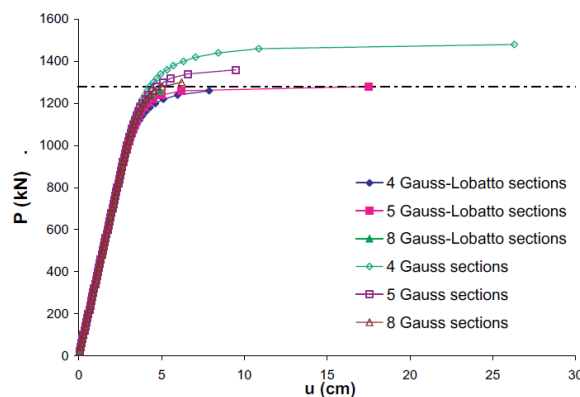


Figure 4.12 – Performance of force-based element for various integration schemes (Papaioannou et al., 2005)

As previously mentioned, the numerical integration method used is based on the Gauss-Lobatto distribution, which includes, at least, the monitoring points at each end of the

element. Following, there is a description of the characteristics of each structural member used in the nonlinear analyses:

- Columns
  - Element class – Inelastic force-based frame (1 FB element)
  - 200 fibers
  - 5 Integration Sections
- Beams
  - Element class – Inelastic force-based frame (1 FB element)
  - 200 fibers
  - 5 Integration Sections
- Braces
  - Element class – Inelastic force-based frame (2 FB element)
  - 200 fibers
  - 4 Integration Sections

Concerning the dynamic analyses, a 2% Rayleigh tangent stiffness damping has been used at both first and second mode. Indeed, differently from initial damping formulation, it does not produce artificial overdamping at high ductility demand as shown by D'Aniello et al. (2013); Priestley and Grant (2005); Priestley (2005).

#### 4.5.1 *Restraints and boundary conditions*

The nonlinear models need to have the same restraints and boundary conditions applied on the seismic design in order to have a reliable comparison. For each typology, the conditions assumed on the model are described, accounting for the special characteristic present in different typologies.

**Moment-resisting frame** – In this structural system, all the beam-to-columns connections were assumed as rigid and full strength. The base column is considered rigid.

**Concentrically braced frame** – Only the beam-to-columns connections from CBFs are rigid while the MRF parts were assumed as pinned in end. Braces were considered pinned in both end connections.

**Dual-concentrically braced frame** – In this case, both concentrically and moment-resisting systems have rigid and full strength beam-to-columns connections. Again, the braces were considered to be pinned in both connections.

The pinned connection have been simulated in the SeismoStruct (2011) as *link* element. The *link* corresponds to a generic element, capable of reproducing a large number of options to

a similar a behaviour of a structural members or connections. In order to simulate a pinned connection for the end braces and end beam out of the braced bay of the CBFs, a rotational spring was modelled in this region, where the stiffness is close to zero. The element is composed by only a linear curve without a limit defined by force or moment. Figure 4.13 depicts the model used by the end braces, for instance.

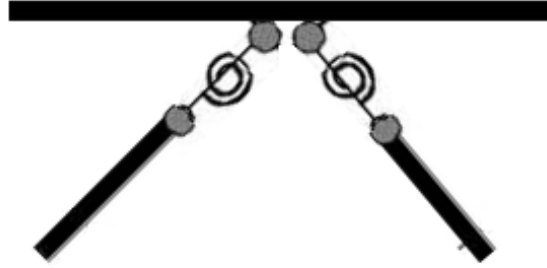


Figure 4.13 – Rotational spring to simulate the pinned connections

#### 4.5.2 *P-delta effects*

The second order effects have been accounted for in all analyses by assuming large displacements/rotations and large independent deformations related to the chord of the frame element through the employment of the total co-rotational formulation given by Correia and Virtuoso (2006) implemented in SeismoStruct (2011). The model proposed is based on kinematic transformations associated to large displacements and three-dimensional rotations of the beam-column member. In the local chord system of the beam-column element, six basic displacement degrees-of-freedom and internal forces are shown in Figure 4.14.

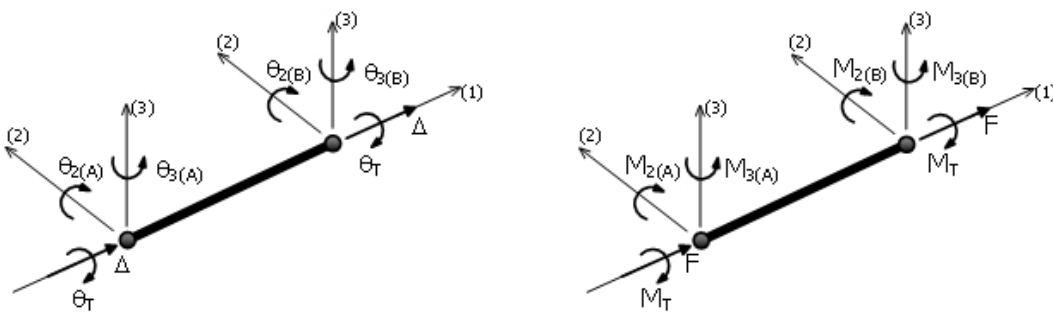


Figure 4.14 – The basic displacement degrees-of-freedom and forces of beam-column element (SeismoStruct, 2011)

Furthermore, in order to evaluate the P-Delta effects of the seismic mass that is not tributary to the frame, the employment of a leaning column was considered, as in Figure 4.15.

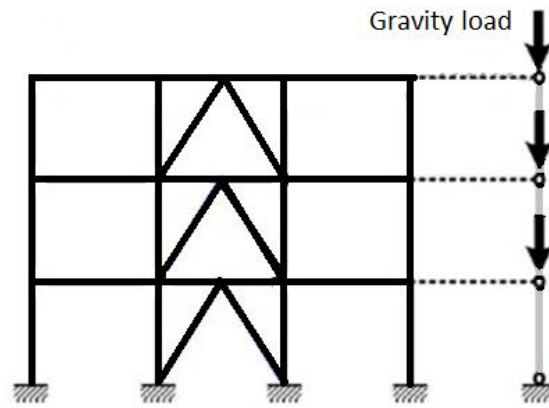


Figure 4.15 – Learning column

#### 4.5.3 Material properties

For the seismic design, concrete compression strength and steel yield stress have been used according to EN1992-1-1 (2004) and EN1993-1-1 (2005). Different values of material overstrength factor ( $\gamma_{ov}$ ) according to steel grade were used. In particular,  $\gamma_{ov}$  equal to 1.25 was assumed for S355, while 1.10 for S460 and S690 (RFSR-CT-2007-00039, 2013). Below, a list of the material properties of nonlinear analyses for both, steel and concrete:

- **Concrete**
  - Compressive Strength: 38 MPa
  - Poisson's Ratio: 0.2
  - Density: 24 kN/m<sup>3</sup>
- **Steels**
  - Yielding Strength (S355): 443.75 MPa
  - Yielding Strength (S460): 506.00 MPa
  - Yielding Strength (S690): 759.00 MPa
  - Yielding Strength (Rein.): 625.00 MPa
  - Poisson's Ratio: 0.3
  - Density: 78.5 kN/m<sup>3</sup>
  - Young Modulus: 210 MPa

The concrete behaviour was simulated considering the stress-strain relationship proposed by Martinez-rueda and Elnashai (1997). This model reproduces the loading and unloading when the member is under cyclic loading. Figure 4.16 illustrates the typical proposed stress-strain curve of concrete for cyclic loading used for the nonlinear analyses.



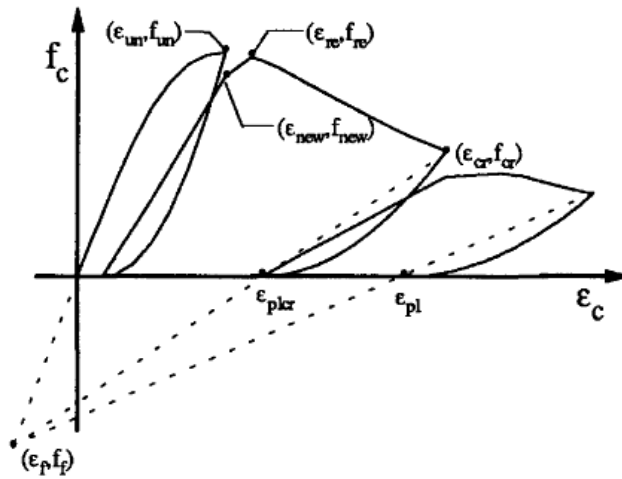


Figure 4.16 – Concrete stress-strain curve (Martínez-rueda and Elnashai, 1997)

For the stress-strain relationship of steel members, the model proposed by Menegotto and Pinto (1973) was chosen. This model simulates the following characteristics of material: Elastic, yielding and hardening branches; Baushinger effect which consists of the reduction of the yield stress after a reverse that increases with the enlargement of the plastic strain component of the last excursion and decreases with the curvature in the transition zone between the elastic and the plastic branches; Isotropic strain hardening, which consists of an increase of the envelope curve, proportional to the plastic strain component of the last excursion. From Figure 4.17 to Figure 4.19, stress-strain curve and material properties to steel grades S355, S460 and S690 used in analyses can be seen.

It is important to mention that, in order to establish the behaviour of composite columns, the confinement effect provided by steel profile and/or reinforcement was evaluated whereby constant confining pressure is assumed throughout the entire stress-strain range.

The effects of confinement provided by steel profile and/or reinforcement have been determined according to Mander et al. (1988) and Susantha et al. (2001), for fully/partially encased and concrete filled tube, respectively.

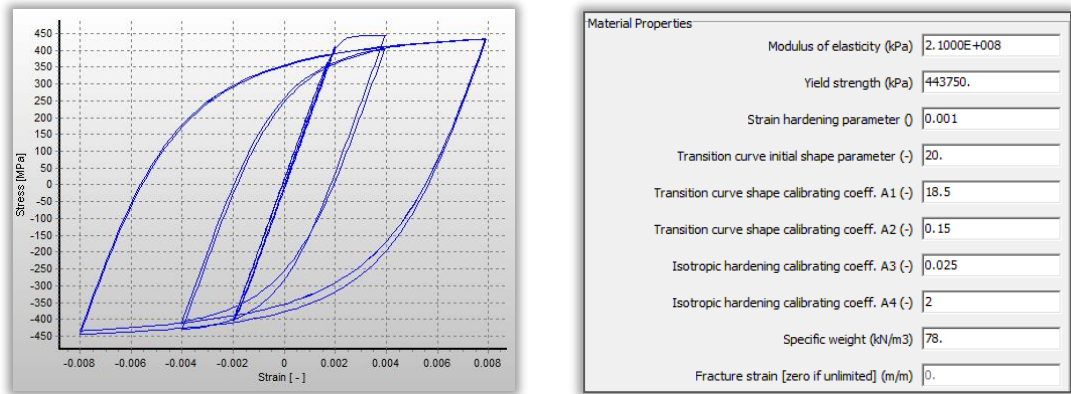


Figure 4.17 – Material properties and stress-strain curve for the S355

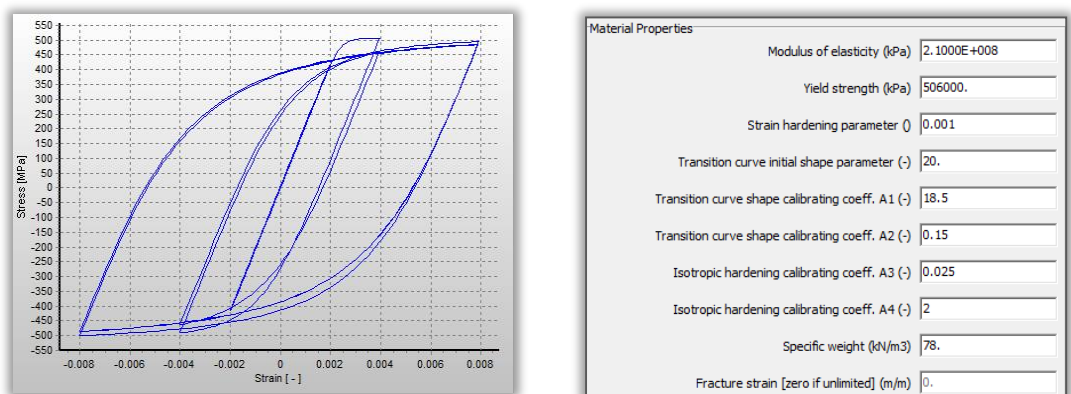


Figure 2.18 – Material properties and stress-strain curve for the S460

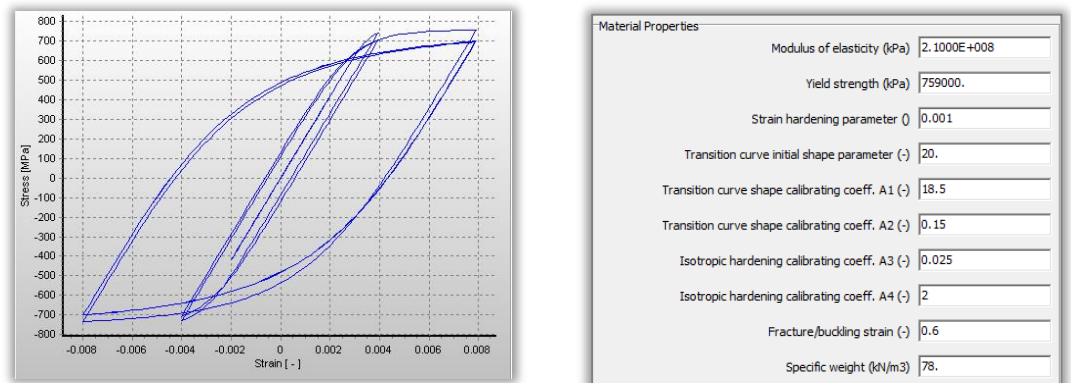


Figure 4.19 – Material properties and stress-strain curve for the S690

The typical cross section of composite column is divided in three main parts: an unconfined region, a partially confined one within the hoops and a highly confined region between the flanges of the steel profile. Each region presents a distinct stress-strain behaviour based on level of confinement. In unconfined concrete, there is no increase of strength nor increase of ductility; however, for partially and highly confined concrete this increase may occur.

The strength and ductility of partially confined region is defined taking into account the maximum transverse pressure from transverse reinforcement. However, for highly confined

part, the strength and ductility of concrete is bigger than a partially confined one, because there is influence of steel profile in the calculation of confinement factor.

Concerning the different types of composite column cross sections assessed the fully and partially encased sections have the three regions defined and the concrete filled tubes have only main one confined region because, in this case, there is no reinforcement (see Figure 4.20).

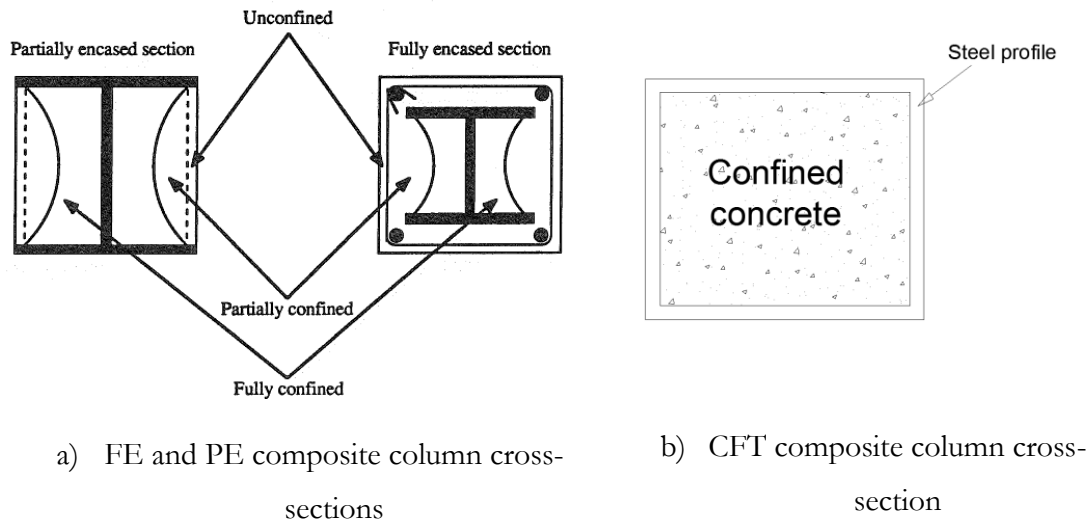


Figure 4.20 – Characterization of the confined regions on the composite column sections

#### 4.5.4 Calibration of the numerical model for the unbraced frames

In order to calibrate the implemented model for the MRFs in this research, experimental tests carried out by Wakabayashi et al. (1974) and D'Aniello et al. (2012) have been used to validate the assumptions assumed in the nonlinear analyses of the study cases.

Wakabayashi et al. (1974) have, under monotonic and reversed horizontal loading, performed tests in steel frame with single story (Figure 4.21) subjected or not to large constant vertical load on the columns in order to make it possible to know the behaviour of lower storey of tall buildings. The frame has lateral supporting to prevent lateral buckling.



CBFs. They are responsible for the energy dissipation and an accuracy of numerical models becomes extremely important to avoid unreliable response of the structures, since the formation of the first nonlinear event may mostly affect the prediction of collapse mechanism. Thus, it is fundamental to have an accurate prediction of brace buckling on the seismic assessment as well as for the evaluation of structural robustness under exceptional loads.

It is recognized that the physical theory models are the most efficient approach to simulate the nonlinear response of CBFs (Uriz, 2005). In this approach, the braces are usually schematized with two elements connected by a generalized plastic hinge for braces or accounting for distributed plasticity. An initial out-of-straightness imperfection (or camber) is used at the intersection of the two connected elements to reproduce the buckling effects (see Figure 4.23). The value of this eccentricity has been studied (Uriz, 2005; D'Aniello et al., 2014a; Dicleli and Mehta, 2007; Goggins and Salawdeh, 2013) in recent years in order to have a reliable formulation to simulate the buckling effects.

Although in the study carried out by D'Aniello et al. (2014a), the formulation presented by Dicleli and Mehta (2007) to determine the camber showed better seismic performance in comparison with other approaches, a constant value for the camber equal to  $L/500$  (being  $L$  the brace length) was assumed. Such value has no significant error to predict the seismic performance of the CBFs with V-inverted.

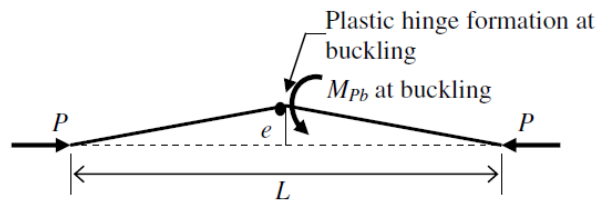


Figure 4.23 – Example of braces with out-of-straightness ( $e$ ) (Dicleli and Mehta, 2007)

The braces can be modelled considering two approaches: (a) the use of two beam elements with lumped plastic hinges at both ends of each elements (Marino and Nakashima, 2006) and (b) the use of at least two distributed inelasticity fibre elements to account for plasticity across the section and along the member (Uriz, 2005). In this research, the latter approach has been used to model the brace elements. As it was seen, the use of the distributed inelasticity elements does not require a calibration of the section response.

In order to verify the accuracy of the assumptions employed on the numerical models of brace, the experimental tests from the study carried out by Black et al. (1980) were used. The examined brace is a simple pinned W8x20 (US measurements) wide flange steel brace, having geometric slenderness equal to 118 and non-dimensional slenderness equal to 1.4.

Figure 4.24 shows the performance of both, experimental and numerical responses for the axial and lateral behaviours. In both cases, a good agreement between the experimental and numerical curves could be achieved.

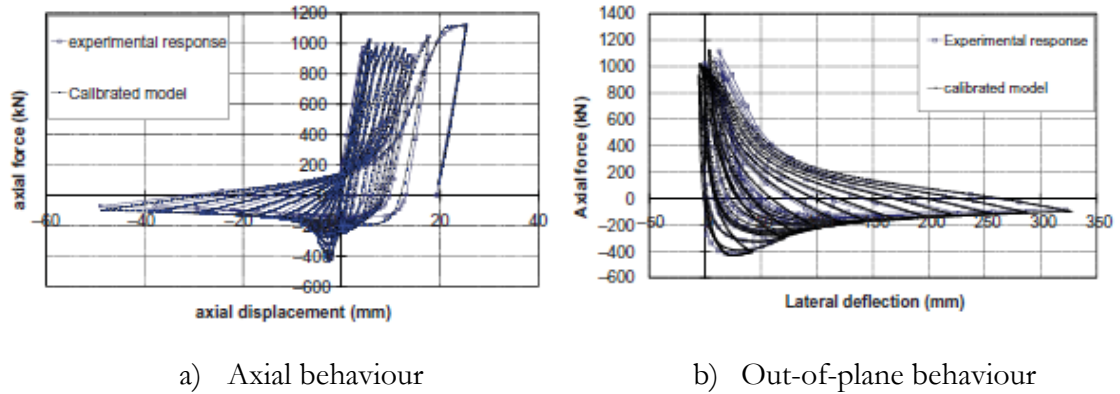


Figure 4.24 – Comparison between the experimental and numerical responses

Furthermore, the experimental results from the shake table tests carried out by Uang and Bertero (1986) are used in order to verify the overall behaviour of the implemented model. This test consists of a steel concentrically braced building with six-storey (see Figure 4.25). The bracing members are made of welded square hollow profiles characterized by non-dimensional slenderness of about 0.4. (Stocky braces). The accelerograms record, namely, the Miyagi-ken-okiu earthquake of 1978, North-South (N-S) component only, with PGA scaled to 0.33g is applied to all nodes at the basis of the model, which correspond to those physically attached to the shake table platform. Figure 4.25 reveals the comparison of both, numerical and experimental results based on roof displacements. It is interesting to note that the numerical response has good agreement with those from experimental test allowing confidence on the proposed assumptions.

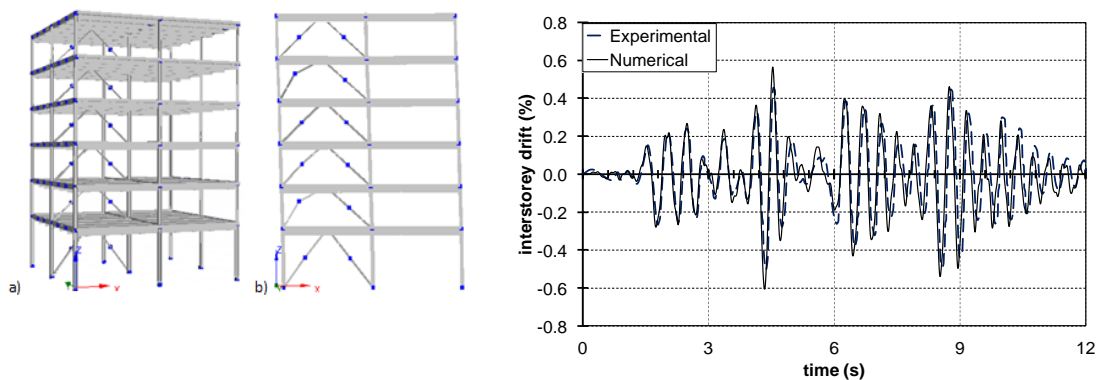


Figure 4.25 – Comparison between the experimental and numerical responses

## *Chapter V*

# Moment-resisting Dual-Steel Frames

The nonlinear performance of the Moment-resisting frames using HSS on the non-dissipative structural members are herein described and discussed. Based on the nonlinear procedures introduced in the previous chapter, the aim of this chapter is to provide a detailed analysis of the nonlinear behaviour of the study cases directed to Moment-resisting frames. The influence of the parameters examined, namely, the geometrical characteristics, the steel-concrete composite column and the soil type on the seismic performance is also reported.

The study is focused on the evaluation of the behaviour and overstrength factors, as well as on seismic performance of MRFs on the three limit states defined in Chapter IV. The performance indicators that have been particularly monitored for all limit states are the following: i) peak inter-storey drift ratios; ii) residual inter-storey drift ratios; iii) peak storey accelerations; iv) beam ductility demand; v) beam flexural overstrength.

In order to evaluate the influence of the design parameters on the construction costs, the material consumption has been calculated for all the examined cases, specially the steel consumption, which has been computed in terms of total weight, while concrete consumption in terms of total cast volume. The amounts of steel grade S355 (MCS) used for beams, steel grade S460 (HSS) used for column and reinforcement steel (RS) are presented separately.

### 5.1 Static-nonlinear analysis

Figure 5.1 shows the capacity curves from pushover analyses for both patterns of lateral load, obtained by normalizing the base shear  $V$  with the design base shear  $V_d$ . As it can be noted, all frames possess an actual capacity considerably higher than the one assumed in design. This effect is most probably due to the design procedure, which is governed by the requirements to satisfy both inter-storey drift limits and to control the P-delta effect.

The frames under 1<sup>st</sup> mode pushover showed an almost uniform inter-storey drift distribution up to the formation of the first plastic hinge, while pushover analyses under uniform load pattern showed a pronounced concentration of drifts at lower storeys also in elastic range. In the final phase of both, 1<sup>st</sup> mode and uniform pushover lower storeys exhibit significant inter-storey drifts compared to upper levels, but soft storey mechanism occurred only for the uniform load pattern on the first storey.

The comparison of response curves allows highlighting the influence of the investigated parameters. In particular, when it comes to the influence of number of storeys, it can be noted that the four-storey frames experience larger  $V/V_d$  ratios than the eight-storey frames. This implies that the smaller the number of stories, the larger the design overstrength.

In the examined cases (namely within the range 5 - 7.5 m) the influence of span length is found to be less significant. Longer span frames showed a slightly larger overstrength. This result is ascribable to the design process. Indeed, longer beams imply larger beam depth, thus leading to stiffer and stronger columns to satisfy capacity design rules.

Concerning the column type, no substantial differences can be recognized in terms of lateral capacity. Only the cases with FE columns have exhibited slightly smaller base shear ratio. This result can be explained by analysing the failure mode and the damage distribution as showed in Figure 5.2 and Figure 5.3. Indeed, although they are designed to satisfy hierarchy criteria, FE columns are characterized by having a slightly smaller flexural stiffness than the relevant PE and CFT sections. As a consequence, in such cases the distribution of damage tends to be less uniform than in the frames with stiffer columns. Hence, the damage tends to be concentrated on the lower stories, thus resulting in smaller base shear forces.

Considering the soil conditions, the base shear ratio of frames located on stiff soil are higher than those located on soft soil conditions. This result is mainly related to the adopted design criteria. Indeed, in the former cases (namely stiff soil) the design forces are noticeably smaller than those in the second (namely soft soil), while the design displacement demand is similar. Hence, in order to satisfy the drift limitations, larger cross sections were selected for frames founded on stiff soils, thus resulting in larger normalized base shear ratios.

The inelastic distribution and the sequence of plastic hinges are pointed out by the numbering close to the symbol of plastic hinge (i.e. bold circle) shown in Figure 5.2 and Figure 5.3. These figures were obtained when the frames reached the maximum base shear for only the 1<sup>st</sup> Mode pattern, once they are responsible for the severe distribution in terms of plastic hinge. Both are observed, the effectiveness of capacity design criteria and the influence of the building aspect ratio (namely the ratio between the building height and the



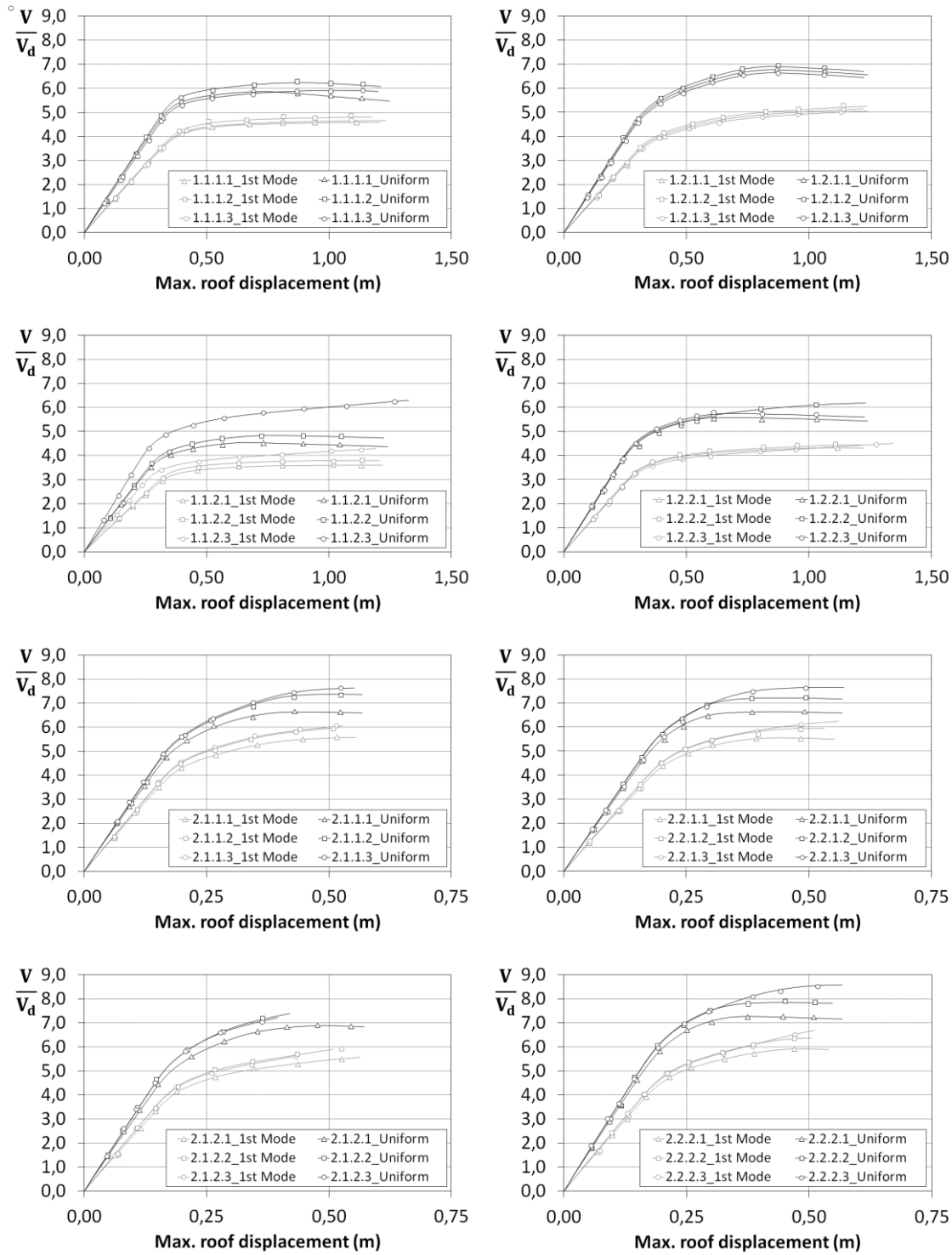
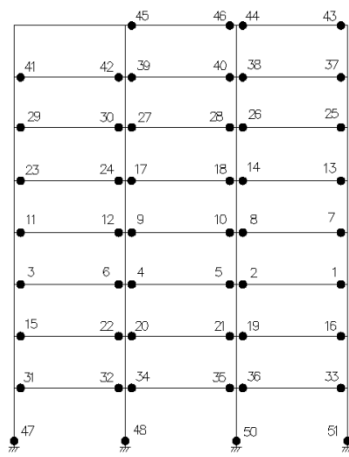
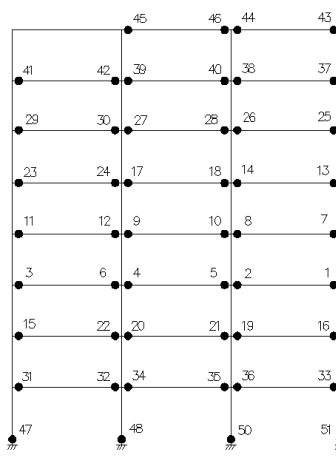


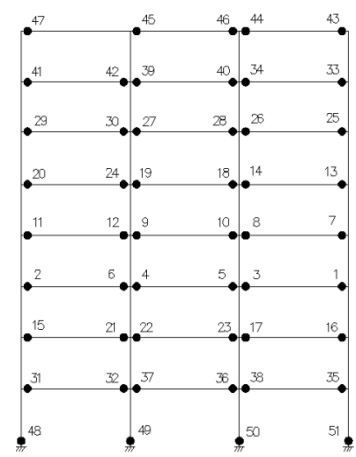
Figure 5.1 – Normalized pushover response curves



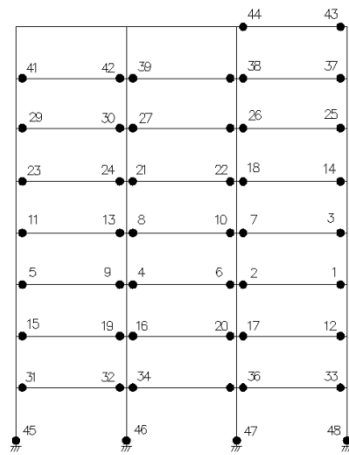
MRF\_1.2.1.1



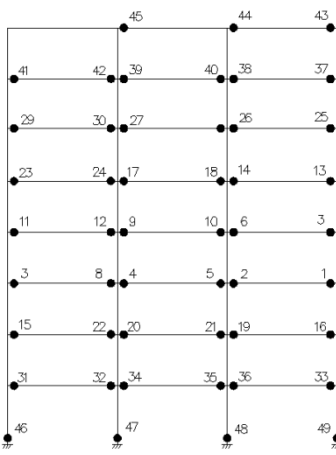
MRF\_1.2.1.2



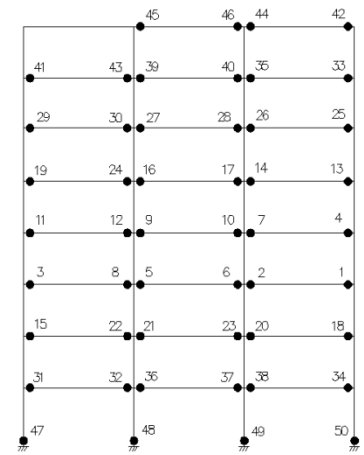
MRF\_1.2.1.3



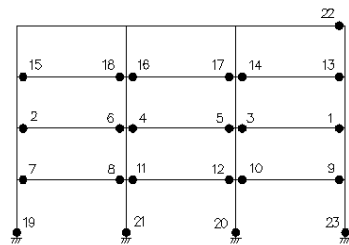
MRF\_1.2.2.1



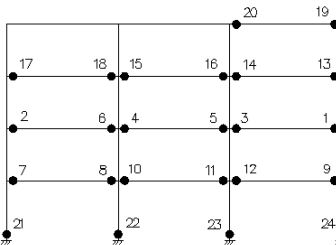
MRF\_1.2.2.2



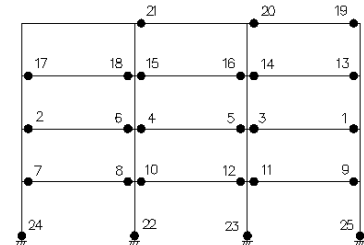
MRF\_1.2.2.3



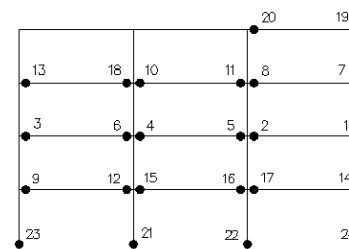
MRF\_2.2.1.1



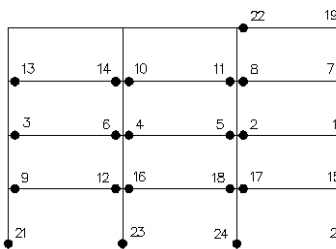
MRF\_2.2.1.2



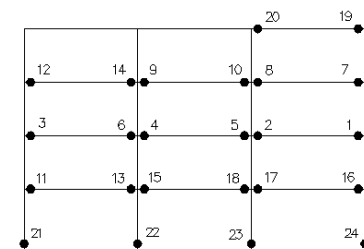
MRF\_2.2.1.3



MRF\_2.2.2.1



MRF\_2.2.2.2



MRF\_2.2.2.3

Figure 5.2 – 1<sup>st</sup> Mode Pushover: Damage distribution for frames with 7.5m of span

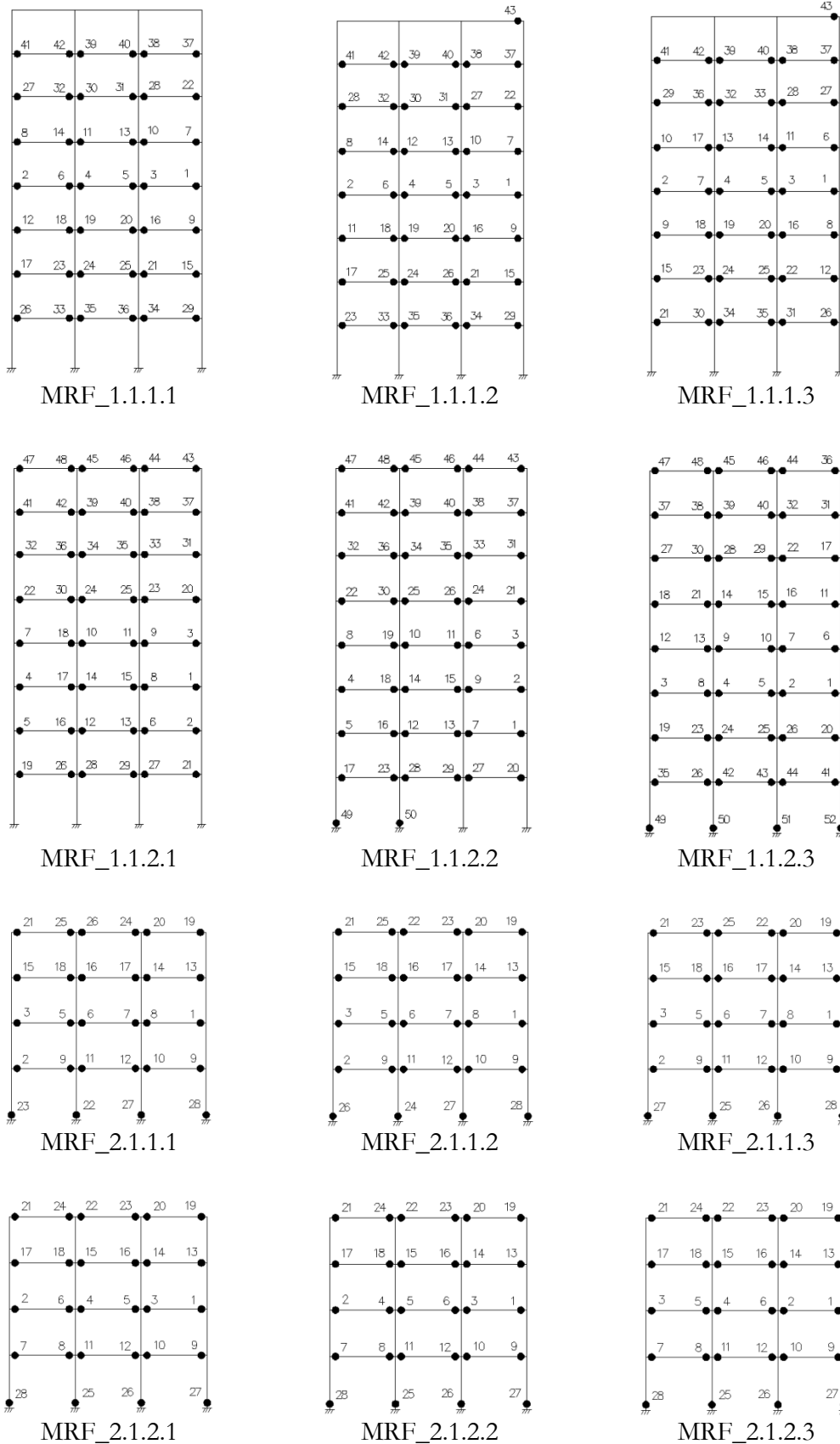


Figure 5.3 – 1<sup>st</sup> Mode Pushover: Damage distribution for frames with 5.0m of span

width), in relation to the damage evolution up to the attainment of the defined collapse limit. The former is evidenced by the weak-beam/strong-column behaviour, being all plastic hinges located on ends of beam and column base. The influence of the latter can be recognized by the different distribution of damage along the building height. Indeed, the shorter the bay, the larger the plastic beam rotation at the same total rotation demand, as compared to a longer span beam.

In general, shorter-span structures (i.e. 5.0 m) can fully develop the plastic mechanism with plastic hinge formed at all beam-ends, as well as at the column bases. On the other hand, longer-span frames (i.e. 7.5 m) do not achieve the complete formation of plastic mechanism, even though the damage redistribution is fully satisfactory. This difference is due to the lateral stiffness and to the profile of lateral displacements exhibit in both ensembles of frames. Indeed, 5.0 span structures show a dominant cantilever's behaviour, leading to large rotation demand on the top. Conversely, 7.5 span frames present a shear-type dominant response, which is characterized by large rotation demand on lower storeys.

#### 5.1.1 Overall overstrength factor

Table 5.1 reports both overstrength factor associated to seismic design assumptions and those indicated in EN1998-1-1 (2004). Analysing the first term in Equation (4.1) the pushover curves obtained from uniform load distribution show lower values. As general outcome, the median value is equal to 1.33, thus very close to 1.30 recommended by EN1998-1-1 (2004). Concerning the examined parameters, it is noticeable that frames having CFT columns show the higher overstrength factors, while the cases with FE and PE columns exhibit similar overstrength factors. On the other hand, the cases with FE columns exhibit slightly smaller base shear ratio. This fact is once again justified by slightly smaller flexural stiffness of the FE column in comparison with the PE and CFT sections. The other parameters have no appreciable influence on the  $\Omega_1$  factors.

In relation to the second term of Equation (4.1), the pushover curves obtained with first mode load distribution show the lower  $\Omega_2$  ratios. Table 5.1 shows that significantly large values have been obtained, since the median of  $\Omega_2$  is equal to 3.85, thus very close to the design behaviour factor ( $q = 4$ ). This result is ascribable to the need to satisfy the code drift requirements, which compels to oversize the structural members to provide adequate lateral stiffness. This issue often arises in the design of ductile seismic resistant MRFs. However, in case of dual-steel frames this design procedure is even more necessary. Indeed, although the use of HSS allowed to guarantee the hierarchy criteria, the higher the steel grade of non-dissipative members the smaller the corresponding size of cross sections, potentially resulting in very flexible frames. Analysing the influence of design parameters, no

Table 5.1 – Overstrength factors

<i>Frames</i>	$\left(\frac{V_y}{V_{1y}}\right)$		$\left(\frac{V_{1y}}{V_{dy}}\right)$		$\left(\frac{V_y}{V_{1y}}\right)_{min}$	<i>Load pattern</i>	$\left(\frac{V_{1y}}{V_{dy}}\right)_{min}$	<i>Load pattern</i>	$\Omega$	<i>Load pattern</i>
	<i>1<sup>st</sup> Mode</i>	<i>Uniform</i>	<i>1<sup>st</sup> Mode</i>	<i>Uniform</i>						
MRF_1.1.1.1	1.22	1.17	3.78	5.05	1.17	Uniform	3.78	1 <sup>st</sup> Mode	4.60	1 <sup>st</sup> Mode
MRF_1.1.1.2	1.25	1.19	3.84	5.23	1.19	Uniform	3.84	1 <sup>st</sup> Mode	4.80	1 <sup>st</sup> Mode
MRF_1.1.1.3	1.21	1.20	3.86	4.92	1.20	Uniform	3.86	1 <sup>st</sup> Mode	4.66	1 <sup>st</sup> Mode
MRF_1.1.2.1	1.23	1.21	2.94	3.76	1.21	Uniform	2.94	1 <sup>st</sup> Mode	3.60	1 <sup>st</sup> Mode
MRF_1.1.2.2	1.23	1.21	3.09	4.00	1.21	Uniform	3.09	1 <sup>st</sup> Mode	3.79	1 <sup>st</sup> Mode
MRF_1.1.2.3	1.58	1.54	3.11	4.24	1.54	Uniform	3.11	1 <sup>st</sup> Mode	4.91	1 <sup>st</sup> Mode
MRF_1.2.1.1	1.46	1.43	3.44	4.57	1.43	Uniform	3.44	1 <sup>st</sup> Mode	5.02	1 <sup>st</sup> Mode
MRF_1.2.1.2	1.49	1.44	3.52	4.79	1.44	Uniform	3.52	1 <sup>st</sup> Mode	5.26	1 <sup>st</sup> Mode
MRF_1.2.1.3	2.06	1.54	3.71	4.83	1.54	Uniform	3.71	1 <sup>st</sup> Mode	7.46	Uniform
MRF_1.2.2.1	1.36	1.28	3.18	4.34	1.28	Uniform	3.18	1 <sup>st</sup> Mode	4.32	1 <sup>st</sup> Mode
MRF_1.2.2.2	1.37	1.31	3.24	4.38	1.31	Uniform	3.24	1 <sup>st</sup> Mode	4.44	1 <sup>st</sup> Mode
MRF_1.2.2.3	1.45	1.44	3.08	4.28	1.44	Uniform	3.25	1 <sup>st</sup> Mode	4.46	1 <sup>st</sup> Mode

Table 5.1 – Overstrength factors (*Continued*)

Frames	$\left(\frac{V_y}{V_{1y}}\right)$		$\left(\frac{V_{1y}}{V_{dy}}\right)$		$\left(\frac{V_y}{V_{1y}}\right)_{min}$	Load pattern	$\left(\frac{V_{1y}}{V_{dy}}\right)_{min}$	Load pattern	$\Omega$	Load pattern
	1 <sup>st</sup> Mode	Uniform	1 <sup>st</sup> Mode	Uniform						
MRF_2.1.1.1	1.40	1.35	4.00	4.96	1.35	Uniform	4.00	1 <sup>st</sup> Mode	5.59	1 <sup>st</sup> Mode
MRF_2.1.1.2	1.47	1.45	4.16	5.08	1.45	Uniform	4.16	1 <sup>st</sup> Mode	6.10	1 <sup>st</sup> Mode
MRF_2.1.1.3	1.50	1.49	4.19	5.11	1.49	Uniform	4.19	1 <sup>st</sup> Mode	6.28	1 <sup>st</sup> Mode
MRF_2.1.2.1	1.44	1.43	3.71	4.82	1.43	Uniform	3.71	1 <sup>st</sup> Mode	5.34	1 <sup>st</sup> Mode
MRF_2.1.2.2	1.60	1.46	3.92	5.24	1.46	Uniform	3.92	1 <sup>st</sup> Mode	6.27	1 <sup>st</sup> Mode
MRF_2.1.2.3	1.57	1.49	3.96	5.10	1.49	Uniform	3.96	1 <sup>st</sup> Mode	6.23	1 <sup>st</sup> Mode
MRF_2.2.1.1	1.32	1.26	4.22	5.26	1.26	Uniform	4.22	1 <sup>st</sup> Mode	5.55	1 <sup>st</sup> Mode
MRF_2.2.1.2	1.35	1.29	4.38	5.59	1.29	Uniform	4.38	1 <sup>st</sup> Mode	5.94	1 <sup>st</sup> Mode
MRF_2.2.1.3	1.39	1.36	4.53	5.65	1.36	Uniform	4.53	1 <sup>st</sup> Mode	6.30	1 <sup>st</sup> Mode
MRF_2.2.2.1	1.31	1.24	4.52	5.84	1.24	Uniform	4.52	1 <sup>st</sup> Mode	5.91	1 <sup>st</sup> Mode
MRF_2.2.2.2	1.37	1.29	4.67	6.05	1.29	Uniform	4.67	1 <sup>st</sup> Mode	6.37	1 <sup>st</sup> Mode
MRF_2.2.2.3	1.46	1.38	4.76	6.20	1.38	Uniform	4.76	1 <sup>st</sup> Mode	6.96	1 <sup>st</sup> Mode
Statistics (percentile)	16 <sup>th</sup>	1.24	1.21	3.16	4.32	1.21	3.22	4.45		
	50 <sup>th</sup>	1.40	1.36	3.85	5.01	1.36	3.85	5.45		
	84 <sup>th</sup>	1.52	1.47	4.42	5.61	1.47	4.42	6.29		

appreciable difference can be recognized for  $\Omega_2$  factors. However, some differences for tall frames (i.e. eight-storey) can be observed for different soil types. Indeed, in the cases with stiff soil, the design base shear is about 20% smaller than in the cases with soft soil, while the design displacement demand are comparable. Therefore, the selected cross sections are proportionately larger for frames located on stiff soils, resulting in larger normalized base shear ratios.

This effect can also be recognized in the overall  $\Omega$  factors. Indeed, the mean  $\Omega$  factors are smaller for frames designed for soft soil than those for stiff soil. However, it should be noted that four-storey frames exhibit larger  $\Omega$  than eight-storey ones, namely the former from 5.43 to 5.97 and the latter from 4.25 to 4.97. This pronounced difference is due to the fact that the design forces for shorter frames are quite small, while the displacement demand is proportionally larger. Thus, it clarifies the reason for so large values of overstrength.

## 5.2 Dynamic performance evaluation

In order to investigate the dynamic performance of the MRFs, nonlinear incremental dynamic analyses have been performed taking into consideration the three reference limit states defined by EN1998-1-3 (2005). The performance indicators monitored for all limit states are the following: i) peak inter-storey drift ratios; ii) residual inter-storey drift ratios; iii) peak storey accelerations; iv) beam ductility demand; v) beam flexural overstrength. The results are presented hereinafter.

### 5.2.1 *Peak inter-storey drift ratios*

Figure 5.4 depicts the median value of inter-storey drift ratio (IDR) demand along the building height for the three limit states, while Table 5.2 reports the values obtained for the 16<sup>th</sup>, 50<sup>th</sup> and 84<sup>th</sup> percentiles.

As a general remark, the examined design parameters do not reflect any appreciable influence on the IDR demand. However, it is interesting to note that the numerical results show a quite uniform distribution of IDR along the building height, except for the first storey.

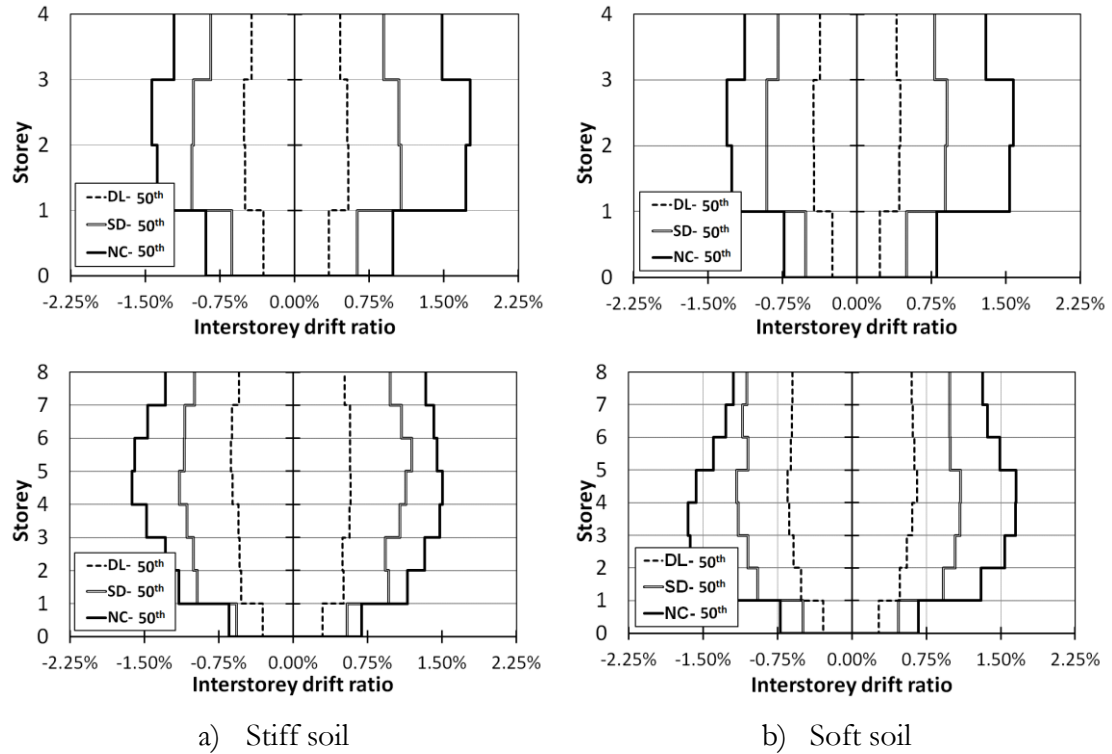


Figure 5.4 – Inter-storey drift demand for the three limit states

The IDR demand at each limit state is fairly lower than the performance limits. It is interesting to note that although the seismic design of the examined frames has been governed by drift limitation, the median values of IDR at DL state are significantly lower than the limit of 0.75%. At DL state, all frames behave in elastic field, being the yield IDR larger than 1% in most of the cases. Thus, consistently with the results from pushover analyses, very limited inelastic demand can be observed at both SD and NC limit state. In particular, the median IDR for the SD also in the range 1% - 1.2% for four- and eight-storey frames, significantly lower than the limit of 3.0%. Such results seem to suggest that dual-steel solution may lead to inefficient and uneconomical structures. However, such considerations have been also drafted for EN1998-1-1 (2004). compliant MRFs made of one steel grade (Castro et al., 2009). The reason of that may be found in the severe requirements for both drift limitations and stability criteria.

### 5.2.2 Residual inter-storey drift ratios

The residual inter-storey drift ratios (RIDR) have been monitored at each limit state, because they provide useful data on the damage distribution and on the post-quake reparability of the frames.

As discussed in the previous section, at DL state, all frames behave elastically and no nonlinear events are observed, except for some cracking in the composite columns. Hence, the RIDRs are close to zero at this limit state.



Table 5.2 – Dispersion of inter-storey drift ratio demand (*values in %*)

Percentiles at each limit state		4-Storey		8-Storey	
		Stiff soil	Soft soil	Stiff soil	Soft soil
DL	16 <sup>th</sup>	0.38	0.36	0.52	0.49
	50 <sup>th</sup>	0.54	0.44	0.63	0.66
	84 <sup>th</sup>	0.83	0.54	0.74	0.82
SD	16 <sup>th</sup>	0.83	0.71	0.89	0.98
	50 <sup>th</sup>	1.07	0.91	1.19	1.16
	84 <sup>th</sup>	1.43	1.29	1.48	1.64
NC	16 <sup>th</sup>	1.39	1.08	1.19	1.35
	50 <sup>th</sup>	1.72	1.58	1.62	1.65
	84 <sup>th</sup>	2.37	1.78	1.98	2.10

Small RIDRs have been recognized at SD and NC limit states, as depicted in Figure 5.5 and Table 5.3 the maximum values are lower than the limit of 0.40%. In particular, the maximum median RIDRs are about 0.05% and 0.19% at SD and NC limit state, respectively. It is interesting to observe that, owing to the smaller design overstrength, all eight-storey frames show the larger demand and consequently residual drift ratios larger than those experienced by four-storey frames. Regarding the soil conditions, the larger RIDRs are observed in frames designed for stiff soil, namely, a value of 0.19% against 0.16% is observed for the eight-storey frames, in addition, it is possible to see a difference of 0.14% - 0.05% for the four-storey frames.

Anyway, the extent of the residual drifts is relatively small, and it easily admits the repair after the earthquake. Nowadays, this issue has a primary importance when it comes to the recent earthquakes (e.g. L'Aquila in 2009, Emilia in 2012, Christchurch in 2010 and 2011, etc.). Indeed, in some cases, the repairing costs may overcome the constructional cost of the new building. Hence, although the performance of the examined frames is less efficient, rough economic considerations may suggest that the examined frames might potentially result in cheaper structures by also taking into consideration the repairing costs in case of a refined benefit-cost analysis. This matter is relatively recent in European design practice, being the current codes (e.g. EN1998-1-1 (2004), EN1998-1-3 (2005), etc.) strictly oriented to design ductile structures experiencing plastic deformations even under moderate seismic action (as also those at DL limit state). More detailed investigation of this topic is beyond the scope of this study but it is clearly a research field that deserves further analysis.

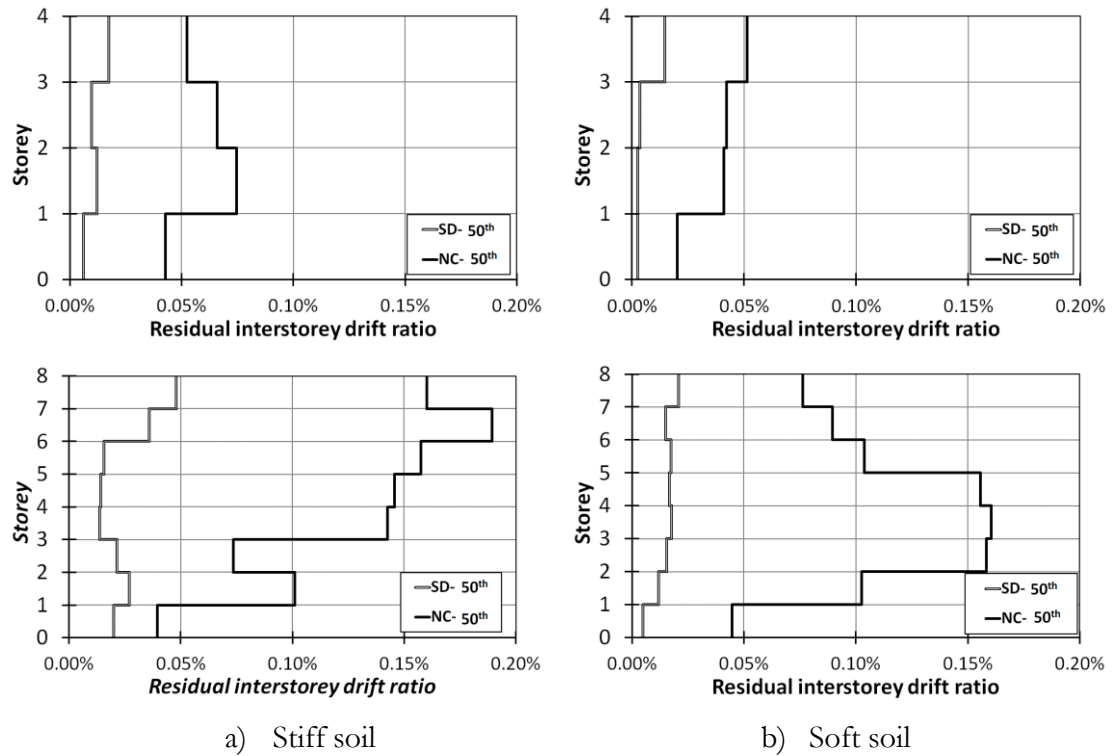


Figure 5.5 – Residual inter-storey drift ratios

Table 5.3 – Dispersion of residual inter-storey drift ratio demand (*values in %*)

Percentiles at each limit state		4-Storey		8-Storey	
		Stiff soil	Soft soil	Stiff soil	Soft soil
SD	16 <sup>th</sup>	0.00	0.00	0.01	0.01
	50 <sup>th</sup>	0.02	0.01	0.05	0.02
	84 <sup>th</sup>	0.08	0.03	0.20	0.05
NC	16 <sup>th</sup>	0.04	0.01	0.04	0.05
	50 <sup>th</sup>	0.14	0.05	0.19	0.16
	84 <sup>th</sup>	0.25	0.16	0.35	0.36

### 5.2.3 Peak storey accelerations

Peak storey accelerations (PSAs) are usually related to the non-structural damage. They allow us to quantify the potential economic loss depending on the type of facilities and non-structural elements.

Figure 5.6 and Table 5.4 show the distribution of the median values of PSA along the building height for each limit state and their percentiles. The results are shown varying the number of storeys and the soil conditions, because these design parameters are those actually influencing the PSAs. It is interesting to note that the median maxima PSA are similar for

both four- and eight-storey buildings located on stiff soil, with values of about 1.6, 3 and 4 times the design acceleration  $A_d$  at DL, SD and NC respectively. As predictable due to the larger input acceleration at the fundamental period, the buildings located on soft soil show larger values for PSAs, ranging from 2, 4 to 5 times  $A_d$  for DL, SD and NC, respectively.

The significant dynamic magnification of storey accelerations in all examined cases clearly highlights that very severe non-structural damage can be expected, which corresponds to a very limited structural damage. Indeed, most of the architectural components (i.e. cladding systems, ceiling and lighting systems, interior partition walls, etc.), as well as, the mechanical and electrical equipment and systems (i.e. heating, ventilation and cooling systems, fire protection systems, and emergency power systems, etc.), and also the building contents and inventory are prone to high amplitude of storey accelerations, according to what is shown by recent earthquakes (FEMAE-74, 2011). Hence, it should be observed that such kind of structural systems may be unsuitable for critical facilities, like hospitals where the indirect losses due to damaged equipment and lost inventory represent more than 80% of the total construction cost (FEMAE-74, 2011).

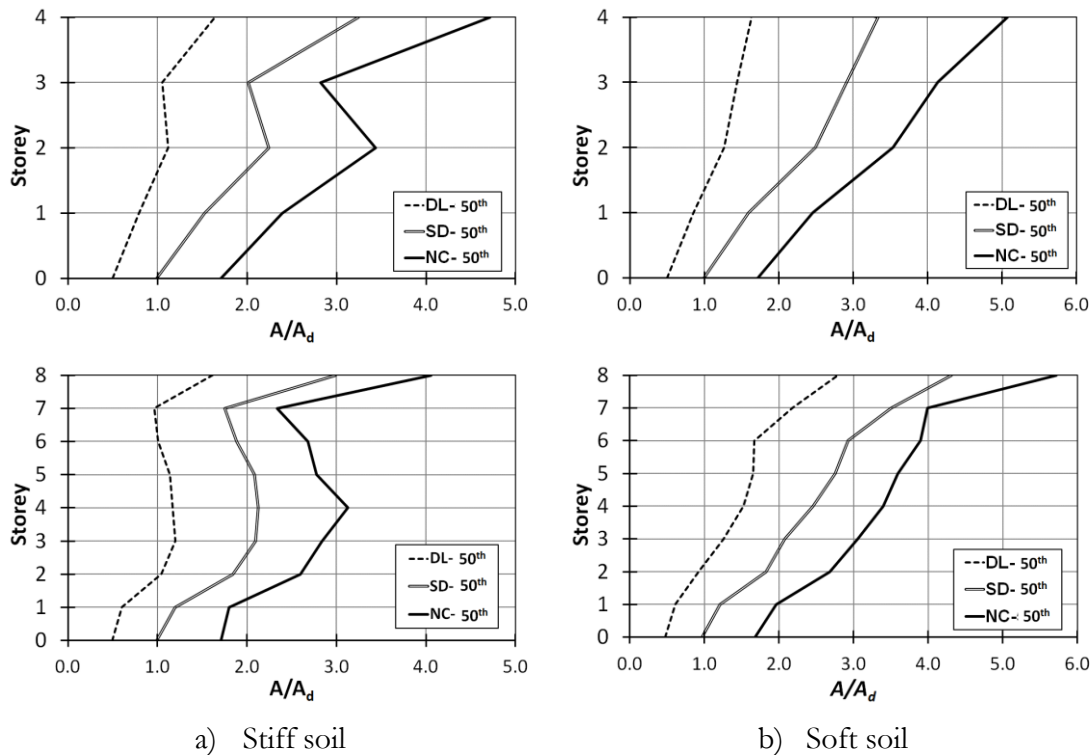


Figure 5.6 – Storey acceleration for DL, SD and NC limit states

Table 5.4 – Maximum ratios obtained for PSAs

Percentiles at each limit state		4-Storey		8-Storey	
		Stiff soil	Soft soil	Stiff soil	Soft soil
DL	16 <sup>th</sup>	1.34	1.45	1.40	2.07
	50 <sup>th</sup>	1.64	1.63	1.61	2.79
	84 <sup>th</sup>	1.94	2.10	1.92	3.48
SD	16 <sup>th</sup>	2.69	2.76	2.54	3.75
	50 <sup>th</sup>	3.24	3.33	2.98	4.30
	84 <sup>th</sup>	3.71	4.27	3.65	5.14
NC	16 <sup>th</sup>	3.77	4.66	3.51	4.90
	50 <sup>th</sup>	4.71	5.07	4.05	5.71
	84 <sup>th</sup>	5.43	5.70	4.88	6.50

#### 5.2.4 Beam ductility demand

The ductility demand for dissipative beams of MRFs is expressed in terms of total chord rotation. The beams should have adequate rotation capacity to assure that a determined portion of the input seismic energy is dissipated by plastic behaviour. Therefore, steel beams need to develop a ductile behaviour with high rotation capacity (D'Aniello et al., 2012; D'Aniello et al., 2014b).

According to EN1998-1-1 (2004), the beam plastic rotation capacity should be no lesser than  $10\theta_y$ ,  $60\theta_y$  and  $80\theta_y$ , respectively for the DL, SD and NC, being  $\theta_y$  the beam yield rotation.

Figure 5.7 illustrates the median ductility demand along the building height. As it can be observed, most of the beams are in elastic range at SD limit state, while very limited plastic rotation demand can be recognized at NC limit state. Once more, these results can be explained by the design procedure that led to an oversize of the structural element in order to fulfil the requirement of damage limitation.

The small beam ductility demand suggests that for such rather structures the use of class 2 beams can be more convenient, because the large reserve of ductility of class 1 profiles cannot be exploited. In addition, at the same overall performance cheaper structures would be designed.

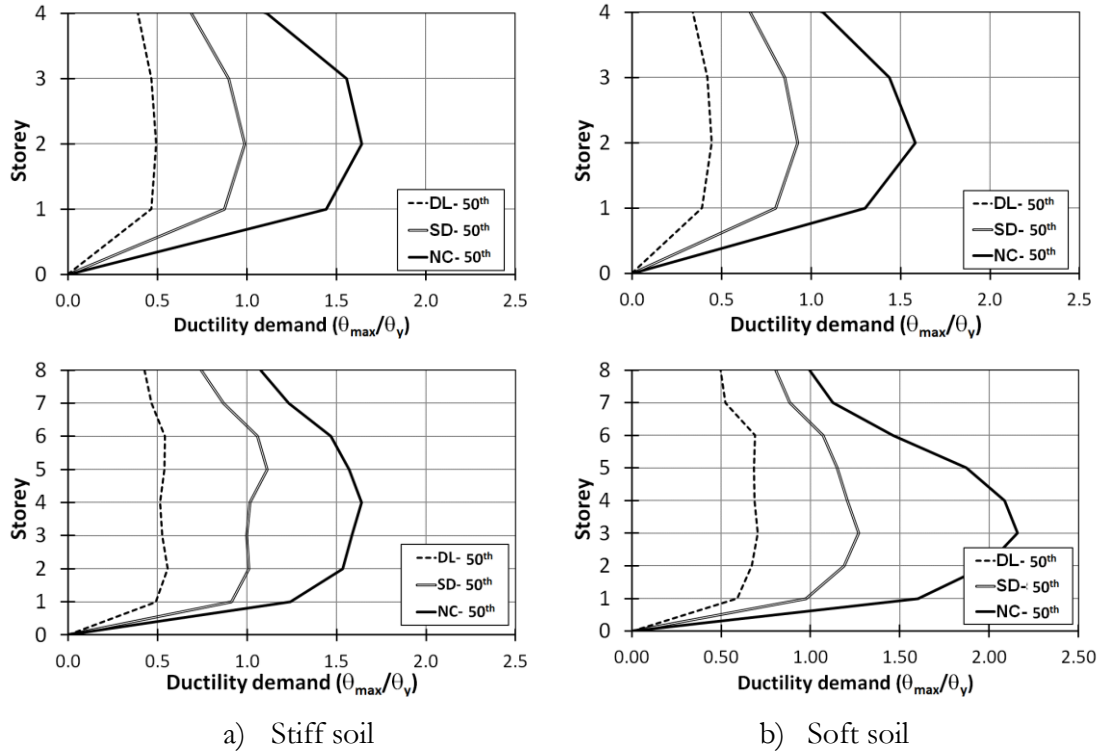


Figure 5.7 – Ductility demand ratios

### 5.2.5 Beam flexural overstrength

The beam flexural overstrength ( $s$ ) is the non-dimensional measure of the ultimate bending capacity of steel beams, due to the amount of strain hardening which can be exhibited prior beam failure (D'Aniello et al., 2012; D'Aniello et al., 2014b).

The maximum flexural overstrength ( $s^*$ ) may be defined in terms of bending moments as follows:

$$s^* = \frac{M_{\max}}{M_p} \quad (5.1)$$

in which,  $M_{\max}$  is the peak bending moment experienced by the beam, and  $M_p$  is the beam plastic bending moment.

This factor plays a key role in the application of hierarchy criteria in seismic design, EN1998-1-1 (2004) accounts only for the possible overstrength due to the random material variability, which considers an overstrength factor equal to  $1.1 \gamma_{ov}$ , for all types of members. Conversely, the amount of beam strain-hardening is neglected, potentially underestimating the real ultimate strength of members, especially for those belonging to class 1 according to EN1993-1-1 (2005).

Figure 5.8 shows the median distribution of  $s^*$  along the building height. As it can be noted, most of the beams behave elastically, thus the median  $s^*$  is lesser than the unity. Some cases slightly larger than 1 occur for 8-storey frames with soft soil at SD and NC limit states. Such results confirm that the design approach of EN1998-1-1 (2004) is consistent with the expected performance of the frames, namely limited ductility demand resulting in small hardening developed by plastic hinge.

Despite the moderate beam plastic engagement, all the analyses showed that the seismic action might induce bi-triangular distribution of bending moments close to the plastic capacity at both beam-ends. This implies that significant shear forces are expected in the panel zone of the columns, especially in the inner columns where the shear force acting on the web panel is almost twice of what is seen in the corner columns.

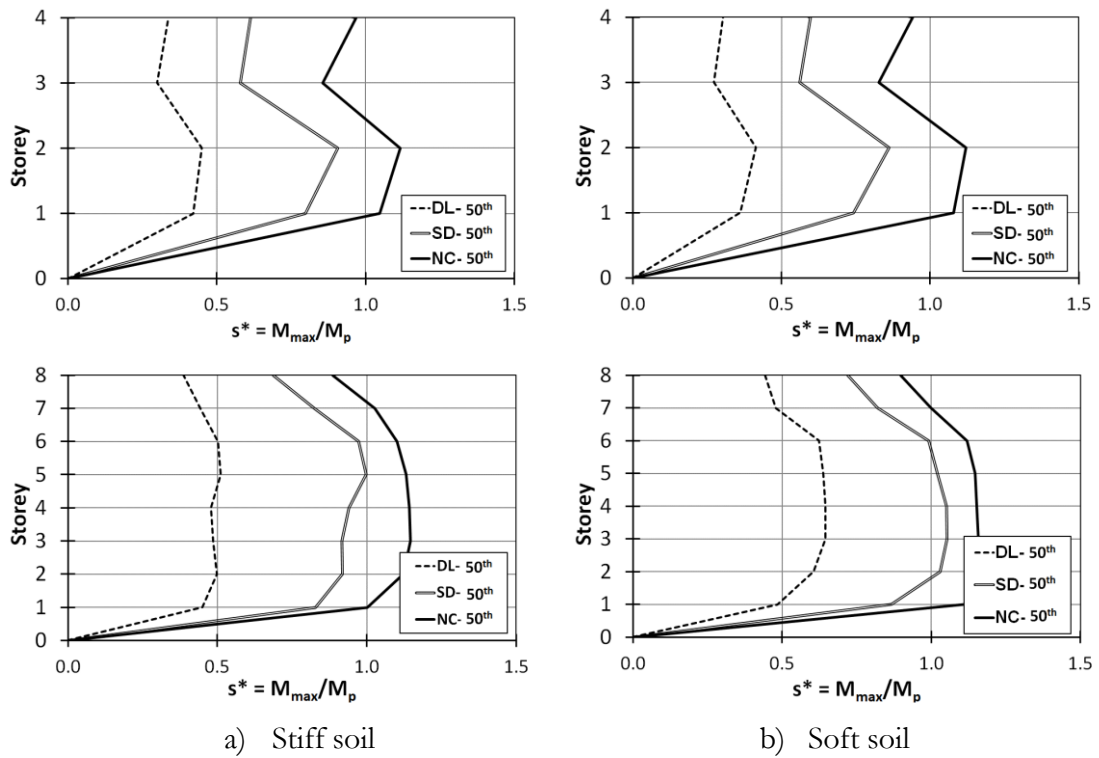


Figure 5.8 – Overstrength demand ratios

The analyses showed that the transformation factor ( $\beta$ ) can vary within the range 1.29 to 2.01 at SD and 1.67 to 2.14 at NC, being  $\beta$  defined according to EN1993-1-8 (2005), which is the ratio between the beam moments  $M_{j,b1,Ed}$  and  $M_{j,b2,Ed}$  at the intersection of the member centrelines into the connections. It is interesting to note that according to EN1993-1-8 (2005)  $\beta$  should be no larger than 2, which corresponds to the contemporary formation of plastic hinge in the two beams belonging to the connections. However, in real cases the amount of strain hardening may lead to overcome the plastic moment in one side of the connections. This effect should be accounted for designing full strength connections according to the provisions of EN1998-1-1 (2004), in which column panel zone should be

designed in order to avoid significant yielding within this component. In the reference frames, in order to satisfy this code requirement, each web panel of interior column was strengthened with one doubler plate thinner than the column web in all cases.

### 5.3 Behaviour factors

As previously mentioned in Chapter IV – Section 4.4, two approaches have been used in order to assess the behaviour factors. The first corresponds to method incorporated in EN1998-1-1 (2004) and will be referred as European approach. The second was proposed by Salvitti and Elnashai approach and will be referred as Salvitti & Elnashai approach. Figure 5.9 and Figure 5.10 summarize the behaviour factors obtained using both approaches. A behaviour factor equal to 1.0 is assumed by the DL limit state, due to the responses of the examined frames that were on the elastic field.

It is notorious to note that the European approach reveals a smaller behaviour factor in comparison with Salvitti and Elnashai approach. Indeed, their formulation performs a verification of the behaviour factor through the level of building overstrength. The large behaviour factors found are consistent with the nonlinear results of the study cases, which presented a large high level of overstrength.

The European approach gives behaviour factor to the SD limit state equal to 3.44 and 3.30 for the frames located on stiff and soft soils, respectively. Using Salvitti and Elnashai approach the values are quite higher, i.e. 9.18 for the stiff soil and 7.96 for the soft soil.

Concerning NC limit state, values of 3.93 and 3.43 according to type of soil are obtained using the European approach, which, again, are much lower than 8.14 and 7.58 obtained using Salvitti and Elnashai approach. Moreover, it is interesting to mention that the values for NC limit state are obviously larger than those for SD limit state, owing to the more demanding collapse criterion for the European approach. On the other hand, the other method delivers smaller behaviour factors for the NC state, because the increasing of the acceleration corresponding to failure criterion is not proportional to the increasing of the PGA of limit state. In other words, the study cases are closer to reach the limit proposed by NC limit state than those assumed for the SD one.

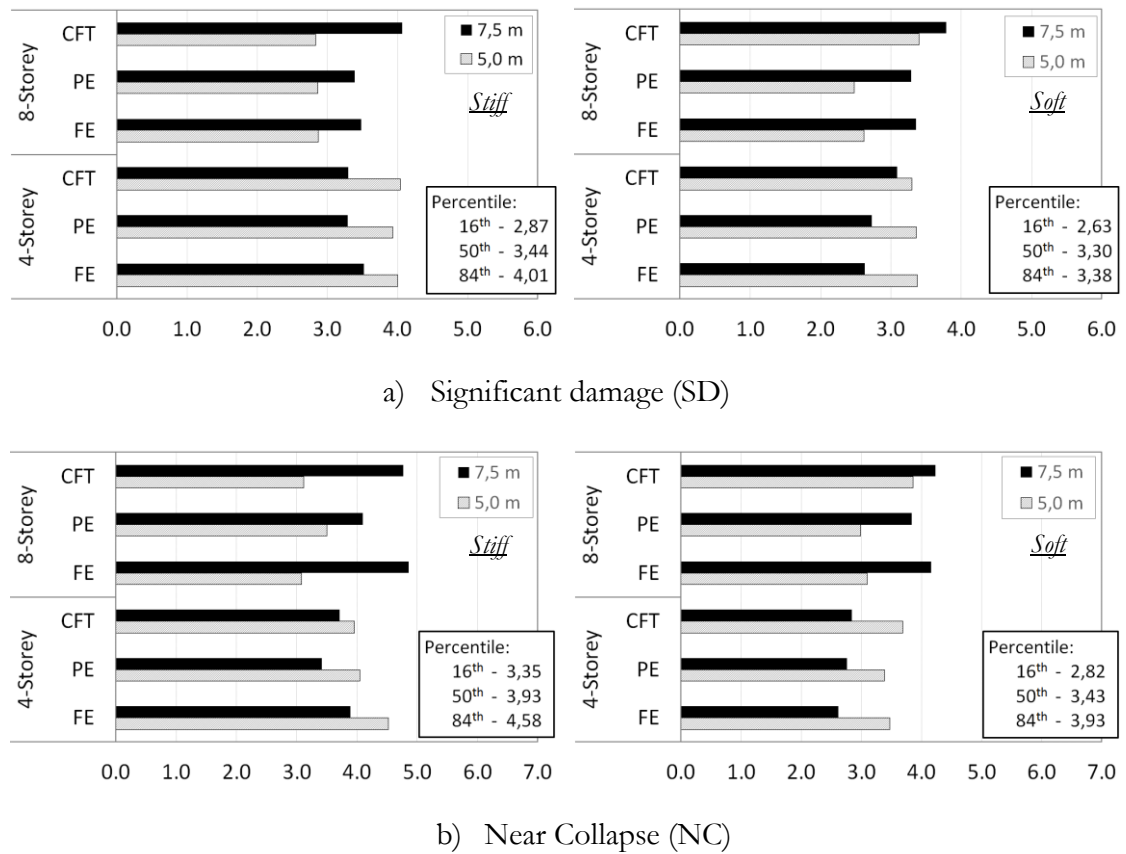


Figure 5.9 – Behaviour factors using European approach

By analysing the role of the examined design parameters, it is not possible to define a general trend. Anyway, it is interesting to note that the frames located on soft soil present behaviour factors, which are slightly lower than those obtained for stiff soil, independently of the approaches. Such results are mainly due to the larger displacement demand of records for soft soil, which are characterized by more severe accelerations within the fundamental periods of the examined frames.

Aside from the soil conditions, Figure 5.9 and Figure 5.10 show that the span length is the geometrical parameter influencing the value of behaviour factor. For four-storey frames, those with the shorter span are characterized by larger behaviour factors. On the other hand, the contrary is seen for eight-storey frames. These results can be explained by considering that for all cases the drift criterion was the main condition limiting the seismic performance. Therefore, in low-rise frames the overall displacement shape at the peak is close to shear type profile, consequently, the lateral stiffness increases reducing the beam length. Thus, a larger acceleration is necessary to overcome the drift capacity and a larger behaviour factor is obtained. In case of taller frames, the lateral displacement profiles differ from the beam length. In particular, the cases with shorter spans tend to present an overall cantilever response, while a shear type shape corresponds to the frames with longer bays. This different



behaviour is associated to different drift demand. The cantilever-type structures show a larger demand especially at the upper storey, leading to smaller  $A_0$  limits and smaller behaviour factors.

As a general remark, it should be noted that the median behaviour factors (namely 3.44 and 3.30 for stiff and soft soil) obtained from IDAs at SD are slightly lower than that used at the design stage (namely  $q = 4$ ) for the European approach. This result is consistent with recent research findings D'Aniello et al. (2014b) that highlight the need to a rational recalibration of the values of behaviour factors reported in EN1998-1-1 (2004).

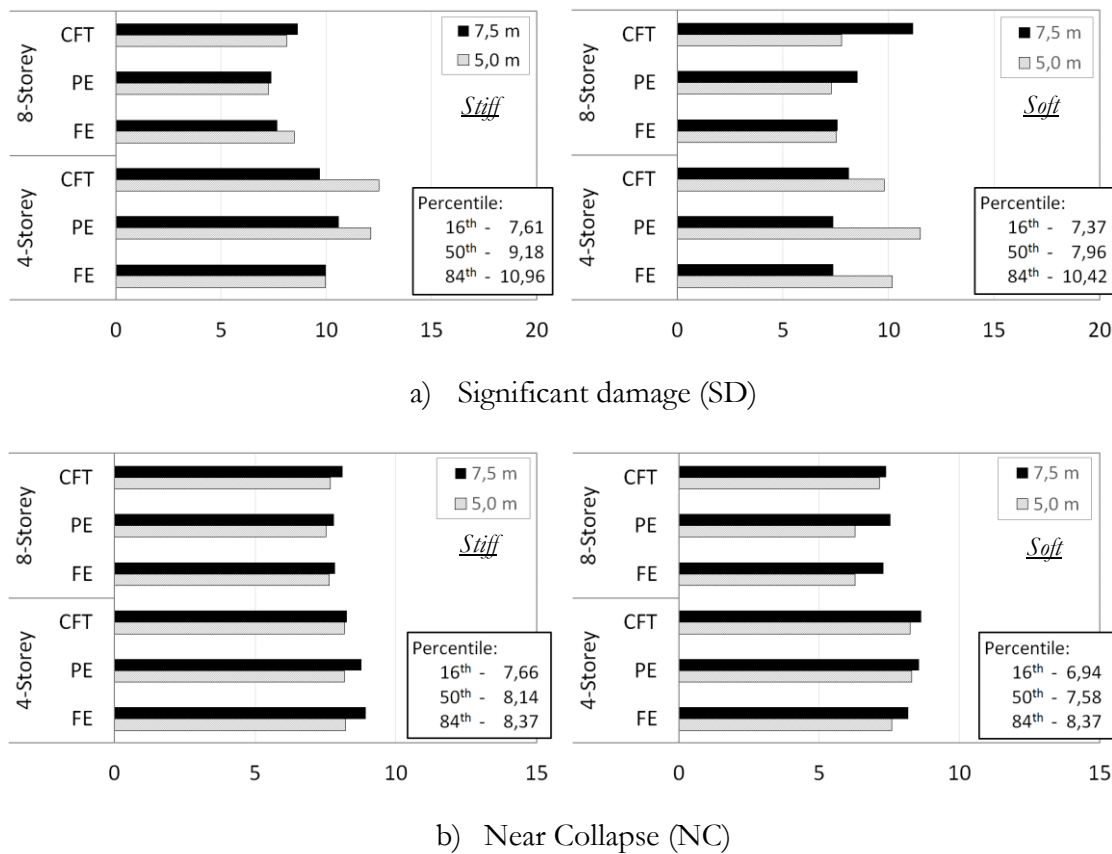


Figure 5.10 – Behaviour factors using Salvitti & Elnashai approach

## 5.1 Material consumption

Steel consumption is computed in terms of total weight, while concrete consumption is computed in terms of total cast volume. The amounts of steel grade S355 (MCS) used for beams, steel grade S460 (HSS) used for columns and reinforcement steel (RS) are presented separately. The total amount obtained has been divided by the tributary area of the frame,  $3L^2$  (see Figure 5.11) and by the number of stories “ $n$ ”, as follows:

$$\gamma_{material} = \frac{Total\ Amount}{3L^2 \times n} \quad (5.2)$$

The average value obtained in Expression (5.2) for each type of material is denoted as “material density” hereafter.

Table 5.5 reports the material density showing the dependency of this indicator on the examined design parameters. The interrelations with those parameters have been clarified in Figure 5.11 to Figure 5.13.

As a general comment, the structures designed for soft soil are characterized by a consumption of materials larger than those designed for stiff soil. This result is even more interesting by considering that the design PGA for frames on soft soil is smaller (namely equal to 0.16g) than that used for cases on stiff soil (namely equal to 0.24g). However, it is not surprising, because the soft soil spectrum is characterized by design accelerations larger than those for stiff soil spectrum at the fundamental periods of the reference buildings.

The influence of column cross section typology is shown in Figure 5.11. As it can be noted, the structures with CFT columns are characterized by a larger consumption of steel, especially for the columns that are made of HSS. In addition, considering that the configuration of beam-to-column connections that should be used in order to have full strength connections are more complex and expensive than those used for wide flange columns. The structures made of CFT are the least effective from an economical point of view. For the cases with FE and PE, columns are characterized by similar material consumptions.

Table 5.5 – Average weight (kg) of steel for each structural element

<i>Span</i>	<i>8-Storey</i>				<i>4-Storey</i>			
	<i>Stiff soil</i>		<i>Soft soil</i>		<i>Stiff soil</i>		<i>Soft soil</i>	
	<i>Column</i>	<i>Beam</i>	<i>Column</i>	<i>Beam</i>	<i>Column</i>	<i>Beam</i>	<i>Column</i>	<i>Beam</i>
5.0 m	12729	8084	17533	9711	6979	3524	8004	3524
7.5 m	29752	12283	33015	16082	10846	5553	13263	5553
$\Delta\gamma = \gamma_{7.5}/\gamma_5$	2.34	1.52	1.88	1.66	1.55	1.58	1.66	1.58

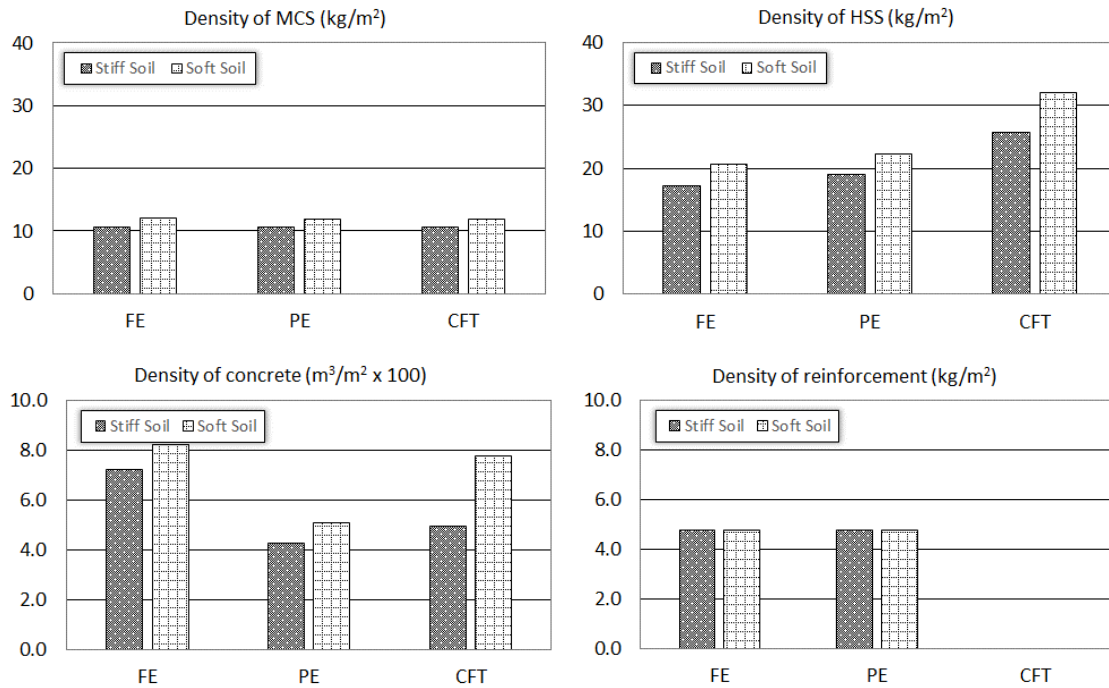


Figure 5.11 – Average of amount of steel and concrete

Figure 5.12 shows the steel densities highlighting the influence of span length. As it can be noted, for both four- and eight-storey frames the cases with 5.0m span show higher density of both MCS and HSS than those with 7.5m span. This result is ascribable to the need to provide adequate lateral stiffness, compelling the designer to select heavy profiles.

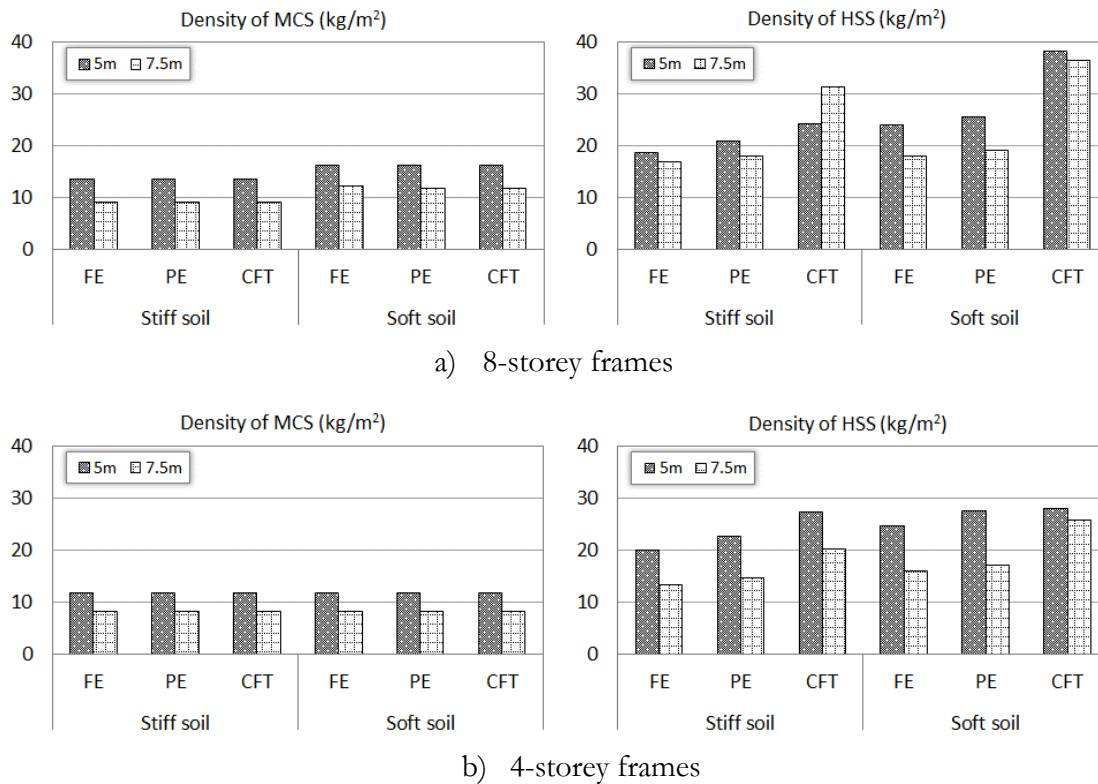
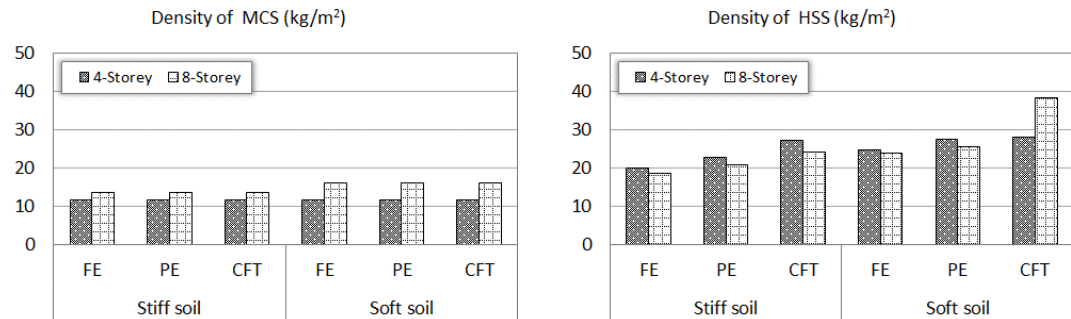
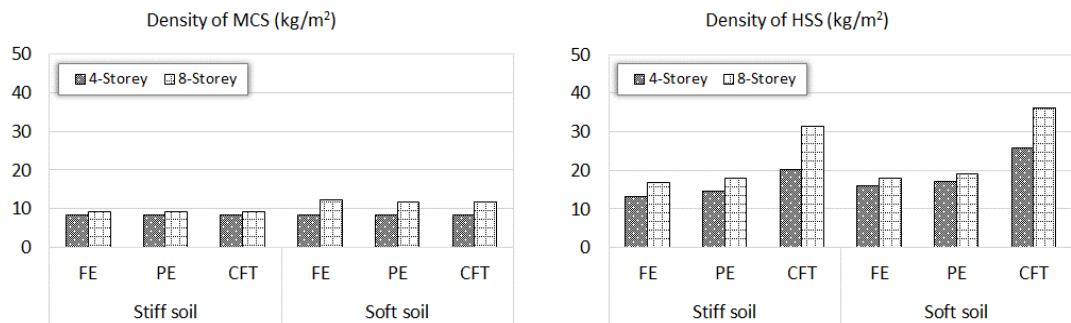


Figure 5.12 – Comparison of material consumption to span length

Figure 5.13 shows the variability of steel density highlighting the influence of number of storeys. As expected, the plots highlight that larger steel density generally characterizes taller frames, which are expected for the cases with four-storeys and span length equal to 5.0 m, where the HSS density is larger. As previously discussed, this outcome derives from the design process to satisfy both drift and stability limitations.



a) Frames with 5.0m of span



b) Frames with 7.5m of span

Figure 5.13 – Comparison of material consumption to number of storey

## ***Chapter VI***

# Concentrically Braced Dual-Steel Frames

In this chapter, the nonlinear behaviour of the Concentrically Braced Dual-Steel Frames is presented with particular focus on the static and dynamic nonlinear analyses. The nonlinear results provide a discussion about the design parameters that affect the overall or local seismic performance. In particular, the overstrength and behaviour factor are obtained from all study case, as well as from seismic performance on the three limit states as EN1998-1-3 (2005). The performance of the frames is evaluated and the role of each design parameter is discussed based on the following global and local indicators: i) peak inter-storey drift ratios; ii) residual inter-storey drift ratios; iii) peak storey accelerations and iv) brace ductility demand.

Furthermore, the material consumption is also examined in this chapter. The aim is to discuss the influence of the design parameters over the material amount. Moreover, the outcomes of the decision adopted on the seismic design, as well as the requirement incorporated on the design stage concerning the material consumption. .

### **6.1 Nonlinear static analysis**

Figure 6.1 and Figure 6.2 depict the pushover curves from the 1<sup>st</sup> Mode and Uniform patterns obtained by normalizing the base shear  $V$  with the design base shear  $V_d$ . These curves show a particular characteristic of the CBFs. It can be clearly seen that after the first plastic event, there is a sudden reduction in the lateral resistance of the building. This trend is justified due to the buckling effect of the braces in compression. The sudden decrease of lateral resistance is immediately followed by an increase with reduced lateral stiffness of the frame. The maximum lateral resistance of the eight-storey frames is larger than the lateral resistance associated with the first buckling event. However, the sudden reduction in lateral

resistance seems to penalize more the taller frames, since for these frames it is not possible to clearly identify an increase of the lateral resistance after the first plastic event, except for the uniform pattern, and when occurs, this is not substantial. This behaviour has an influence on the assessment of the overstrength factors, which will be discussed later.

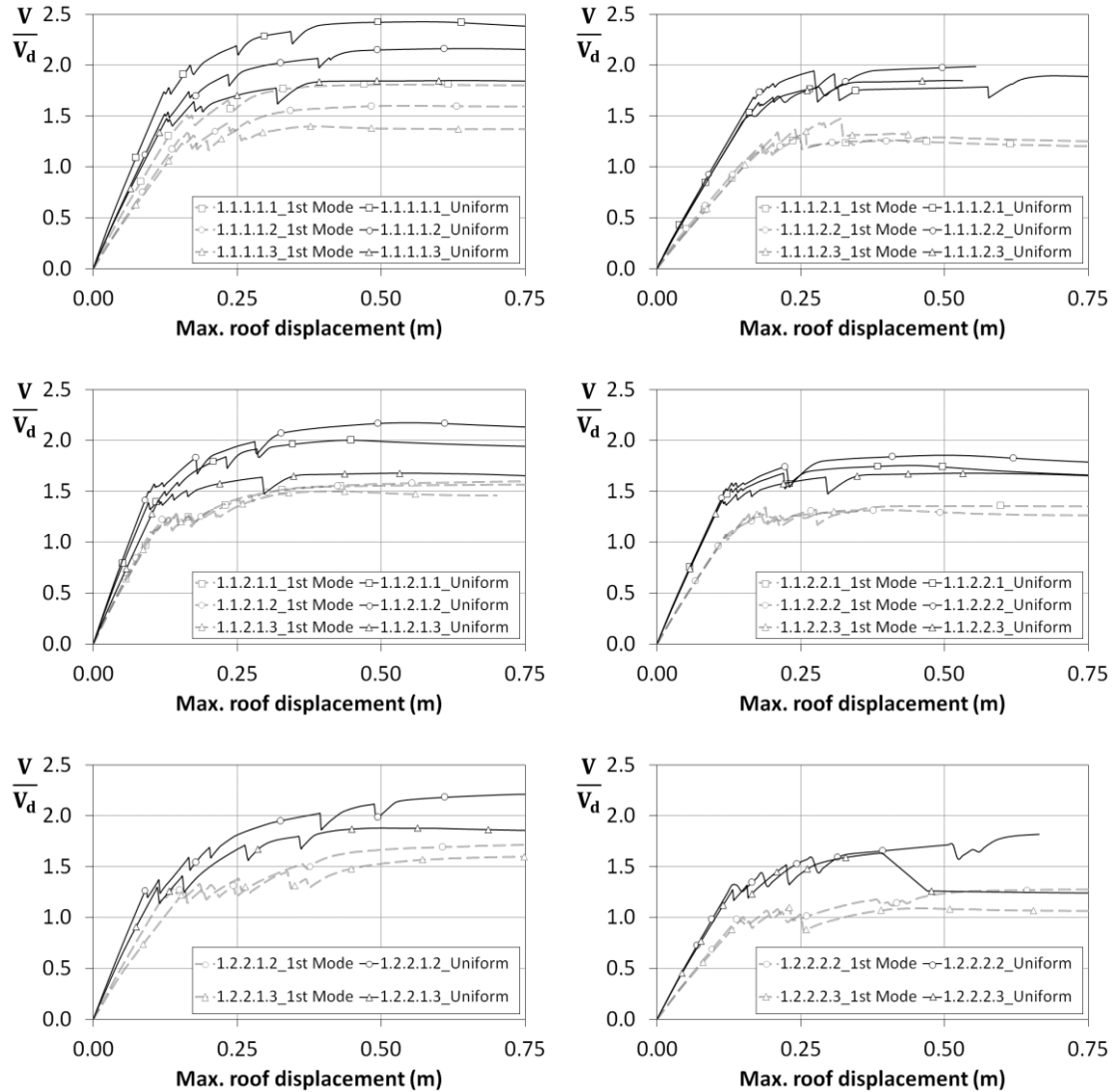


Figure 6.1 – Normalized pushover response curves from eight-storey frames

The curves plotted in Figure 6.1 and in Figure 6.2 allow highlighting the influence of the investigated parameters. By focusing on the number of storeys, it can be observed that eight-storey frames experience larger  $V/V_d$  ratios than the sixteen-storey frames. In fact, the maximum base shear from taller frames is basically determined when the first plastic hinge is formed. As a matter of fact, the poor redistribution of the inelastic demand is more evident for the sixteen-storey resulting on soft storey mechanism. This observation implies that the higher the number of storeys, the smaller the overstrength factor.

Concerning the span length, the frames with shorter span present slightly larger base shear ratio mainly for the cases located on stiff soil condition. Those frames were designed

considering an overstrength factor from dissipative member higher than the frames with larger span, resulting on stiffer structures in order to fulfil the capacity design criteria.

In relation to the column type used, the major differences can be observed when the uniform load pattern is applied. In regard to the modal load pattern, no substantial differences can be recognized in terms of lateral capacity, expect for the taller frames. In general, frames with CFT columns have smaller overall stiffness and smaller base shear ratio in comparison with both FE and PE columns. In order to allow for feasible connections the design took into consideration the geometric restriction of the column instead of its resistance, which was design driving in some situations. Thus, these over-designed structures provide high level of lateral stiffness resulting on higher lateral overall stiffness.

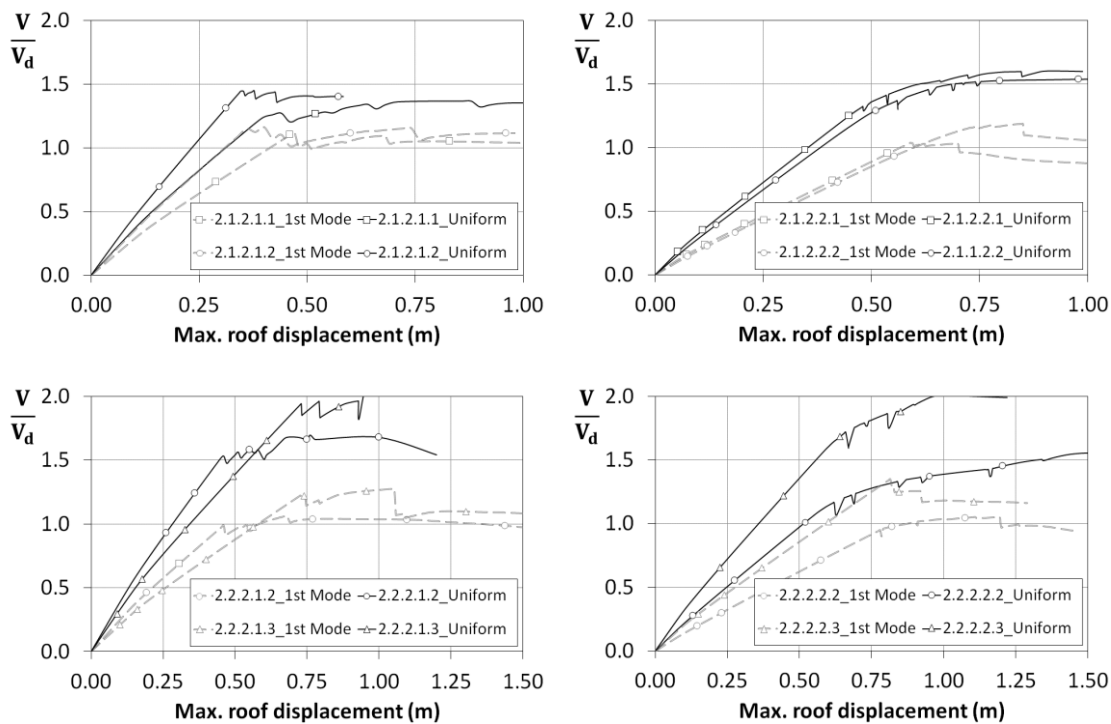


Figure 6.2 – Normalized pushover response curves from sixteen-storey frames

Considering the soil conditions, the base shear ratio of frames located on stiff soil is higher than the one located on soft soil conditions. The frames located in the zone with soft soil condition are designed considering a higher design base shear due to larger ground motion control period,  $T_c$ . Thus, the frames in soft soil are stiffer and strong in comparison with other frames. Moreover, the slenderness brace criterion is less significant for these frames. The sum of these factors causes a reduction between the base shear from first plastic event and maximum base shear. Therefore, the frames on soft soil condition cannot significantly increase the lateral resistance after the first plastic event.

Regarding to HSS steel grades used, the frames designed with S690 show slight larger ratios compared to frames with S460. Indeed, the use of superior steel grade allow having an small increase of the resistance after of the first plastic event. This result can be explained by fact of the good redistribution of the forces for the frames with S690 where another storey also suffer plastic deformation without concentrating on one.

The damage distribution when the structure reaches an inter-storey drift of 2% modal pattern loading pushover is illustrated in Figure 6.3 to Figure 6.6. Observing the plastic hinge sequence, it is worth noting that the first yielding is located in braces in compression. Soon thereafter, the plastic hinges are formed in beams from braced bay, and finally, the inelastic deformation develops in tensioned braces.

As a general remark, the capacity design criteria used on seismic design is confirmed when most of the plastic hinges are concentrated on the dissipative elements, namely, the brace keeping the non-dissipative ones in elastic field. Nevertheless, it is possible to see that some beams from braced bay experience the formation of plastic hinges due to high resistance degradation after the braces buckling. This observation is important because these beams were designed to resist the vertical forces due to contemporary brace yielding in tension and post-buckling in compression. This subject have been addressed in several studies, in particular, a numerical study has recently been carried out by Serra et al. (2010) in order to investigate the post-buckling compressive strength of the braces. The authors have shown that the post-buckling resistance considered in EN1998-1-1 (2004) is not adequate. Results have shown that post-buckling compressive strength is lower than the one included in European code.

The poor distribution of damage in some cases is related to inability of this structural system in redistributing the inelastic demand in the vertical direction, being, therefore, prone to soft storey formation. This fact is more evident in taller frames located on soft soil condition. The number of plastic hinges located on sixteen-storey frames is much smaller in comparison with the eight-storey ones. The increase in the building height allowed high concentration of damage located on specific region mainly in mid-rise. Thus, it was not possible to reproduce a uniform distribution of damage seen in the eight-storey frames. This fact is consistent with the capacity curves in which there is no appreciable increasing of the lateral resistance after the first plastic event in the taller frames.



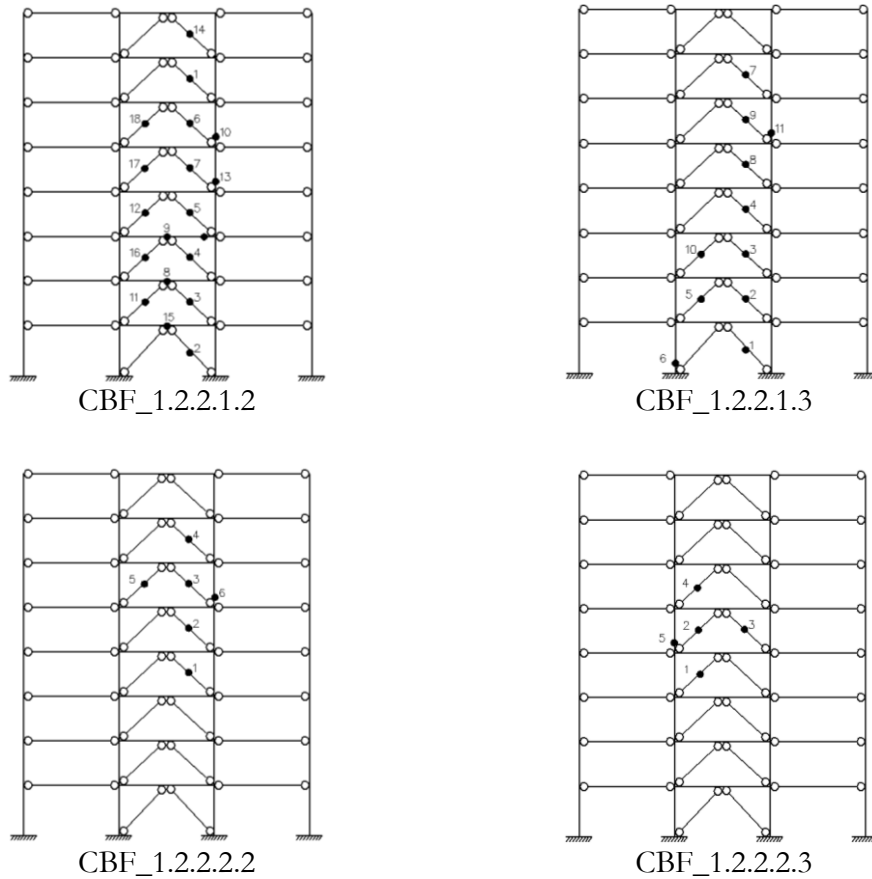


Figure 6.3 – 1<sup>st</sup> Mode Pushover: Damage distribution for eight-storey frames with S690

The use of S690 steel grade in non-dissipative members provides smaller plastic hinges in comparison with the S460. Moreover, the formation of plastic hinge on the beam from braced bay is not pronounced on the cases with S690. In fact, these beams were designed considering the same steel grade of non-dissipative steel grade; therefore, the beam strength of a solution with S690 should be larger, in contrast, with smaller flexural stiffness.

With regard to the type of composite steel-concrete column used, it is not possible to find a clear tendency of behaviour to a particular composite cross-section. However, the frames using FE column on the non-dissipative members experience a higher number of plastic hinge compared to solution with PE and CFT columns.

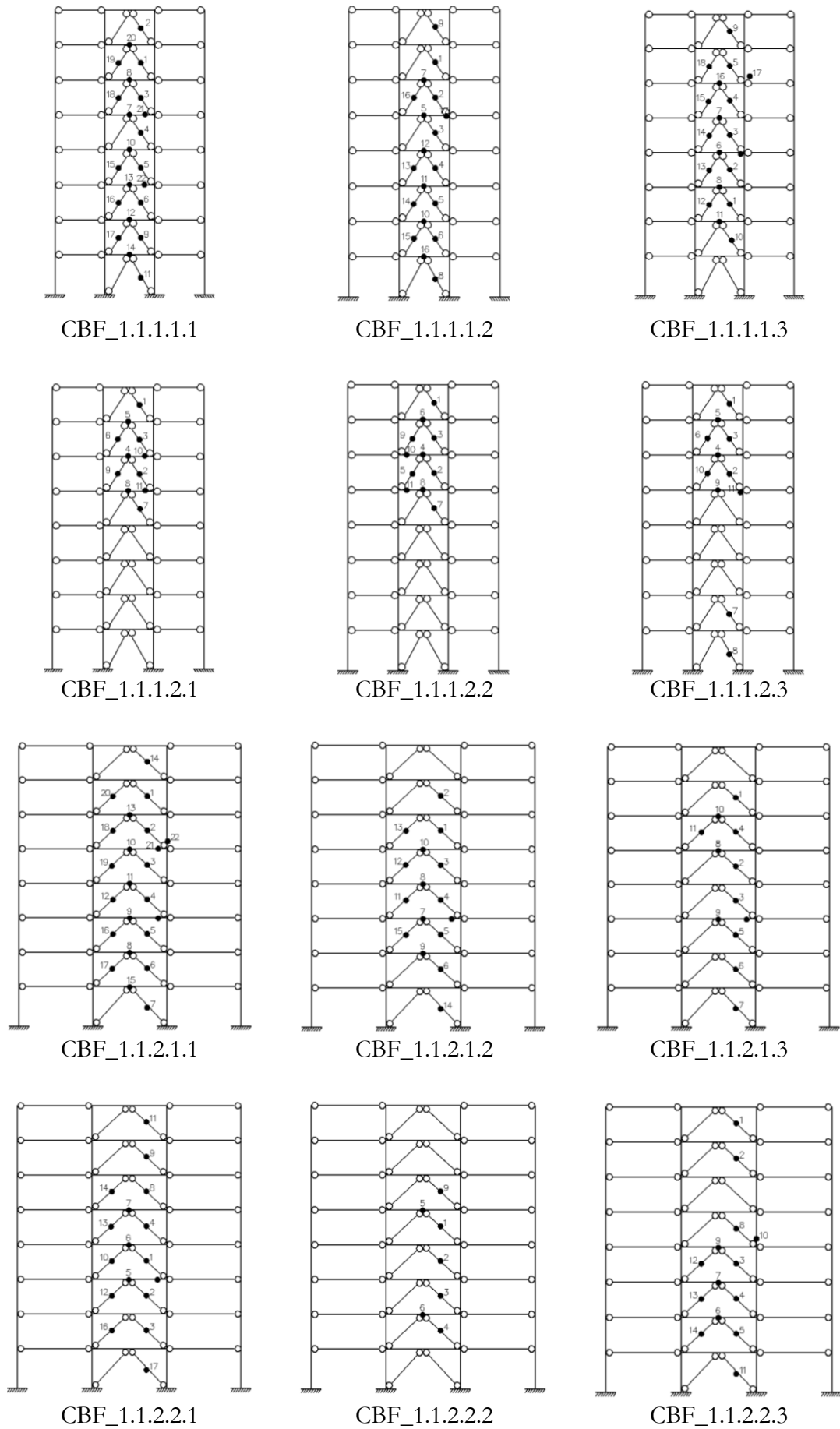
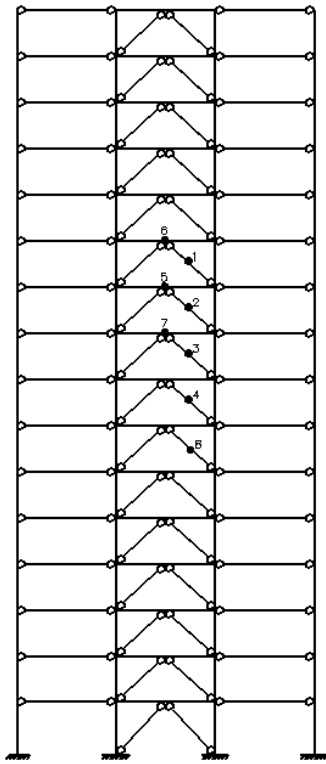
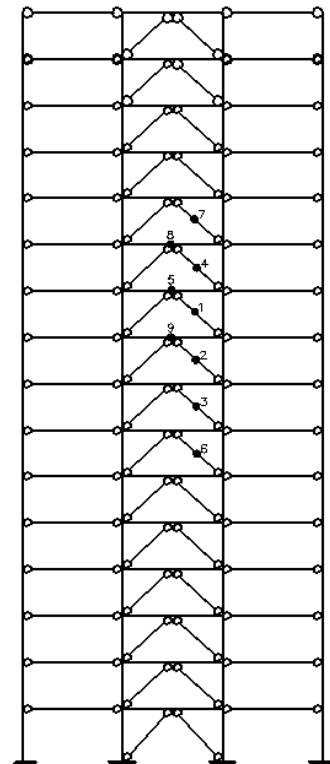


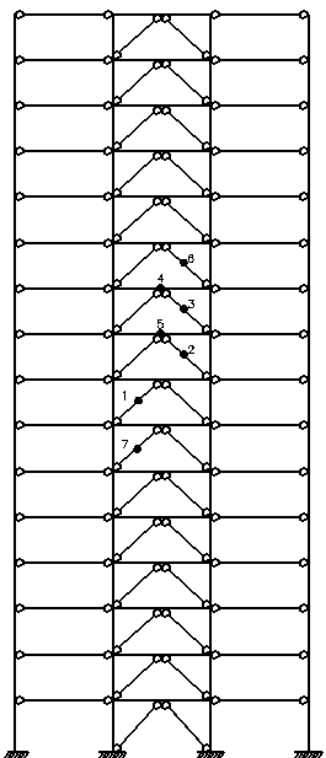
Figure 6.4 – 1<sup>st</sup> Mode Pushover: Damage distribution for eight-storey frames with S460



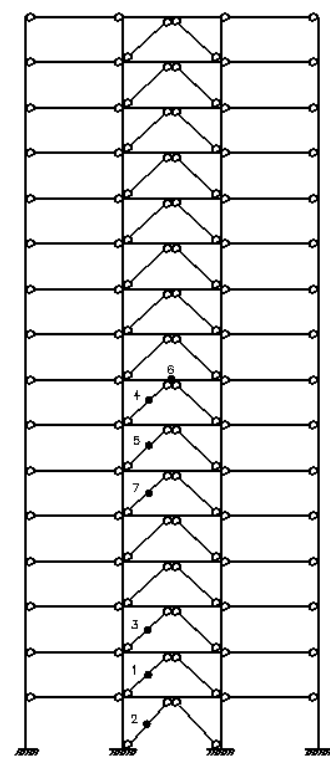
CBF\_2.1.2.1.1



CBF\_2.1.2.1.2

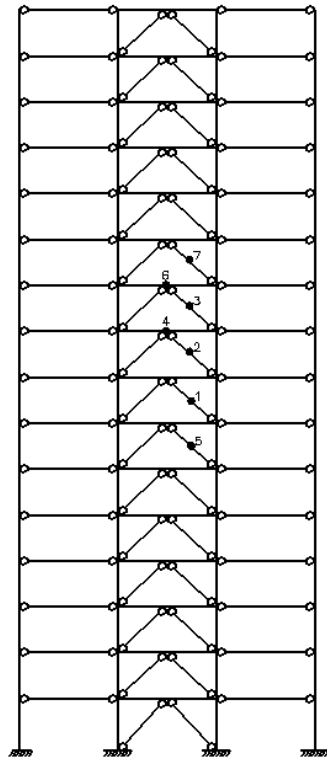


CBF\_2.1.2.2.1

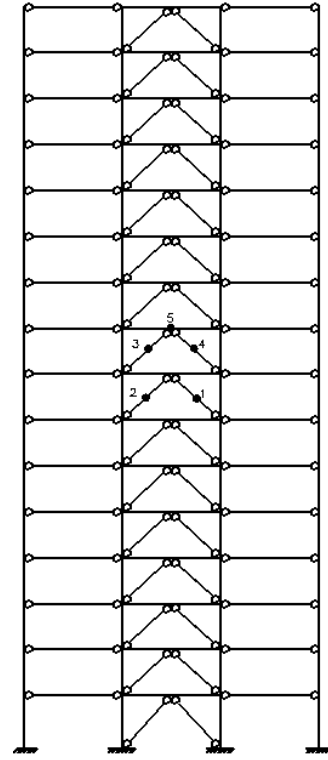


CBF\_2.1.2.2.2

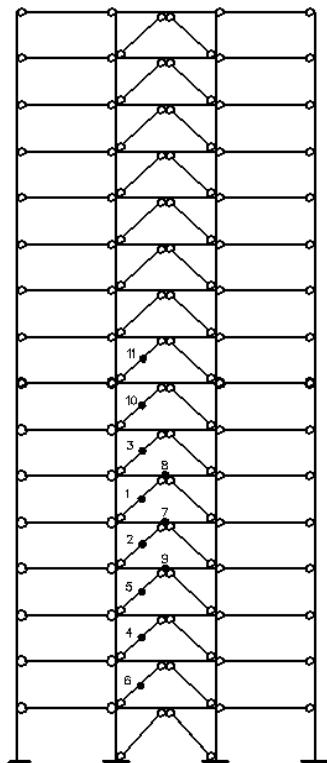
Figure 6.5 – 1<sup>st</sup> Mode Pushover: Damage distribution for sixteen-storey frames with S460



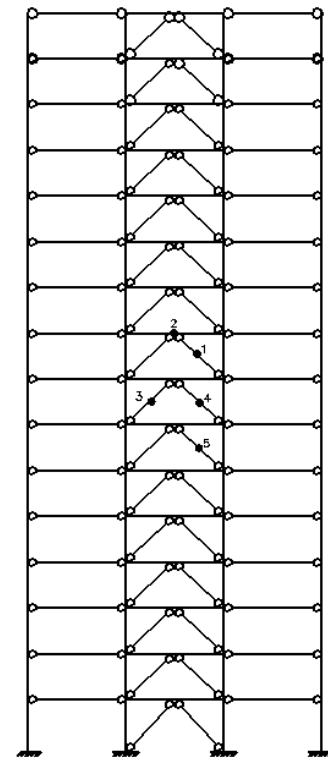
CBF\_2.2.2.1.2



CBF\_2.2.2.1.3



CBF\_2.2.2.2.2



CBF\_2.2.2.2.3

Figure 6.6 – 1<sup>st</sup> Mode Pushover: Damage distribution for sixteen-storey frames with

S690

### 6.1.1 Overall overstrength factor

The study of the overstrength is based on the two terms of the Equation (4.1). The values obtained from pushover analyses, considering the two load patterns, are presented in Table 6.1 for all case studies. In general, the modal pattern is responsible for giving the minimum value for the overstrength associated with design decision and the  $\Omega$  factor. However, there are some cases in which the uniform pattern provides the minimum value for the overstrength fact incorporated in EN1998-1-1 (2004). The frames with minimum overstrength provided by uniform pattern are characterized by high damage concentration in low-rise floors.

When analysing the results concerning the number of storey, sixteen-storey frames exhibit smaller overstrength factor in comparison with eight-storey frames, except for the second term of Equation (4.1). In fact, the taller frames concentrate damage, in most cases, in the mid-height resulting in soft storey mechanism due to poor redistribution of the forces. On the other hand, the eight-storey frames provide larger overstrength factor, due to the better redistribution of damage along the vertical direction. The difference of 23% for overstrength related to EN1998-1-1 (2004) and the difference in the order of 5% for the term related to design decisions are found in the frames with greater height, which is responsible for larger median, 1.14 compared to 1.09 from eight-storey frames. For this latter, this difference may be related to minor contribution of the fundamental mode for the taller frames. Finally, a difference of 22% is found in the  $\Omega$  factor with a median of 1.46 for the smaller frames and 1.20 for other frames.

Concerning the influence of span length, there is no significant difference between the two lengths investigated. Frames with smaller span present medians of 1.25, 1.08 and 1.44, while other frames show values of 1.28, 1.09 and 1.43 for the  $\Omega_1$ ,  $\Omega_2$  and  $\Omega$  factors, respectively. This was expected due to observations presented on previous section concerning capacity curves.

It is also possible to see that soil condition is another parameter that may affect the overstrength factors, since the frames designed considering a stiff soil condition present larger values. For such frames, values of 1.29, 1.14 and 1.54 are observed for the  $\Omega_1$ ,  $\Omega_2$  and  $\Omega$  factors, while values around of 1.21, 1.06 and 1.32 are found for the frames located in soft soil. The larger difference (14%) is given for the  $\Omega$  factor due to contribution of second terms of Equation (4.1). In fact, the frames located in soft soil condition are designed for larger shear base in comparison with stiff soil, which reduces the influence of slenderness braces of the last floor, besides providing stiffer structures. In some cases, especially for the

frames in stiff soil, the slenderness limit governed the seismic design according to EN1998-1-1 (2004) due to the clause that determines a homogenous dissipation of energy where the scatter of overstrength (defined by ratio design resistance of diagonal with the design value of the axial force in same diagonal for seismic combination) should be less of 25%. Therefore, the soft soil condition allowed for structures with smaller ratio design plastic resistance to design buckling resistance.

Concerning the use of HSS steel grade, the frames designed with higher steel grade exhibit slightly increase on both overstrength factors. The frames with S690 present median of 1.23 and 1.10, while the frames designed with S460, a median of 1.21 and 1.07 is observed for the first and second terms of Equation (4.1), respectively. However, this difference is very small compared to other parameters.

No clear correlation was found between overstrength and column type. However, it is possible to see that the frames with CFT column exhibits smaller  $\Omega$  factor in most cases. In addition, there is no noticeable variation in both overstrength factor terms for the FE and PE columns. In fact, other parameters besides the composite column type can influence the overall behaviour of the buildings.

In general, the frames studied present a median of 1.21 for the overstrength mostly related to modal load pattern. It should be noticed that EN1998-1-1 (2004) does not mention values of overstrength for CBFs. The values for the  $\Omega_2$  of the overstrength reveal that the solution adopted on seismic design provides structures of excellent level of optimization, since the values found are close to 1.0, having a median of 1.11.

In conclusion, the frames exhibited overstrength factors ( $\Omega$ ) lower than the behaviour factor employed in seismic design ( $q = 2.5$ ) allowing for the formation of plastic ‘hinges’ under the design earthquake record.

Table 6.1 – Overstrength factor for the CBFs

<i>Frames</i>	$\left(\frac{V_y}{V_{1y}}\right)$		$\left(\frac{V_{1y}}{V_{dy}}\right)$		$\left(\frac{V_y}{V_{1y}}\right)_{\min}$	<i>Load pattern</i>	$\left(\frac{V_{1y}}{V_{dy}}\right)_{\min}$	<i>Load pattern</i>	$\Omega$	<i>Load pattern</i>
	<i>1<sup>st</sup> Mode</i>	<i>Uniform</i>	<i>1<sup>st</sup> Mode</i>	<i>Uniform</i>						
CBF_1.1.1.1.1	1.74	1.40	1.04	1.74	1.40	Uniform	1.04	1st Mode	1.81	1st Mode
CBF_1.1.1.1.2	1.31	1.43	1.22	1.52	1.31	1st Mode	1.22	1st Mode	1.60	1st Mode
CBF_1.1.1.1.3	1.14	1.25	1.23	1.47	1.14	1st Mode	1.23	1st Mode	1.40	1st Mode
CBF_1.1.1.2.1	1.23	1.24	1.04	1.53	1.22	1st Mode	1.04	1st Mode	1.28	1st Mode
CBF_1.1.1.2.2	1.20	1.21	1.11	1.65	1.20	1st Mode	1.04	1st Mode	1.33	1st Mode
CBF_1.1.1.2.3	1.18	1.27	1.24	1.45	1.18	1st Mode	1.24	1st Mode	1.47	1st Mode
CBF_1.1.2.1.1	1.41	1.44	1.11	1.39	1.41	1st Mode	1.11	1st Mode	1.57	1st Mode
CBF_1.1.2.1.2	1.47	1.44	1.10	1.51	1.44	Uniform	1.10	1st Mode	1.62	1st Mode
CBF_1.1.2.1.3	1.34	1.52	1.12	1.36	1.34	1st Mode	1.12	1st Mode	1.50	1st Mode
CBF_1.1.2.2.1	1.28	1.21	1.06	1.45	1.21	Uniform	1.06	1st Mode	1.35	1st Mode
CBF_1.1.2.2.2	1.25	1.22	1.07	1.52	1.22	Uniform	1.07	1st Mode	1.34	1st Mode
CBF_1.1.2.2.3	1.23	1.19	1.06	1.41	1.19	Uniform	1.06	1st Mode	1.31	1st Mode

Table 6.1 – Overstrength factor for the CBFs (*Continued*)

<i>Frames</i>	$\left(\frac{V_y}{V_{1y}}\right)$		$\left(\frac{V_{1y}}{V_{dy}}\right)$		$\left(\frac{V_y}{V_{1y}}\right)_{\min}$	<i>Load pattern</i>	$\left(\frac{V_{1y}}{V_{dy}}\right)_{\min}$	<i>Load pattern</i>	$\Omega$	<i>Load pattern</i>
	<i>1<sup>st</sup> Mode</i>	<i>Uniform</i>	<i>1<sup>st</sup> Mode</i>	<i>Uniform</i>						
CBF_1.2.2.1.2	1.51	1.75	1.16	1.26	1.51	1st Mode	1.16	1st Mode	1.76	1st Mode
CBF_1.2.2.1.3	1.26	1.45	1.27	1.29	1.26	1st Mode	1.27	1st Mode	1.60	1st Mode
CBF_1.2.2.2.2	1.27	1.30	1.00	1.32	1.27	1st Mode	1.00	1st Mode	1.27	1st Mode
CBF_1.2.2.2.3	1.10	1.22	1.00	1.27	1.10	Uniform	1.00	1st Mode	1.10	1st Mode
CBF_2.1.2.1.1	1.00	1.10	1.12	1.49	1.00	1st Mode	1.12	1st Mode	1.12	1st Mode
CBF_2.1.2.1.2	1.01	1.01	1.15	1.68	1.01	1st Mode	1.15	1st Mode	1.16	1st Mode
CBF_2.1.2.2.1	1.02	1.21	1.05	1.30	1.02	1st Mode	1.05	1st Mode	1.07	1st Mode
CBF_2.1.2.2.2	1.08	1.20	1.10	1.37	1.08	1st Mode	1.10	1st Mode	1.24	1st Mode
CBF_2.2.2.1.2	1.11	1.51	1.04	1.61	1.11	1st Mode	1.04	1st Mode	1.16	1st Mode
CBF_2.2.2.2.3	1.02	1.62	1.36	2.36	1.02	1st Mode	1.36	1st Mode	1.39	1st Mode
CBF_2.2.2.2.2	1.13	1.22	1.21	1.49	1.13	1st Mode	1.21	1st Mode	1.37	1st Mode
CBF_2.2.2.2.3	1.04	1.17	1.29	1.71	1.04	1st Mode	1.29	1st Mode	1.35	1st Mode
16 <sup>th</sup>	1.03	1.20	1.04	1.31	1.03		1.04		1.16	
50 <sup>th</sup>	1.24	1.24	1.11	1.48	1.21		1.11		1.35	
84 <sup>th</sup>	1.36	1.47	1.22	1.66	1.36		1.22		1.60	



## 6.2 Dynamic performance evaluation

Nonlinear incremental dynamic analyses have been performed to characterize both, the inelastic behaviour and the performance compared to the three-reference limit states defined in Chapter VI. In this section, the outcomes concerning the dynamic analyses are discussed considering the three limit states previously described. The performance of the frames is evaluated and the role of each design parameter is discussed taking into consideration the following global and local indicators: i) peak inter-storey drift ratios; ii) residual inter-storey drift ratios; iii) peak storey accelerations and iv) brace ductility demand.

### 6.2.1 Peak inter-storey drift ratios

The median profile of IDRs obtained for all the examined cases in the three limit states is summarized in Figure 6.7. The results are divided in three groups according to the parameters that significantly influence IDRs, i.e. soil, steel grade and span length. Table 6.2 summarizes the maximum value found for each plotted curve in Figure 6.7.

The eight-storey frames experiment higher inter-storey drift demand for the upper storeys and a more uniform profile in comparison with sixteen-storey frames. On the other hand, the taller frames show maximum drifts around the mid-height. This fact was expected and had already been observed on the pushover analyses. The taller frames suffer higher damage concentration in a particular zone resulting in larger inter-story drift demand. This can be explained by cantilever-behaviour from the taller frames.

Focusing on the soil type, it is observed that the frames founded in soft soil suffer larger inter-storey drift demand when comparing to the frames located in stiff soil, specially the frames designed with higher steel grade. These frames are lighter and more flexible structures resulting in increased inter-storey drift demand, as it can be observed in the sixteen-storey frames. However, this difference tends to decrease when there is an increase of damage in structures, except for the cases in which a soft storey mechanism appears in a specific storey. Indeed, the frames with soft soil have fundamental period located on the constant acceleration spectrum range resulting in larger seismic demand.

Also shown in Figure 6.7 is the comparison concerning span length presenting larger responses for the frames with larger span due to larger flexibility of beams in braced bay. Comparing to shorter span frames, those beams provide a higher level of axial deformation to braces due to higher flexural stiffness and, consequently, larger displacement of mid-span.

In Figure 6.7 the comparison between the two type of HSS steel grades can be assessed as well. In most cases, the displacement profiles presented are similar at a certain point. This observation is true for the sixteen-storey frames and for the DL and SD limit states, expect

for the frame located in soft soil, considering S690, in which a soft mechanism in NC limit state is seen. Although the increasing steel grade provides more flexible structures, it is important to note that the frames designed with S690 present lower IDRs. Taking into consideration the eight-storey frames, those designed with a higher steel grade suffered a slightly larger inter-storey drift demand than those designed with S460, mainly for the DL limit state. A 17% reduction of IDRs is observed for the SD and NC limit state for the frames located in stiff soil, whereas for soft soil that reduction is only present for the NC limit state. This fact is related to better redistribution of the damage for the frames with high steel grade on the non-dissipative element being consistent with the results from pushover analyses where these structures presented larger overstrength factors

In general, the eight-storey frames present an inter-storey drift below the limit adopted in the seismic design for the DL limit state. In contrast, this is not true for the sixteen-storey frames located in soft soil showing values ranging from 1.25% to 1.50% and therefore larger than the 0.75% limit. Moreover, it is interesting to note that the frames experience drifts higher than the 3% (value assumed by the NC limit state for the MRFs) due to the appearance of the soft storey mechanism arising of the large damage concentration.

Table 6.2 – Maximum median of inter-storey drift ratio demand (*value in %*)

Percentiles at each limit state		8-Storey				16-Storey	
		5.0 m		7.5 m		7.5 m	
		Stiff soil	Soft soil	Stiff soil	Soft soil	Stiff soil	Soft soil
S460	DL	0.41	0.40	0.41	0.44	0.69	1.48
	SD	0.89	0.84	1.19	1.39	1.59	2.09
	NC	1.59	1.45	2.14	2.44	3.68	3.87
S690	DL	-	-	0.52	0.72	0.63	1.22
	SD	-	-	1.01	1.66	1.35	2.06
	NC	-	-	1.75	2.13	4.52	2.23

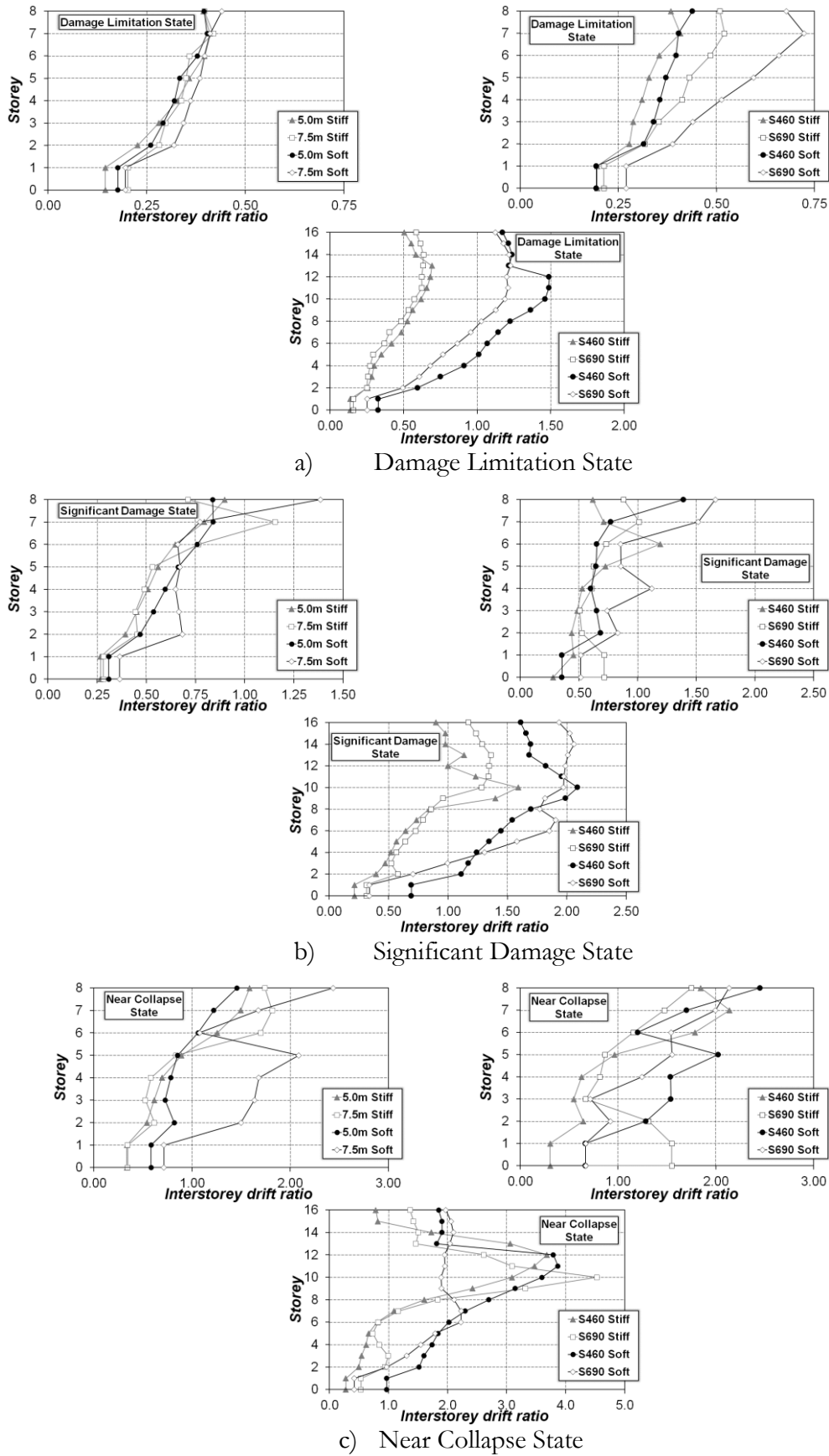


Figure 6.7 – Influence of studied parameters in inter-storey median drift demand for the three limit states (*values in %*)

### 6.2.2 Residual inter-storey drift ratios

The RIDRs is an important parameter when the structures suffer severe damage imposed by the seismic event being necessary to perform rehabilitation of the building. Monitoring of the residual displacement along of height allows the calculation of the median profiles based on seven records, which are shown in Figure 6.8 and whose maxima are given in Table 6.3. As expected, the lower frames show lower values, around zero for the DL limit state, due to their higher lateral stiffness. The large RIDRs reported are related to soft storey-mechanism presented by the some study cases, mainly for the sixteen-storey frames. In contrast to MRFs, the CBFs show to be susceptible to large RIDRs being justified by poor redistribution of the inelastic demand.

When the focus is on the three parameters that showed larger influences in RIDR, i.e. steel grade, soil type and span length, it is observed that frames in soft soil experience the higher ratios, especially for the DL and SD limit states, except for few cases that exhibit severe damage concentration in a specific floor developing soft-storey mechanism. The frames with the smaller span present similar values for both soil types as well as had already been recognized on the IRDs. In the frames with shorter length span, no formation of weak storey mechanism is identified. This fact is related to high flexural stiffness provided by shorter span reducing the axial deformation of the braces. Thus, the flexural stiffness of beam from braced bay reveal to be an important seismic parameter response of CBFs.

Although the increasing of steel grade allowed the structures to be more flexible, the frames designed with S690 in non-dissipative elements exhibit up to three times lower RIDRs (0.36%-to-0.12%). This result is consistent with the IDRs where, once again, the frames with S690 provides an adequate redistribution of the damage in comparison with frames with S460.

Table 6.3 – Maximum median of residual inter-storey drift ratio demand (*values in %*)

Percentiles at each limit state		8-Storey				16-Storey	
		5.0 m		7.5 m		7.5 m	
		Stiff soil	Soft soil	Stiff soil	Soft soil	Stiff soil	Soft soil
S460	DL	0.00	0.00	0.00	0.02	0.01	0.09
	SD	0.02	0.02	0.12	0.14	0.31	0.54
	NC	0.13	0.12	0.36	0.32	0.69	0.55
S690	DL	-	-	0.00	0.01	0.01	0.01
	SD	-	-	0.10	0.18	0.09	0.26
	NC	-	-	0.12	0.85	0.58	0.36

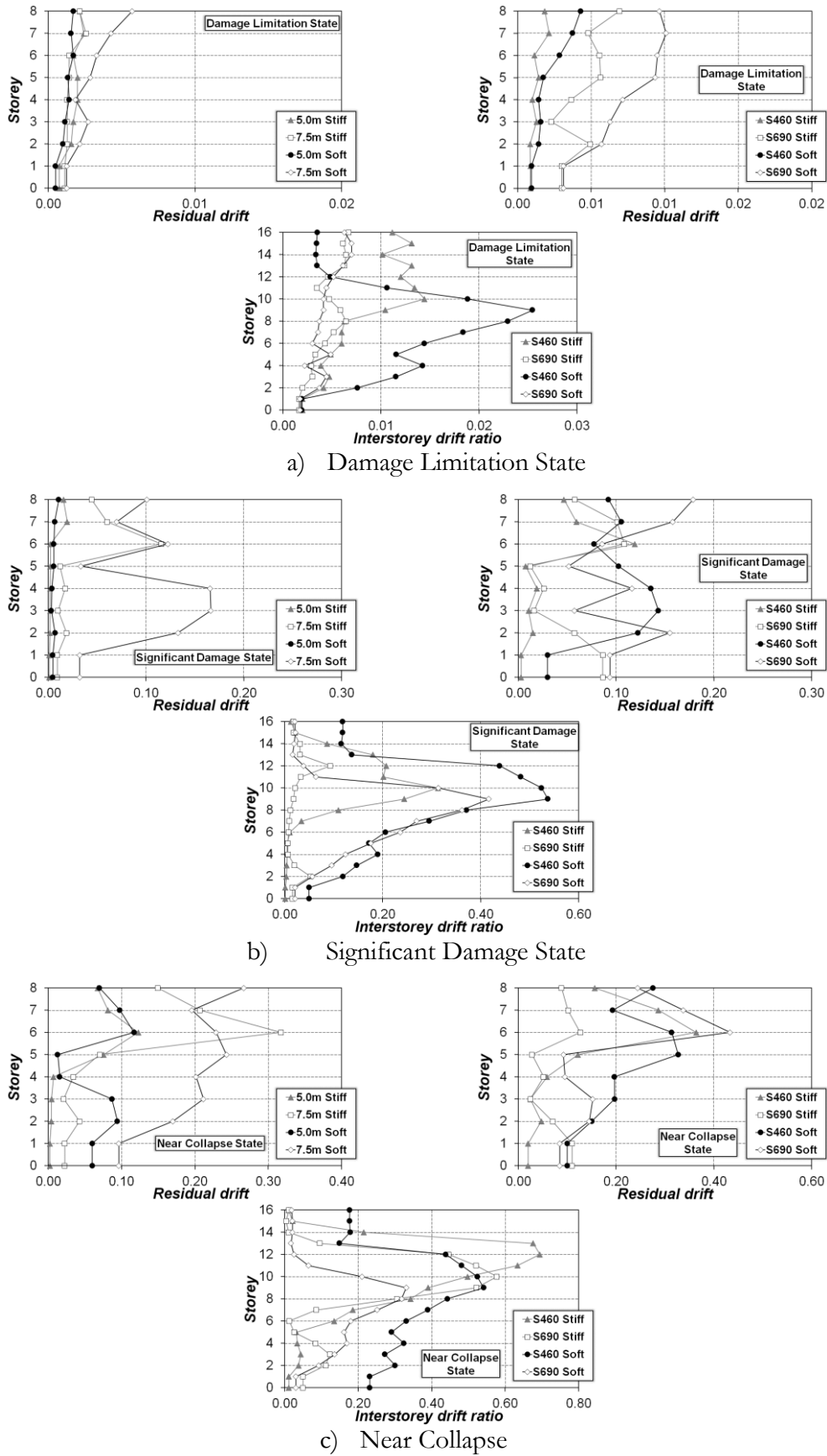


Figure 6.8 – Influence of studied parameters in residual drift ratio for the three limit states (*values in %*)

### 6.2.3 *Peak storey accelerations*

The plots in Figure 6.9 show the median profile of normalized PSA along of the building height obtained from seven records. Table 6.4 summarizes the maxima of the PSA profiles. In general, the higher PSA values are found on the top floor whatever the soil type, span length or building height. This reason is attributed to the higher modes in nonlinear condition and it is more evident in the sixteen-storey frames where the cantilever-dominant is characterized. In detail, it is worth noting that the higher values are related to frames located in soft soil. They exhibit a profile less uniform along the height than the frames in stiff soil.

In general, the taller frames show “S”-shaped profiles evidencing the influence of higher modes in PSAs response. This scenario corresponds to have shear-dominated behaviour at the bottom floors, flexural-dominated behaviour at the upper floors, and a combination of these two behaviour contributes to the middle floors level response.

Concerning the span length, shorter span frames show lower values for both residual and transient inter-storey drift when compared with larger span frames. Results presented in Figure 6.9 and Table 6.4 gather evidence that the former exhibit higher PSA for both soil types and for the three limit states. This indicates that the degradation of braces is not related to floor acceleration since the response of the PSAs is not proportional.

As it was observed for both residual and transient inter-storey drifts, the increase of steel grade shows to be beneficial allowing a reduction of PSAs in the majority of cases reaching differences around 11% for frames located in stiff soil and 37% for those located in soft soil. Once again, the frames located in soft soil condition present larger seismic demand, namely PSAs, in comparison with the frames designed considering a stiff soil.

As general comments, the significant amplification of the storey acceleration in study cases indicate that severe damage in the non-structural members can be expected, as it was seen for the MRFs (FEMAE-74, 2011). In contrast, there is a mitigation of the PSAs amplitudes for the CBFs compared to value obtained for the unbraced frames. In detail, the CBFs with eight-storey experience values around of 3.67 to 3.97 for the SD limit state while the eight-storey MRFs present values of 4.05 to 5.71 for the stiff and soft soil, respectively.

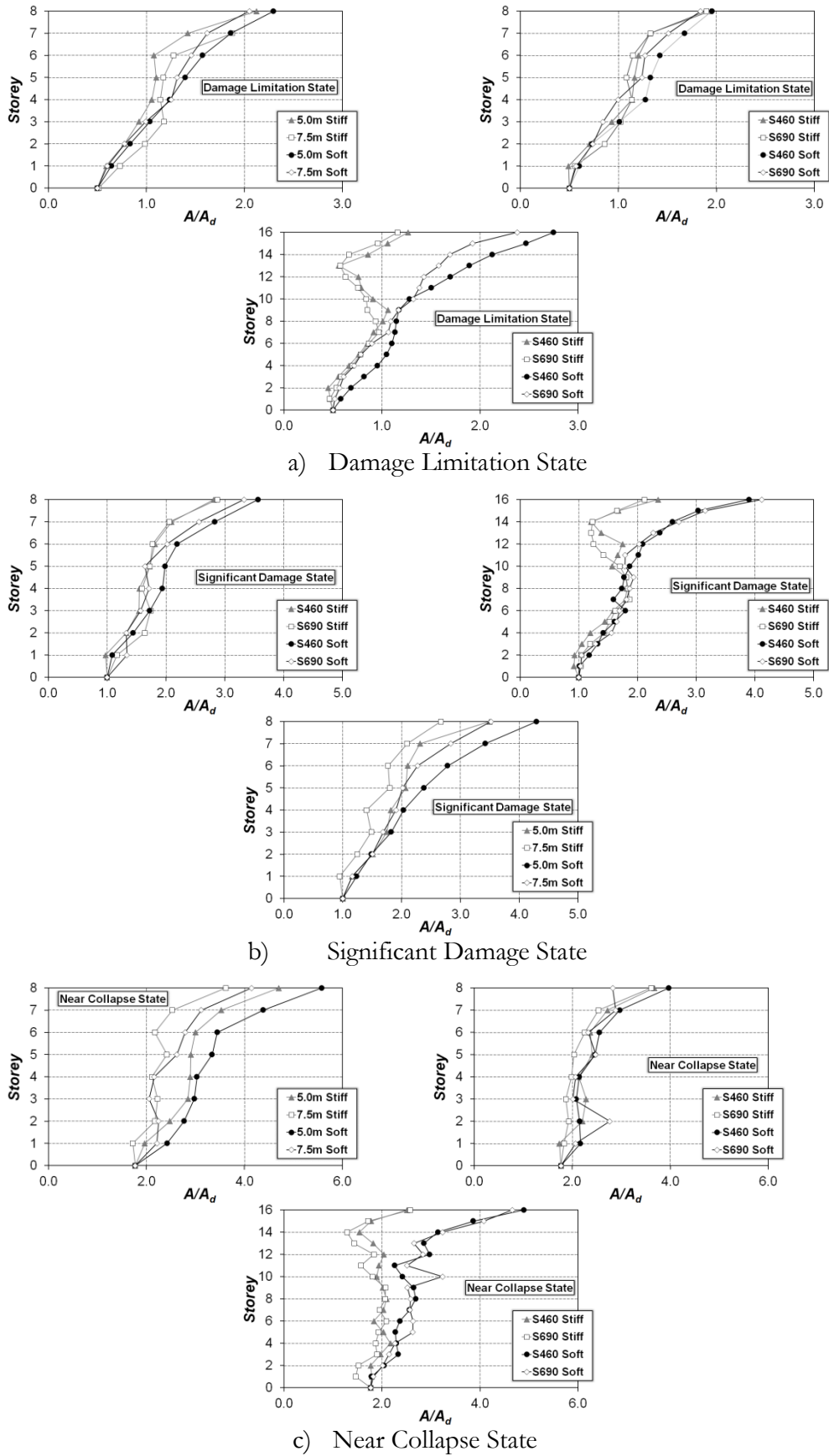


Figure 6.9 – Profiles of the peak storey acceleration

Table 6.4 – Maximum values found for the PSAs (*values in %*)

Percentiles at each limit state		8-Storey				16-Storey	
		5.0 m		7.5 m		7.5 m	
		Stiff soil	Soft soil	Stiff soil	Soft soil	Stiff soil	Soft soil
DL		2.12	2.24	1.94	1.96	1.26	2.75
S460	SD	3.49	4.29	2.81	3.56	2.35	3.89
	NC	4.70	5.57	3.67	3.97	2.51	4.89
DL		-	-	1.90	1.84	1.16	2.38
S690	SD	-	-	2.87	3.32	2.11	4.11
	NC	-	-	3.61	2.89	2.57	4.65

#### 6.2.4 Brace ductility demand

EN1998-1-3 (2005) determines that the inelastic capacity of braces in compression is a percentage of the axial deformation at buckling load,  $\Delta_c$ . The limit values for braces cross section Class 1 are  $0.25\Delta_c$ ,  $4.0\Delta_c$  and  $6.0\Delta_c$  for Class 2 are  $0.25\Delta_c$ ,  $1.0\Delta_c$  and  $2.0\Delta_c$ , respectively for the DL, SD and NC limit states. For braces in tension, the corresponding limits are  $0.25\Delta_t$ ,  $7.0\Delta_t$  and  $9.0\Delta_t$ , disregarding the cross section class. The axial deformation of braces has been investigated for the CBFs. The ratio of the maximum median value obtained for the seven records of each soil condition and the maximum value recommended in EN1998-1-3 (2005) are presented in Figure 6.10 for each limit state. Table 6.5 reports the maximum median for each level of peak ground acceleration in accordance with EN1998-1-3 (2005).

The results show an inadequate performance of the frames, in special the values obtained for the DL that are heavily higher than the limit of  $0.25\Delta_c$  showing a ratio ranging from 2.28 to 3.34 for the frames with S460 while this difference varies from 2.60 to 2.91 for the frames with higher steel grade. Indeed, the recommended value for the inelastic capacity incorporated in the EN1998-1-3 (2005) clearly determines that there is no buckling effect occurs.

The span length shows to be an important parameter affecting the brace ductility demand. In particular, the ductility demand in shorter span frames remain below the SD limit imposed by EN1998-1-3 (2005) and close to the NC limit. This behaviour is related to the flexural stiffness of beams in braced frames, since a shorter and consequently stiffer beam allows lower axial deformation in braces due to displacement of mid-point where the braces are connected. Worth to be mentioned is that sixteen-storey frames show lower brace deformation demand than eight-storey frames, mainly for the DL limit state. As the brace slenderness is increased for the eight-storey frames, buckling occurs at a smaller



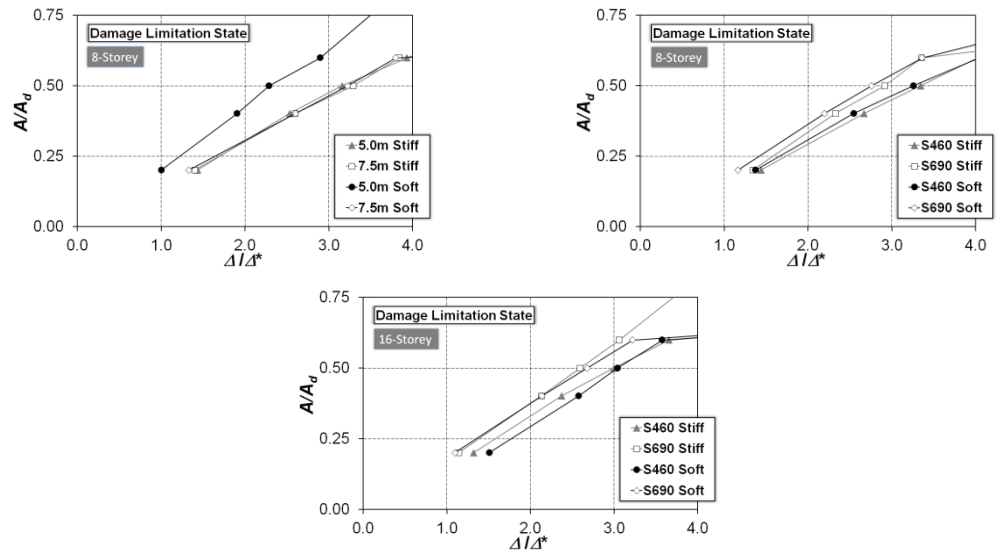
deformation, therefore, the ductility demand for the taller frames is smaller (Tremblay, 2002).

Concerning to steel grade used, its increase provides a reduction of ductility demand mainly for the DL and NC limit states. This is as expected looking for the results of the before assessment. The frames with S690 allow to have more uniform of the damage, being more notorious because the beam from braced bays are made up of the same steel grade employed on the non-dissipative member (namely S690) resulting in large axial deformation for the braces.

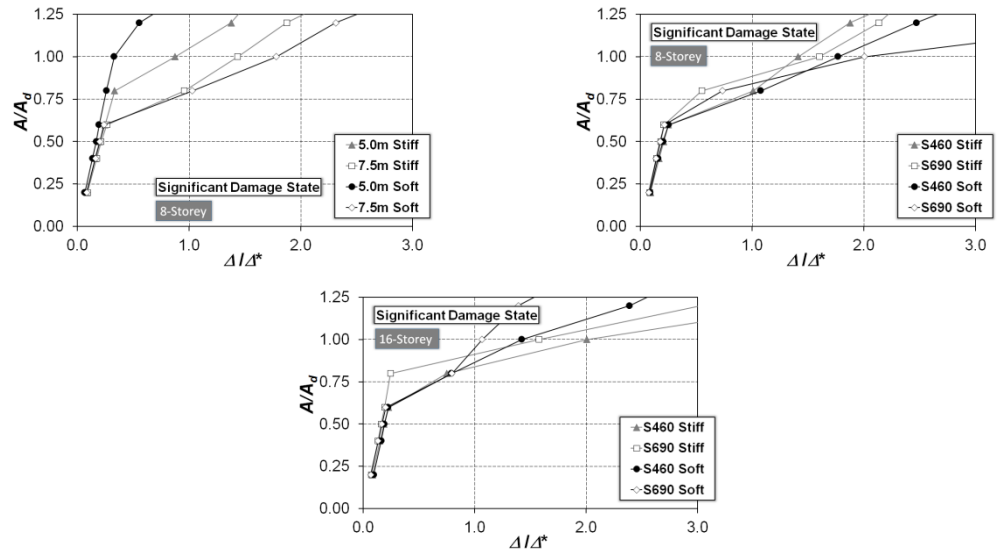
It is also possible to observe that there is a reduction of ductility demand for the sixteen-storey frames located in soft soil when comparing them with lower rise frames. Moreover, the soil condition influence on the seismic performance in which the frames found on soft soil experience larger brace ductility demand. However, it is possible to see some cases where the stiff soil provides the greater demand being justified by formation of the soft storey mechanism.

Table 6.5 – Maximum value of brace ductility demand

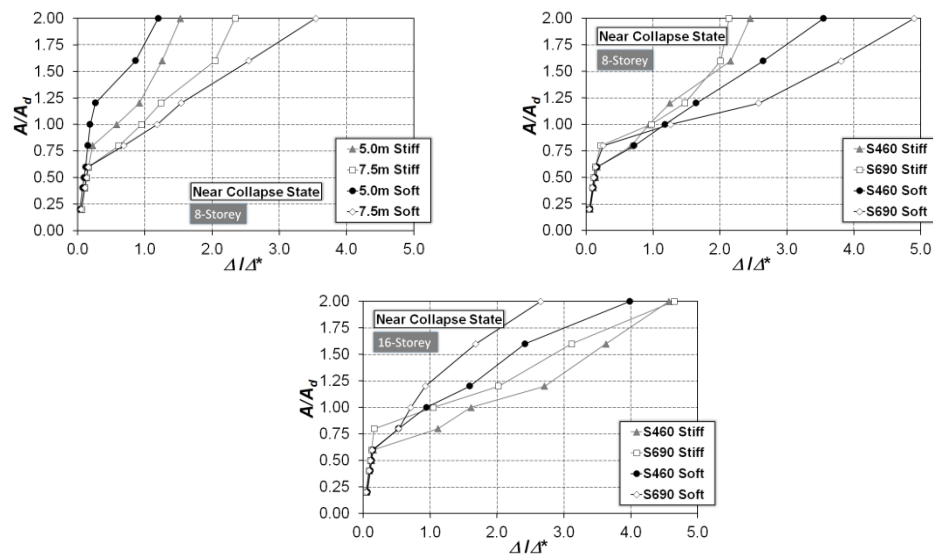
Percentiles at each limit state		8-Storey				16-Storey	
		5.0 m		7.5 m		7.5 m	
		Stiff soil	Soft soil	Stiff soil	Soft soil	Stiff soil	Soft soil
S460	DL	3.15	2.28	3.34	3.26	2.99	3.04
	SD	0.87	0.33	1.41	1.77	2.00	1.42
	NC	1.37	1.00	2.28	3.03	4.03	3.08
S690	DL	-	-	2.91	2.76	2.60	2.68
	SD	-	-	1.60	2.00	1.57	1.06
	NC	-	-	2.06	4.27	3.77	2.10



a) Damage Limitation State



b) Significant Damage State



c) Near Collapse State

Figure 6.10 – Brace ductility demand for the three limit states

### 6.3 Behaviour factors

The influence of the soil condition the HSS steel grade and the span length using the two different methods to determine the behaviour factors for each limit state are discussed hereafter. Since EN1998-1-3 (2005) imposes an elastic behaviour for DL limit state, only SD and NC limit states are considered.

As a general comment, the both methods deliver smaller behaviour factors in comparison with that used on the seismic design, mainly for the European approach. In particular, the European approach gives behaviour factors around 1.70 for the both soil condition. Salvati & Elnashai approach delivers behaviour factors equal to 2.22 and 2.17 for stiff and soft soil, respectively. This outcome shows the relevance of performing a recalibration of the values given in EN1998-1-1 (2004). Furthermore, the brace ductility demand was responsible by smaller behaviour factor for both methodologies

#### 6.3.1 Influence of soil condition

The influence of soil condition in behaviour factors considering the two methods previously stated was evaluated and all the results are presented in Figure 6.11. There is a reduction of behaviour factors when a soft soil condition is considered with differences for the NC limit state up to 2.3% and 15.3%, for the first and second method, respectively. Concerning the SD limit state, the differences between soil types are not significant, even when applying European approach and there is a decrease of 6.0% for the second method. This is an evidence that, for low damage levels, the influence of soil condition is not relevant in seismic behaviour of concentrically braced frames where there is not large plastic deformation of the braces.

The European approach presents a median of 1.70 for both stiff soil and soft soil in SD limit state, which is lower than the behaviour factor of 2.5 considered in design. In contrast, the second method delivers higher values with medians of 2.22 and 2.17 for stiff and soft soil respectively. The overstrength factors close to 1.0 obtained from pushover analyses determine the behaviour factor in the European approach. In contrast, the method proposed by Salvati and Elnashai approach makes the behaviour factor to depend on the ratio between peak ground acceleration of seismic design and acceleration necessary to obtain the failure criteria established.

Focusing on NC limit state, an increase of behaviour factors is seen for European approach. In opposition, the Salvati & Elnashai method shows a decrease in comparison with DL limit state. The first result was expected because the overstrength factor and acceleration are constant in the European method. Therefore, the increase is given by enlargement of limit

imposed for NC limit state that consequently result in higher failure accelerations. The decrease of q-factor obtained from the second method shows that the scatter within the acceleration of limit state to failure criteria is larger. Therefore, the frames are closer to fulfil the limit from SD than the values imposed by NC limit state.

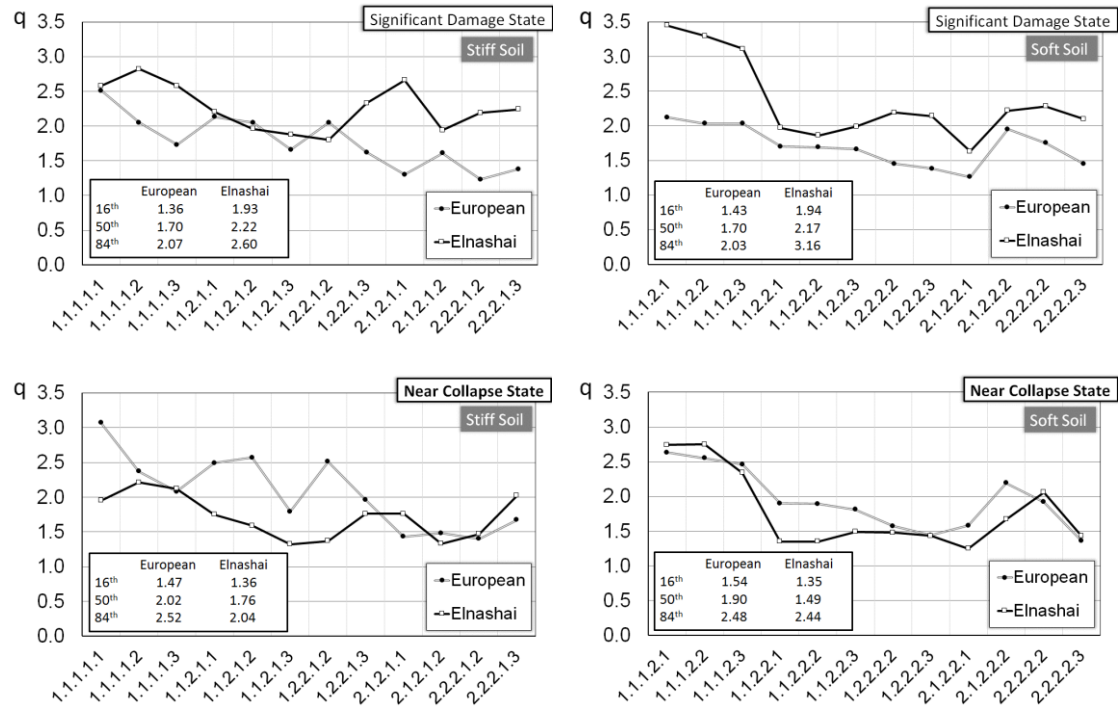


Figure 6.11 – Comparison of behaviour factors for soil type

### 6.3.2 Influence of HSS steel grade

The influence of different steel grades in the behaviour factors are summarized in Figure 6.12 that shows the median of behaviour factors for the seven records analysed in each type of soil. Interesting to note is that the increase of steel grade provides higher q-factors computed with Salvitti & Elnashai approach and lower values when European one is used. In the first case, the frames designed considering S690 for the non-dissipative elements show an increase of 12% for the SD limit state and 4% for the NC limit state in comparison with the frames designed for a lower steel grade. In the second case (namely the European approach), a reduction of 9% and 5% is obtained, respectively for SD and NC limit states. This difference is consistent with the drift previously discussed where the use of the S690 provide a better damage distribution with smaller drift demand. Therefore, the Salvitti & Elnashai approach deliver higher behaviour factor for the frames designed with S690.

In other words, the frames designed with S690 need higher accelerations to reach the limit states when compared with the frames designed with S460. However, they exhibit lower transient and residual drift ratios, as previously concluded and, therefore, when a determined

structure presents a soft mechanism, there is a large concentration of damage on a unique floor resulting in precocious plastic hinges located in braces.

In contrast, the decreasing of the behaviour factor when a superior steel grade is used for the European method is justified by the acceleration of the first plastic hinge because the differences found for the overstrength factor is not significant. Due to more uniform damage along of height, the first plastic hinge is formed for an acceleration superior than that observed for a frame with S460.

In general, both methods deliver q-factors lower than the value used in seismic design independently of the steel grade. Once more, Salvitti & Elnashai method shows a decreasing for NC limit state in comparison with DL limit state and there is an increasing of behaviour factors when using European method.

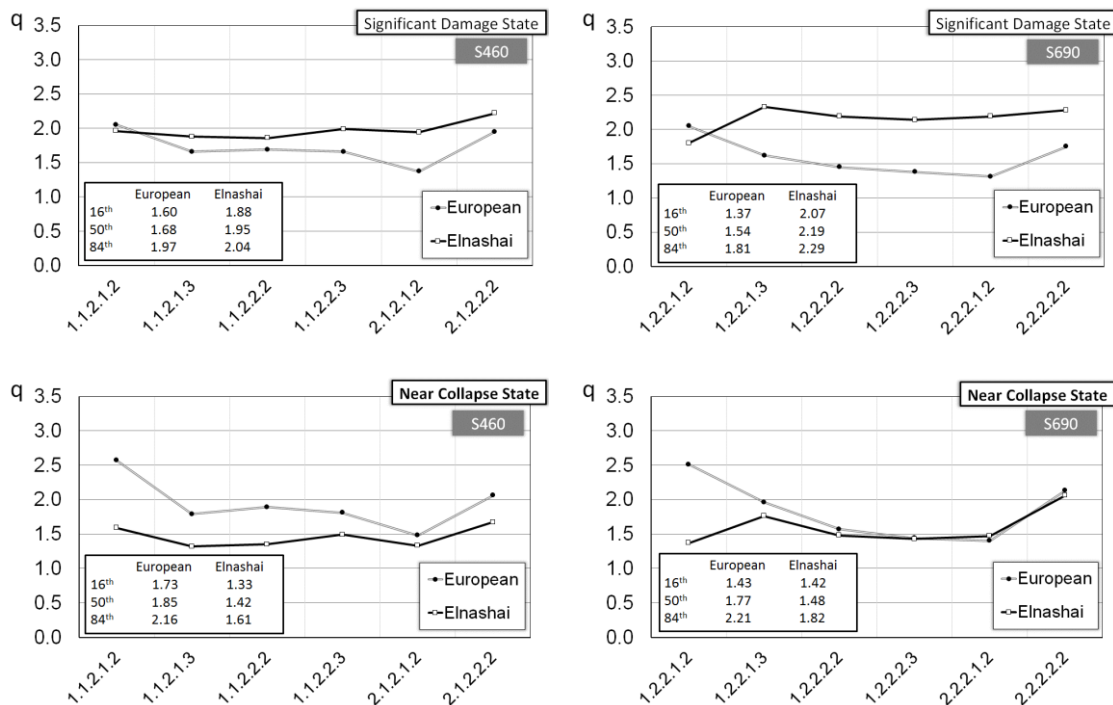


Figure 6.12 – Comparison of behaviour factors according to steel grade

### 6.3.3 Influence of span length

The curves plotted in Figure 6.13 show the q-factor median according to two different span lengths. Following the results of brace ductility demand obtained previously, the frames with smaller span length indicate higher behaviour factors. The justification is similar to the one proposed before and it is also based on the fact that the stiffer beams in 5.0m span beams allow lower axial deformation in braces due to lower displacement of mid-span. This issue has been recently investigated in (Tenchini et al., 2013).

The 5.0m span frames present a median q-factor of 2.04 and 2.51 according to European method and 1.70 and 1.90 according to Salvitti & Elnashai method for the SD and NC limit states, respectively.

Applying Salvitti & Elnashai method for the shorter span frames, median q-factors of 2.97 and 2.28 can be obtained for the SD and NC limit states, respectively. For the frames with larger spans, those values are 1.97 and 1.42.

In general, the frames with smaller span present behaviour factor close to the design value, mainly when the second calculation method is used. Furthermore, this method provides values, which are larger than the European approach for the SD limit state.

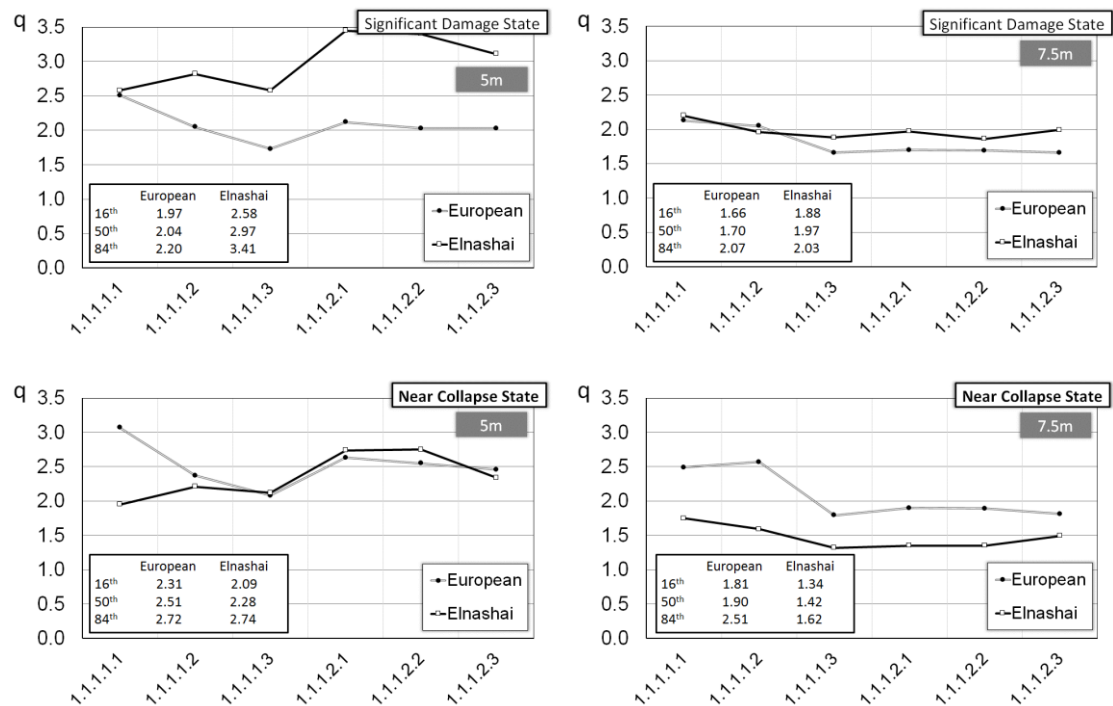


Figure 6.13 – Comparison of behaviour factors according to span length

#### 6.3.4 Influence of number of storey

In Figure 6.14, a comparison between the two number of storey is devoted. Some differences can be recognized comparing eight-storey frames with those designed with sixteen-storey. In particular, the taller frames present smaller behaviour factor for the European approach for both limit states. On the other hand, the Salvitti & Elnashai method provides larger behaviour factor for the taller frames.

As expected, the capacity curves showed that sudden reduction in lateral resistance penalized more the taller frames, and consequently, smaller overstrength factor are delivered compared to eight-storey frames. This fact influences the results presented by European method since this depends on the overstrength factor. In detail, a median behaviour factor of 1.70 for SD limit state and 1.93 for the NC is observed for the for smaller frames.

Concerning to behaviour factor from taller frames, the study cases present median of 1.37 and 1.53 for SD and NC limit states, respectively.

Applying Salvitti & Elnashai method for the taller frames, it is observed a median q-factors of 2.21 and 1.57 for the SD and NC limit states, respectively. The eight storey-frames deliver median value of the 2.06 for SD limit state and 1.46 for NC one. These values are higher than those seen for the European approach when compared to eight-storey frames. In fact, the Salvitti & Elnashai is not influenced by the overstrength factor, therefore, the large behaviour factor is attributed to brace dimensions where the eight-storey frames have brace less slender.

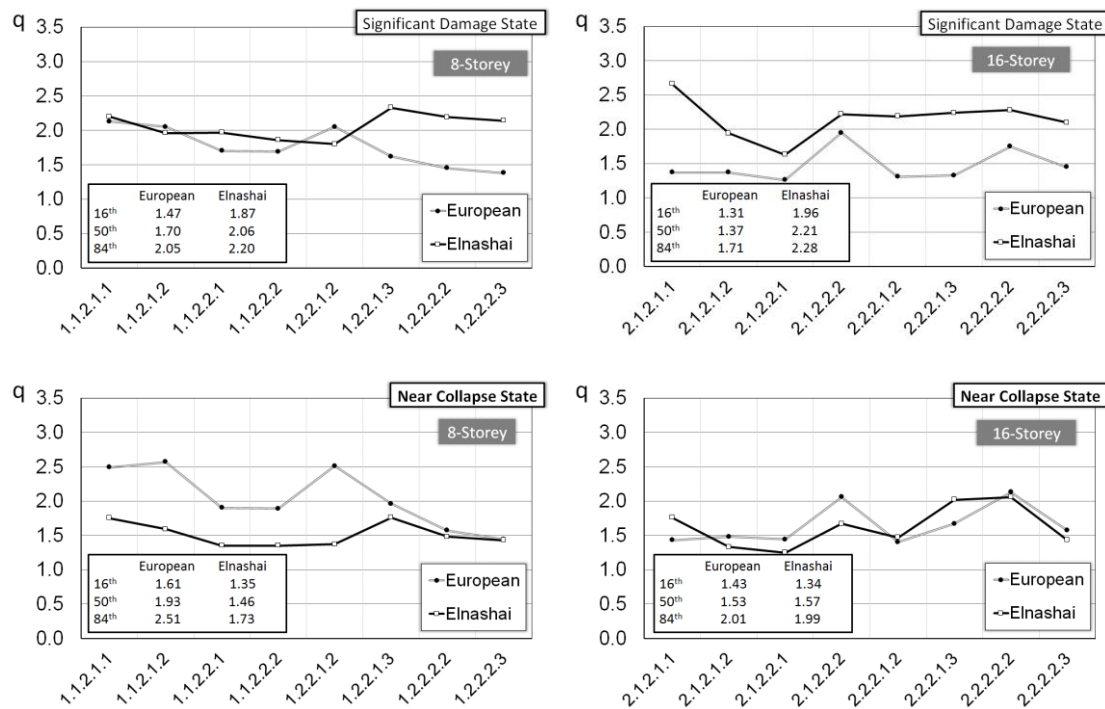


Figure 6.14 – Comparing the behaviour factors concerning to number of storey

## 6.4 Material consumption

The material consumption of the CBF is calculated in accordance with the Equation (5.2) from previous chapter. The steel consumption is computed in terms of total weight while the concrete is defined in terms of the total cast volume. Again, the term material density is used here in order to compare the influence of the parameters on the material consumption.

Figure 6.15 depicts a comparison that takes the soil type as reference. It is worth noting that the frames located on soft soil condition have presented larger material densities, namely steel profile, reinforcement and concrete. Although for both soil types the same PGA has been considered, a type of soil with larger corner  $T_c$  shows to be an important factor on the cost of the building. Note that the frames that were designed considering a soft soil have presented smaller overstrength factor on the seismic design in which a priori would result

in reduced material consumption. However, this difference is not sufficient to have lower material consumption. In particular, the difference shown on the steel profile consumption is attributed exclusively to the HSS amount. The major contribution on the consumption reduction is associated to non-dissipative element in which the HSS are employed.

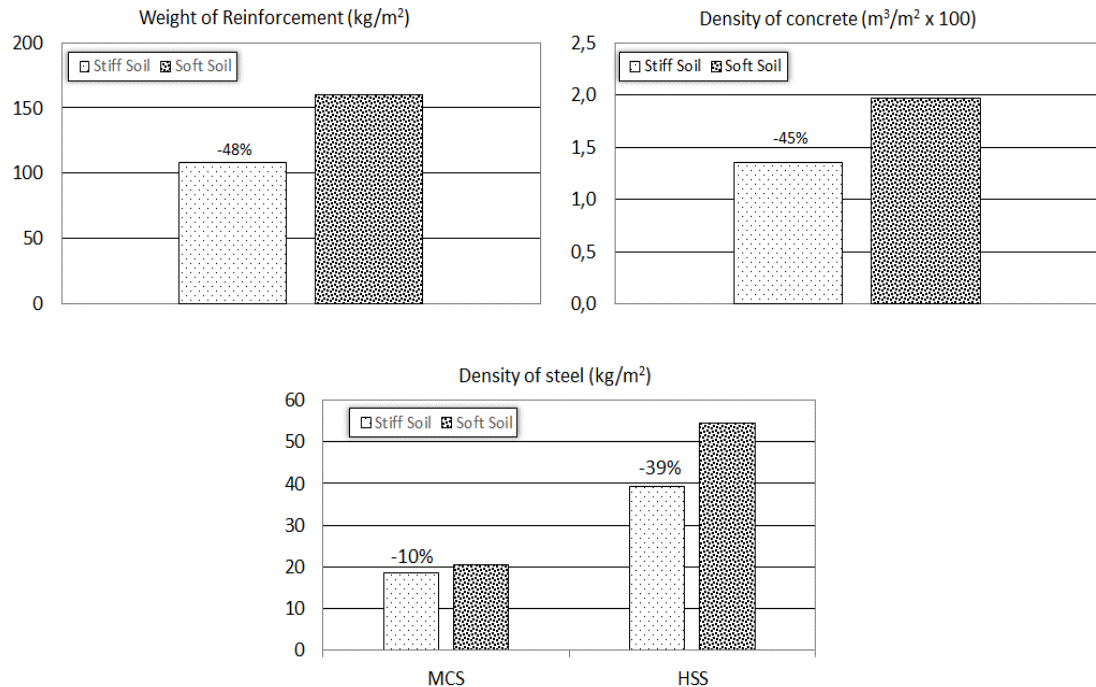


Figure 6.15 – Average of amount of steel, concrete and reinforcement

Figure 6.16 shows the steel densities highlighting the dependency on the steel grade. As it can be noted, the larger amount of density of steel is obtained for the cases with S460 steel grade. In particular, the use of the high steel grade shows to be more efficient for the frames located on soft soil. The result presented in Figure 6.16 is justified in evaluating the seismic design of the CBFs. The seismic design was not governed by damage limitation criterion, so the resistance played an important role to determine the structural members mainly for the non-dissipative ones resulting on lighter structures when a high steel grade is used. Moreover, the MCS steel consumption shows not to be sensitive to the increase of HSS steel grade. Indeed, the differences are observed only for the braces because the beams from un-braced bay were designed based on the non-seismic combination.



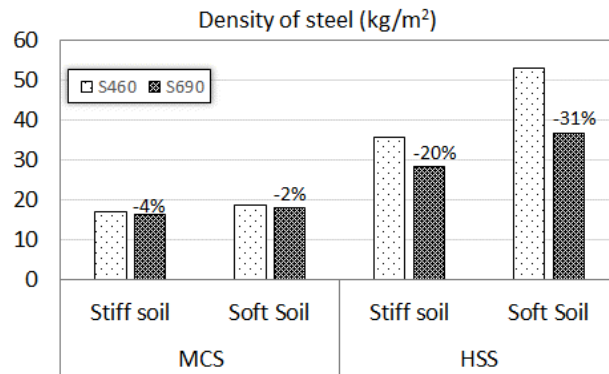


Figure 6.16 – Comparison between the HSS steel grades

Figure 6.17 illustrates the variability of steel density highlighting the influence of number of stories. The plots show that larger steel density generally characterizes taller frames. In contrast, the eight-storey frames located on stiff soil condition present higher steel density. This fact can be explained by higher fundamental periods of taller structures resulting in lower seismic action, especially for the stiff soil where the intensity of the seismic action is not so pronounced.

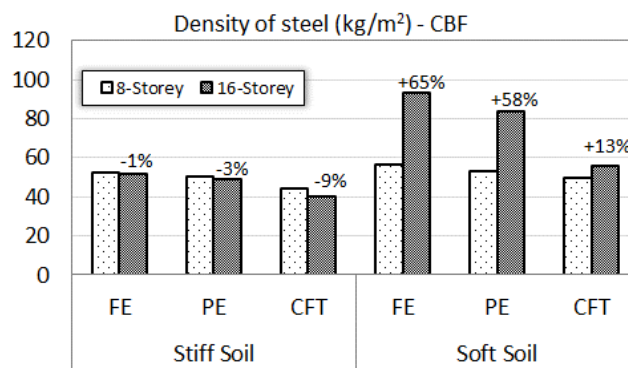


Figure 6.17 – Comparison of material consumption to number of storey

It is also important to mention that, according to Figure 6.18, composite steel-concrete column affects the material consumption of the buildings. The larger amount of steel is obtained for the cases with PE column. On the other hand, the CFT columns were the most efficient solution in terms of overall weight of the structure. Hence, this aspect can also be taken into account on the economic planning of the building.

Furthermore, Figure 6.19 and Table 6.6 show the steel densities highlighting the influence of span length. The cases with 5.0m span show higher density for both soil conditions. This issue addresses the difference in the influence area. The increase of the steel density is not proportional to the influence area resulting in larger amount for the frames with 5.0m of span.

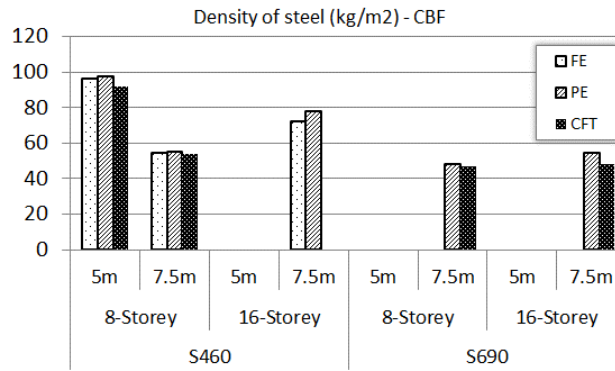


Figure 6.18 – Influence of the composite steel-concrete column

Table 6.6 – The steel weight (kg) for the frames with 5.0m and 7.5m of span

Span	Stiff soil			Soft soil		
	Column	Beam	Brace	Column	Beam	Brace
5m	19705	29055	3033	24349	34151	3975
7.5m	21944	44141	4088	26403	46301	5108
$\Delta$ (%)	111	152	135	108	136	128

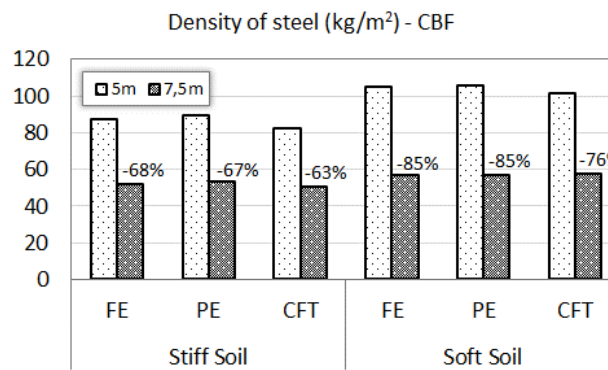


Figure 6.19 – Influence of the length span on the steel density

## ***Chapter VII***

# Dual-System Concentrically Braced Dual-Steel Frames

This Chapter is devoted to the presentation and discussion of the nonlinear performance of Dual-system frames composed by Concentrically Braced and Moment Resisting bays, including the effect of using two different steel grades in the elements according to the hierarchy defined for seismic resistance. Following the nonlinear procedure presented in the previous chapters, the static and dynamic nonlinear analyses are carried out in order to provide information about the overstrength factor, as well as the behaviour factor for these type of structures. Moreover, the seismic dynamic response is evaluated considering the three limit states proposed in Chapter IV and using the following parameters for discussion: i) peak inter-storey drift ratios; ii) residual inter-storey drift ratios; iii) peak storey accelerations and iv) brace ductility demand. In addition to these, the flexural ductility of the beams from MRF part is also investigated and discussed.

The nonlinear results from pushover analyses are first discussed and the basis of the overstrength factor. The dynamic performance is then outlined and the main results are presented and examined. The material consumption is also investigated providing a comparison between the Simple and Dual-Concentrically Braced Frames. The aim is to assess the possible advantages/limitations in the use of Dual-System in seismic zones.

### **7.1 Static-nonlinear analysis**

The capacity curves from pushover analyses for both 1<sup>st</sup> Mode and Uniform patterns are shown in Figure 7.1 and Figure 7.2. In these plots, the axis of ordinates correspond to base shear normalized with the design base shear while, in abscissas, the maximum roof displacement is represented.

Concerning the outcome, it is interesting to underline that after the first nonlinear event, the frames present a sudden reduction in lateral resistance, and then, there is an increasing in their resistance and a decreasing of the overall stiffness in comparison with the initial one. Such fact has also been observed in the CBFs. This behaviour is attributed to buckling of the braces. In particular, the eight-storey frames experience ratios that range from 2.0 to 3.5 for the 1<sup>st</sup> Mode pattern, while a variation that ranges around 2.0 to 2.5 is observed for the taller frames. The uniform pattern gives the major ratios where values between 2.5 and 4.0 are seen for both height investigated.

Focusing on the examined parameter, the frames founded in soft soil condition are responsible for smaller base shear ratios. Moreover, the difference between the base shear of the first plastic event and the maximum base shear is larger, concerning the study cases with stiff soil. Indeed, the frames located in soft soil are designed considering a larger base shear due to their design spectrum with large corner period  $T_c$ . This fact results in strong and stiffer structures in comparison with those designed considering as soil type a soil Type C (stiff soil). In addition, this increase of the design base shear mitigates the influence of the slenderness brace criterion in the seismic design. Therefore, these two factors may justify the smaller base shear ratio given by study cases located on soft soil condition. This outcome is consistent with the results presented for the CBFs.

The curves plotted in Figure 7.1 and Figure 7.2 allow highlighting the influence of the number of storey. The taller frames experience smaller base shear ratios compared to eight-storey frames, mainly for the 1<sup>st</sup> Mode pattern. In fact, applying this lateral load pattern to the taller frames, the increase of the base shear is not significant due to a probable soft mechanism usually seen in this structural system. The poor redistribution of the damage is proved to be more pronounced for the sixteen-storey frames. This behaviour will have consequences on the overstrength factors which will be discussed later.

Comparing the two span lengths examined, the differences found are mainly due to geometric restrictions of cross sections aiming at realistic frames. Some frames, mainly for those of 7.5m span and located on stiff soil, present larger base shear ratio, once they are stiffer and stronger. However, when there is no this influence, the study cases with two span lengths present similar base shear ratios.

Furthermore, the frames designed with S690 show larger ratios compared to frames with S460, mainly for the taller frames. This fact is related to overstrength factor used and to good redistribution of the damage provided by increase of the steel grade. Analysing Figure 3.15 in Chapter 3 it can be observed that the frames with S690 have been designed for a

larger overstrength factor resulting in stiffer and stronger structures in comparison with the frames with S460.

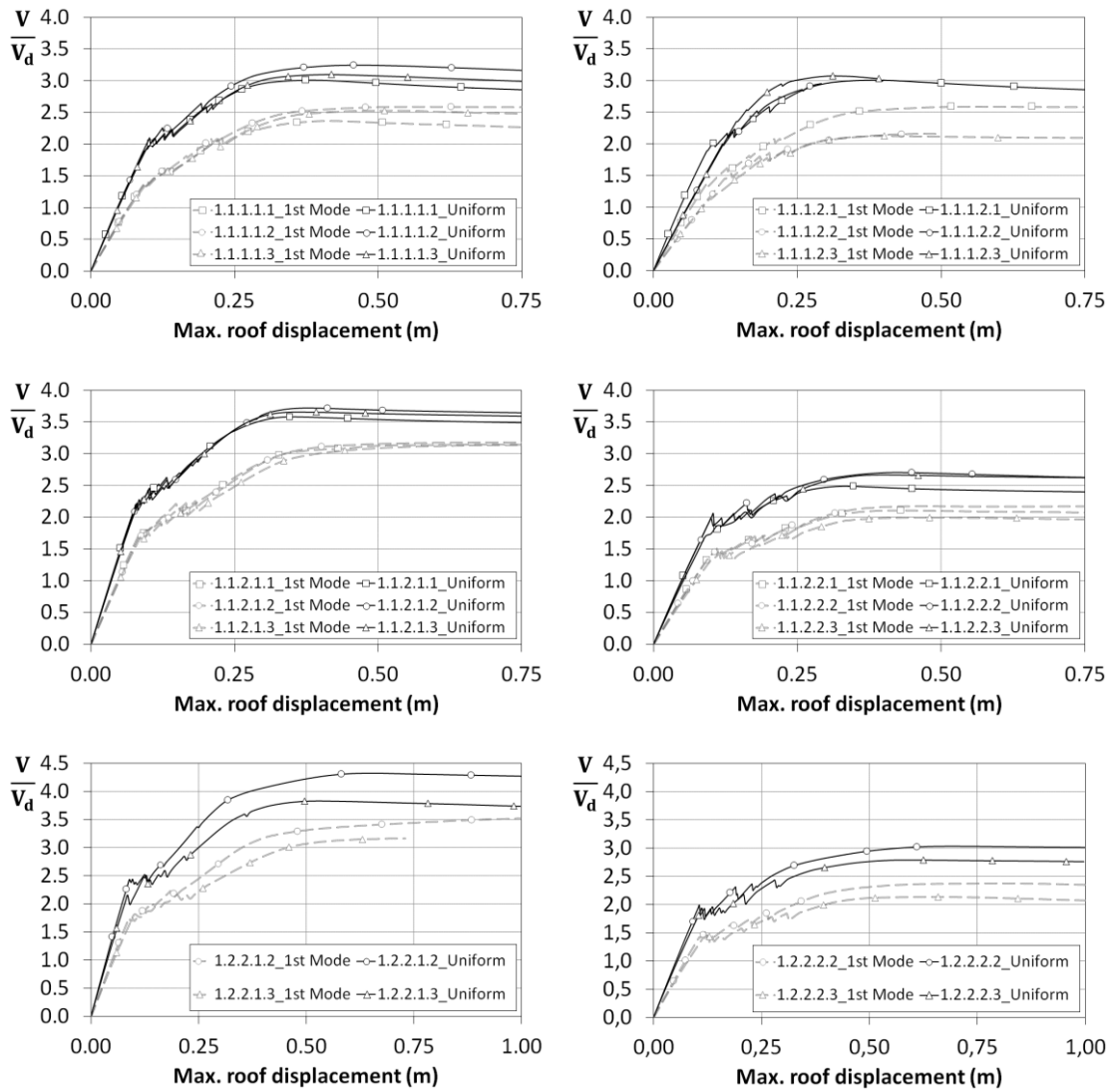


Figure 7.1 – Normalized pushover response curves from eight-storey frames

Moreover, the frames with S460 do not present an appreciable increase in their resistance after the first nonlinear event indicating a soft storey mechanism.

Regarding the composite columns, there is no substantial difference among the three types of columns, especially for the eight-storey frames. However, where there is a slight difference, the CFT columns are responsible for smaller base shear ratio compared to FE and PE columns. In fact, frames with CFT column are characterized by a smaller overall stiffness; in addition, they are less susceptible to geometrical restriction with lower reserves of resistance.

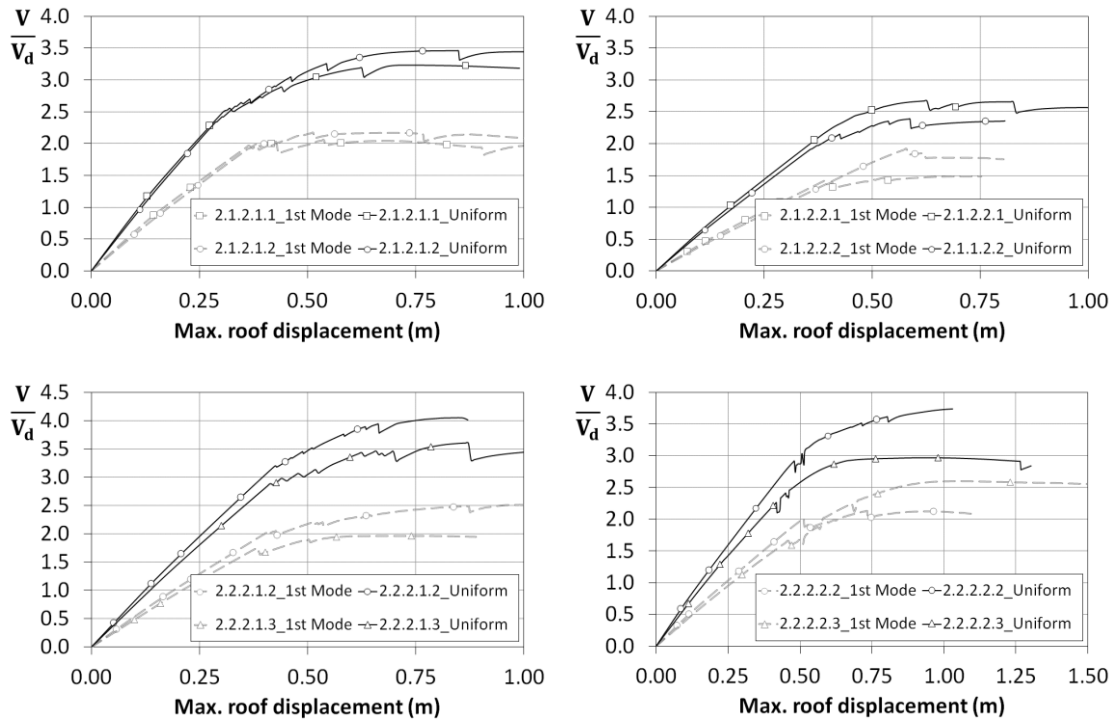


Figure 7.2 – Normalized pushover response curves from sixteen-storey frames

The plastic hinge pattern has also been assessed in this section. Analysing Figure 7.3 to Figure 7.6 it is possible to have an overview of the damage distribution and its sequence when the study cases reach an inter-storey drift of 2% for the 1<sup>st</sup> Mode. In particular, the first plastic event is given by the braces in compression. As it was seen in the capacity curves this event results in a sudden reduction of the lateral resistance. Afterwards, the “dual” effect is triggered and the plastic hinges can be seen on the end beam of the MRF system. Soon thereafter, the plastic hinges are formed in beam from braced bay and in braces from tension.

The plastic hinges in the MRF subsystem appear when the primary bracing subsystem has significant damage resulting in smaller overall lateral stiffness. In fact, the study cases confirm the idea of a dual-system structure where the secondary subsystem withstands the earthquake motion after the failure of the primary subsystem that is expected to primarily resist the earthquake.

As general remarks, the study cases experience excessive concentration of damage in mid-height. On the other hand, the capacity design criteria used on seismic design is confirmed where most of the plastic hinges are concentrated on the dissipative structural members, except for some composite columns from mid-rise. Analogous to CBFs, some beams from braced bay experience the formation of plastic hinges due to unbalance of vertical forces provided by contemporary brace yielding in tension and post-buckling in compression.

Once again, the post-buckling resistance considered in EN1998-1-1 (2004) seems to be not adequate confirming results from Serra et al. (2010).

In general, the D-CBFs show a poor distribution of damage where large damage concentrations are located in the mid-rise of the buildings, being prone to soft storey mechanism. In detail, the number of plastic hinges formed in the sixteen-storey frames is smaller in comparison with the eight-storey ones. Basically the MRF subsystem is not nearly triggered. It is not possible to reproduce a uniform distribution of damage when there is a wide resistance degradation of the braces resulting in plastic hinge on the beams from braced bay.

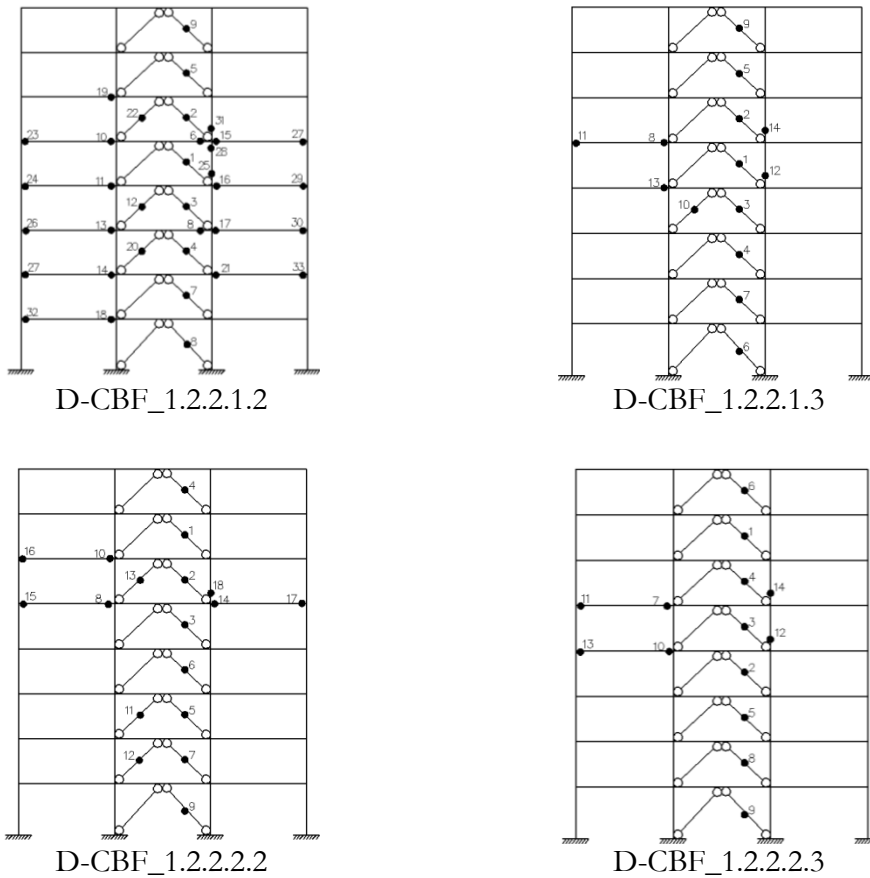


Figure 7.3 – 1<sup>st</sup> Mode Pushover: Damage distribution for frames with eight-storey frames with S690

Concerning another parameter, the increase of the strength steel used on the non-dissipative structural members provides fewer plastic hinges in comparison with those designed with S460. In fact, the use of S690 steel grade resulted in structures that are more flexible. Moreover, the formation of plastic hinges on the beam from braced bay is not pronounced on the cases with S690. Indeed, these beams were designed considering the same steel grade of non-dissipative steel grade; therefore, the beam strength of a solution with S690 should be larger, in contrast, with smaller flexural stiffness.

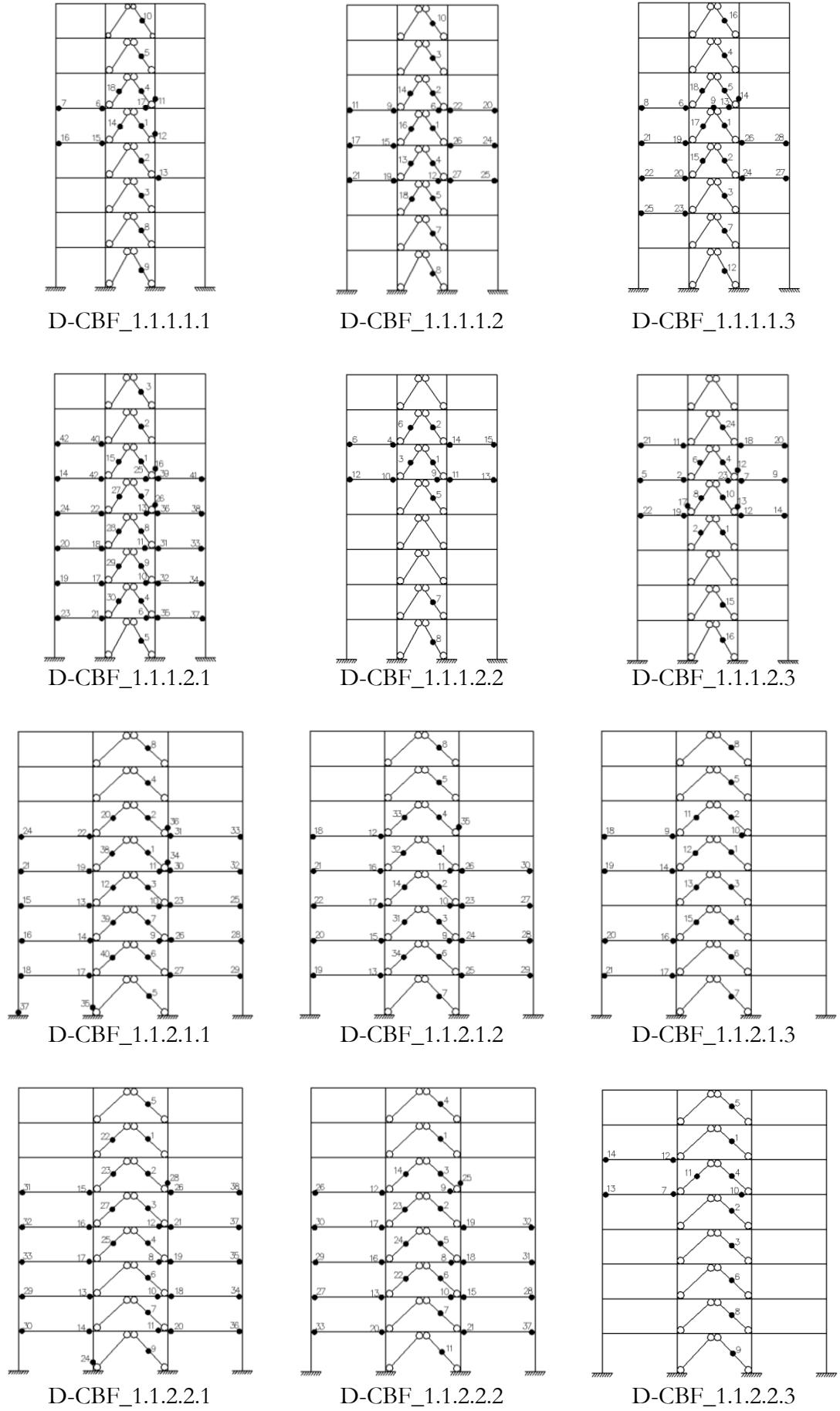
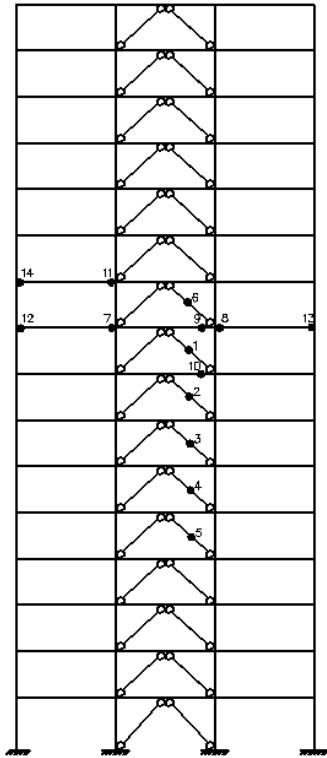
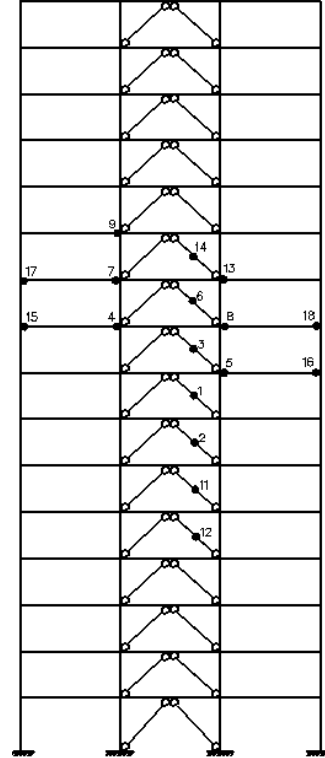


Figure 7.4 – 1<sup>st</sup> Mode Pushover: Damage distribution for eight-storey frames with S460

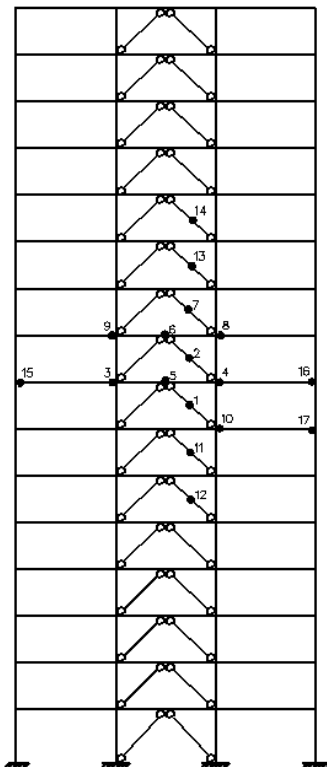




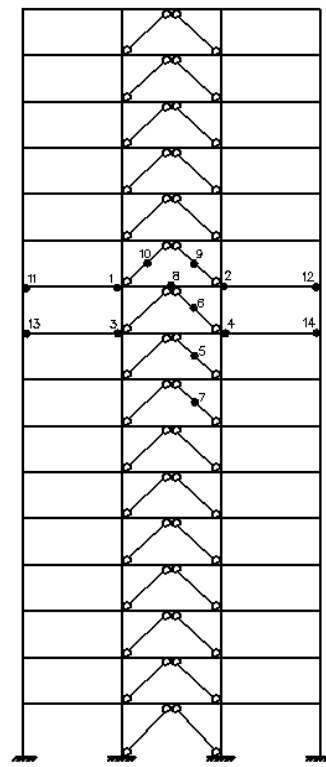
D-CBF\_2.1.2.1.1



D-CBF\_2.1.2.1.2

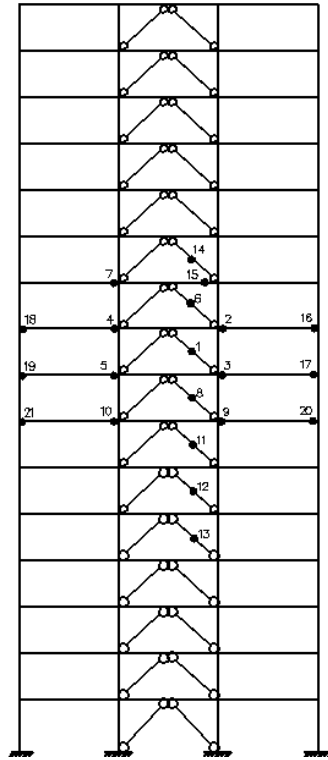


D-CBF\_2.1.2.2.1

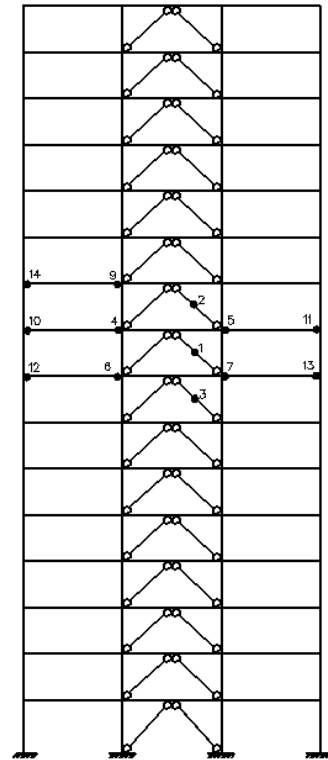


D-CBF\_2.1.2.2.2

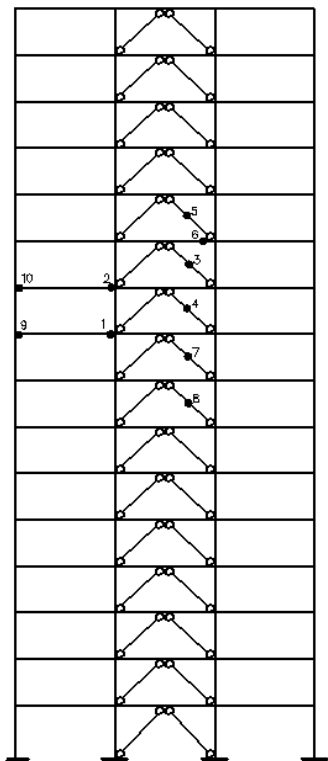
Figure 7.5 – 1<sup>st</sup> Mode Pushover: Damage distribution for frames with sixteen-storey frames with S460



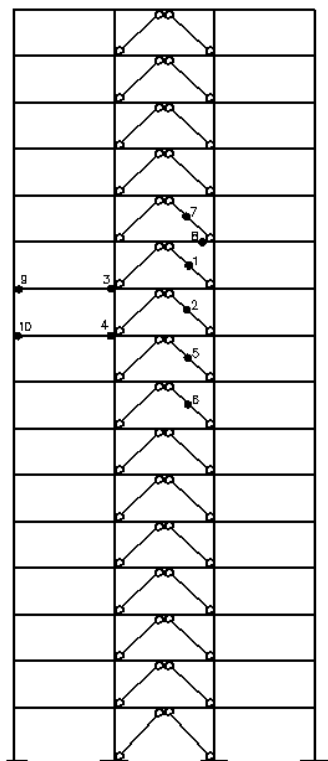
D-CBF\_2.2.2.1.2



D-CBF\_2.2.2.1.3



D-CBF\_2.2.2.2.2



D-CBF\_2.2.2.2.3

Figure 7.6 – 1<sup>st</sup> Mode Pushover: Damage distribution for frames with sixteen-storey frames with S690

In relation to column type, it is not easy to find a tendency for the composite column used. However, the frames using FE column on the non-dissipative members experience a slight increase of the number of plastic hinge compared to the solution with PE and CFT columns, as it was seen for the CBFs. There is not appreciable differences between the two span lengths studied.

#### 7.1.1 Overall overstrength factor

Regarding the overstrength factors, Table 7.1 reports the overstrength factor for the two lateral pattern used in the pushover analyses and the values found are shown according to the two overstrength examined. As general comment, the uniform pattern is the lateral loading in which it is possible to find the minimum overstrength factors associated to  $\Omega_1$  factor, mainly for the eight-storey frames. The modal pattern results in wide damage in the upper storey, it is more serious when it comes to the taller frames where a cantilever-behaviour is more pronounced. Moreover, this last pattern is also responsible for giving the minimum value for the overstrength associated with design decision and the  $\Omega$  factor.

Analysing the number of storey, the taller frames exhibit smaller  $\Omega_1$  and  $\Omega$  factors in comparison with eight-storey frames, as it was also evidenced in the CBFs. This outcome is consistent with the plastic deformation and capacity curves evaluated in the previous section. The sixteen-storey frames have a wide damage concentration in the mid-height resulting in soft storey mechanism due to poor redistribution of the forces. On the other hand, the eight-storey frames provide larger overstrength factor, due to a better redistribution of damage along the vertical direction. Regarding some other overstrength factors ( $\Omega_2$ ), the sixteen-storey frames are responsible for major values. This fact may be related to minor contribution of the fundamental mode for the taller frames.

In quantitative terms, an increasing of 42% of the overstrength given by EN1998-1-1 (2004) is observed for the eight-storey frames. For what concerns the overstrength related to design criteria, a median of 1.54 is observed for the eight-storey frames, while the taller frames present a value of 1.88 resulting in a decrease of 18%. Finally, a difference of 32% is found in the  $\Omega$  factor with a median of 2.76 for the smaller frames and 2.08 for the other frames.

The length span does not play an important role when it comes to the overstrength factors. In particular, frames with smaller span have medians of 1.52, 1.42 and 2.26, while other frames show values of 1.53, 1.52 and 2.65 for the  $\Omega_1$ ,  $\Omega_2$  and  $\Omega$  factors, respectively.

It can be stated that the soil type also affects the overstrength factors. The values reported in Table 7.1 indicate that the frames located in stiff soil condition present larger  $\Omega_1$  and  $\Omega$  factors. As observed on the CBFs, the large base shear from soft design spectrum reduced

the influence of slenderness braces, especially on the last floor, on the seismic design. It resulted in structures with lower  $\Omega_{\text{design}}$  factors in order to define the load in the non-dissipative elements. Therefore, the soft soil condition allowed structures with smaller ratio between design plastic resistance and design buckling resistance. All the frames found in soft soil are stiffer and strong in comparison with others, resulting in a poor redistribution of damage right after the first plastic event, it tends to have a soft storey mechanism. The frames in stiff soil present values of 1.61, 1.68 and 2.55 for the  $\Omega_1$ ,  $\Omega_2$  and  $\Omega$  factors, while values around 1.37, 1.43 and 2.11 are found for the frames located in soft soil. The major difference is given for the  $\Omega$  factor with a value of 21%.

The increase of the HSS steel grade provides structures with slightly higher overstrength factor, especially for the  $\Omega$  factor. The values indicated in Table 7.1 show that the frames designed with S690 have an increasing of 7%, 6% and 11% for the  $\Omega_1$ ,  $\Omega_2$  and  $\Omega$  factors, respectively. In fact, the buildings with this steel grade allow for a better distribution of the damage causing an increase of the lateral strength after the first plastic event. On the other hand, when it compare it with another parameter examined, namely the soil type, the use of either S690 or S460 on the non-dissipative structural members does not show any appreciable differences for the D-CBFs.

Concerning the type of composite steel-concrete column, in most cases, the CFT and FE composite columns give the smaller overstrength factors. This fact is related to the relation between the stiffness and strength of the column type. The frames with CFT columns are more flexible because this column type is efficient when the ratio weight and strength is taken into account. This issue is verified in the next section, which presents an assessment of the material consumption.

Summarizing, the frames studied here present a median of 1.45 for the overstrength incorporated in the EN1998-1-1 (2004). It should be noticed that in the seismic design when the behaviour factor was assumed, this study used a value of 4.8 considering as reference q-factor a value of 4.0. This reference value was then multiplied by 1.2, being the overstrength factor assumed, resulting in the value of 4.8. Therefore, the study cases show an increasing overstrength factor in comparison with those employed on the seismic design.

Table 7.1 – Overstrength factor for the D-CBFs

<i>Frames</i>	$\left(\frac{V_y}{V_{1y}}\right)$		$\left(\frac{V_{1y}}{V_{dy}}\right)$		$\left(\frac{V_y}{V_{1y}}\right)_{\min}$	<i>Load pattern</i>	$\left(\frac{V_{1y}}{V_{dy}}\right)_{\min}$	<i>Load pattern</i>	$\Omega$	<i>Load pattern</i>
	<i>1<sup>st</sup> Mode</i>	<i>Uniform</i>	<i>1<sup>st</sup> Mode</i>	<i>Uniform</i>						
D-CBF_1.1.1.1.1	1.74	1.60	1.36	1.87	1.60	Uniform	1.36	1st Mode	2.37	1st Mode
D-CBF_1.1.1.1.2	1.90	1.57	1.36	2.07	1.57	Uniform	1.36	1st Mode	2.59	1st Mode
D-CBF_1.1.1.1.3	1.82	1.62	1.39	1.92	1.62	Uniform	1.39	1st Mode	2.52	1st Mode
D-CBF_1.1.1.2.1	1.44	1.38	1.47	2.34	1.38	Uniform	1.47	1st Mode	2.11	1st Mode
D-CBF_1.1.1.2.2	1.48	1.52	1.45	1.52	1.48	1st Mode	1.45	1st Mode	2.15	1st Mode
D-CBF_1.1.1.2.3	1.37	1.36	1.55	2.32	1.36	1st Mode	1.55	1st Mode	2.12	1st Mode
D-CBF_1.1.2.1.1	1.89	1.64	1.66	2.18	1.64	Uniform	1.66	1st Mode	3.14	1st Mode
D-CBF_1.1.2.1.2	1.88	1.68	1.70	2.22	1.68	Uniform	1.70	1st Mode	3.18	1st Mode
D-CBF_1.1.2.1.3	1.90	1.62	1.65	2.25	1.62	Uniform	1.65	1st Mode	3.14	1st Mode
D-CBF_1.1.2.2.1	1.51	1.25	1.40	1.99	1.25	Uniform	1.40	1st Mode	2.11	1st Mode
D-CBF_1.1.2.2.2	1.57	1.33	1.39	2.03	1.33	Uniform	1.39	1st Mode	2.17	1st Mode
D-CBF_1.1.2.2.3	1.45	1.57	1.38	1.70	1.45	1st Mode	1.38	1st Mode	2.00	1st Mode

Table 7.1 – Overstrength factor for the D-CBFs (*Continued*)

Frames	$\left(\frac{V_y}{V_{1y}}\right)$		$\left(\frac{V_{1y}}{V_{dy}}\right)$		$\left(\frac{V_y}{V_{1y}}\right)_{\min}$	Load pattern	$\left(\frac{V_{1y}}{V_{dy}}\right)_{\min}$	Load pattern	$\Omega$	Load pattern
	1 <sup>st</sup> Mode	Uniform	1 <sup>st</sup> Mode	Uniform						
D-CBF_1.2.2.1.2	2.01	1.78	1.75	2.43	1.78	Uniform	1.75	1st Mode	3.52	1st Mode
D-CBF_1.2.2.1.3	1.75	1.77	1.81	2.16	1.75	1st Mode	1.81	1st Mode	3.16	1st Mode
D-CBF_1.2.2.2.2	1.67	1.53	1.42	1.98	1.53	Uniform	1.42	1st Mode	2.37	1st Mode
D-CBF_1.2.2.2.3	1.51	1.44	1.40	1.93	1.44	Uniform	1.40	1st Mode	2.13	1st Mode
D-CBF_2.1.2.1.1	1.07	1.28	1.94	2.61	1.07	1st Mode	1.94	1st Mode	2.08	1st Mode
D-CBF_2.1.2.1.2	1.13	1.50	1.93	2.38	1.13	1st Mode	1.93	1st Mode	2.18	1st Mode
D-CBF_2.1.2.2.1	1.07	1.24	1.41	2.12	1.07	1st Mode	1.41	1st Mode	1.51	1st Mode
D-CBF_2.1.2.2.2	1.03	1.15	1.86	2.22	1.03	1st Mode	1.86	1st Mode	1.92	1st Mode
D-CBF_2.2.2.1.2	1.24	1.22	2.02	2.65	1.22	Uniform	2.02	1st Mode	2.50	1st Mode
D-CBF_2.2.2.2.3	1.20	1.29	1.63	3.29	1.20	1st Mode	1.63	1st Mode	1.96	1st Mode
D-CBF_2.2.2.2.2	1.10	1.13	1.90	2.37	1.10	1st Mode	1.90	1st Mode	2.09	1st Mode
D-CBF_2.2.2.2.3	1.28	1.29	1.63	1.94	1.64	1st Mode	1.63	1st Mode	2.09	1st Mode
16 <sup>th</sup>	1.12	1.25	1.39	1.93	1.12		1.39		2.05	
50 <sup>th</sup>	1.50	1.47	1.59	2.17	1.45		1.59		2.16	
84 <sup>th</sup>	1.88	1.63	1.87	2.40	1.64		1.87		3.14	

Opposed to CBF, the values found for the  $\Omega_2$  factor are considerably greater than 1.0 showing that the decision making did not result in structures with excellent level of optimization with a median of 1.59. This factor perhaps indicates a use of smaller behaviour factor since the frames with larger base shear, namely those located on soft soil condition, exhibit lower  $\Omega_2$  factor. This issue is an important observation that can be studied in further works but it does not match the scope of this work.

Finally, the frames also exhibit overstrength factors ( $\Omega$ ) which were lower than the behaviour factor employed in seismic design ( $q = 4.8$ ) as it was seen in the CBFs. Thus, the seismic response for the design earthquake is not elastic range where the formation of plastic hinges can be observed.

## 7.2 Dynamic performance evaluation

In order to understand the nonlinear dynamic behaviour and the influence of the investigated parameters on the seismic performance of the D-CBFs, incremental dynamic analyses were carried out following the procedure described in Chapter IV.

According to nonlinear procedures, the outcomes of dynamic analyses are assessed according to the three limit states proposed by EN1998-1-3 (2005). The evaluation addresses the role of each parameter examined in this study, concerning not only the overall, but also the global seismic response.

The nonlinear dynamic performance is based on the evaluation of the following global and local indicators: i) peak inter-storey drift ratios; ii) residual inter-storey drift ratios; iii) peak storey accelerations, iv) brace ductility demand and v) beams of MRF part ductility. In addition, the flexural ductility of the beams of MRF part is also studied and described.

### 7.2.1 Peak inter-storey drift ratios

The IDR was also monitored for the D-CBFs considering the three limit states previously proposed. Figure 7.7 reveals the median profile for all the study cases and Table 7.2 provides the maximum value found in each curve of this figure. These plots also show the influence of the parameters that significantly modify the seismic response. The plots are divided into three different groups for each limit state: soil condition, steel grade and span length.

The first observation to be made is about the difference between the median profile considering the number of storey as reference. Figure 7.7 indicates that the eight-storey frames present higher IDRs in the upper storey having a more uniform profile in comparison with the taller frames. These last ones are characterized by higher drift demand compared with the smaller frames. Moreover, the maximum values are located around the

mid-height. It is important to note that the taller frames are more flexible and there is a large concentration of localized damage in the given floor resulting in a soft storey mechanism. This general behaviour is attributed to cantilever-behaviour from the taller frames to be more pronounced than the eight-storey frames with shorter span length, for instance.

The soil condition is another parameter that strongly influence the seismic performance of the D-CBFs. It is worth to highlight that the frames located on soft soil experiment higher IDR demand in comparison with those that are designed considering only the stiff soil. In some cases, especially for the taller frames, the values more than double. This large difference is mainly attributed to the soft storey mechanism of the frames on the soft soil due to frames are located in the constant acceleration range of the spectrum resulting in large demand. On the other hand, the frames with 5.0m of span located on soft soil condition experience smaller drift demand. This observation is related to the appearance of the soft mechanism for the frames located on stiff soil condition. Indeed, this last case presents more abrupt variation of the drift demand along the height. In contrast, for the CBFs, this difference decreased when the seismic intensity increased. When it comes to the D-CBFs, it is not possible to state that with such certainty, due to the higher tendency of the soft storey mechanism.

It is interesting to note that the HSS steel grade has an affect on the response of the D-CBFs. The increase of the steel strength of the non-dissipative members provides more flexible structures, mainly when a high value behaviour factor is used on the seismic design. The median profiles comparing the two HSS steel grades indicate a similar behaviour employing either S460 or S690 on the non-dissipative members for the taller frames, even though, there is a significant difference for the eight-storey frames. This difference ranges from 13% up to 62% for the eight-storey, when a minimum value of 3% is regarded and a maximum of 13% is considered for the taller frames. The use of S690 for the eight-storey frames results in a large drift demand that is concentrated in a specific region, and the employment of S460 enables a more uniform distribution of the damage along the height. In the previous Chapter, it was observed that the use of the higher steel grade provided a better redistribution of the drift. Here, the result is the opposite due to high flexibility given by S690 in association with large behaviour factor assumed in the design.

In terms of span length, Figure 7.7 and Table 7.2 indicate that the frames with 5.0m of span experience higher IDRs in comparison with those designed with larger span length.



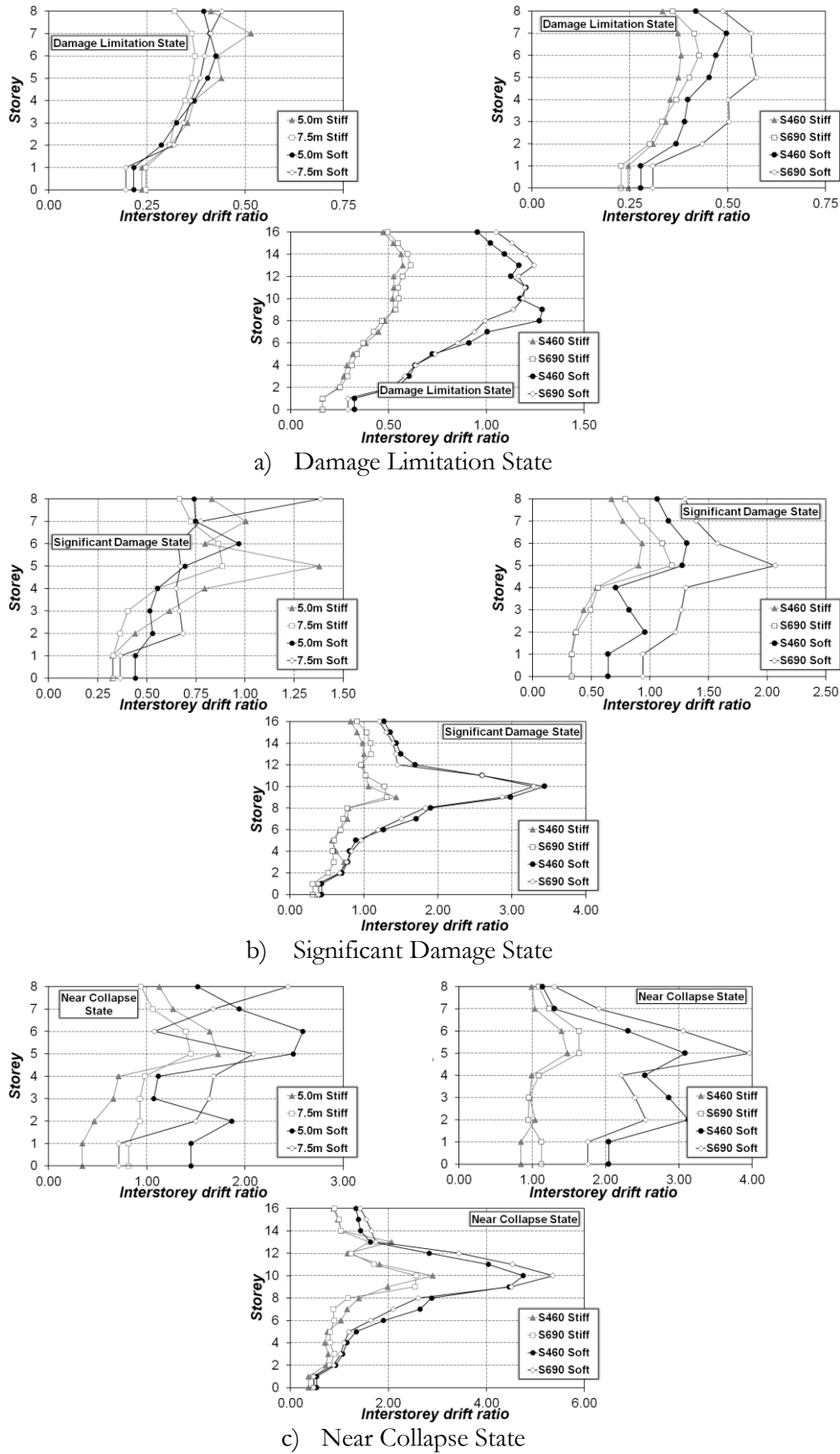


Figure 7.7 – Influence of studied parameters in inter-storey drift demand for the three limit states (*values in %*)

This observation is justified by the fact that some structural members of the frames with larger span length were designed considering geometrical restrictions. Thus, the flexibility of beams in braced bay has less influence on the overall behaviour since the lateral stiffness has increased for the eight-storey frames.

In general, the eight-storey frames present drift demand below the limit adopted in seismic design for the DL limit state for both soil condition investigated. On the other hand, the large drift demand obtained for the sixteen-storey frames located on the soft soil exceed the value assumed for the DL limit state. In detail, the IDRs of the taller frames reach a value of 1.28% for the ones with S460 and 1.24% for those with S690. It is worth noticing that some cases present a large drift demand for the DL and for the NC limit state, surpassing 3%.

Table 7.2 – Maximum median of inter-storey drift ratio demand for the D-CBFs (*values in %*)

Percentiles at each limit state		8-Storey						16-Storey	
		5.0 m			7.5 m			7.5 m	
		Stiff soil	Soft soil		Stiff soil	Soft soil		Stiff soil	Soft soil
S460	DL	0.51	0.42		0.37	0.44		0.57	1.28
	SD	1.37	0.96		0.88	1.38		1.43	3.44
	NC	1.72	2.58		1.44	2.44		2.90	4.75
S690	DL	-	-		0.42	0.57		0.61	1.24
	SD	-	-		1.18	2.06		1.30	3.29
	NC	-	-		1.63	3.96		2.56	5.35

### 7.2.2 Residual inter-storey drift ratios

This section presents the RIDRs experienced by the study cases. The plots with the median profiles are depicted by Figure 7.8 and the maximum values found in these curves are presented in Table 7.3. Again, the data is presented in terms of soil condition, HSS steel grade and geometric, hiding the reviews about the composite steel-concrete column because the differences are not relevant. In general terms, the study cases experience lower residual drift demand for the DL limit state. This fact is associated to high lateral stiff provided by braces. On the other hand, the large drifts are seen for the NC limit state especially for the taller frames.

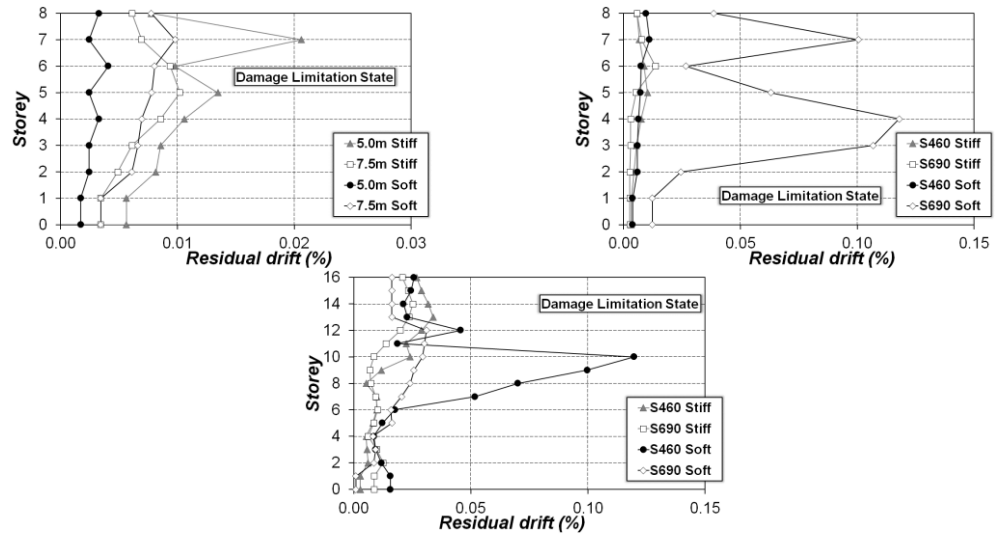
Furthermore, the curves in Figure 7.8 show the same high drift demand region seen previously on the IDRs. In fact, the residual drift profiles show a reflection of the transient drift profiles. Therefore, the eight-storey frames experience large residual drift demand on the upper storey due to large brace strength degradation resulting in large deformation in

this zone. For the taller frames, their profiles are less uniform compared to eight-storey frames and high demand are seen in the mid-height.

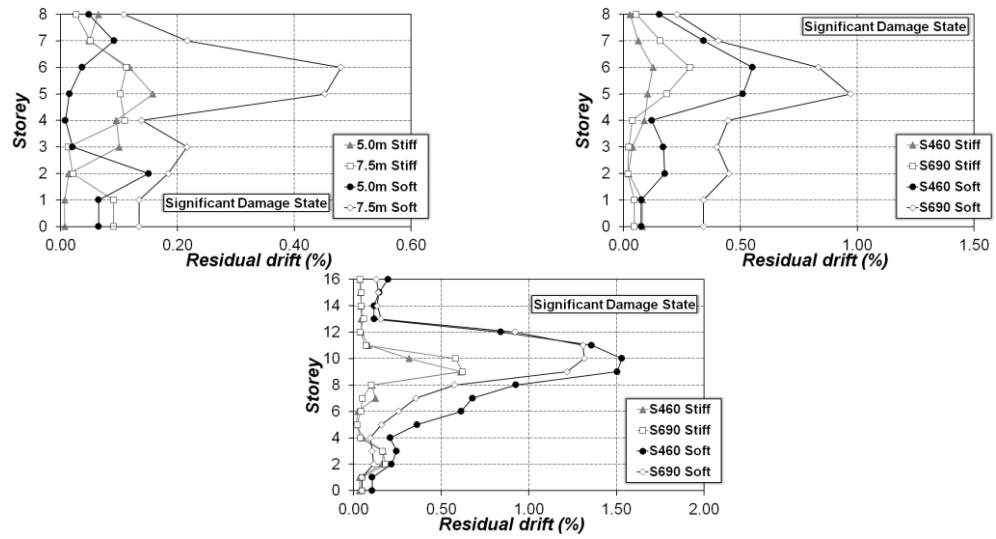
Focusing on the influence of parameters, it is important to note that the frames located on soft soil experience higher ratios. This observation was expected due to the profiles of the transient inter-storey drifts. The soil condition plays an important role in order to assess the overall seismic performance of the D-CBFs. Although high seismic action on seismic design for the soft soil has provided stiffer structures, large drift demand is seen for the D-CBFs.

Again, frames with shorter frames exhibit larger drift ratio in comparison with the frames with 7.5m span. The same observation stated previously also applies here. Therefore, the decision taken on the seismic design influences the behaviour of longer frames. In particular, the geometric restriction provided structural member with high overstrength. Thus, the flexural stiffness of beam from braced bay reveals that there are no major influences on the seismic response.

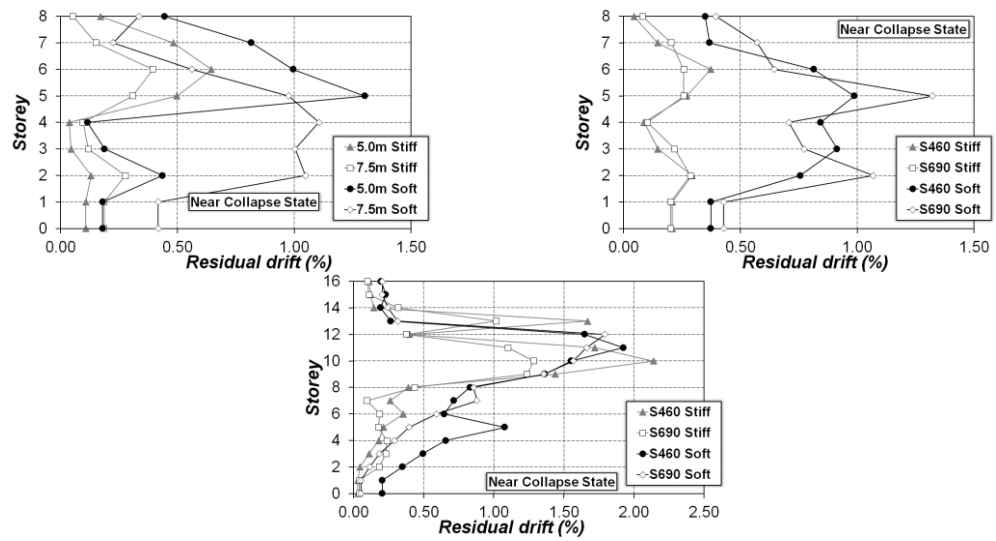
Some comments can be made concerning HSS steel grade and applied to the non-dissipative members. It is recognized that the increase of the steel strength provides a mitigation of material consumption when the seismic design is not governed by deformation criterion that in the case of D-CBFs, this results in more flexible structures. However, the median profiles for both HSS steel grades are very similar, mainly for the taller frames. The frames designed with S690 (more flexible) experience RIDRs smaller than the frames with S460. On the other hand, the increase of the HSS steel grade does not result in smaller RIDRs for the eight-storey frames. In detail, there are some cases in which the eight-storey frames with S690 present values twice larger than the others. This fact is more evident for frames in soft soil and DL and SD limit states where the soft storey mechanism is more pronounced.



a) Damage Limitation State



b) Significant Damage State



c) Near Collapse State

Figure 7.8 – Influence of studied parameters in residual drift ratio for the three limit states

Table 7.3 – Maximum median of residual inter-storey drift ratio demand (*values in %*)

Percentiles at each limit state	8-Storey				16-Storey	
	5.0 m		7.5 m		7.5 m	
	Stiff soil	Soft soil	Stiff soil	Soft soil	Stiff soil	Soft soil
DL	0.02	0.00	0.01	0.01	0.03	0.10
S460 SD	0.15	0.15	0.11	0.48	0.61	1.53
NC	0.64	1.30	0.39	1.10	2.14	1.92
DL	-	-	0.01	0.12	0.02	0.03
S690 SD	-	-	0.28	0.97	0.62	1.31
NC	-	-	0.29	1.32	1.28	1.79

### 7.2.3 Peak storey accelerations

The PSA along the height of the buildings structures is here investigated using the seven records selected for each soil condition. Figure 7.9 illustrates the median profiles of the PSA comparing the soil type, length span and number of storey. The plotted values represent the amplification of the storey acceleration where the absolute peak storey acceleration is divided by design acceleration. Table 7.4 and Figure 7.9 show the maximum value obtained for each curve.

It is possible to underline that the taller buildings follow the “S” shaped curve with the maximum PSA located on the top floor. This implies that for these frames, shear-dominated behaviour is observed on the bottom floors, flexural-dominated behaviour is observed at the upper floors, and a combination of these two behaviours contributes to the middle floors level response. On the other hand, the frames with eight-storey frames present a more linear behaviour over the height in which the maximum values are achieved on the top floor. In particular, the taller frames exhibit larger amplification of storey acceleration reaching value around 4.0 and the shorter frames, mainly for the soft soil, experience PSA of 3.0 for the NC limit state.

It is interesting to notice that the PSA level achieved is sensitive to soil condition especially for the taller frames. The difference found between the two soil types reaches values in order of 40%. Again, the soil condition is an important parameter, which may influence the seismic performance of the buildings.

Another aspect to be assessed is related to span length. It was seen for both transient and residual drift that the frames with 5.0m of span presented larger demand compared to

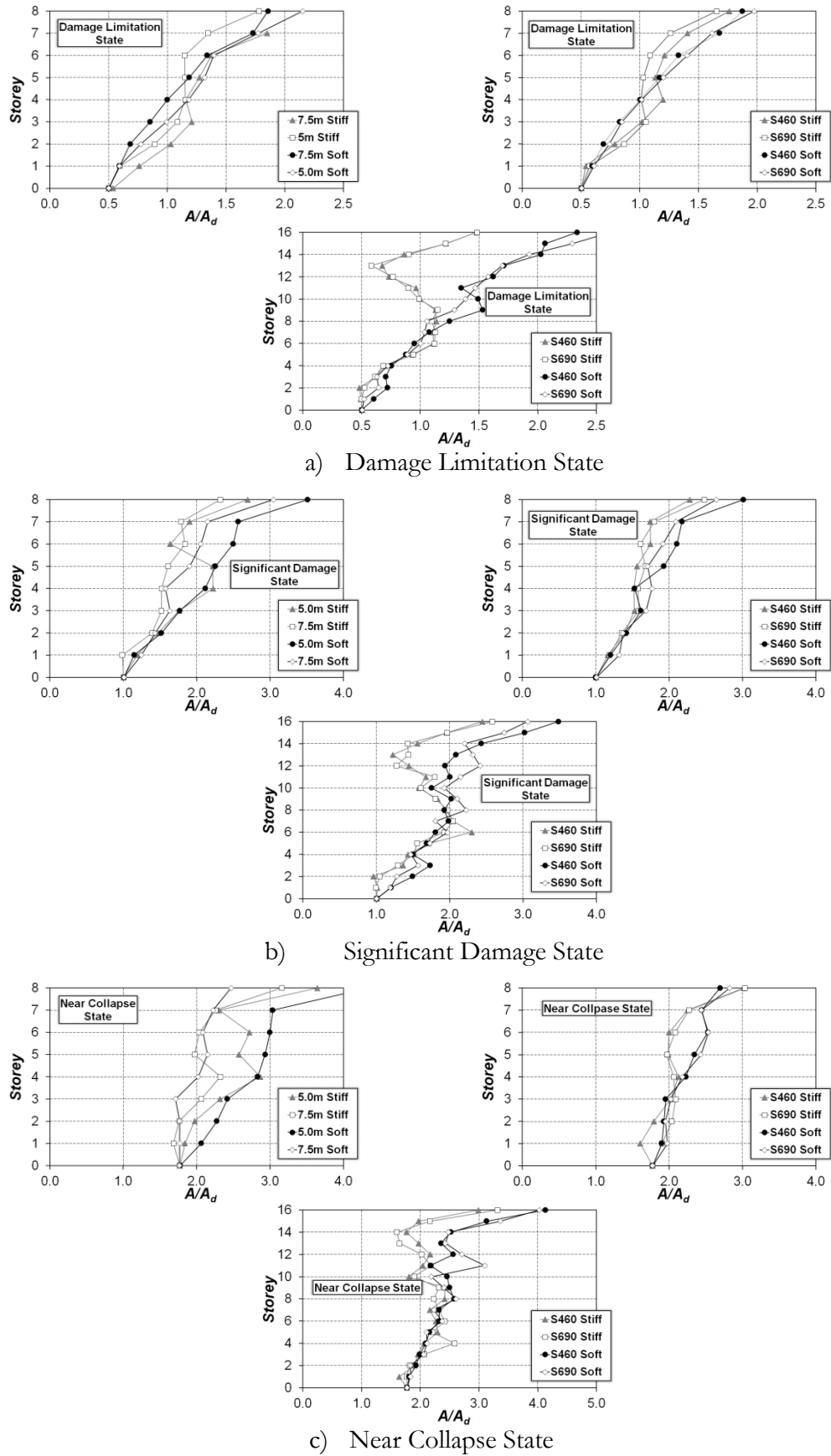


Figure 7.9 – Profiles of the peak storey acceleration for the D-CBFs

frames with longer span. For the PSAs, this trend is repeated. The frames with shorter length span are responsible for major amplitudes.

Table 7.4 – Maximum values found for the PSAs for the D-CBFs

Percentiles at each limit state		8-Storey				16-Storey	
		5.0 m		7.5 m		7.5 m	
		Stiff soil	Soft soil	Stiff soil	Soft soil	Stiff soil	Soft soil
S460	DL	1.78	2.15	1.84	1.85	1.48	2.33
	SD	2.69	3.51	2.32	3.04	2.44	3.48
	NC	3.64	4.34	3.16	2.47	2.99	4.13
S690	DL	-	-	1.64	1.97	1.48	2.62
	SD	-	-	2.47	2.64	2.58	3.06
	NC	-	-	3.03	2.83	3.31	4.02

Concerning HSS steel grade used on non-dissipative members, the plots for both steel grades investigated are very similar. The HSS steel grade is the parameter that less influences the PSAs in comparison with the other. In general, the increase of the steel strength of the non-dissipative elements provides a reduction of the PSAs in most cases. It can be observed a reduction of 13% for the NC limit state, in contrast, there are some cases in which an increase of PSAs is observed, namely for the SD limit state.

Analogous to CBFs and MRFs, significant amplification of the storey acceleration are also observed for the D-CBF. This means that wide damage in the non-structural members can be expected (FEMAE-74, 2011).

#### 7.2.4 Brace ductility demand

The inelastic capacity of the braces evaluated in this section corresponds to the same one defined in the previous chapter. It follows the recommended values for the CBFs according to EN1998-1-3 (2005). Figure 7.10 reveals the median of the ratio of the ductility demand for braces with larger rates, namely the braces in compression because the tension braces present smaller ductility demand. In Table 7.5, the maximum median for each performance level in accordance with EN1998-1-3 (2005) is indicated.

The results underlined by Figure 7.10 and Table 7.5 reveal large difference among the three performance levels investigated. In particular, the frames experience high axial deformation with values heavily superior to the recommended limit by EN1998-1-3 (2005). According to DL limit state, the braces should be provided with adequate resistance in order to ensure that the axial deformation does not reach the limit of  $0.25\Delta_c$ . In this scenario, there is no inelastic deformation in the buildings since the braces in compression are the first structural member to behave nonlinear. Therefore, the study cases are well far away from the proposed

limits to fulfil the assumption of the DL state. On the other hand, the values indicated on Table 7.5 show that the frames are closer to fulfil the proposed limit for the SD limit state.

As expected, the soil condition also plays an important role on the brace ductility demand in the D-CBFs. The frames with larger span length and located in soft soil condition experience an average increasing of the 93% on the ductility demand. In contrast, the frames with shorter frames experience smaller ductility demand for the soft soil condition. This fact is related to the appearance of a soft storey mechanism on the upper floors resulting in larger damage concentration and consequently greater axial deformation in the braces.

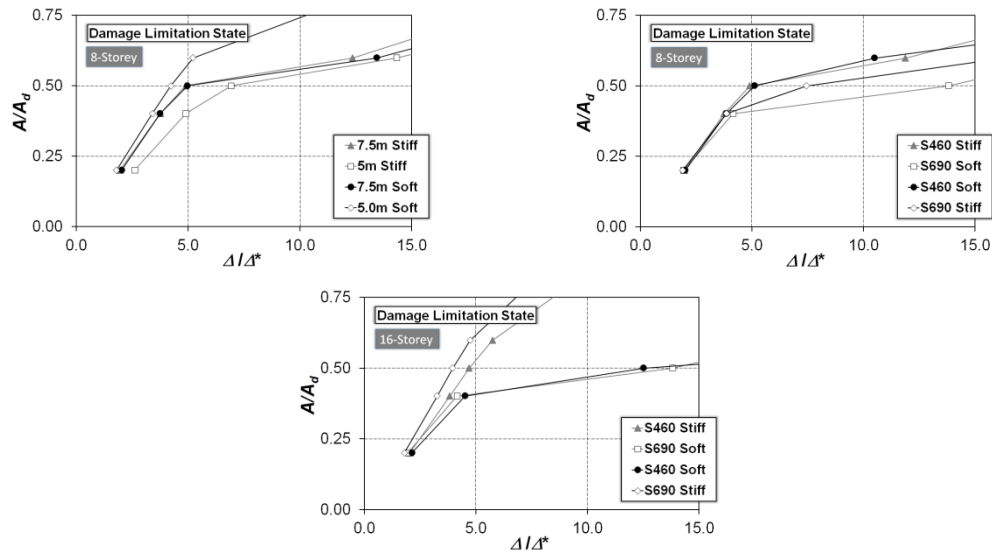
Due to oversize of the cross-section, the frames with 7.5m of span present smaller ratio in comparison with the shorter length span frames expect for the cases with soft soil conditions. It is interesting to notice that probably if there was greater damage concentration in a particular zone for the frames with shorter span length in stiff soil, the behaviour of these frames could be the same as in the soft soil.

Regarding the HSS steel grade, the increasing of the steel strength brings few benefits for the frames in terms of brace ductility demand in comparison with another parameter stated previously. This outcome is consistent with another parameters monitored where it is observed a large seismic demand for the frames with S690.

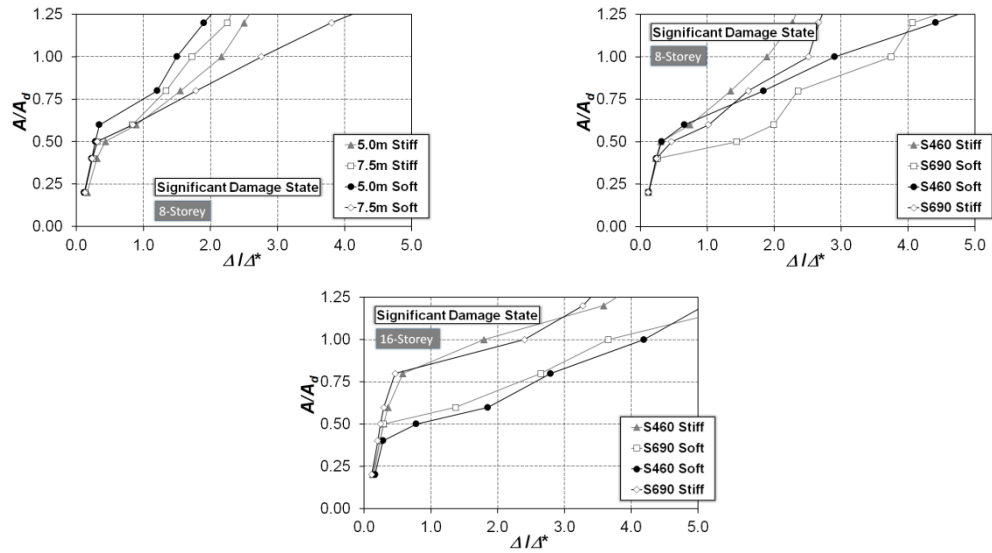
Table 7.5 – Maximum value of brace ductility demand

Percentiles at each limit state	8-Storey				16-Storey	
	5.0 m		7.5 m		7.5 m	
	Stiff soil	Soft soil	Stiff soil	Soft soil	Stiff soil	Soft soil
S460 DL	6.92	4.22	4.90	5.11	4.70	12.52
S460 SD	2.16	1.50	1.89	2.90	1.80	4.19
S460 NC	2.58	2.29	1.93	5.47	3.97	4.59
S690 DL	-	-	7.45	13.81	3.95	4.64
S690 SD	-	-	2.51	3.74	2.40	3.66
S690 NC	-	-	2.38	5.19	3.20	5.00

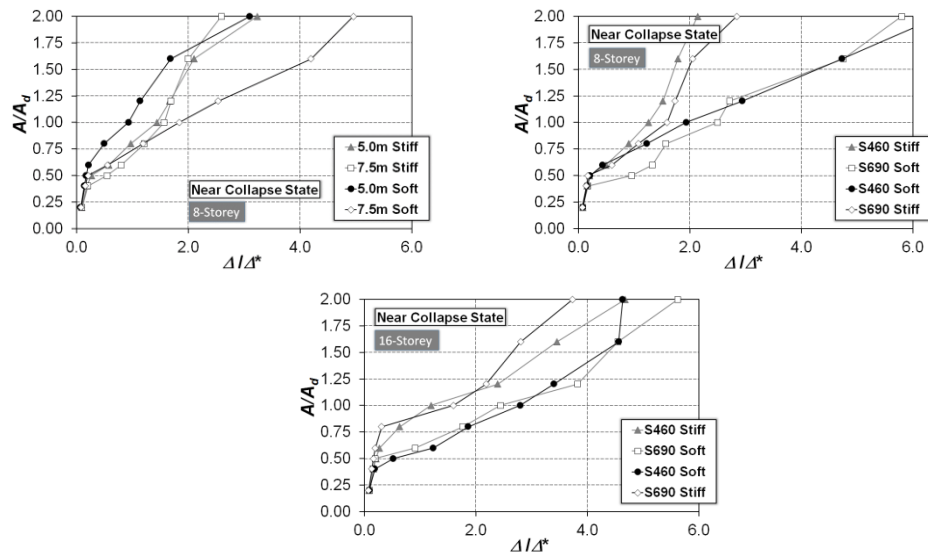




a) Damage Limitation State



b) Significant Damage State



c) Near Collapse State

Figure 7.10 – Brace ductility demand from D-CBFs for the three limit states

### 7.2.5 Beam ductility demand in MRF subsystem

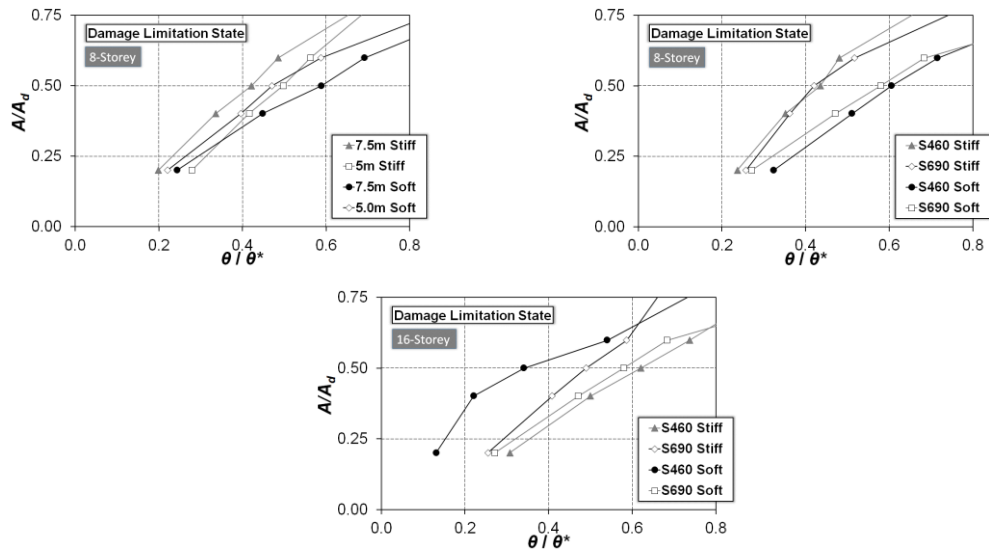
The aim of the “dual-system” is to improve the energy dissipation capacity of the structures allowing additional dissipative zones provided by the beams from MRFs part of the D-CBFs. Therefore, it is important to assess the rotation capacity to assure the formation of a full plastic ductile mechanism, in which it becomes compulsory to verify the rotation demand and then to compare it with the rotation capacity (D'Aniello et al., 2014b; D'Aniello et al., 2012).

In order to investigate the beam ductility demand from MRF part, the limits for beam plastic rotation capacity defined in EN1998-1-3 (2005) are also used here. In particular, the norm recommends that the beam plastic rotation capacity should be no lesser than  $10\theta_y$ ,  $6\theta_y$  and  $8\theta_y$ , respectively for the DL, SD and NC, being  $\theta_y$  the beam yield rotation. Figure 7.11 and Table 7.6 show the ratio between the maximum rotation obtained on the dynamic analyses and plastic rotation capacity of the beams. Once more, Figure 7.11 illustrates the median curves while Table 7.6 provides the maximum associated to each performance level.

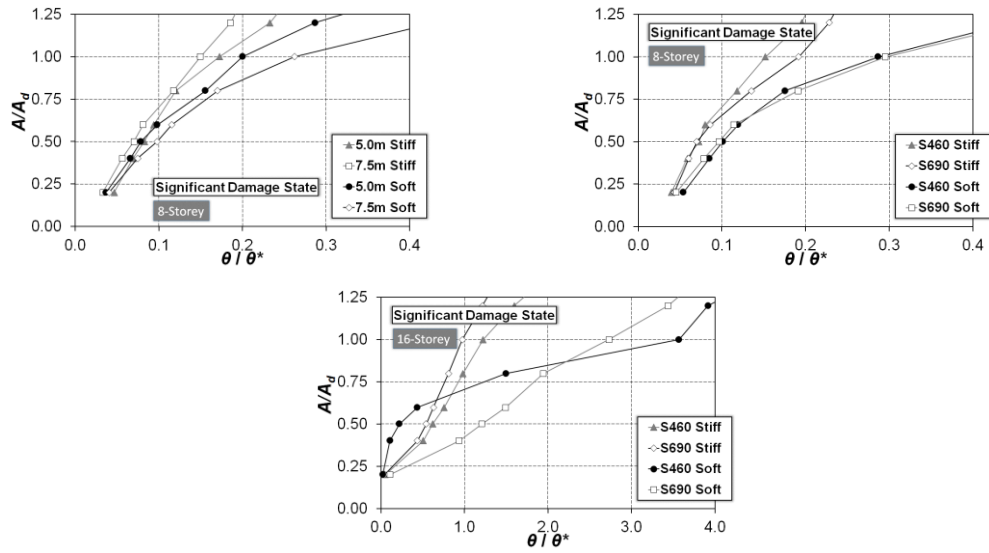
In general, the eight-storey frames provide an adequate performance with values below the proposed limit for the three limit states. However, the taller frames have beams where the demand is of major capacity. Indeed, this result was expected due to the high demand observed in previous chapters. It is clear to see that the high damage concentrated on a specify zone affects the local behaviour of the structural elements causing large deformation. Overall, the SD limit states are more stringent in comparison with DL and NC limit states for the taller frames; however, the DL limit state gives the major ratios.

Evaluating the investigated parameters, it can be observed that, once again, the soil condition influences the seismic behaviour of the frames. The frames designed considering a soft soil condition experience larger beam ductility demand. It is worth to notice that due to a high design load caused by a design spectrum, stiffer structures were created, and consequently, braces with larger size.

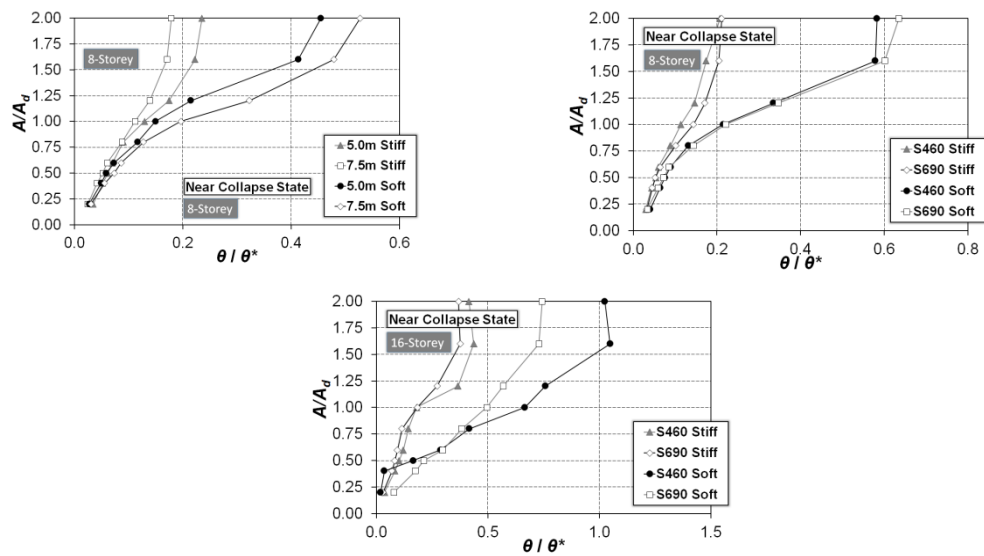
This observation about soft soil becomes very important because the beams from the MRF parts are larger and stronger (remembering that the seismic design of these structural elements depend on the brace strength of the brace on each floor), therefore, the flexural demand provided by records plays an important role in seismic performance, again.



a) Damage Limitation State



b) Significant Damage State



c) Near Collapse State

Figure 7.11 – Beam ductility demand from MRF part of the D-CBFs for the three states

It is important to point out that the increase of the HSS steel grade is beneficial only for the taller frames, because there is no appreciable difference between the two HSS steel grades for the eight-storey frames. Regarding to length span, the distinctions are observed only for the soft soil condition where an increasing of the beam ductility demand for the frames with longer span is of 26%.

Although the frames with shorter frames have presented larger inter-storey drift, both transient and residual, the frames with 7.5m experience higher beam ductility demand. This observation is attributed to length span where the smaller span results in stiffer beam.

Table 7.6 – Maximum value of beam ductility demand from MRF part of the D-CBFs

Percentiles at each limit state	8-Storey				16-Storey	
	5.0 m		7.5 m		7.5 m	
	Stiff soil	Soft soil	Stiff soil	Soft soil	Stiff soil	Soft soil
DL	0.49	0.47	0.42	0.60	0.62	0.34
S460 SD	0.17	0.20	0.15	0.29	1.22	3.56
NC	0.20	0.43	0.17	0.58	0.43	1.04
DL	-	-	0.42	0.57	0.48	1.33
S690 SD	-	-	0.19	0.29	0.97	2.72
NC	-	-	0.21	0.61	0.37	0.73

### 7.3 Behaviour factors

Within this section, the behaviour factor using the two different methods has been evaluated. The effects of the soil condition, HSS steel grade and span length on the behaviour factor in the examined cases are emphasized herein. Analogous to CBFs, a behaviour factor equal to 1.0 is imposed due to criterion previously defined by EN1998-1-3 (2005).

In general terms, the following plots show that the behaviour factor delivered by both approaches is smaller than those assumed in the seismic design, mainly for the European approach. In particular, it is worth noticed that the European approach gives behaviour factors equal to 2.61 for stiff soil and 2.12 for frames in soft soil analysing the SD limit state. On the other hand, Salvitti and Elnashai method delivers larger behaviour factor in comparison with the former being 3.03 and 2.74 for stiff and soft soil condition, respectively. With these values, it is notorious to understand that a recalibration of the values given in EN1998-1-1 (2004) is required, taking into account the limit imposed by EN1998-1-3 (2005). Furthermore, the brace ductility demand was responsible by smaller behaviour factor for both methodologies.

### 7.3.1 *Influence of soil condition*

Comparing the two soil types investigated, Figure 7.12 depicts the outcomes for both approaches where the soft soil condition is responsible by smaller values. In particular, the frames located in soft soil condition present a reduction of 23% for the European approach, and an reduction of 10% is observed by Salvitti and Elnashai method in the SD limit states. In case the of NC limit state, the reduction is more pronounced for the European method with values around 31% and there are no appreciable differences for the second method with a similar reduction of 9%. This larger distinction between the two soil types is attributed mainly to overstrength factor from pushover analyses and to large ductility demand. In the section regarding the outcomes related to the overstrength factors, it is shown that the frames designed considering a soft soil condition present lower overstrength factors and this parameter plays an important role in determining the behaviour factor for the European approach. As also observed for the CBFs, the difference is smaller for the SD limit state indicating that for low damage levels, the influence of soil condition is not relevant especially for what concerns the European approach.

In detail for the SD limit state, the European approach delivers a median of 2.61 for the stiff soil and 2.12 for the soft soil condition. These values are not close to the value employed on the seismic design, namely 4.8. This shows that the seismic performance of the study cases is not adequate and does not fulfil the criteria established for what concerns the ductility demand. The approach presented by Salvitti and Elnashai method shows an increase in the behaviour factor in comparison with the former, however, the values found do not reach the behaviour factor assumed on the seismic design. In particular, a value of 3.03 for stiff soil and 2.74 for soft soil condition is observed. This aspect is related to the needlessness to have an overstrength factor in the formulation, so that the method of Salvitti and Elnashai method can become a method that is less sensitive to the variation of the soil condition.

Concerning NC limit state, Salvitti and Elnashai approach exhibits values of 2.27 and 2.07 for both stiff and soft soil condition, respectively. As it can be observed, there is a reduction when comparing these values with the ones obtained from the SD limit state. This means that the frames are closer to match the limit imposed upon SD than those assumed for the NC limit state are. The enlargement of limit imposed on NC limit state is not proportional to higher of the failure criterion.

In contrast, the European approach delivers larger values where 3.21 and 2.45 are seen for the stiff and soft soil conditions, respectively. Indeed, the overstrength factor and acceleration are constant in the European method and there is only an enlargement of the

limit imposed on the NC limit state resulting in increased values. In general, the values for the NC limit state are also not close those assumed on the seismic design.

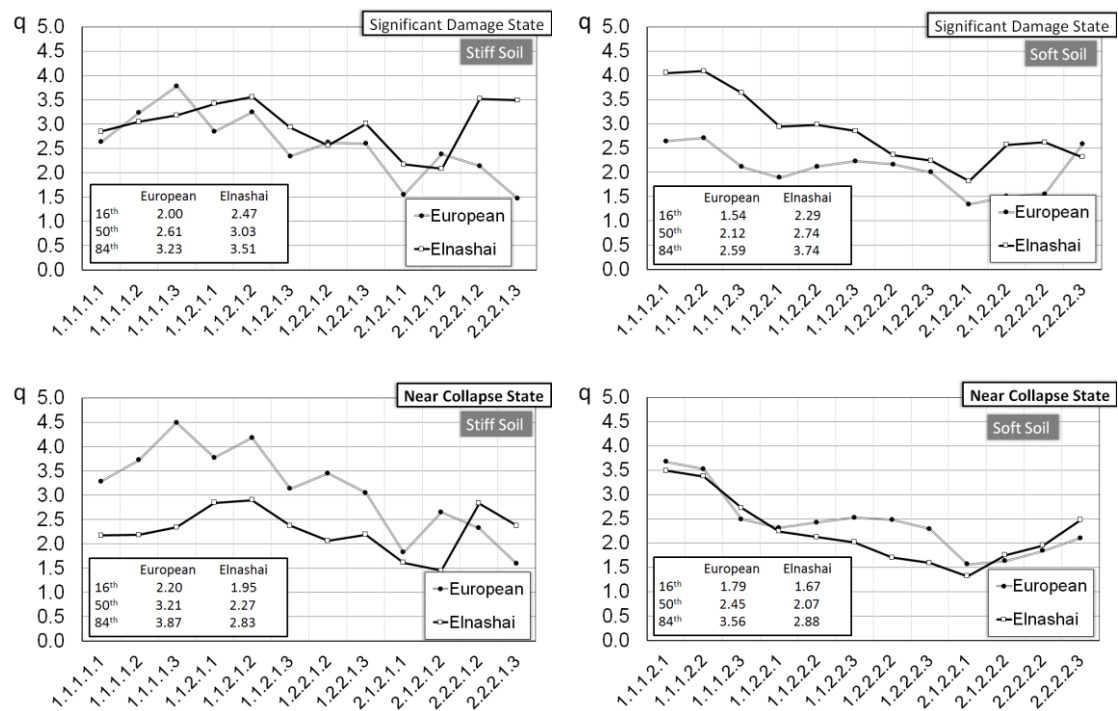


Figure 7.12 – Comparison of behaviour factors for soil type

### 7.3.2 Influence of span length

The span length plays an important role in the seismic performance of the D-CBFs, and consequently, has some influence on the behaviour factors for both methodologies examined. The curves plotted in Figure 7.13 highlight the behaviour factor median according to the two different span length. The frames with shorter frames have behaviour factors with median of 2.68 for the European approach and 3.41 for Salvitti and Elnashai method, while the other frames exhibits values around 2.29 and 2.96 considering the SD limit state as reference.

Indeed, the flexural stiffness of the beams from braced bay is a key parameter because the stiffer beams provide lower axial deformation in braces. This issue has been recently investigated in (Tenchini et al., 2013). In contrast to this larger behaviour factors, it was also seen in the section regarding the brace ductility demand that the frames with 7.5m of span present smaller ratio in comparison with the shorter length span frames due to their oversize. Although it seems to be a nonsense, this result can be explained through a performance to be investigated in a specific value of acceleration, on the other hand, behaviour factor is determined when the building achieves the failure criterion assumed to characterize the limit state.

For the NC limit state, behaviour factors equal to 3.60 and 2.83 are observed for the European approach in both stiff and soft soil conditions, respectively, and for other methods, the values are 2.53 and 2.31. Once again, the second approach presents values that are lower for the NC limit state than for the SD limit state. In general, the frames with length span of 5.0m are responsible for major behaviour factor, and consequently, are closer to value assumed in seismic design.

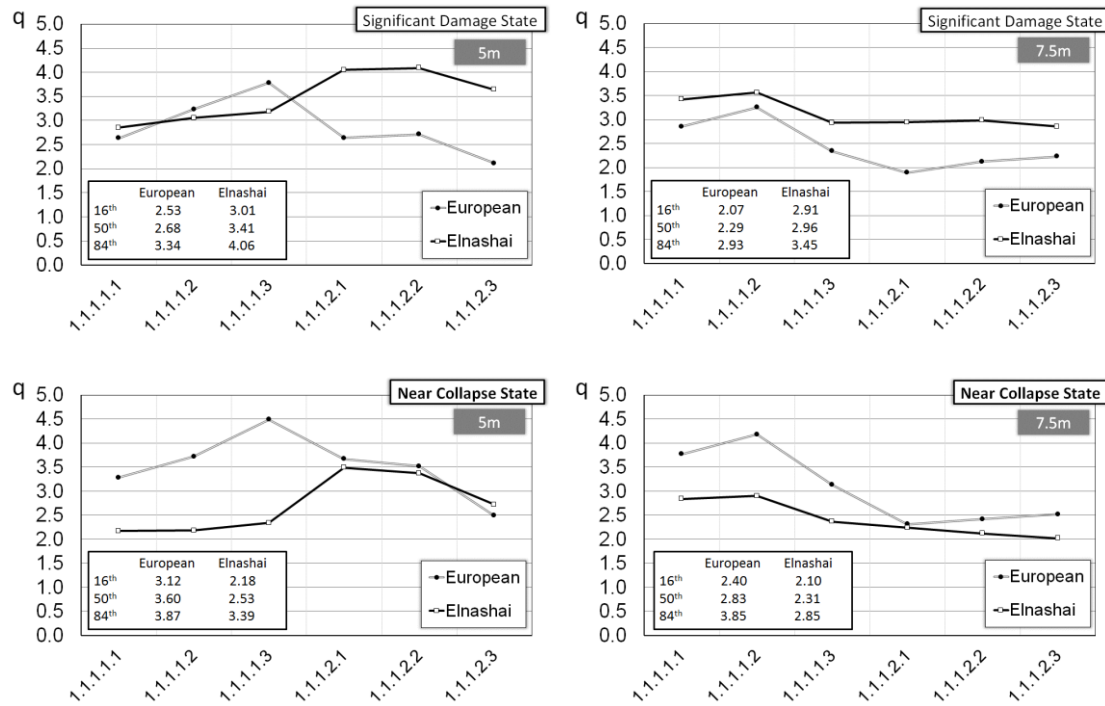


Figure 7.13 – Comparison of behaviour factors for pan length

### 7.3.3 Influence of HSS steel grade

Some differences can be recognized comparing the frames designed with S460 or S690. The frames using S460 in their non-dissipative member show lower median of behaviour factor for the seven records in comparison with the frames designed with S690. This difference is shown in Figure 7.14. This fact can once again be attributed to flexural stiffness of the beam from braced bay. Indeed, this structural members have been designed with the same steel grade of the non-dissipative member. This solution results in minor cross-section because the steel resistance is increased resulting in section with smaller flexural stiffness. On the other hand, this solution also results in smaller formation of plastic hinge on the beam from braced bay.

In particular, the European approach delivers behaviour factors equal to 2.29 and 2.59 for the frames using S460 in SD and NC limit state, respectively. For the cases with S690, there is a reduction of 6% and 7%. It is interesting to notice that the frames with S690 present larger overstrength factor, thus the issue regarding the flexural stiffness becomes more

important for the European approach where the frames with major overstrength factor still result in lower behaviour factors.

According to results found in Salvitti and Elnashai method, the difference between the two steel grade is more pronounced for the SD limit state with value of 11% while a small difference of 3% is identified for the NC limit state. This fact is justified by a small behaviour factor from taller frames in comparison with the frames with eight-storey frames

As a whole, both methods deliver q-factors lower than the value used in seismic design independently of the steel grade. Once more, Salvitti and Elnashai approach show a decreasing for NC limit state in comparison with DL limit state and there is an increase of behaviour factors when using the other method.

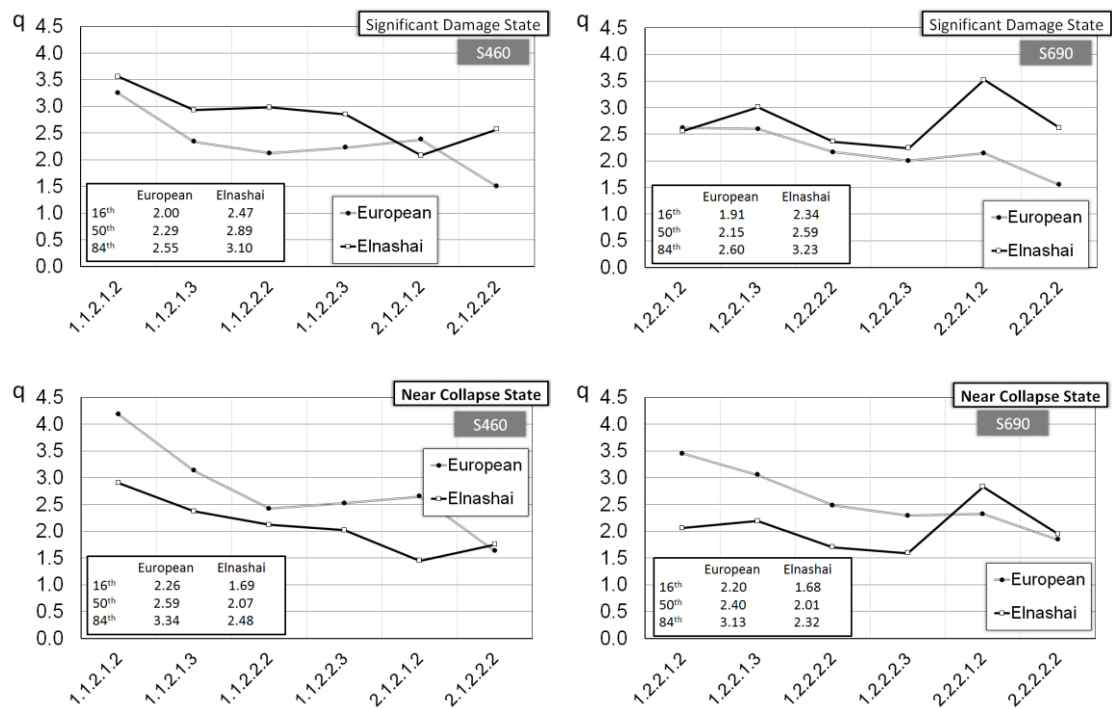


Figure 7.14 – Comparison of behaviour factors for steel grade

#### 7.3.4 Influence of number of storey

Figure 7.15 depicts the median values of the behaviour factors comparing the number of storey. In these plots, it can be recognized some difference where the taller frames are responsible by smaller behaviour for both methods. In particular, the Salvitti & Elnashai approach deliver the larger value in comparison with another except for the NC limit state of the eight-storey frames.

As seen in the pushover results, the sudden reduction in lateral resistance is more detrimental for the taller where lower overstrength factor is observed. Therefore, the smaller behaviour factors deliver by European approach is justified by the lower overstrength factor from the



taller frames. This trend is also observed for the Salvitti & Elnashai approach. This results is contrary to what was observed for the CBF where the taller frames present higher behaviour factor for the Salvitti & Elnashai approach. This fact can be explained due to high flexibility of the D-CBF due to use of high behaviour factor. In addition, the taller frames present poorer seismic performance where, basically, the MRFs subsystem is not nearly triggered. Therefore, the large axial deformation demand is observed for the taller frames in comparison with eight-storey frames.

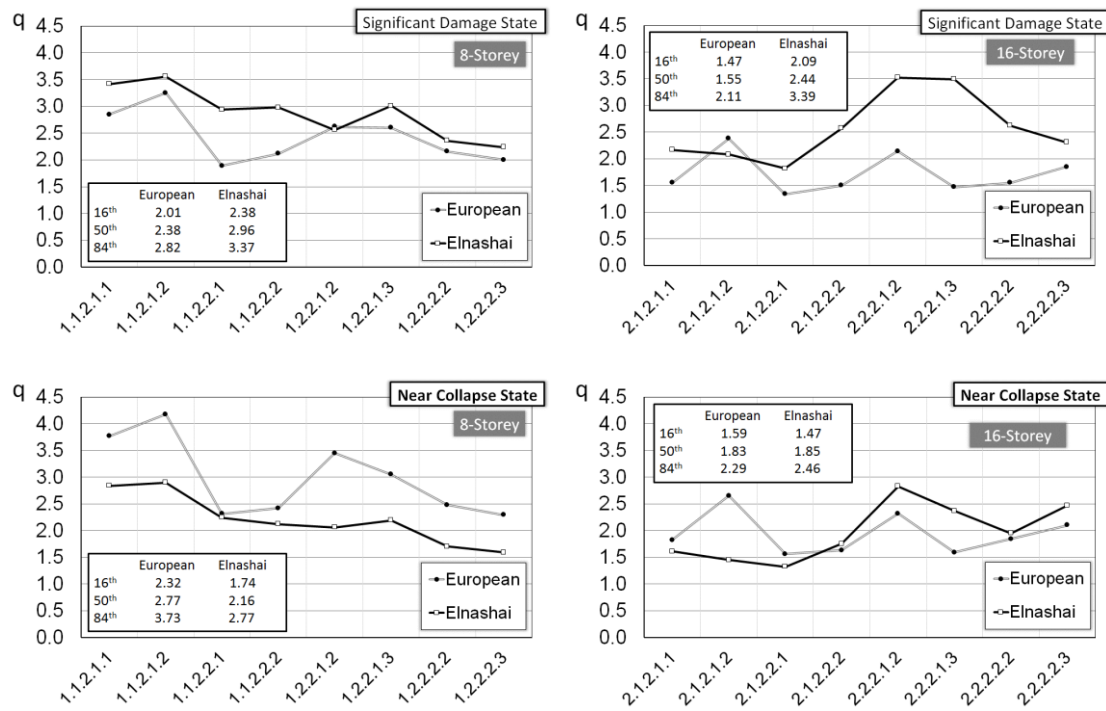


Figure 7.15 – Comparing the behaviour factors concerning to number of storey

## 7.4 Material consumption

As previously stated, the material consumption has been evaluated in this work for the investigated study cases using the Equation (5.2) in order to obtain the material density. Thus, the steel consumption is computed in terms of total weight while the concrete is given in terms of the total cast volume.

Figure 7.16 illustrates the material consumption performing a comparison between the two soil types. It is interesting to notice that the frames located on soft soil condition exhibit larger material densities taken into account the amount of steel, concrete and reinforcement. Once again, the enlargement of the corner  $T_c$  is an important factor in order to obtain heavier structures because the PGA for both soil types is the same ( $a_g = 0.32g$ ). Indeed, depending on the fundamental period of the structure, the base shear to be considered on the seismic design is superior for the cases in region with soft soil. The high base shear provided by design spectrum allowed reducing the overstrength used on determining the

load for the non-dissipative structural members; in contrast, it is not possible to decrease the material consumption. Furthermore, Figure 7.16 also reveals that the influence of the structural members made with HSS is smaller than the ones with MCS. This increased contribution certainly affects the final cost of the building when there is a comparison with a conventional solution, i.e., the whole structure designed with MCS.

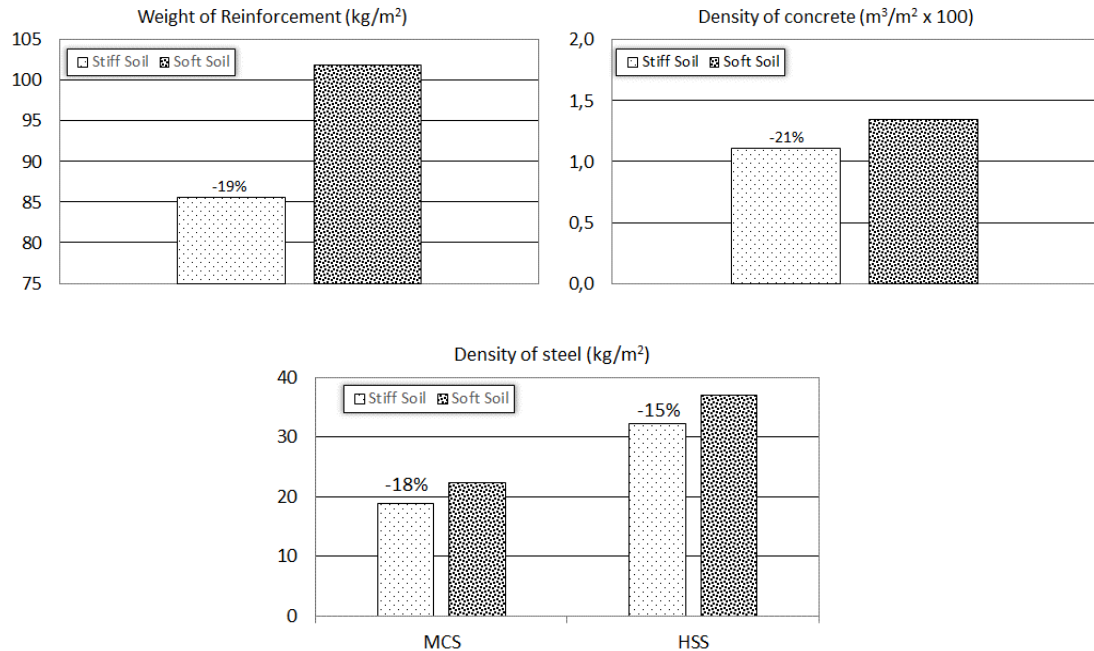


Figure 7.16 – Average of amount of steel, concrete and reinforcement

In Figure 7.17, the focus is given for the dependency of the steel grade used on the non-dissipative structural members. In detail, the use of superior steel grade provides a reduction of the steel density. This result is expected because the seismic design of D-CBFs was governed by resistance expect by some cases in which the upper columns were chosen in order to have realistic building with workable connections. On the other hand, the increase of the steel grade is not as sensitive for the cases on soft soil condition in which large base shear are developed, increasing the need for resistance: However, the cases where geometrical restriction are observed, there is an increase of the material consumption, mainly for the cases on stiff soil. Furthermore, it is noticed that there is no difference on the amount of MCS steel grade. Indeed, the contribution of the braces and beams on the steel density for both steel grades is not significant in comparison with the elements with HSS. In other words, the cross-sections are similar and the gain is attributed to non-dissipative structural members.

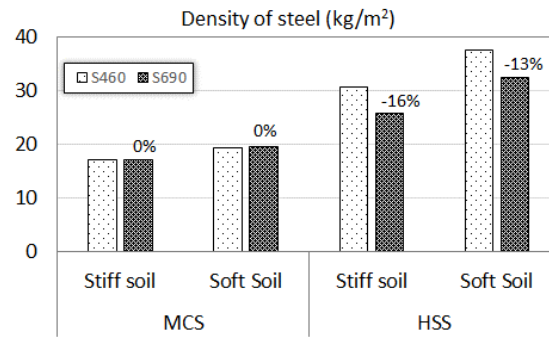


Figure 7.17 – Comparison between the HSS steel grades

The steel density highlighting the influence of number of storey is revealed by Figure 7.18. This figure shows that the larger steel density is visualized for the taller frames. This increase is sharp for the soft soil condition where the major base shear is observed due to factors already mentioned. The result presented in this plot is attributed to higher fundamental period from sixteen-storey that results in smaller seismic action. This aspect was also observed in the CBFs.

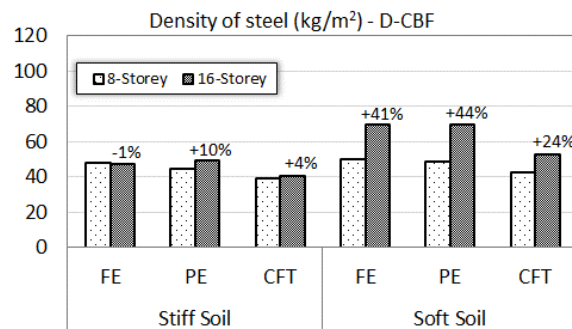


Figure 7.18 – Comparison of material consumption and number of storey

Analysing the type of composite steel-concrete column used in Figure 7.19, it is interesting to mention that the CFT column is the most efficient solution in terms of overall weight of the building. In fact, due to its geometric shape, it is possible to have a same level of resistance but with a reserve of the steel density. In contrast, the PE column is responsible for greater steel density due to the higher contribution of the concrete given by the FE column.

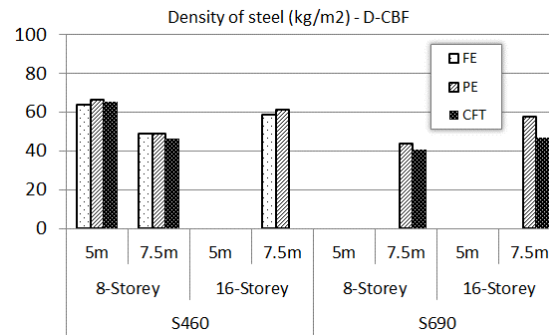


Figure 7.19 – Influence of the composite steel-concrete column

According to Figure 7.20 and Table 7.7, the steel densities highlighting the influence of span length is indicated. As it was also seen for the CBFs, the frames with shorter span show higher density regardless of soil type adopted. Once again, it is justified by the increase of the area, that is not proportional to steel density.

Table 7.7 – The steel weight (kg) for the frames with 5.0m and 7.5m of span

Span	Stiff soil			Soft soil		
	Column	Beam	Brace	Column	Beam	Brace
5m	9900	24478	1865	13287	27394	2307
7.5m	18947	41722	2927	20146	43162	3439
$\Delta$ (%)	191	170	157	152	158	149

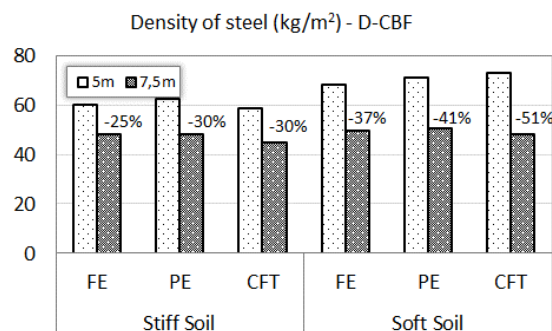


Figure 7.20 – Influence of the length span on the steel density

### 7.5 Comparison between the Dual and Simple Concentrically Braced Dual-Steel Frames

The comparison between the two braced systems investigated, namely the D-CBFs and CBFs, is now presented. In particular, the outcomes concerning the CBFs are stated in Chapter VI. The assessment is based in the seismic performance of the study cases

comparing the outcomes obtained from dynamic nonlinear analyses giving focus on: peak inter-storey drift ratios, residual inter-storey drift ratios, peak storey acceleration and brace ductility demand. Furthermore, the analyses addresses results evaluating the capacity curves, damage distribution, material consumption as well as the overstrength factors.

#### 7.5.1 Analysing of the results from Pushover analyses

Figure 7.21 reveals some plots concerning the normalized pushover capacity curves from both CBFs and D-CBFs outcomes. In this figure, it can be pointed out that after the first nonlinear event, both structural systems present a sudden reduction of the lateral resistance. This fact is attributed to buckling effect of the braces in compression where there is a reduction of the lateral stiffness of the building after this phenomenon. Moreover, the first plastic event occurs for a similar roof displacement. On the other hand, the normalized base shear in this point is different comparing both structural types.

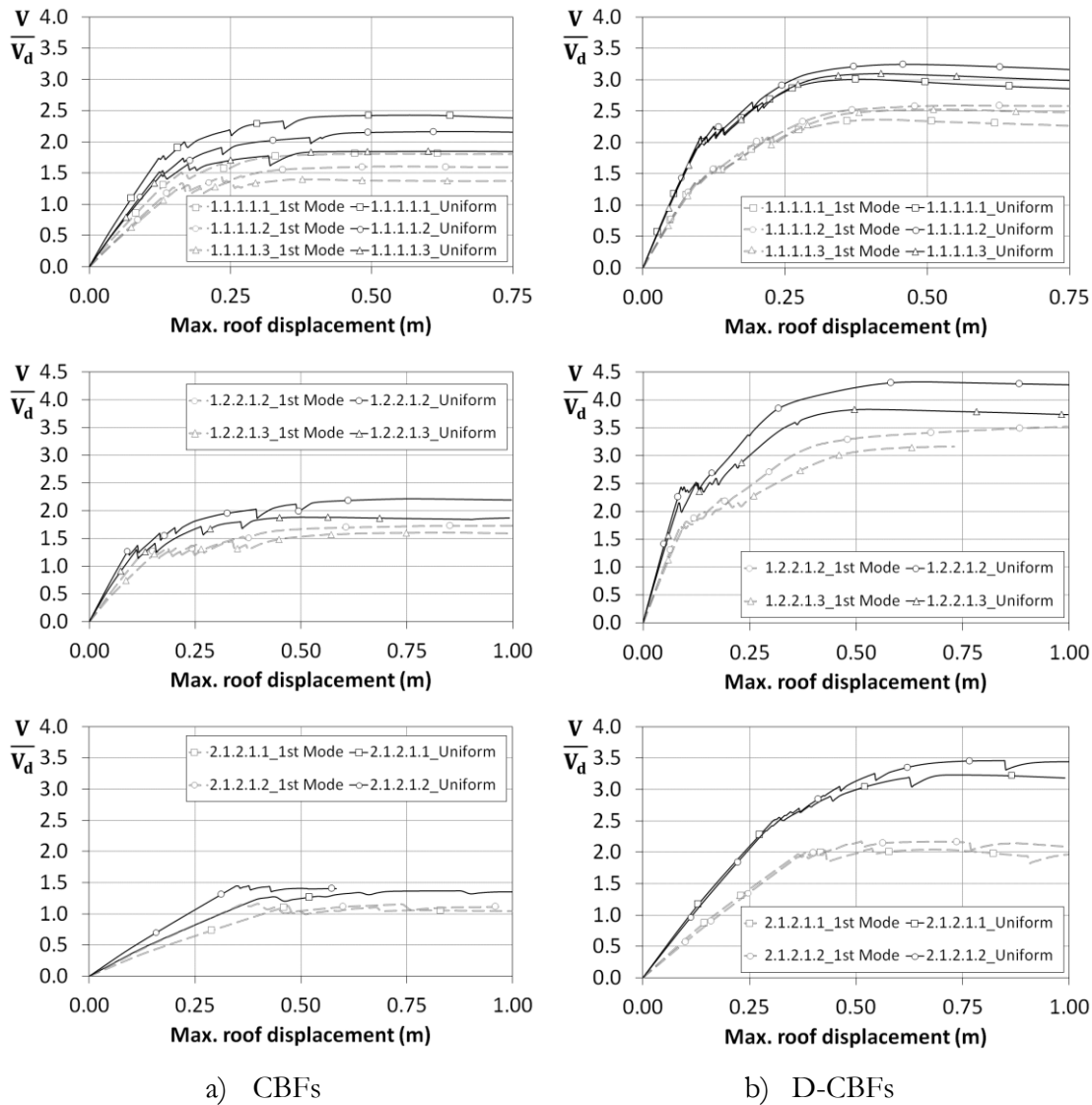


Figure 7.21 – Comparing the normalized pushover response curves

It is noticed that the plots of this figure show that the D-CBFs exhibit higher base shear ratios compared to CBFs. This result is related to fact that the D-CBFs have a subsystem, namely the MRF system, that provides an redundancy level in the entire system: Indeed, the D-CBFs can still have a overstrength after the collapse of the braced system that shows an increase around 60% while the CBFs disclose a value of 25%.

This fact has been observed after the last earthquakes where buildings with a structural system consisting of braced framing survived the earthquake motion, because the connections were rigidly connected and thus the damaged structure behaved as a moment-resisting structure without the braces (Iyama and Kuwamura, 1999). This observation justifies the small increase of the lateral resistance derived from the CBFs.

The redundancy from the D-CBFs consequently influences the overstrength factors. A summary of the results obtained from the pushover analyses is presented in Figure 7.22 and Figure 7.23. Indeed, the dual-system are responsible for larger overstrength factors analysing the three terms:  $\Omega_1$ ,  $\Omega_2$  and  $\Omega$  factors.

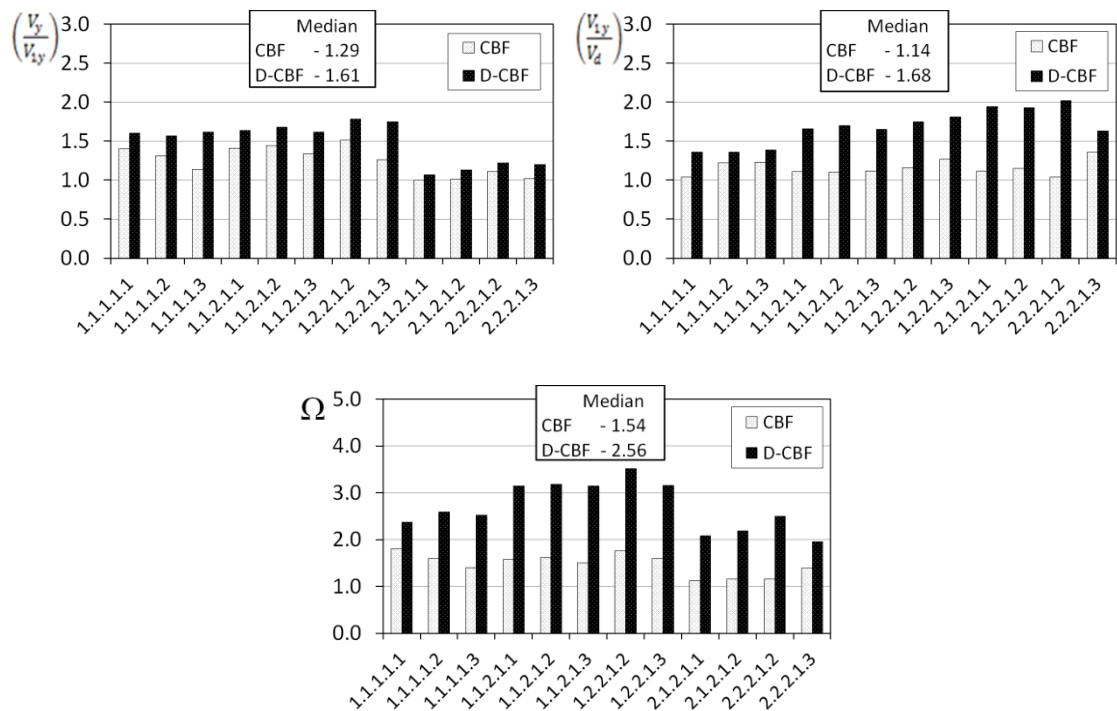


Figure 7.22 – Comparing the overstrength factors for stiff soil condition

For the frames located in stiff soil, the D-CBFs present an increasing of 25%, 47% and 66% for the  $\Omega_1$ ,  $\Omega_2$  and  $\Omega$  factors, respectively. The main aspect to be underlined is the difference obtained for the overstrength factor related to structural optimization state the need to assess the decisions taken in order to perform the seismic design among the behaviour factor. This is an important topic for future works in order to evaluate the seismic behaviour of the D-CBFs with smaller behaviour factors.

When it comes to frames in soft soil condition, it is observed a difference around 15%, 35% and 59% for the following overstrength factors:  $\Omega_1$ ,  $\Omega_2$  and  $\Omega$ . Giving once again focus on the  $\Omega_2$  factor, there is slight reduction of the difference between two typologies. The high base shear from design spectrum results in lower dependency of the slenderness braces on the seismic design. Hence, it makes sense to use a small behaviour factor in order to decrease this parameter.

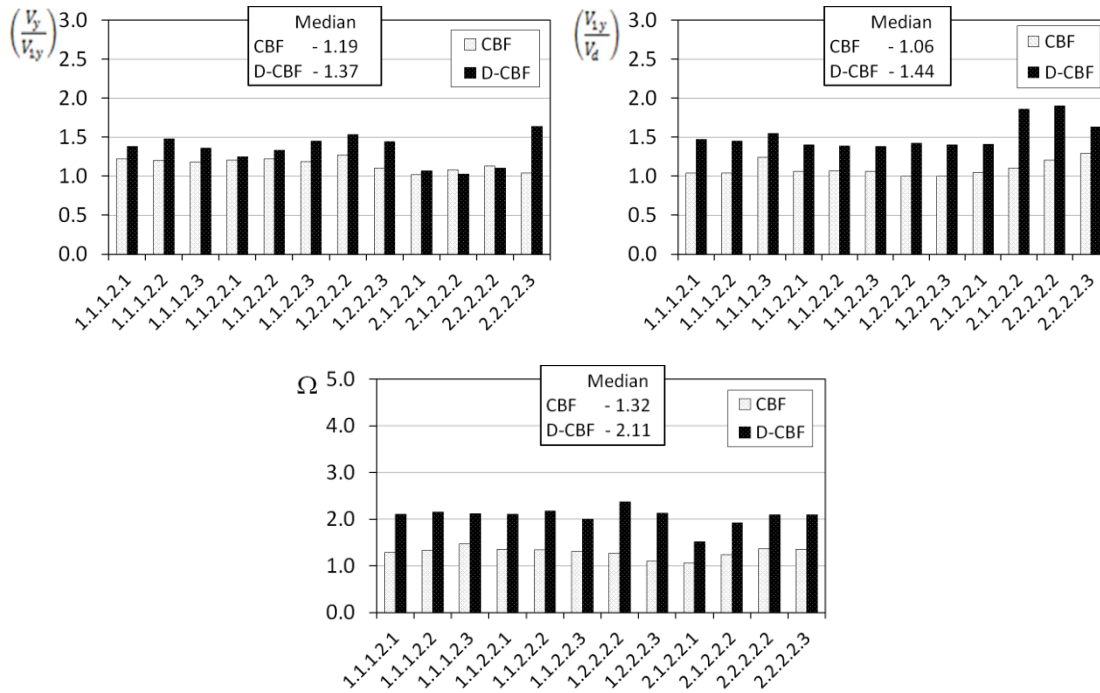


Figure 7.23 – Comparing the overstrength factors for soft soil condition

On the basis of the damage distribution illustrated by Figure 7.24, it is clear to verify beyond yielding of the braces, the dual-system experiences plastic hinges end beam from the subsystem. For both systems, the braces in compression are the first structural members to have the formation of plastic hinges. As feature of the dual-system, after the buckling of braces in compression, the beam outside the braced bay may be the elements where plastic hinges will be formed or the tensioned braces take their place. On the other hand, there is no possibility to have another structural member in order to be responsible for inelastic deformation, but the braces in tension, excluding the beams from braced bay. In the other words, there is the contribution of the beams from subsystem on the energy dissipation when a moderate earthquake reaches the frames.

Another important observation concerns the yielding of the beams from braced bay. This issue has already been raised in a previous section in which EN1998-1-1 (2004) is not safe enough to ensure that there is no plastic formation in this beams. However, a small number of cases with plastic hinges in these structural members is observed for the D-CBFs. In fact,

with the introduction of the beam from MRFs part in energy dissipation, the D-CBFs have more appropriate redistribution of the load after the first plastic event in comparison with the CBFs.

The general point of view, the two structural system show a poor distribution of damage where large damage concentration is located in mid-rise of the buildings, being, therefore, prone to soft storey mechanism. Notwithstanding, this behaviour is recognized by structures of this kind.

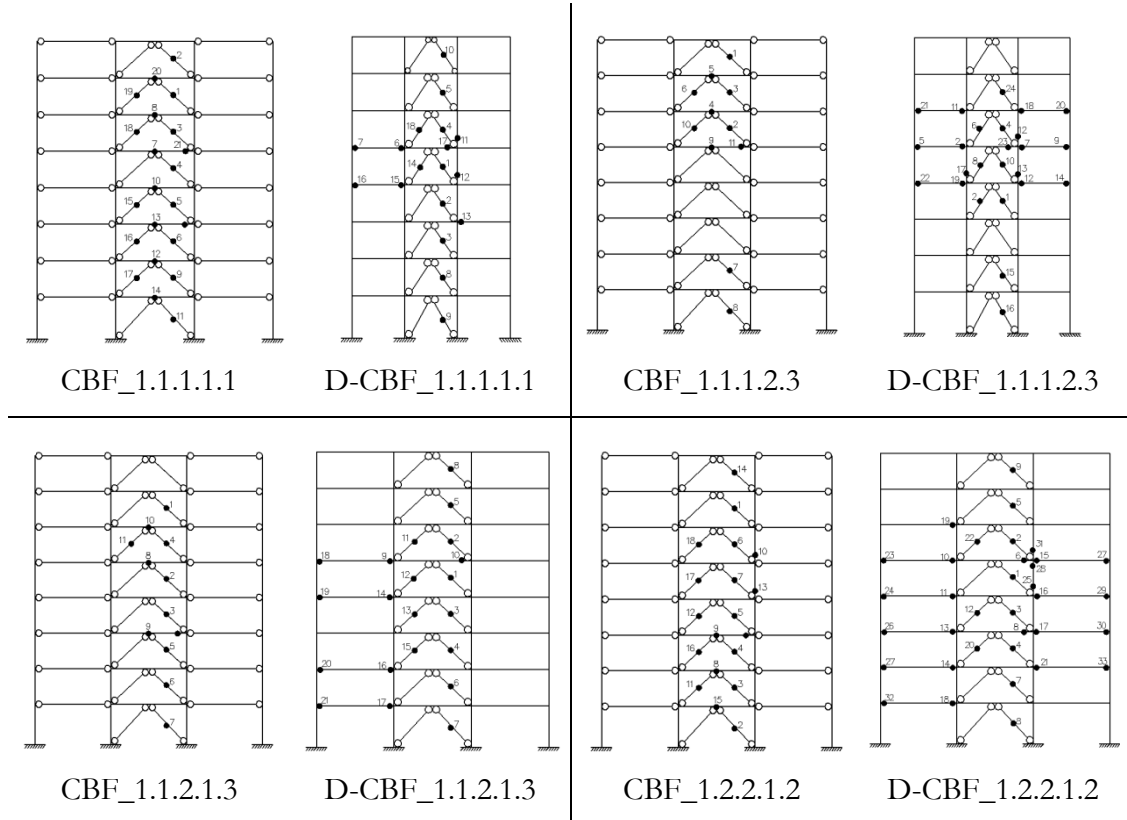


Figure 7.24 – Examples of damage distribution for the two systems

### 7.5.2 Evaluation of the dynamic response

The influence of structural system on the seismic performance is presented in Figure 7.25. In this figure, the values shown correspond to median obtained from all the study case by separating the plot according to the soil type assumed. Visual inspection of the this figure indicates that the D-CBFs experience larger PIDRs, RIDRs and brace ductility demand. This outcome was expected due to high flexibility of the D-CBFs.

It is worth to notice that the dual-system has been designed considering a higher capacity of energy dissipation. Therefore, the frames with dual-system have been designed for a behaviour factor equal to 4.8 while the simple system has been assumed a value of 2.5. This difference makes the frames lighter because the design base shear is lower. Moreover, there is a larger seismic demand, either global or local, for a same seismic intensity.



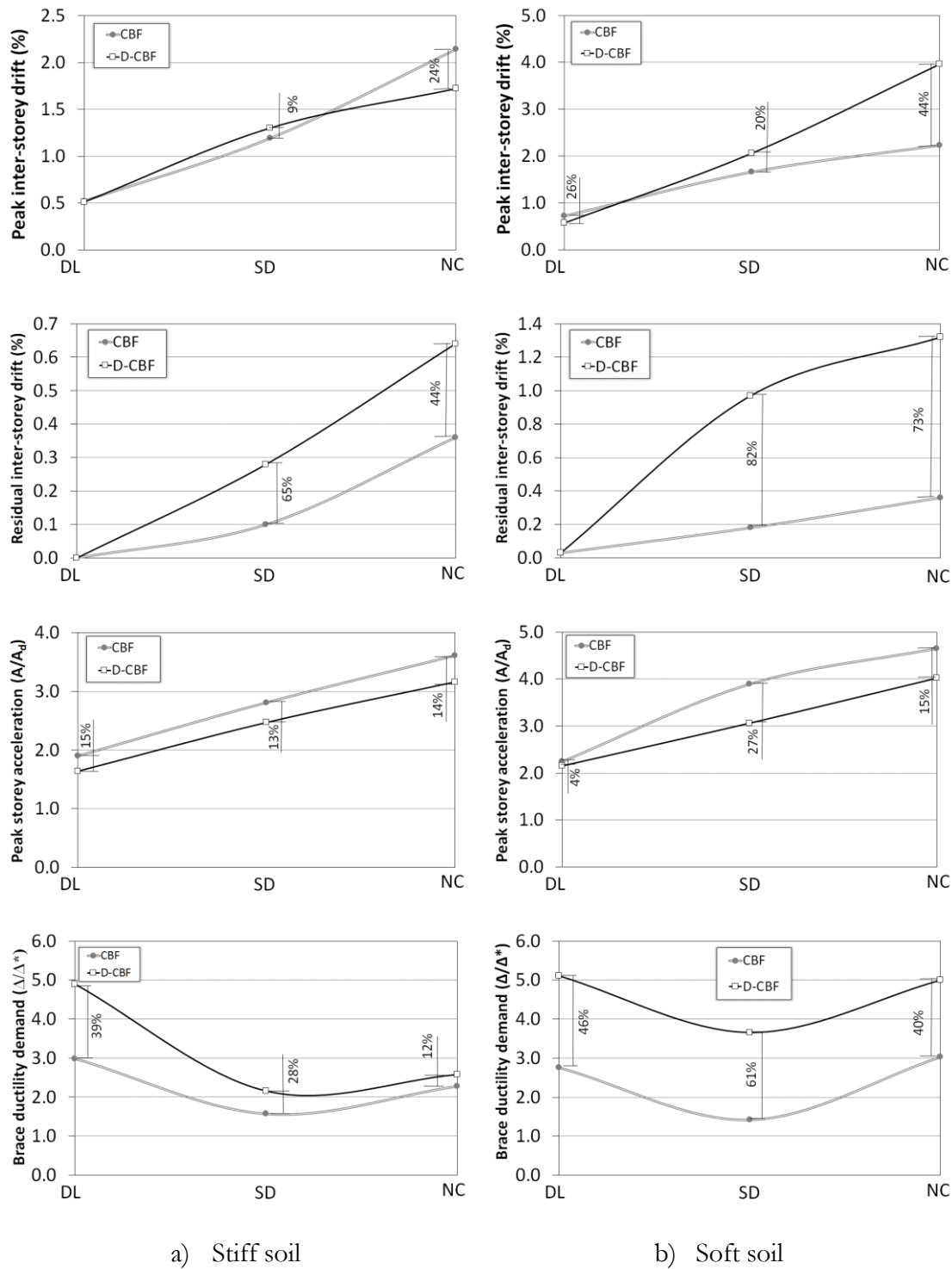


Figure 7.25 – Seismic performance of both CBFs and D-CBFs

Furthermore, this distinction of the two structural systems is more notorious for the soft soil condition. Indeed, most of the frames located in soft soil condition are in constant acceleration range resulting in larger demand in comparison with the frames in stiff soil.

In contrast, the storey acceleration amplitudes are lower for the D-CBFs. As previously stated, it is recognized that the PSA is related to damage of the non-structural elements. Therefore, with this outcome it can be concluded that while the global and local deformation

are larger for the cases with dual-system, the damage non-structural of the buildings are smaller. This issue plays an important role when an economical assessment is performed taken into account the cost related to non-structural members. Thus, this is another important topic to be studied in future works.

### 7.5.3 Behaviour factors

Although the simple system provides more appropriate seismic behaviour in terms of global and local deformation, the dual-system shows a higher energy dissipation capacity in comparison with the former. Figure 7.26 and Figure 7.27 illustrate the behaviour factor using the European and Salvitti and Elnashai approaches performing a comparison between the two structural systems.

In fact, both methodologies deliver behaviour factors larger for the study cases with the dual-system. This result may initially seem contradictory but it is not. The larger deformation presented mainly by braces were responsible for determining the maximum acceleration in which the limit proposed by the limit state is achieved.

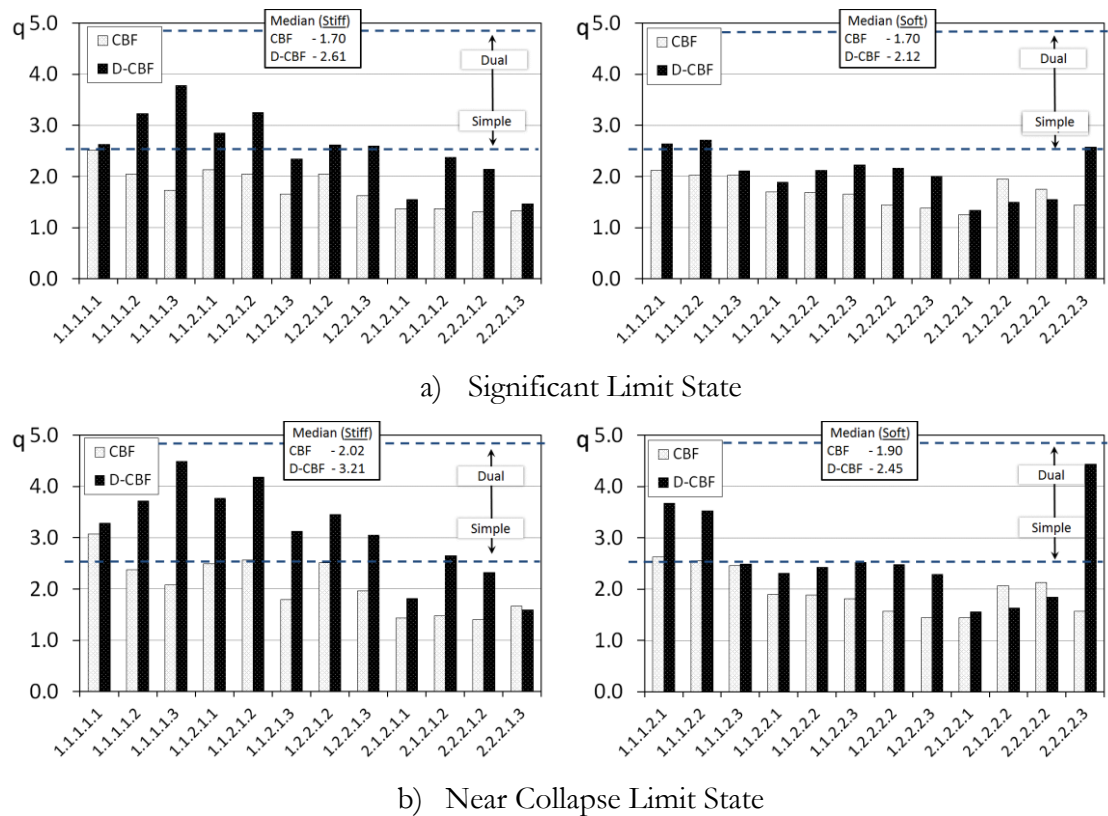


Figure 7.26 – Behaviour factor for both CBFs and D-CBFs using the European approach

This fact can be explained using the formulation of Salvitti and Elnashai approach. Following this expression, the issue is to find the acceleration which the building reaches the limit proposed when other parameters are constant no matter the structural system of

the building. Therefore, when the acceleration of the D-CBFs reach the maximum local deformation, they become higher than those obtained from the CBFs. This observation can conclude that even though the dual-system has higher local deformation due to its redundancy, the frames have a larger capacity to ensure a specific deformation for a given earthquake no collapse.

In terms of differences, there is a reduction of the energy dissipation capacity around 55% for the frames located in stiff soil and 25% for those designed considering a soft soil condition using the European approach. This difference is related to the employment of the overstrength factor used in the formulation of the European approach. Indeed, this parameters plays an important role where the increase of the seismic performance of the building is conditioned to a reduction of its capacity due to the overstrength factor obtained in pushover analyses.

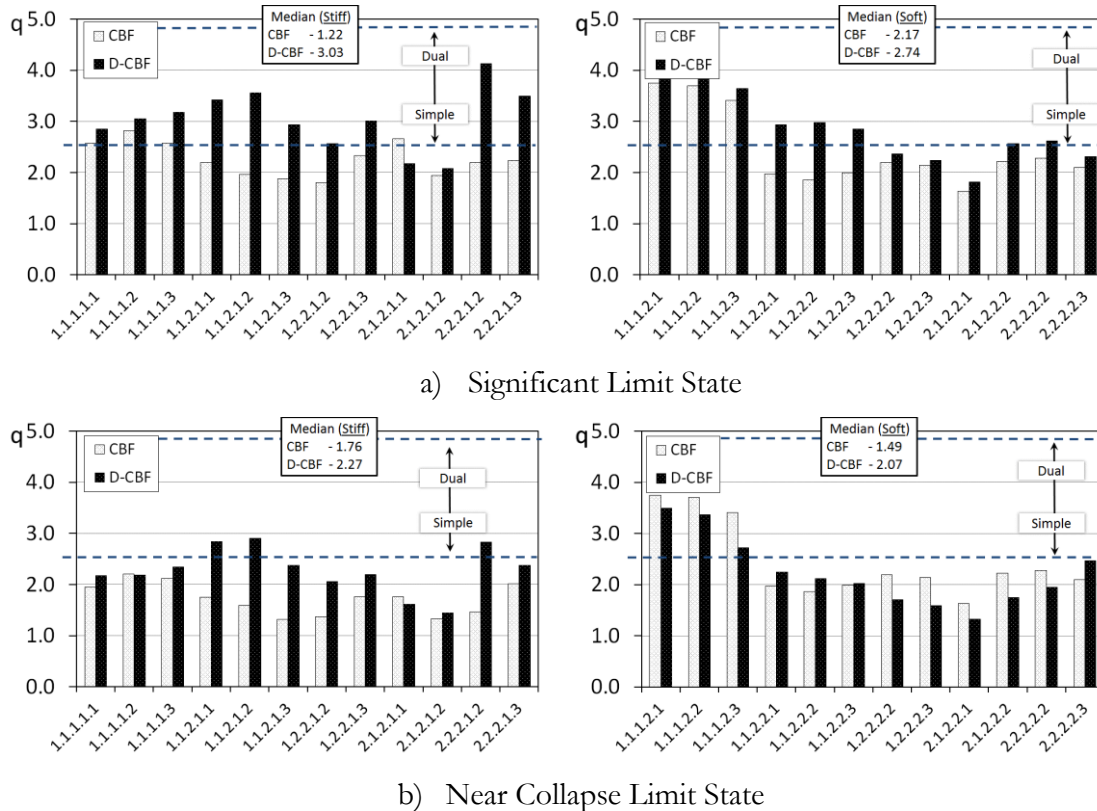


Figure 7.27 – Behaviour factor for both CBFs and D-CBFs using the Salvitti and Elnashai approach

For the Salvitti and Elnashai method, it is possible to observe that for the frames in stiff soil, the behaviour factor from D-CBF corresponds to more than twice of the CBFs for the SD limit state while only an increasing of 28% is seen for the NC one. Considering a soft soil condition as reference, it is worth mentioning that an increasing of 26% is stated for stiff soil and a value of 38% is seen in soft soil.

As previously stated, the plots reveal lower behaviour factor for both approaches compared to that one assumed in the seismic design for both structural systems. This outcomes show a need to verify the behaviour factor incorporated in EN1998-1-1 (2004) for CBF and D-CBF using HSS in the non-dissipative elements.

#### 7.5.4 *Material consumption*

In this subsection, the material consumption has also been compared. It is important to notice that the comparison carried out herein is based only in the amount of material, namely, the steel. It is recognized that the dual-system is composed by rigid connection in MRF part in order to take into account the energy dissipation from end beam. However, comparing with the CBFs, connecting columns and beam rigidly, it is not efficient with respect to construction cost comparing with the pinned connection from the beam without the braced bay of the CBFs.

Figure 7.28 depicts the material consumption for both typologies highlighting the steel density. It is clear to see that the cases with D-CBFs have a lower material consumption in comparison with the CBFs. This outcome was expected because the base shear considered in the seismic design is also lesser for the D-CBFs resulting in lighter structures. In contrast, there are some cases in which this is not true, because the geometric condition is an important factor that influences the amount of material consumption.

In particular, the CBFs in stiff soil present a median of  $58\text{kg/m}^2$  while for the soft soil condition, the value reaches  $75\text{kg/m}^2$ . Analysing the values reported by D-CBFs, it is noticed a median of  $49\text{kg/m}^2$  and  $59\text{kg/m}^2$  for stiff and soft soil condition, respectively. As it can be seen, the difference gains more notoriety for the soft soil. In fact, the use of high behaviour factor provides lower base shear design, and it also results in lighter structures. These light structures have lesser fundamental periods that consequently have smaller base shear design. Summarizing, the small behaviour factor provides lighter structures which in turn have lower fundamental period resulting in lesser base shear design as well. This fact is true when there is no geometrical restriction or slenderness criteria, which may cause an increase in the load to be considered for the non-dissipative members due to increase of the overstrength.

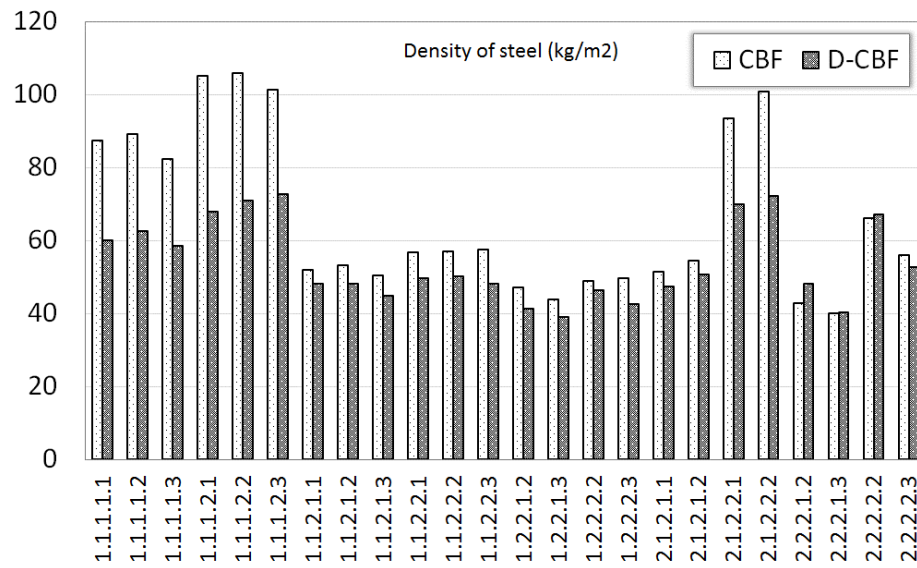


Figure 7.28 – Comparison taking into account the steel consumption

## *Chapter VIII*

# Dual-Steel vs Conventional Frames: Economic and Technical comparative evaluation

This Chapter is devoted to the technical and economic comparison between dual-steel and conventional frames in order to evaluate the efficiency of dual-steel structures. It is selected a set of study cases for each typology examined in this Thesis. In the conventional solution the frames are designed considering the S355 for all the elements. Both solutions have been designed considering the same design assumptions used in the previous chapters. The EN1998-1-1 (2004) is used as reference code in order to perform the seismic design while the AISC-341 (2005) have been used to design the dual-system structures.

For the economical evaluation, the indexes provided in Dubina et al. (2014) have been used. In particular, the indexes provided by STAHLBAU PICHLER SRL have been considered to determine the total cost of the frames taking into account the design, drawings, materials, and production costs. Regarding to concrete cost, the price provided by PREVETON CALCESTRUZZI SPA for a concrete C30/37 has been considered.

### **8.1 Selection of the study cases**

An additional set of three frames representative of MRF, CBF and D-CBF was defined considering steel grade S355, stiff soil condition, 7.5m span length, eight stories, and FE columns for the MRFs while CFT have been selected for the braced frames. This set of parameters was identified as the one that provided lower standardized consumption of material. These frames have been designed considering the same assumptions used for the dual-steel frames, namely those prescribed in EN1998-1-1 (2004) and in AISC-341 (2005) for the minimum resistance of 25% ensured by the MRF subsystem.

Concerning the behaviour factors, 4.0, 2.5 and 4.8 have been assumed for the MRF, CBF and D-CBF, respectively. The same PGA for stiff soil has been considered, namely a value of 0.24g for the MRF and 0.32g for CBF and D-CBF frames.

Figure 8.1 depicts the cross-sections of the both conventional and dual-steel structures for the CBF and D-CBF. For MRF the design with S355 provides the same cross-section as for a solution with S460 since the resistance of the structural elements is not a key design parameter. Therefore, it was concluded that the MRFs using the dual-steel concept are not economically efficient.

Observing Figure 8.1 it is interesting to note that a solution with MCS or HSS deliver the same bracing frames. The only change is related to the columns. In fact, there is no significant changes in the fundamental period of the structures and overstrength factor from the seismic design present slightly differences which the frame with S690 are responsible by larger value. This fact is related to reduction of the overall mass resulting in higher fundamental periods, however, there is an increasing of the overstrength factor because the slenderness of the brace from the last floor influence of the minimum factor.

## 8.2 Comparison in terms of seismic performance

In order to assess the seismic performance of the dual-steel structures comparing with structures using single MCS, dynamic nonlinear analyses have been performed for both solutions keeping the same assumptions and monitoring the same indicators as for Dual-steel frames.

### 8.2.1 *Moment-resisting Frames*

The analyses carried out on the single steel MRFs showed a seismic performance very close to that of dual steel frames in terms of overall displacements. Indeed, the IDR demand of single steel frames is almost equal to that experienced by the relevant dual steel structures at DL, while some slight differences can be recognized at both SD and NC limit states especially for eight-storey frames as depicted in Figure 8.2 where the median IDR demand along the building height is plotted for both dual steel (i.e. tagged as “HSS”) and single steel (i.e. tagged as “MCS”) frames.

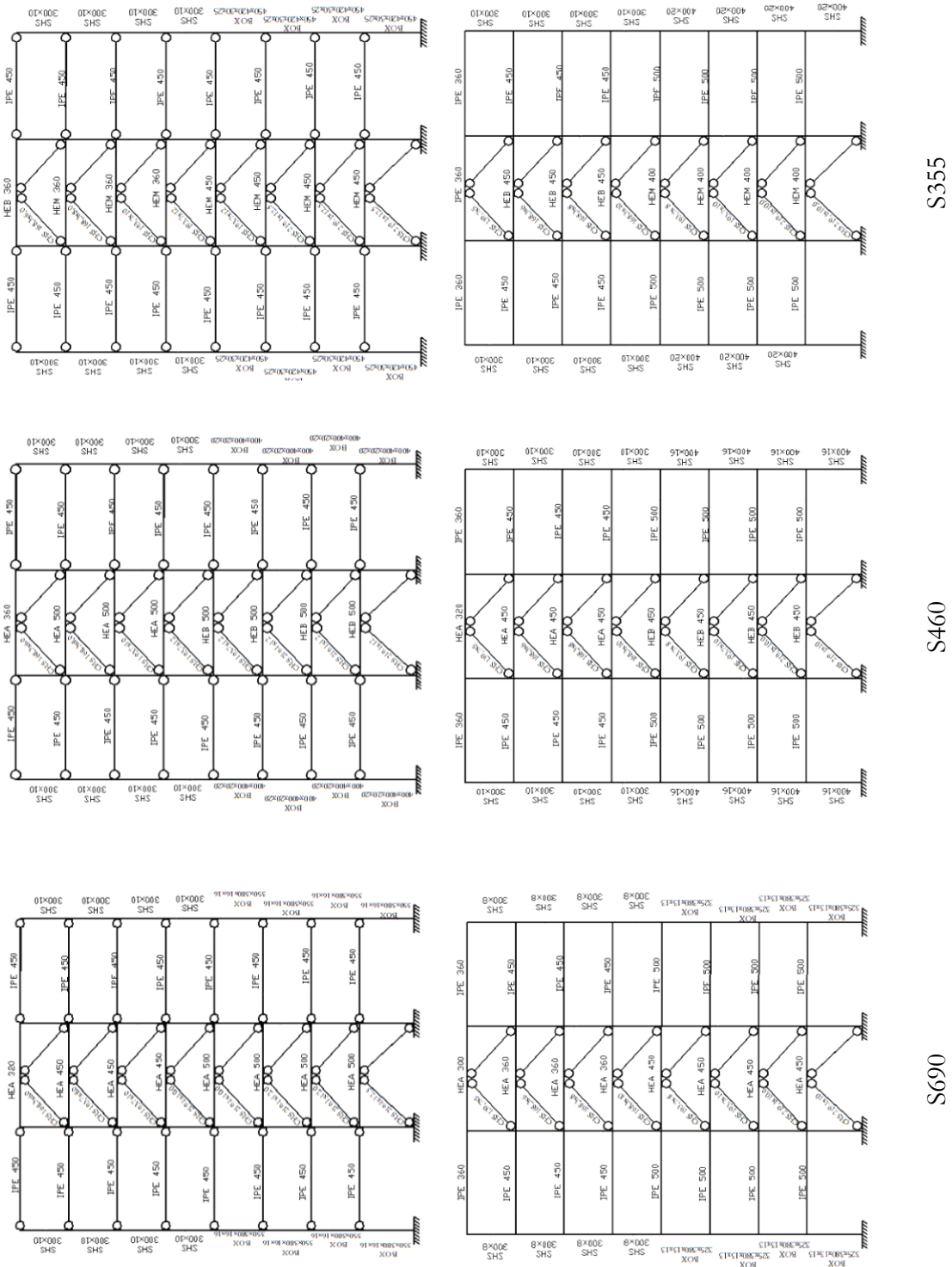


Figure 8.1 – Description of the study cases comparing the conventional structures with dual-steel ones

The comparison at SD shows that the maxima IDRs for single steel frames are larger in comparison with dual-steel structures with a variation equal to 15%. At NC this variation is larger achieving a value of 29%. Such results are mainly due to the different plastic engagement exhibited by single grade frames as compared to dual-steel ones. Indeed, for the



former case moderate plastic deformations can occur in interior columns at building mid-height. The differences enlarge at NC where the plastic deformations in the columns increase. As a consequence, larger RIDRs are observed for single steel frames than for dual steel frames, as illustrated in Figure 8.3.

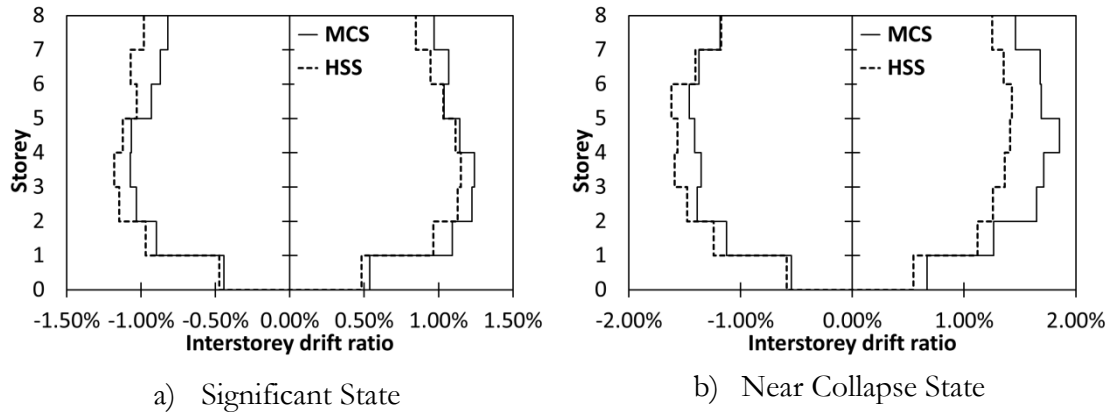


Figure 8.2 – Dual-steel *versus* single steel MRFs: Transient inter-storey drift ratios

In addition, concerning the shear demand in the column web panel it is observed that for single steel frames the additional plates necessary to strengthen the connections should be thicker than the column web thickness, thus theoretically ineffective according to EN1998-1-1 (2004). On the contrary, dual-steel frame do not show this problem. This comparison suggests that dual-steel solution allows controlling better the plastic mechanism, thus avoiding the formation of plastic deformations into the column and minimizing the repairing costs even though the initial constructional prices may be larger than those for the single steel solution. This outcome is not easily predictable, since limited seismic demand was expected for both solutions because of the significant design overstrength resulting from EN1998-1-1 (2004) provisions.

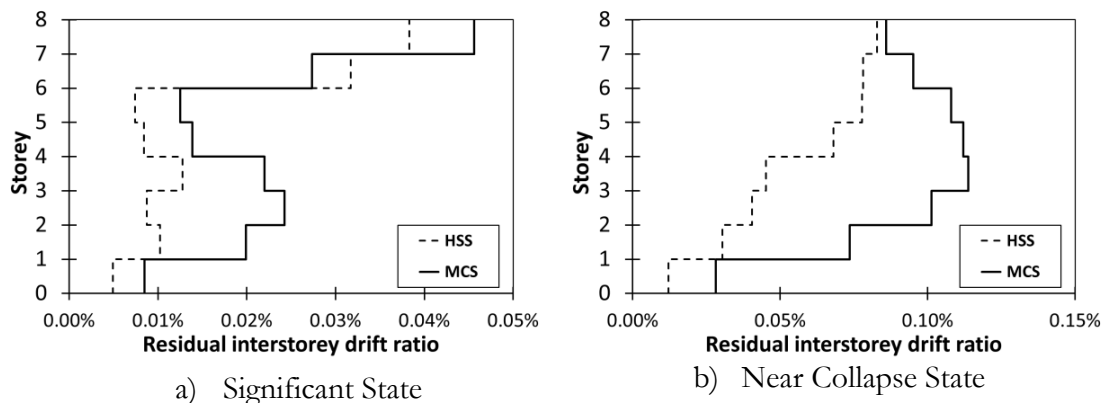


Figure 8.3 – Dual-steel *versus* single steel MRFs: Residual inter-storey drift ratios

### 8.2.2 Concentrically Braced Frames

Figure 8.4 to Figure 8.7 reveal the outcomes from the dynamic nonlinear analyses analysing the three limit states showing the median values obtained.

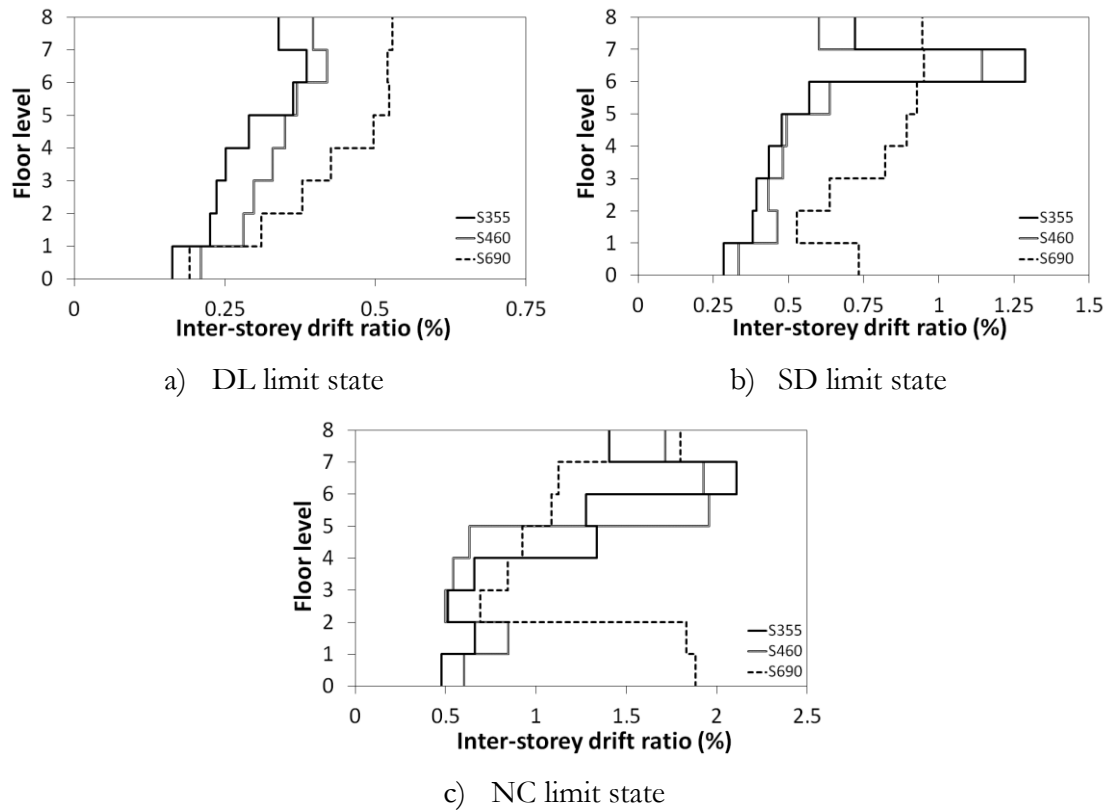


Figure 8.4 – Dual-steel *versus* single steel CBFs: Inter-storey drift demand

As a general remark, the analyses show that the seismic performance of the single steel CBF are very close to that of dual-steel frames. In particular, the frames designed considering a S690 steel grade presents a more appropriate behaviour in terms of overall displacements, brace ductility demand and storey acceleration when the comparison is addressed to maximum values.

The IDRs profiles show that differences which are more appreciable is devoted to DL and SD limit state. In fact, the frames with S690 are more flexible having larger drift demand in comparison with the frames with S460 and S355. The use of the MCS did not prevent a very common behaviour from this structural type, namely weak storey mechanism. The three cases examined presented problem concerning to high concentrations of damage in a specify floor. While the frames with S355 and S460 present large deformation in the upper floor, the frames designed show high drift demand in the first floor.

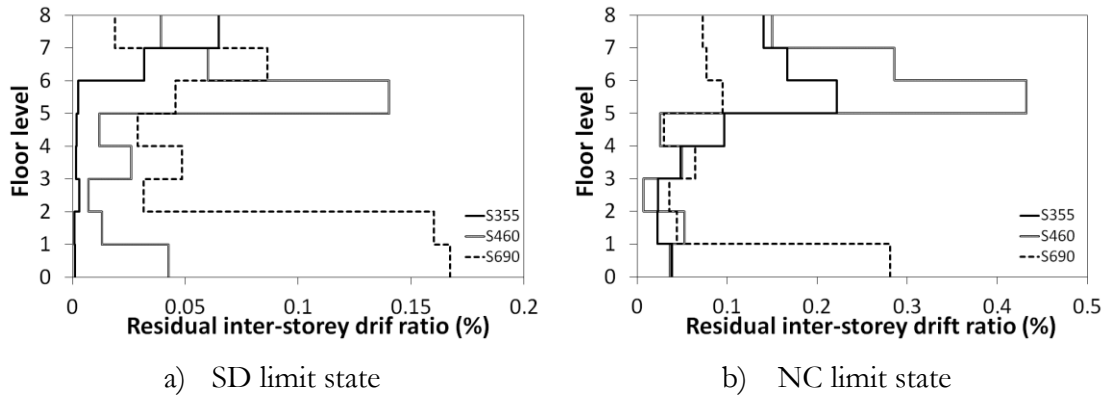


Figure 8.5 – Dual-steel *versus* single steel CBFs: Residual inter-storey drift demand

Concerning to RIDRs, Figure 8.5 illustrates the plots comparing the three study cases. In this figure, only the curves from SD and NC limit states are shown because the response in terms of residual drift is very close to zero for the DL. Interesting to note is that the frames with S355 are responsible for smaller residual drift. This result can be explained by use of the S355 in the beams from braced bays. In fact, the increasing of the flexural stiffness of these structural members allow to have smaller brace resistance deterioration, and consequently, lower residual drift.

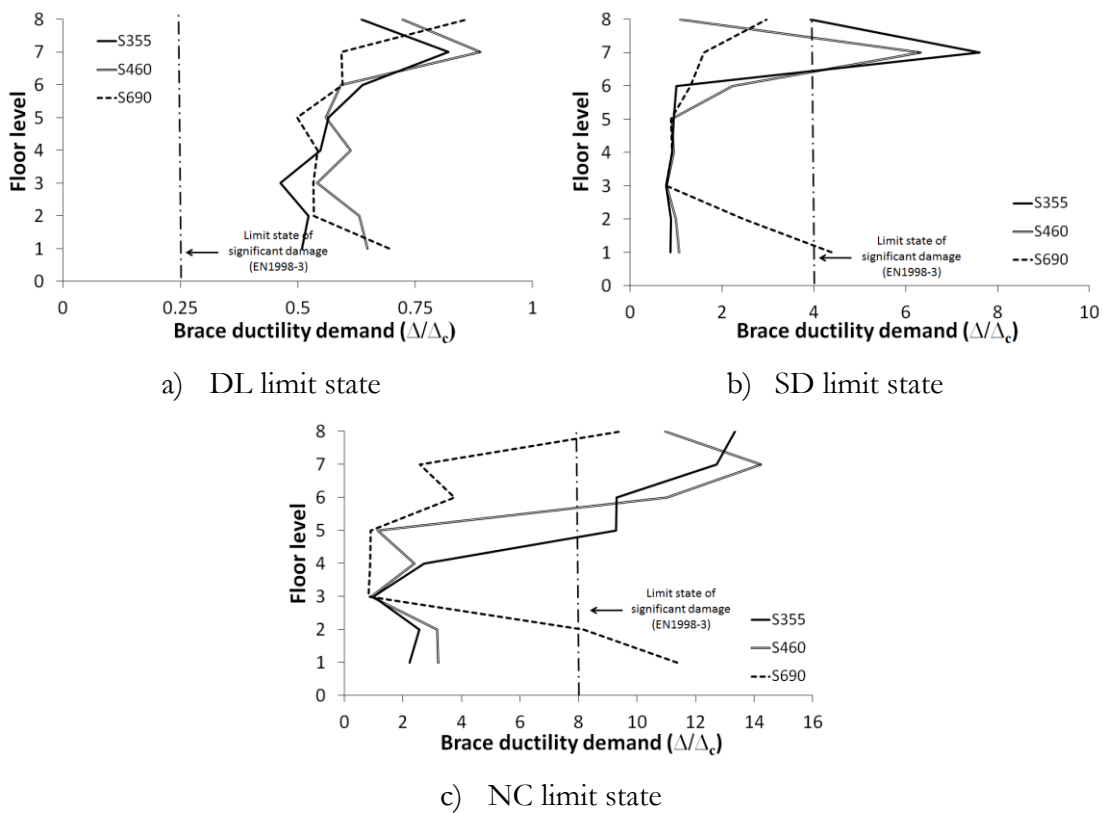


Figure 8.6 – Dual-steel *versus* single steel CBFs: Brace ductility demand

The drift profile is consistent with the brace ductility demand profile shown by Figure 8.6. It is noticed that large ductility demand is observed in the braces of upper floor for the

frames with S355 and S460 while the other frame present high brace ductility demand in the first floor.

Comparing only the frames with S355 and S460 because they present similar behaviour, it can be observed that the issue regarding to flexural stiffness of the beams is addressed to brace ductility demand where the frames with S355 have stiffer beams due to use of the MCS in these members. On the other hand, the frame with S690 present lower values due to more adequate redistribution of the frame along the height. However, all study cases present values superior to limit proposed by EN1998-1-3 (2005), especially for the DL limit state.

The curves from the storey acceleration also are very similar. In particular, the frames designed considering S690 steel grade present lower storey acceleration as can be observed in Figure 8.7. The frames with S460 and S355 present profiles very similar. In all study cases, the maximum value is observed in the last floor.

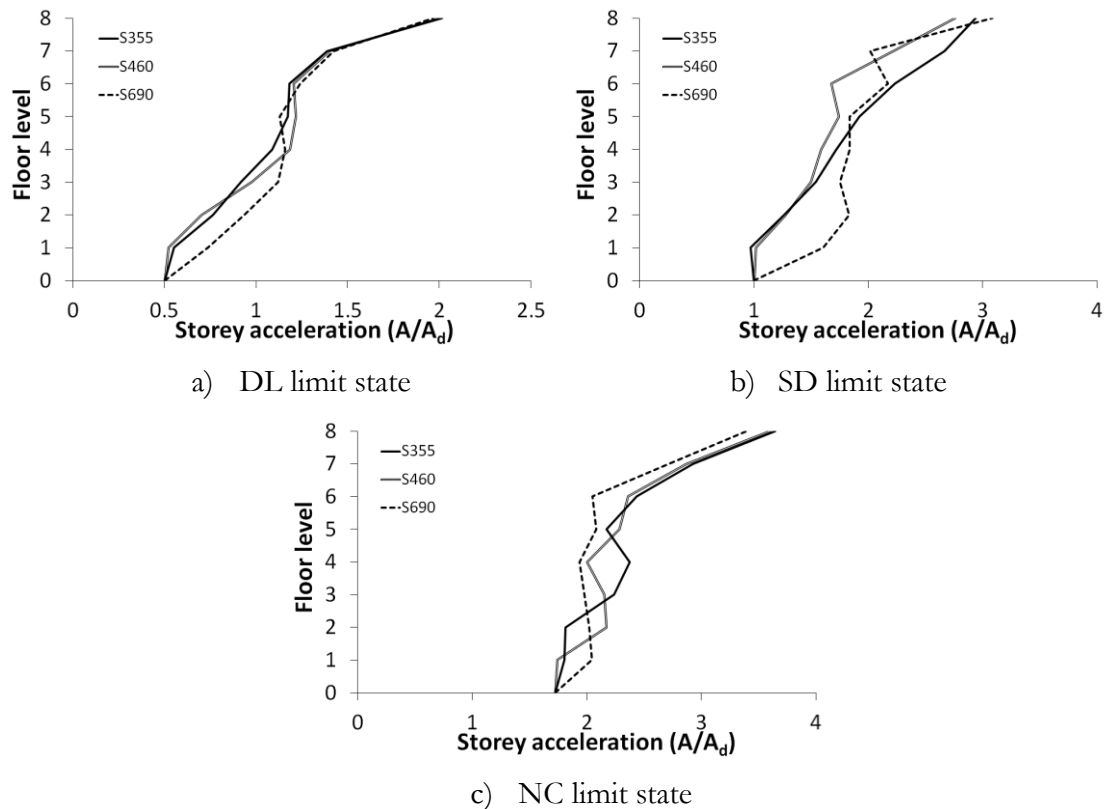


Figure 8.7 – Dual-steel *versus* single steel CBFs: Storey acceleration

### 8.2.3 Dual-Concentrically Braced Frames

Analysing the seismic response for the three study cases given in Figure 8.8 to Figure 8.11, it can be observed that the profiles are very similar regardless of the steel grade applied on the non-dissipative members. Slight differences can be seen for the frames with S355 where the brace ductility demand is smaller than other ones. Once again, the issue concerning the

flexural stiffness of the beam from braced bay is addressed. On the other hand, this difference is smaller in comparison with the CBF. In fact, due to high local ductility provided by use of the high behaviour factor and the redundancy from the MRF subsystem, the dual-system structures showed to be not so sensitive.

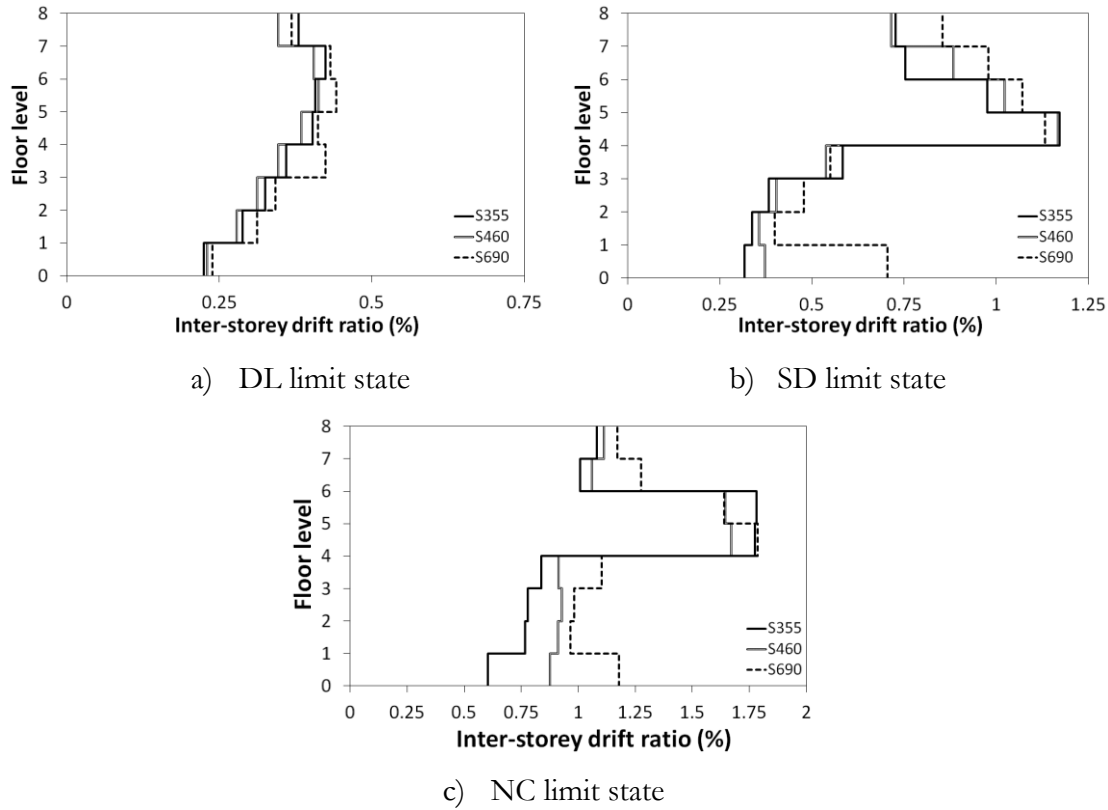


Figure 8.8 – Dual-steel *versus* single steel D-CBFs: Inter-storey drift demand

The IDRs for both study cases present similar profiles. In particular, the upper floor are responsible for the large drift demand. All the frames experience drift below the limit given by the DL limit state (0.75%).

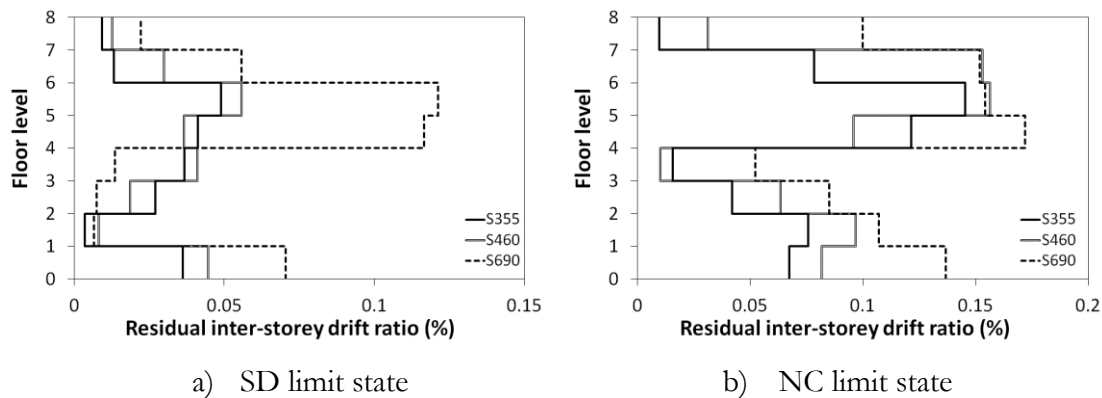


Figure 8.9 – Dual-steel *versus* single steel D-CBFs: Residual inter-storey drift demand

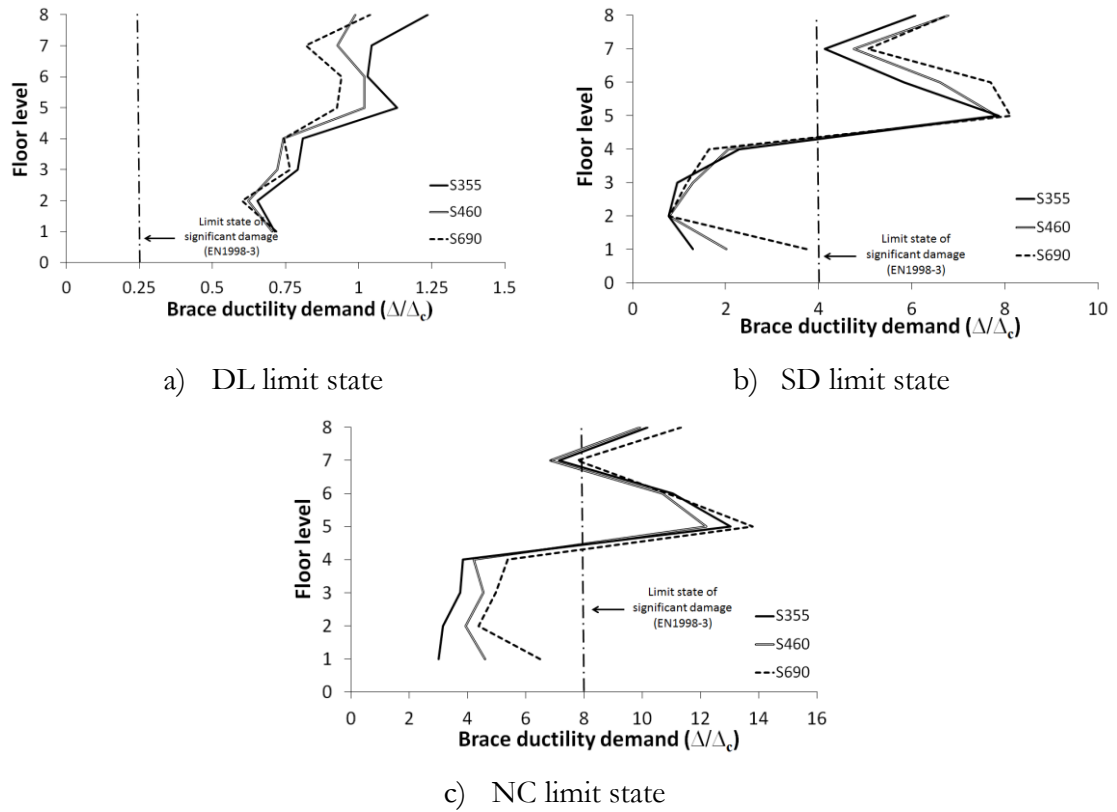


Figure 8.10 – Dual-steel *versus* single steel D-CBFs: Brace ductility demand

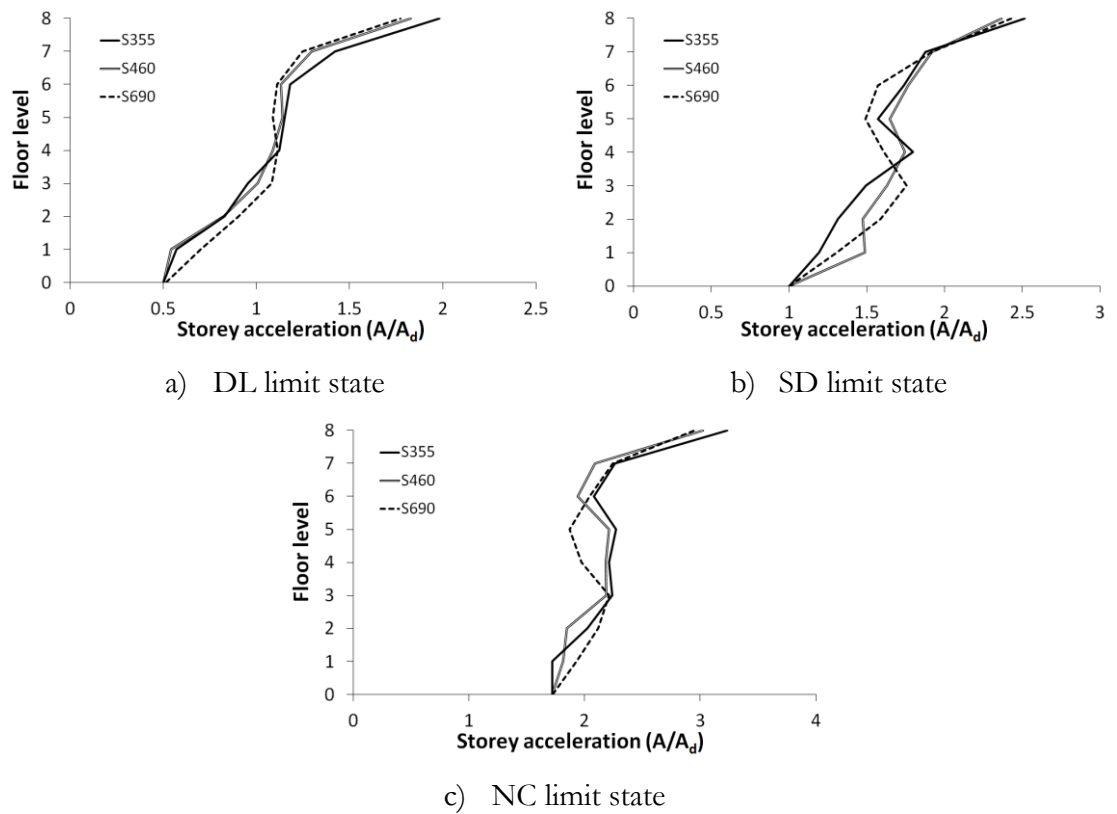


Figure 8.11 – Dual-steel *versus* single steel D-CBFs: Storey acceleration

As expected, the residual drift profiles present behaviour consistent with IRDs. The large damage concentration is located in the upper floors. The significant difference is observed for the SD limit state due to flexibility of the frames with S690. However, for the NC limit state, this difference is not so pronounced.

Concerning to brace ductility demand and storey acceleration, there is no appreciable differences from the plots presented in Figure 8.10 and Figure 8.11. Maybe, a small difference is observed for the brace ductility demand where the frames with S355 present lower values in comparison with another frames. Once again, the D-CBFs present poorest behaviour related to the brace ductility demand considering the DL limit state. For the other limit states, the soft storey mechanism is responsible for high values presented exceeding the limit proposed in EN1998-1-3 (2005).

It is noteworthy that the number of cases presented in this section is small. It is necessary to perform further analyses with a larger study cases.

### 8.3 Economic evaluation

In this section, an economic evaluation is conducted to provide a comparison between the three steel grades in terms of general price of each frame. In general, there is a large set of factors that can affect directly or indirectly building costs: codes, site location, frame structure, construction time, capital costs, social and environmental factors, raw material costs, use of recycled materials, etc. Therefore, to perform an economic evaluation is a complex task depending on tangible and intangible factors that can decisively influence the final result. Nevertheless, since only a comparison between different solutions is aimed the procedure followed in this dissertation should be robust enough to provide reliable conclusions.

The indices used are applied to the total weight for different steel grades and concrete materials. The connections are considered by increasing 20% of the total steel weight.

Table 8.1 reports the value considered for each item that can affect the frame costs. The average price for current S255 MRFs is estimated in 2150 €/ton taking into account the design, drawings, material, production, quality controls, transportation, installation and bolts. The prices presented in this table are based on the concept of prefabricated structural elements, i.e. beam and column elements are pre-realized in the factory by welding plates and dimensions must allow an easy transportation and assemblage in the building site.

Some items have not been taken into account in the price building, such as fire protection and surface treatment.

Table 8.1 – Prices from each task to be considered in the economic evaluation

Item	Description	Economic indices
<b>DESING</b>	Technical Office; Details “Engineerization”; Calculations Executive design; Design checks	16 €/t
<b>DRAWINGS</b>	Static elements approval drawings	60 €/t
<b>MATERIALS</b>	Steel (beams, columns and plates); Concrete	1080 €/t
<b>PRODUCTION</b>	Pre-manufacturing within the factory	450 €/t
<b>QUALITY CONTROLS</b>	Performed within the factory	54 €/t
<b>TRANSPORTATION</b>	Supposed a range of transportation of 500 km; Means of transportations	40 €/t
<b>INSTALLATION</b>	Necessary equipment; Laying; Need of high altitude works	370 €/t
<b>BOLTS</b>	Supposed hot zinc-coated	80 €/t
Frame reference		2150 €/t

The concrete for the composite columns has been considered with the price of 142 €/m<sup>3</sup> taken from PREBETON CALCESTRUZZI S.P.A. catalogue. The price established in the Table 8.1 applies to frames designed with S355. For different steel grades differences in price are given in Table 8.2. A variation of 3% and 5% is considered for frames designed with S460 and S690, respectively, in comparison with the S355 frames.

Table 8.2 – Differences of prices depending of the steel grade

STEEL GRADE	FRAME PRICE (AVERAGE)	DIFFERENCE	PERCENTAGE
S355	2150 €/t	REFERENCE	
S460	2200 €/t	30 - 70 €/t	3 %
S690	2250 €/t	100 - 150 €/t	5 %

It is important to mention that particular attention has been taken for the minimum amount of HSS, which the industry refuses to produce. The can be evaluated in around 50 t/profile.



### 8.3.1 Concentrically Braced Frames

Table 7.7 to Table 8.8 indicate the total weight for the previously considered frames. It is presented the weight for each set of structural member, namely columns, braces and beams. As stated before, the connection weight is considered as 20% of the steel weight. In addition, the concrete are has been evaluated on basis of the dimensions of the column cross-sections.

Analysing the total weight, it is interesting to note that there is a reduction of the 12% if the S460 steel grade is used considering the frames with S355 as reference. For the S690 steel grade, it is observed a reduction of the total weight of 29%. The larger parcels that have contributed to this reduction is addressed to columns and beams from the braced bay. The contribution of the bracing and concrete is not so significant in comparison with other elements. Moreover, the reduction obtained for the total weight is not proportional to the increase of the steel strength.

#### **CBF with S355**

Table 8.3 – The steel weight (kg) for the columns and beams of the CBF with S355

Floor	COLUMNS		INNER BEAMS		OUTER BEAMS	
	Steel profile	Weight (kg/m)	Steel profile	Weight (kg/cm²)	Steel profile	Weight (kg/cm²)
1	BOX 450x420x30x25	376	HEM 450	263	IPE 450	78
2						
3						
4						
5	SHS 300x10	90	HEM 360	250		
6						
7			HEB 360	142		
8						

Table 8.4 – The steel weight (kg) for the columns and beams of the CBF with S355

Floor	BRACES		Weight
	Steel profile	Weight (kg/m)	
1	CHS 219,1x12,5	64	Columns Inner Beams Outer Beams Bracing Connections 66t
2	CHS 219,1x12,5	64	
3	CHS 219,1x12,5	64	
4	CHS 193,7x12,0	54	
5	CHS 193,7x12,0	54	
6	CHS 193,7x10,0	45	Concrete Total
7	CHS 168,3x8,0	32	
8	CHS 168,3x6,0	24	

***CBF with S460***

Table 8.5 – The steel weight (kg) for the columns and beams of the CBF with S460

Floor	COLUMNS		INNER BEAMS		OUTER BEAMS	
	Steel profile	Weight (kg/m)	Steel profile	Weight (kg/cm²)	Steel profile	Weight (kg/cm²)
1	BOX 400x400x20x20	267	HEB 500	187	IPE 450	78
2						
3						
4						
5	SHS 300x10	90	HEA 500	155		
6						
7			HEA 360	112		
8						

Table 8.6 – The steel weight (kg) for the columns and beams of the CBF with S460

Floor	BRACES				Weight
	Steel profile	Weight (kg/m)			
1	CHS 219,1x12,0	61	Columns		21t
2	CHS 219,1x12,0	61	Inner Beams		10
3	CHS 219,1x12,0	61	Outer Beams		9t
4	CHS 193,7x12,0	54	Bracing		4t
5	CHS 193,7x12,0	54	Connections		9t
6	CHS 193,7x10,0	45			53t
7	CHS 168,3x8,0	32	Concrete		48t
8	CHS 168,3x6,0	24	Total		100t

***CBF with S690***

Table 8.7 – The steel weight (kg) for the columns and beams of the CBF with S690

Floor	COLUMNS		INNER BEAMS		OUTER BEAMS	
	Steel profile	Weight (kg/m)	Steel profile	Weight (kg/cm²)	Steel profile	Weight (kg/cm²)
1	BOX 350x380x16x16	183	HEA 500	155	IPE 450	78
2						
3						
4						
5	SHS 300x10	90	HEA 450	140		
6						
7			HEA 320	98		
8						

Table 8.8 – The steel weight (kg) for the columns and beams of the CBF with S690

Floor	BRACES			Weight
	Steel profile	Weight (kg/m)		
1	CHS 219.1x12,5	64	Columns	16t
2	CHS 219.1x12,0	61	Inner Beams	9
3	CHS 219.1x12,0	61	Outer Beams	9t
4	CHS 219.1x10,0	52	Bracing	4t
5	CHS 219.1x10,0	52	Connections	8
6	CHS 193,7x10,0	45		45
7	CHS 193,7x8,0	37	Concrete	42t
8	CHS 168,3x6,0	24	Total	87t

Figure 8.12 illustrates the total cost of the three study cases examined for the CBF structural system. The comparison is carried out taking into account the indices previously stated together with the adaptation depending on the steel grade applied on the non-dissipative elements.

Interesting to note that the use of HSS provided smaller cost for the CBFs with a reduction of about 21% for S460 and 37% for S690. Comparing these reductions with those obtained for the weight, it is important to note that the total cost reduction is larger than the reduction of the weight..

This results show to be quite satisfactory where the technical behaviour of the CBFs is not affected by the use of the dual-steel concept.

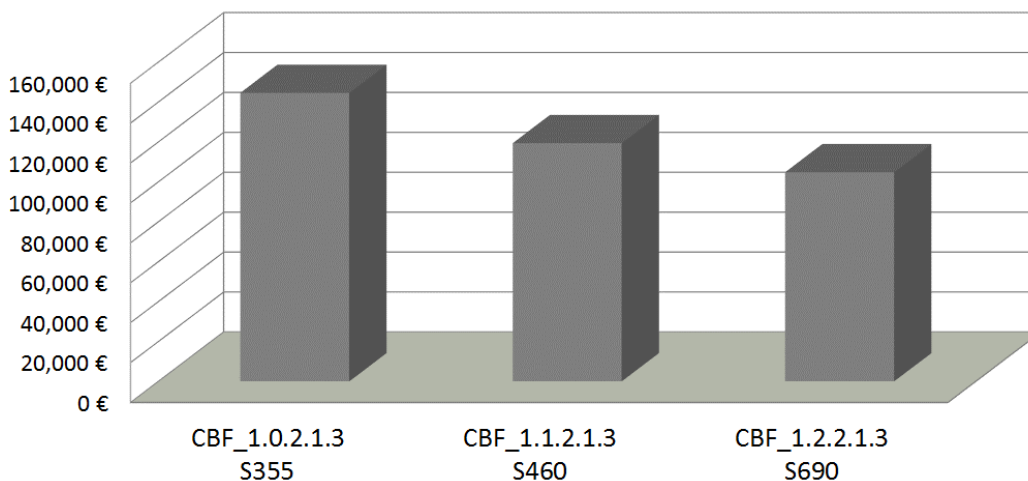


Figure 8.12 – Total costs of the CBFs comparing the S355, S460 and S690 structures

### 8.3.2 Dual-Concentrically Braced Frames

In Table 8.9 to Table 8.14, the weight of the frames examined for the D-CBFs is presented showing in detail the parcel of each structural member. Once again, the connections have been considered through of the total weight of the frame where a value of the 20% should be added taking into account the weight connections. In addition, the concrete are has been evaluated on basis of the dimensions of the column cross-sections.

Evaluating the results presented in these tables, there is a reduction of the weight of the frames when an HSS is applied in the non-dissipative elements. Indeed, the seismic design was not governed by damage limitation and therefore the resistance plays an important role. The frame designed with S460 results in reduction of the weight of 10% and when S690 is used the reduction is 22%. Similar to CBF, the contribution of the columns and inner beams are responsible for this reduction.

#### **D-CBF with S355**

Table 8.9 – The steel weight (kg) for the columns and beams of the D-CBF with S355

Floor	COLUMNS		INNER BEAMS		OUTER BEAMS	
	Steel profile	Weight (kg/m)	Steel profile	Weight (kg/cm <sup>2</sup> )	Steel profile	Weight (kg/cm <sup>2</sup> )
1	SHS 400x20	235	HEM 400	256	IPE 500	91
2						
3						
4						
5	SHS 300x10	90	HEB 450	171	IPE 450	78
6						
7			HEB 300	117	IPE 360	57
8						

Table 8.10 – The steel weight (kg) for the columns and beams of the D-CBF with S355

Floor	BRACES	
	Steel profile	Weight (kg/m)
1	CHS 219,1x10,0	52
2	CHS 219,1x10,0	52
3	CHS 193,7x10,0	45
4	CHS 193,7x8,0	37
5	CHS 168,3x10,0	39
6	CHS 168,3x8,0	32
7	CHS 168,3x6,0	24
8	CHS 139,7x5,0	17

	Weight
Columns	19t
Inner Beams	12t
Outer Beams	10t
Bracing	3t
Connections	9t
	53
Concrete	42t
Total	99t

***D-CBF with S460***

Table 8.11 – The steel weight (kg) for the columns and beams of the D-CBF with S460

Floor	COLUMNS		INNER BEAMS		OUTER BEAMS	
	Steel profile	Weight (kg/m)	Steel profile	Weight (kg/cm <sup>2</sup> )	Steel profile	Weight (kg/cm <sup>2</sup> )
1	SHS 400x16	190	HEB 450	171	IPE 500	91
2						
3						
4						
5	SHS 300x10	90	HEA 450	140	IPE 450	78
6						
7			HEA 320	98	IPE 360	57
8						

Table 8.12 – The steel weight (kg) for the columns and beams of the D-CBF with S460

Floor	BRACES		Weight (kg/m)
	Steel profile	Weight (kg/m)	
1	CHS 219,1x10,0	52	
2	CHS 219,1x10,0	52	
3	CHS 193,7x10,0	45	
4	CHS 193,7x8,0	37	
5	CHS 168,3x10,0	39	
6	CHS 168,3x8,0	32	
7	CHS 168,3x6,0	24	
8	CHS 139,7x5,0	17	

		Weight
Columns		16t
Inner Beams		9t
Outer Beams		10t
Bracing		3t
Connections		8t
		46t
Concrete		44t
Total		90

In Figure 8.13, a price comparison among the steel grades is shown taking into account the values calculated above. The use of S460 represented a reduction of 12% and for S690 the reduction is 21%.

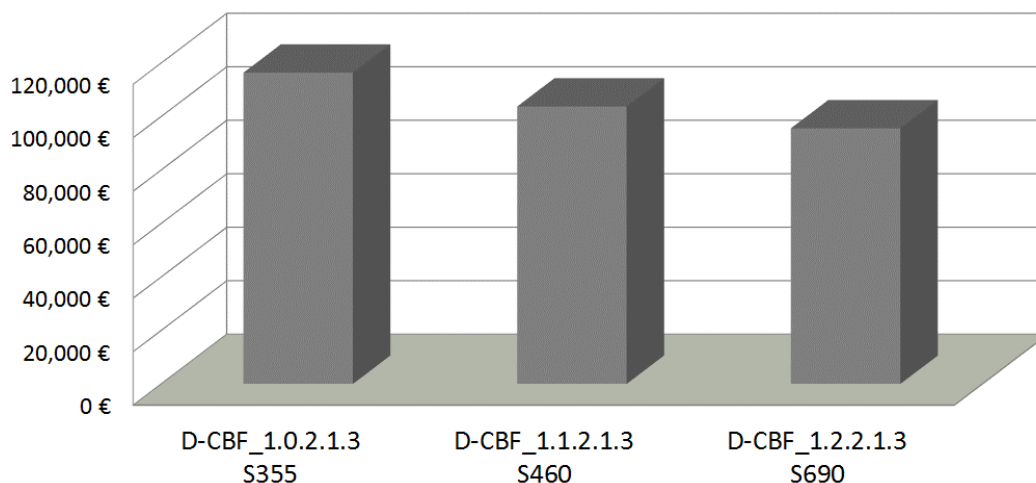


Figure 8.13 – Total costs of the D-CBFs comparing the S355, S460 and S690 structures

***D-CBF with S690***

Table 8.13 – The steel weight (kg) for the columns and beams of the D-CBF with S690

Floor	COLUMNS		INNER BEAMS		OUTER BEAMS	
	Steel profile	Weight (kg/m)	Steel profile	Weight (kg/cm <sup>2</sup> )	Steel profile	Weight (kg/cm <sup>2</sup> )
1	BOX 325x380x13x13	138	HEA 450	171	IPE 500	91
2						
3						
4						
5	SHS 300x8	73	HEA 360	140	IPE 450	78
6						
7						
8			HEA 300	98	IPE 360	57

Table 8.14 – The steel weight (kg) for the columns and beams of the D-CBF with S690

Floor	BRACES	
	Steel profile	Weight (kg/m)
1	CHS 219.1x10,0	52
2	CHS 219.1x10,0	52
3	CHS 193,7x10,0	45
4	CHS 193,7x8,0	37
5	CHS 168,3x10,0	39
6	CHS 168,3x8,0	32
7	CHS 168,3x6,0	24
8	CHS 139,7x5,0	17

	Weight
Columns	12t
Inner Beams	9t
Outer Beams	10t
Bracing	3t
Connections	7t
	41t
Concrete	40t
Total	81t

## *Chapter IX*

# Conclusions

In this Thesis, a numerical parametric study was carried out in order to verify the seismic performance of the building using the dual-steel concept in which frames use High Strength Steel grade in the non-dissipative structural elements while the dissipative elements are designed using Mild Carbon Steel.

The focus was given in three structural systems: Moment-resisting Frames, Concentrically Braced Frames and Dual-Concentrically Braced Frames. For each structural typology, a set of parameter was selected in order to investigate the nonlinear static and the dynamic behaviour and to provide an economic assessment. This set of parameters was chosen based on the type of soil condition, composite steel-concrete columns, span length, building height and the two HSS grades.

The seismic performance-based evaluation was carried out considering three limit states according to EN1998-1-3 (2005), namely damage limitation (DL), significant damage (SD) and near collapse (NC).

Furthermore, this work performed a comparison in technical and economic aspects considering both conventional and dual-steel approaches. In other words, a solution applying HSS in non-dissipative elements (S460 and S690) is compared to another solution but with the non-dissipative elements with MCS (S355).

The main conclusions drawn from this study are summarized in the following sections for the different structural typologies. Also, proposals for seismic design guidelines of dual-steel frames and for future developments are included in the final part of this chapter.

## 9.1 Moment-resisting Frames

For the study cases using the MRF structural system, the following conclusions can be drawn:

- The use of HSS is efficient when it comes to guarantee the weak-beam/strong-column behaviour;
- In most cases, pushover analyses showed overall overstrength factors  $\Omega = \frac{V_y}{V_d} = \frac{V_y}{V_{1y}} \times \frac{V_{1y}}{V_d}$  larger than the design behaviour factor ( $q = 4$ ). This result is ascribable to the codified design procedure, which leads to increase the member size to satisfy the drift limitations. Indeed, using HSS for columns small sections need to satisfy hierarchy criteria, thus conducting to flexible structures;
- The median ratio  $\frac{V_y}{V_{1y}}$  obtained from pushover curves confirmed the value of 1.3 recommended by EN1998-1-1 (2004);
- Nonlinear dynamic analyses showed that the frames have a seismic demand (namely, transient and residual drift ratios, beam ductility) fairly below the proposed limit for DL, SD and NC states. In particular, at SD limit state, most frames behave elastic;
- The median peak storey accelerations range between 2 to 3 times the design PGA. Therefore, significant amplification effects can occur and should be accounted for preserving the integrity of facilities and non-structural elements;
- The behaviour factors obtained from incremental dynamic analyses (IDAs) for SD limit state are smaller than the code value with a median value equal to 3.4 for stiff soil and 3.3 for soft soil condition. The average behaviour factor at NC limit state is equal to 3.9 and 3.4 for both stiff and soft soil conditions, respectively; hence, still smaller than the code value. These results suggest the need to calibrate the behaviour factors given by EN1998-1-1 (2004).

Regarding the material consumptions, the following remarks can be drawn:

- As expected, the taller the building height was, the larger the material consumption in terms of steel density;
- The frames with CFT columns are characterized by a larger amount of HSS and concrete than the cases with FE and PE columns, which are characterized by similar material consumptions;



- All frames located on soft soil are characterized by a larger consumption of material than the corresponding ones designed for stiff soils. This result is worth noticing especially considering that the design PGA for frames on soft soil is smaller (namely equal to 0.16g) than that used for cases on stiff soil (namely equal to 0.24g). Hence, this aspect should be carefully accounted for the economic planning at design stage.

## 9.2 Concentrically Braced Frames

Concerning the outcomes from the nonlinear analyses for the CBFs, the main observations are:

- The capacity design philosophy used in the seismic design was confirmed when most of the plastic hinges are concentrated on the dissipative elements. On the other hand, it is possible to see that some beams from braced bay experience the formation of plastic hinges;
- The overstrength factors,  $\frac{V_y}{V_{ly}}$ , obtained from pushover analyses have a median of 1.25. The taller frames were responsible for smaller values due to the development of a soft storey mechanism. It should be noted that in the European code there is no specific value for the Concentrically Braced Frames with V-inverted braces;
- The median ratio  $\frac{V_{ly}}{V_d}$  are close to 1.0 showing that the assumption adopted on seismic design resulted in structures with excellent level of optimization;
- In general, the nonlinear dynamic analyses showed that the CBFs have a severe seismic demand of brace ductility for DL, SD and NC states. In particular, at DL limit state most of the frames exhibit a very poor response. This result is mainly due to the low stiffness of the beams in the braced bay;
- Moreover, the results have shown that the soft soil, larger span lengths and higher frames result in higher transient and residual drifts together with larger peak storey accelerations. The median of peak storey accelerations range between 2 to 5 times the design PGA. Therefore, significant amplification effects can also occur and should be accounted similar to MRFs;
- The investigated frames experienced brace ductility demand ratio higher than the one recommended by EN1998-1-1 (2004) for the DL, SD and NC limit states. The median varies from 2.28 to 3.34 for the DL limit state, 0.33 to 2.0 for the SD limit state and 1.0 to 4.03 for the NC limit state. In particular, the 5.0m span frames have presented ratios below 1.0 for the SD limit state. This fact contribute to the recommendation of the use of MCS in beams from braced bay;

- The increase of steel grade is beneficial in seismic response in the sense that there was a reduction of transient and residual inter-storey drift ratio. Peak storey accelerations and brace ductility demand were also observed;
- Salvitti & Elnashai approach, used to compute behaviour factors, leads to higher values than those obtained by the European method. The overstrength factors obtained from pushover analysis control the q-factor in European approach. Being those factors close to 1.0, no increase of term  $\left( \frac{A_u}{A_{1,y}} \right)$  is possible, i.e., the structure cannot achieve a yielding strength larger than the one provided by the first plastic event;
- The importance of the flexural stiffness of the beams from braced bay is also verified in order to assess the span length. In detail, the frames with smaller span length presented larger behaviour factor for both methods investigated in this Thesis. Furthermore, the increase of HSS steel grade provides a reduction of behaviour factor for the European method. In contrast, Salvitti & Elnashai approach has shown that the increase of steel grade provides larger behaviour factors. Indeed, as the frames with S460 are more susceptible to the development of the soft storey mechanism, there is larger axial deformation for the braces located in the floor where this mechanism is observed;
- As a whole, the behaviour factors obtained from incremental dynamic analyses (IDAs) for SD limit state are smaller than the code value with a median value equal to 1.7 for both soil conditions. The median behaviour factor at NC limit state is equal to 2.0 and 1.9 for both stiff and soft soil conditions, respectively; hence, still smaller than the code value. Therefore, a calibration of the behaviour factor from EN1998-1-1 (2004) is suggested.

Regarding the material consumptions, the following comments can be drawn:

- Comparing the number of storey, it is possible to say that the taller the building is, the larger the steel density. Moreover, the frames with smaller span length present higher steel density. This last observation was expected since steel becomes competitive for longer span;
- In general, the CFT columns were the most efficient solution in terms of overall weight of the structure. Hence, this aspect can also be taken into account on the economic planning of the building;
- Soft soil condition was responsible for larger consumption of material than the corresponding designed for stiff soil. This is explained by the fundamental period of

the study cases, which are located in the constant acceleration for the soft soil design spectrum resulting in higher base shear;

- Furthermore, the frames with S690 present steel density lower than those designed with S460. The seismic design of the CBFs was not governed by damage limitation criterion, so the resistance is the key parameter to determine the structural members.

### 9.3 Dual-Concentrically Braced Frames

The main observation obtained from the nonlinear analysis of the D-CBFs can be identified as follows:

- As a whole, the philosophy employed in the seismic design was confirmed in the plastic pattern with hinges developed on beams of the secondary subsystem and non-linear behaviour of the braces. The plastic hinges in the MRF subsystem appear when the primary bracing subsystem has significant damage resulting in smaller overall lateral stiffness. In fact, the study cases confirm the idea of a dual-system structure where the subsystem withstands the earthquake motion after the failure of the primary subsystem that is expected to primarily resist the earthquake. On the other hand, it is possible to see that some beams from braced bay experience the formation of plastic hinges for the pushover nonlinear analyses;
- The median ratio,  $\frac{V_y}{V_{1y}}$  was around 1.45. Similarly, to CBFs, the taller frames were responsible for smaller value. Since EN1998-1-1 (2004) does not recommend any value for the overstrength factor of the D-CBFs with V-inverted braces this study can be a contribution to future revision of the code;
- Regarding the ratio,  $\frac{V_{1y}}{V_d}$ , associated to criteria of the seismic design, the median value is higher than 1.0 showing that the assumptions adopted in the seismic design stage does not provide structures with good level of optimization;
- The nonlinear dynamic analyses showed that the D-CBFs are prone to severe seismic demand in terms of brace ductility for DL, SD and NC limit states, while small ductility demand is expected for the beams of the MRF parts. The DL limit state is the one which the study cases presented results more distant from those recommended value by EN1998-1-3 (2005);
- The influence of the soil condition plays a significant role in the seismic performance of the study cases. The frames located in soft soil exhibit larger demand concerning the inter-storey drift (both transient and residual), brace ductility demand and peak

storey acceleration. Regarding the latter, it is noticed that median peak storey accelerations range between 2.0 to 3.5 for stiff soil and 2.0 to 4.5 for the soft soil. These outcomes evidence that significant amplification effects can also occur and should be accounted similar to CBFs and MRFs;

- The ductility brace demand is a critical parameter presented by the study cases. The brace ductility demand ratios were higher than the value recommended by three limit states given by EN1998-1-3 (2005). In particular, the amplification varies from 4.7 to 13.8 for the DL limit state, 1.5 to 3.7 for the SD limit state, and finally, for the NC limit state a value from 1.9 up to 5.5 is observed. These values are much major than the ones proposed by the code, so the question can be related to large deformability due to either the use of the HSS together with the use of high behaviour factor or to the ineffectiveness of code design rules;
- In most frames, the use of an increased steel grade proved not to be advantageous in order to improve the seismic performance in the sense that there is no reduction of the drifts and brace ductility demand. Only for the storey acceleration and for the beams from MRF part, the use of S690 is slightly more suitable. Once again, this behaviour is related to large behaviour factor employed in the seismic design for the D-CBFs together with the greater flexibility provided by HSS;
- Once again, Salvitti & Elnashai approach was responsible for a larger behaviour factor especially when it comes to the SD limit state. Indeed, the frames examined presented an even poorer behaviour for the NC limit state with smaller values applying to Salvitti & Elnashai approach. The influence of the overstrength factor from pushover analyses plays an important role in the European approach;
- Analogous to CBFs, the frames with shorter span length presented larger behaviour factors for both approaches. Once again, the flexural stiffness of the beams becomes a parameter, which should be taken into account. Furthermore, the increase of HSS steel grade provides a reduction of behaviour factor for both methodologies. This is explained by the larger flexibility of the beams from braced bay that was designed with superior steel grade for the frames with S690;
- Analysing the values computed for the European approach, the behaviour factors obtained for SD limit state are smaller than the values assumed in the seismic design with a median of 2.6 for stiff soil and 2.1 for soft soil. For the NC limit state, a median of 3.2 and 2.5 for both stiff and soft soil conditions were obtained, respectively; hence, still smaller than the value assumed. Once again, it is recommend

to perform a calibration of the behaviour factors recommended by EN1998-1-1 (2004).

Regarding the material consumptions, the following comments can be drawn:

- The sixteen-storey frames are responsible for a larger steel density especially when it comes to the soft soil condition in comparison with other frames. It is also important to note that the frames with smaller span length present higher steel density. Once again, this observation was expected since steel becomes competitive for longer spans;
- In general, the CFT columns were also the most efficient solutions in terms of overall weight of the structure. Hence, this aspect can also be taken into account on the economic planning of the building;
- As expected, the frames located in soft soil condition presented a larger material consumption than the corresponding designed for stiff soil. This is explained by the greater base shear design from the design spectrum;
- As most of the frames were designed considering the resistance as a main parameter (expect for the upper columns in order to have realistic building), the frames with S690 present steel density lower than those designed with S460.

#### 9.4 Dual versus simple concentrically braced Frames

A comparison between the Simple and Dual concentrically Braced Frames also was performed. As main observation, the following topics can be mentioned:

- Comparing the pushover results, both typologies exhibit similar behaviour. The first nonlinear event is characterized by the buckling of the braces with sudden reduction of the lateral resistance. In particular, due to presence of the MRF subsystem, the D-CBFs have an increasing of the lateral resistance after of first plastic event in comparison with the CBFs;
- The increase of lateral resistance is reflected in ratio  $\frac{V_y}{V_{1y}}$ . Indeed, the D-CBFs have an increase of 20% for the overstrength incorporated in the EN1998-1-1 (2004). In particular, the frames with dual-system exhibit a median of 1.6 while the cases with simple system show a median of 1.3;
- Concerning the overstrength associated to design criteria, the D-CBFs present a value larger than those given by CBFs. In fact, the CBFs show that the criteria

assumed in the seismic design stage provide structures with good level of optimization;

- Evaluating the damage distribution, the difference between the two structural systems is addressed to beams from the braced bay. Inelastic deformation in these structural members are more pronounced by simple system. In fact, with the introduction of the beam from MRFs part in energy dissipation, the D-CBFs have more appropriate redistribution of the load after the first plastic event in comparison with the CBFs;
- In general, the two structural systems show a poor damage distribution where large damage concentration is located on the mid-rise of the buildings, being, therefore, prone to soft storey mechanism. Notwithstanding, this behaviour is recognized by structures of this kind;
- For the dynamic performance, the dual-system experience larger inter-storey drift ratios, residual drifts and brace ductility demand. This outcome was expected due to flexibility of the D-CBFs given by higher behaviour factor assumed in the seismic design. On the other hand, the storey acceleration amplitudes are lower for the D-CBFs. As previously stated, it is recognized that the peak storey acceleration is related to the damage of the non-structural elements. Therefore, with this outcome it can be concluded that while the global and local deformations are larger for the cases with dual-system, the damage non-structural of the buildings are smaller. This issue plays an important role when an economical assessment is performed, due to the fact that it takes into account the cost related to non-structural members;
- Concerning to behaviour factors for both methods, the dual-system deliver larger behaviour factors. They have a higher energy dissipation capacity in comparison with the simple system given by MRF system.

Considering now the material consumptions for two typologies, it can be said that:

- Due to the use of larger behaviour factor, the dual-system presents lower material consumption in comparison with the simple one, being this difference more notorious for the soft soil condition. In fact, the use of the high behaviour factor provides lower base shear design resulting in lighter structures. These lighter structures have lesser fundamental periods and consequently smaller base shear.

### 9.5 Comparing the conventional with HSS solution

The dual-steel approach is compared with a conventional approach, in which the frame is designed considering a single steel grade. The comparison is devoted to economic and technical terms for the three typologies examined in this Thesis. The main observations are following:

- The comparison between dual-steel and single steel frames showed that the former solution is more effective to control the plastic mechanism for the MRFs;
- On the other hand, similar seismic response is observed for the CBFs and D-CBFs. The poor seismic performance of the CBF and D-CBF using dual-steel approaches is also observed for the conventional frames. In particular, the frames designed with S690 for the CBF structural system are more efficient in terms of maximum value;
- Bending of the beam in braced bay plays an important role for the brace ductility demand. However, this factor does not show any influence in the D-CBFs. This fact can be attributed to high flexibility given by high behaviour factor assumed in the seismic design stage. In addition, the redundancy of the dual-systems attenuates the deterioration of the braced system;
- From the economic point of view it was observed that the use of HSS in non-dissipative structural elements represented an effective solution for the braced frames. On the other hand, the high flexibility of the MRF resulted in seismic designed governed by damage limitation criterion where the stiffness is a key parameter. Thus, in this structural system, the resistance of the non-dissipative elements is not important and the use of HSS seems not to be advantageous;
- For the CBFs, there was a reduction of weight of 12% when S460 is applied in the non-dissipative element, while a decrease of 21% of cost is observed. These values increase to 29% and 37% respectively when a S690 is employed. The equivalent results for D-CBFs are similar. A reduction weight of 10% for the S460 and 22% for the S690 was found compared to conventional solution. Concerning costs, the reduction is 12% for S460 and 21% for S690. These outcomes are only indicative, since the costs for HSS varies according to delivered quantities and place of construction.

## 9.6 Design recommendations

This section summarizes recommendations that can be followed when performing a seismic design using the Dual-Steel concept. The proposed guidance concerns the results of the numerical computations and the conclusions obtained in the previous chapter and all the experience gained during the development of the HSS-SERF project (Dubina et al., 2014). The design proposals are in accordance with the capacity design philosophy underlying the European code (EN1998-1-1, 2004). Three structural systems have been investigated using the Dual-Steel concept and are addressed here:

- **Moment-resisting Frames** – This structural system is composed by beams and columns. The columns may or not have composite steel-concrete columns; however, it is advised to use the composite column in order to provide stiffness to the entire building. Similarly, the beams may or not have composite steel-concrete beam. The use of composite beam may increase the stiffness of the building, however, its contribution is lower in comparison with the column, and therefore, it is necessary to perform an evaluation in terms of cost. The MRFs are dual only in terms of the employment of two steel grades. The developed study covered MRFs up to 8-storey;
- **Concentrically Braced Frames** – They are composed by diagonal bars beyond columns and beams. A bay is braced using the V-inverted shape linked in the mid-length of the beams. The other two bays have the beams with pinned connection in their ends. In general, it is not possible to consider this system as dual due to connection of the beam out of the braced bay. Thus, these beams only contribute to the mass of the system and are not responsible for energy dissipation or lateral resistance. Floor beams may or may not use the composite action, and columns may be of bare steel or composite steel concrete. The developed study covers CBF buildings up to 16-storey;
- **Dual-Concentrically Braced Frames** – In this typology, the sense of dual is used referring to two steel grades and to two structural systems. The former is the main subject of this Thesis while the latter is a composition of the two structural systems previously stated. Similar to CBF, floor beams may or may not be steel-concrete composite, and columns may use bare steel or composite steel concrete. The developed study covers the study cases with height up to 16-storey.



The design philosophy preconized in code EN1998-1-1 (2004) states that the structures located in seismic zones should be able to maximize energy dissipation developing suitable plastic mechanisms according to the predefined hierarchy. Hence, when using dual-steel concept, the MCS steel grade should be located in the dissipative members in order to give adequate ductility for these. On the other hand, the use of HSS is indicated for the non-dissipative elements where plastic hinge is not supposed to form. Figure 9.1 shows in thicker lines the elements (columns) where HSS could be used. It is important to mention that the study cases investigated in this dissertation have the beams in braced bay designed considering the HSS in order to have slim deck slab. However, considering the results, the use of MCS in this structural member can be advantageous since it reduces the axial deformation demand in the braces in compression.

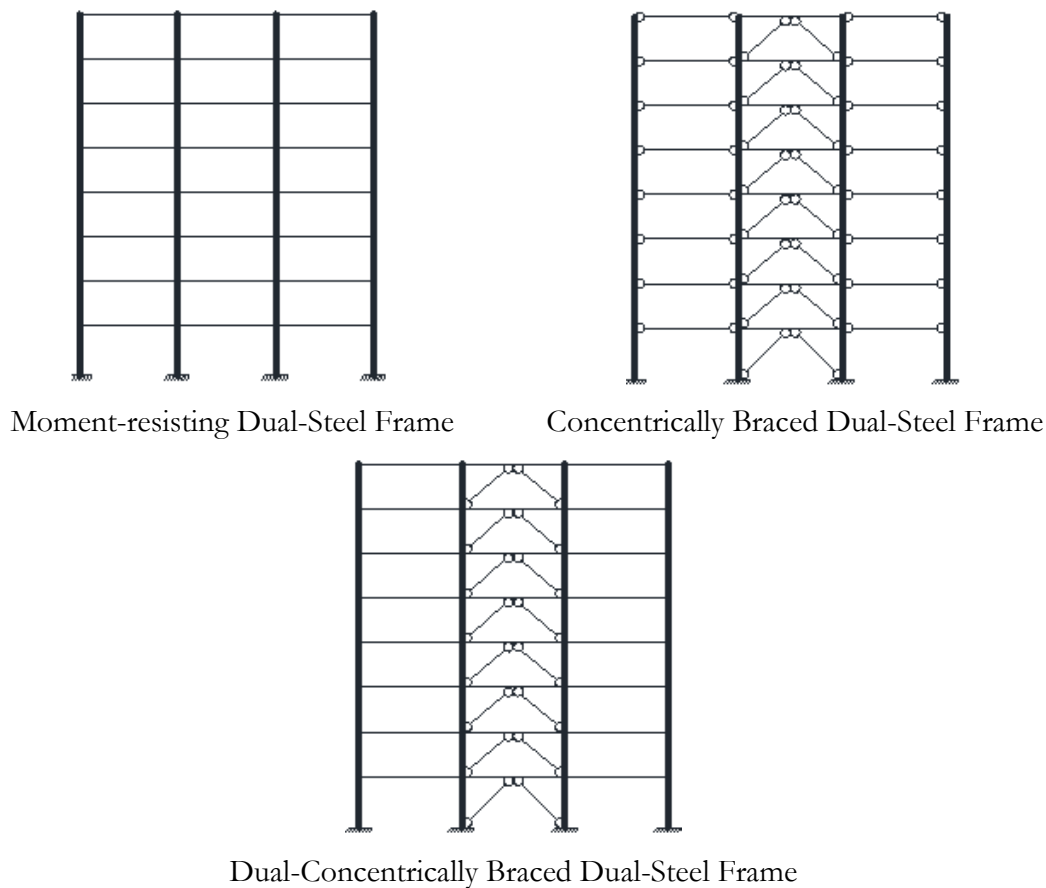


Figure 9.1 – The use of HSS (thicker lines) and MCS (thinner lines) in the studied typologies

This sketch is a proposal for the structures using two steel grades and some variants that can also be considered. For instance, the use of HSS in the beams from non-braced bay of the CBF is an issue that depends on the building cost because the influence of this structural members is not taking into account where there is the influence of the lateral resistance, and consequently, the overall stiffness.

### 9.6.1 *Seismic performance expected*

The dual-steel structures are characterized by the behaviour of their primary resisting member under seismic action. In accordance with the methodology incorporated in EN1998-1-1 (2004), during severe earthquakes, it is expected to form an overall ductility mechanism with uniform formation of plastic zones along the building height. This scenario aims to avoid damage concentration in a limited number of storeys.

Besides MRF and CBF (or EBF not studied in this dissertation), dual configuration, characterized by the presence of a braced system acting together with a MRF part brings together the advantages from both systems and are suitable for extensive use of HSS. It is recognized that the EN1998-1-1 (2004) does not provide specific design rules for the Dual configurations. The expected nonlinear behaviour of EN1998-1-1 (2004) compliant dual structures is characterized by dissipation, simultaneously provided, by beams in MRF part and yielding of tension diagonals in the CBF. Two different behaviours can be targeted by adopting different design strategies. The dissipate behaviour of dual configurations can be viewed as:

- A primary stiff braced frame with a secondary moment frame with the role to provide plastic distribution along the building height thus avoiding formation of weak storey mechanism, or
- A primary ductile MRF stiffened by a secondary braced frame, designed to resist wind loads and to provide lateral stiffness to satisfy service-level drift control.

Dual-steel frames are designed to have a behaviour similar to ordinary steel and steel-concrete composite frames. There are, however some differences that may affect the performance of the frames, which need to be considered during design:

- In the elastic stage, dual-steel frames may be more flexible compared to conventional frames, due to more flexible columns. An increase of flexibility is expected to be more evident for bare steel frames than for composite frames, where the contribution of the concrete is the same either for dual-steel and ordinary steel frames;
- It is advised to use HSS components judiciously in non-dissipative members. On the member level, all non-dissipative sections can be fabricated with HSS with the exception when stiff members are required. For instance, in the case of CBF, the stiffness of the beams from braced bay plays an important role in ensuring formation of global collapse mechanism. The use of HSS for this element is not recommended due to increase of flexibility. There is another sensible set of members, such as the ground floor columns, where two strategies may be adopted: either the use of HSS

columns with rigorous control of the rotation demand on column bases in the DL limit state, or the selective use of ordinary steel for the ground floors columns.

The seismic analyses performed on all structural configurations highlighted that in most cases the behaviour factors are smaller than those given in EN1998-1-1 (2004). Depending on the structural configuration, this result is mainly ascribable to two reasons: 1) the large deformability due to the use of HSS elements; 2) the ineffectiveness of code design rules.

Indeed, for MRFs the use of HSS lead to large lateral flexibility, hence large drift ratios and problems due to P-Delta effects. This leads to the need to oversize the structure, thus impairing the benefit of HSS.

For both CBFs and D-CBFs, the analyses showed that the smaller the beam flexural stiffness the higher is the brace ductility demand in compression. Hence, the use of HSS for beams of braced bays is not advisable.

#### *9.6.2 Design checks for Moment-resisting Dual-steel Frames*

Based on the outcomes from the nonlinear analyses, this guidance recommends the following design provisions:

Design criteria:

- The nonlinear dynamic analyses presented in this Thesis showed that the MRFs have a seismic demand (namely, transient and residual drift ratios, beam ductility) fairly below the proposed limit for DL, SD and NC states. For the SD limit state, for instance, most of frames behave in elastic field. This result is mainly due to the design oversizing. Although this result is consistent with the literature, this guidance recommends the use of the provisions recommended by EN1998-1-1 (2004) in order to consider the second-order effects and inter-storey drifts which are stipulated in Sections 4.4.2.2 and 4.4.3.2 of EN1998-1-1 (2004). The former is associated with ULS whilst the latter is included as SLS;
- The design rules for dual-steel MRFs are basically those given by EN1998-1-1 (2004). Anyway, owing to the need to satisfy the stiffness requirements, it is suggested to design this type of structures in elastic field to satisfy the DL criteria and subsequently to verify the structure against the hierarchy criteria;
- The median obtained of the overstrength factor incorporated in the EN1998-1-1 (2004) from pushover curves confirmed the value of 1.30 recommended by code;
- Based on the nonlinear analyses, it is recommended a calibration of the behaviour factor given by EN1998-1-1 (2004);

- All frames located on soft soil are characterized by larger consumption of material than the corresponding designed for stiff soil. This result is worth of noting especially considering that the design PGA for frames on soft soil is smaller (namely equal to 0.16g) than that used for cases on stiff soil (namely equal to 0.24g). Hence, this aspect should be carefully accounted by designer for the economic planning at design stage in all cases the cost of the building is the leading design parameter.

### 9.6.3 *Design checks for Concentrically Braced Dual-steel Frames*

Once again, on basis of the outcomes from the nonlinear analyses, this guidance recommends the following design provisions for the dual-steel CBFs:

Design criteria:

- The nonlinear dynamic analyses showed that the CBFs have a severe seismic demand in terms of brace ductility for DL, SD and NC states. In particular, at SD limit state most frames exhibit a very poor response. This result is mainly due to the small stiffness of the beams in the braced bay;
- The design rules for dual steel CBFs are basically those given by EN1998-1-1 (2004). In addition, in order to increase the stiffness of the braced beams it is suggested to design these members in mild carbon steel and considering another rule for the post-buckling braces. In particular, this guidance recommends the use of the rule from AISC-341 (2005) which indicates that the post-buckling resistance of the braces should be considered as  $0.3N_{br,d}$  instead of the  $0.3N_{pl}$  from EN1998-1-1 (2004). This measure results in beams with larger flexural stiffness, and consequently, there is a reduction of the axial deformation of the braced frames;
- The median obtained from outcomes of the nonlinear analyses concerns the overstrength factor associated to EN1998-1-1 (2004) is equal to 1.24 for 8-storey frames, while 1.05 for 16 storeys. It is interesting to note that the EN1998-1-1 (2004) does not mention the overstrength factor for the CBF;
- Based on the nonlinear analyses, it is recommended a calibration of the behaviour factor given by EN1998-1-1 (2004);
- All frames located on soft soil are characterized by larger consumption of material than the corresponding designed for stiff soil. Hence, this aspect should be carefully accounted for the economic planning at design stage in all cases the cost of the building is the leading design parameter.

#### 9.6.4 Design checks for Dual-Concentrically Braced Dual-steel Frames

The design recommendations for the dual-steel D-CBFs is here presented based on the outcomes from the nonlinear analyses:

Design criteria:

- The nonlinear dynamic analyses showed that the D-CBFs are prone to severe seismic demand in terms of brace ductility for DL, SD and NC states, while small ductility demand is expected for the beams of the MRF parts. In particular, at SD limit state that most frames exhibit a very poor response. This result is mainly due to the small stiffness of the beams in the braced bays;
- The design rules for dual steel CBFs are basically those given by EN1998-1-1 (2004), namely the requirements for both MRFs and CBFs. However, in order to guarantee that the MRF part has a minimum lateral strength of 25 per cent, the following expression has been taken into account based on shear base of structure:

$$V_{Rd,i}^{MRF} \geq 0.25 \times V_{Rd,i}^{DUAL} \rightarrow V_{Rd,i}^{DUAL} = \frac{1}{0.75} \times (N_{pl}^+ + 0.3 \times N_{pl}^-)_i \times \cos \alpha_i \quad (9.1)$$

in which,  $V_{Rd,i}$  is the base shear resistance at the  $i$ -th storey,  $N_{pl}$  is the plastic axial resistance of the brace in tension(+) or in compression(-) and  $\alpha$  is the angle that the braces make with the horizontal direction. The minimum resistance of the MRF part is derived from the plastic resistance of the brace for a specify storey. This resistance is considered for both compression and tension braces applying the post-buckling effect according to EN1998-1-1 (2004);

- In addition, in order to increase the stiffness of the braced beams it is suggested to design these members in mild carbon steel and considering another rule for the post-buckling braces. In particular, this guidance also recommends the use of the rule from AISC-341 (2005) which indicates that the post-buckling resistance of the braces should be considered as  $0.2N_{br,d}$  instead of the  $0.3N_{pl}$  from EN1998-1-1 (2004);
- The median obtained from outcomes of the nonlinear analyses concerns the overstrength factor associated to EN1998-1-1 (2004) is equal to 1.53 for 8-storey frames, while 1.18 for 16 storeys. It is interesting to note that the EN1998-1-1 (2004) does not mention the overstrength factor for the D-CBF;
- Based on the nonlinear analyses, it is recommended a calibration of the behaviour factor given by EN1998-1-1 (2004);
- All frames located on soft soil are characterized by larger consumption of material than the corresponding designed for stiff soil. Hence, this aspect should be carefully

accounted for the economic planning at design stage in all cases the cost of the building is the leading design parameter.

### 9.7 Future research

During the development of this dissertation some limitations of the European code were recognized which deserve further studies. Following items are considered pertinent for the continuation of the research:

- In this study, the MRFs presented seismic response that are lower than the criteria assumed for the three limit states proposed by EN1998-1-3 (2005). This fact is associated to stringent requirement recommended by the European code for what concerns the second-order effect and drift limitation. The use of composite beam could increase the lateral stiffness avoiding the need to the bigger cross-section;
- The small beam ductility demand obtained for the MRFs suggests that for such structures the use of class 2 beams can be more convenient. Therefore, in order to better study of the seismic performance, it would be important to add a value of the class 2 beam for the MRFs;
- An important issue concerning the braced bays is related to buckling of the braces. These structural members play an important role for the seismic response of the CBFs and D-CBFs. Therefore, it is interesting to study new cases with the use of Buckling Restrained Braces (BRBs) in which yield under both tension and compression have gained acceptance in recent years. The BRB behaves stably under cyclic loads, dissipating large amount of hysteretic energy;
- Although the behaviour factors have been investigated in this Thesis, it should be important to assess a larger number of study cases in order to provide more information about these factors for the building using the dual-steel concept. Moreover, the focus can also be addressed to evaluation of the failure criterion incorporated in the EN1998-1-3 (2005). Some studies show ductility capacity of braces larger than those recommended by this code;
- Another issue is related to storey acceleration, as it was previously stated, this aspect is important for the evolution of the non-structural damage. Hence, it should be important to correlate the amplification of the PGA with a specific building that will suffer with the total cost;
- A study has been performed in this dissertation in order to improve the seismic performance of the CBF and D-CBF. To guarantee a homogeneous plastic engagement over the height and to avoid weak storey mechanism, the difference

between the minimum and maximum overstrength factor of bracing should be at most 25%, where the overstrength is given by ratio between plastic resistance of the bracing and axial loading from seismic combination. In this dissertation, it is proposed to consider the buckling resistance of the braces instead of the plastic one. In addition, the forces in the non-dissipative elements are calculated considering the maximum value of overstrength instead of the minimum value as employed in the EN1998-1-1 (2004). Thus, it is recommended to perform a more detailed study of this approach in order to reduce the brace degradation and the effects of the soft story mechanism.

## 9.8 Published articles and dissemination of results

The main results and conclusion of this Thesis have been presented and/or published in several Conferences and Journals.

The main results and conclusions of the research have been presented and/or published in several conferences and national or international journals. A list of the most important papers and reports is presented below.

### Journals:

Tenchini A, Rebelo C, Lima L and Simões da Silva L (2014) Análise Não Linear de Pórticos “Dual-Steel” simples. *Revista da Estrutura de Aço*, Vol. 3 (1), pp. 1–16.

Tenchini A, D’Aniello M, Rebelo C, Landolfo R, Simões da Silva L and Lima L (2014) Seismic Performance of Dual-Steel Moment-resisting Frames. *Journal of Constructional Steel Research* (in print).

### Conferences:

Silva AT, Rebelo C, Simões da Silva L, Serra M, Lima L, D’Aniello M and Landolfo R (2014) Seismic Evaluation of Concentrically Braced Frames – Influence of the design approach on the V-bracing. In: *EUROSTEEL 2014 – 7<sup>th</sup> European Conference on Steel and Composite Structures*, Naples. (to be published)

Silva AT, Rebelo C, Lima L and Simões da Silva L (2013) Análise não linear de pórticos dual-steel simples. In: *IX Congresso de Construção Metálica e Mista e I Congresso Luso-Brasileiro de Construção Metálica e Sustentável*, Porto, vol. II, pp. II369-II-378.

Silva AT, Rebelo C, Lima L and Simões da Silva L (2013) Avaliação Sísmica de Pórticos com contraventamento centrado. In: *IX Congresso de Construção Metálica e Mista e I Congresso Luso-Brasileiro de Construção Metálica e Sustentável*, Porto, vol. II, pp. 447-456.

Silva AT, Rebelo C, Simões da Silva L, Serra M, Lima L, D’Aniello M and Landolfo R (2012) Seismic Performance of High Strength Steel Moment-resisting Frames. In:

*STESSA 2012 – Behaviour of Steel Structures in Seismic Areas*, Santiago do Chile, Chile, vol. 1, pp. 1-6.

Serra M, Rebelo C, Simões da Silva L, Silva AT, D’Aniello M and Landolfo R (2012) Study on Concentrically V-Braced Frames under cyclic loading. In: *STESSA 2012 – Behaviour of Steel Structures in Seismic Areas*, Santiago do Chile, Chile, vol. 1, pp. 123-129.

Silva AT, Rebelo C, Lima L and Simões da Silva L (2012) Dimensionamento sísmico baseado no desempenho de pórticos simples com aço de alta resistência. In: *4º Congresso Nacional Construção*, Portugal, Coimbra.

Silva AT, Rebelo C, Lima L and Simões da Silva L (2012) Avaliação sísmica de Pórticos “Dual-Steel” com contraventamento centrado. In: *4º Congresso Nacional Construção*, Portugal, Coimbra.

Silva AT, Rebelo C, Lima L, Simões da Silva L, D’Aniello M, Landolfo R (2012) Seismic Performance of Dual-Steel Concentrically Braced Frames. In: *15th World Conference on Earthquake Engineering*, Portugal, Lisbon, Paper 2781.

Silva AT, Rebelo C, Simões da Silva L, Serra M, Lima L, D’Aniello M and Landolfo R (2011) Seismic Performance of High Strength Building – Dual Frame Analysis. In: *EUROSTEEL 2011 – 6th European Conference on Steel and Composite Structures*, Budapest, vol. B, pp. 1179-1184.

Silva AT, Rebelo C, Simões da Silva L, Serra M, Lima L, D’Aniello M and Landolfo R (2011) Análise dos Critérios de Desempenho de Pórticos com Contraventamento Centrado. In: *VIII Congresso de Construção Metálica e Mista*, Guimarães, vol. 1, pp. 1-8.

The results of the numerical studies have been considered into the research European project:

- HSS-SERF (High Strength Steel in Seismic Resistant Buildings Frames – Grant N N0 RFSR-CT-2009-00024).

And also presented in recent international workshop regarding the use of HSS in seismic zones from the HSS-SERF outcomes held in Naples – Italy:

Silva AT, Rebelo C, Simões da Silva L, Serra M, Lima L, D’Aniello M and Landolfo R (2013) Seismic Design of Dual-Steel Structures. In: *High Strength Steel in Seismic Resistant Structures – International Workshop*, Naples.

Silva AT, Rebelo C, Simões da Silva L, Serra M, Lima L, D’Aniello M and Landolfo R (2013) Nonlinear Analysis of Dual-Steel Moment-Resisting Frames. In: *High Strength Steel in Seismic Resistant Structures – International Workshop*, Naples.

D’Aniello M, Portioli F, Landolfo R, Silva AT, Rebelo C and Simões da Silva L (2013) Seismic Performance of Dual-Steel Concentric-braced Frames in simple and dual configuration. In: *High Strength Steel in Seismic Resistant Structures – International Workshop*, Naples.



## References

- Adan S and Hamburger R. (2010) Steel Special Moment Frames: A Historic Perspective. *Structure*.
- AISC-341. (2005) Seismic Provisions for Structural Steel Buildings. Chicago, Illinois: American Institute of Steel Construction, INC.
- AISC. (2010) Will rising ore pricing impact the price of structural steel ?
- Anami K and Miki C. (2001) Fatigue strength of welded joints made of high-strength steels. *Progress in Structural Engineering and Materials* 3: 86-94.
- ATC-40. (1996) ATC-40 - Methodology for seismic evaluation and upgrade of concrete structures. Redwood.
- Bachmann H and Dazio A. (1997) A deformation-based seismic design procedure for structural wall buildings. In: Fajfar P and Krawinkler H (eds) *Seismic Design Methodologies for the Next Generation of Codes*. Rotterdam, 159-170.
- Balling R, Balling L and Richards P. (2009) Design of buckling-restrained braced frames using nonlinear time history analysis and optimization. *Journal of Structural Engineering* 155: 461-468.
- Bjorhovde R. (2004) Development and use of high performance steel. *Journal of Constructional Steel Research* 60: 393-400.
- Black G, Wenger B and Popov E. (1980) Inelastic buckling of steel struts under cyclic load reversals. California, USA.
- Broderick BM, Elghazouli AY and Goggins J. (2008) Earthquake testing and response analysis of concentrically-braced. *Journal of Constructional Steel Research* 64: 997-1007.
- Calvi GM and Sullivan TJ. (2009) Development of a model code for direct displacement based seismic design. *The state of Earthquake Engineering Research in Italy: the ReLUIS-DPC 2005-2008 Project*: 141-171.
- Castro J, Elghazouli A and Villani A. (2009) Improved seismic design procedure for steel moment frames Behaviour of Steel Structures in Seismic Areas. *STESSA 2009: Behaviour of Steel Structures in Seismic Areas*. Philadelphia.
- Celikbas A. (1999) Economics of Damage Controlled Seismic Design. *Dept. of Civil and Environmental Engineering*. Massachusetts Institute of Technology.
- Collins MP and Johansson B. (2006) Bridges in high strength steel. *LABSE - Symposium*. Budapest.

- Correia A and Virtuoso F. (2006) Nonlinear modeling of reinforced concrete structures for seismic applications. *Third European Conference on Computational Mechanics: Solids, Structures and Coupled Problems in Engineering*.
- D'Aniello M. (2007) Steel dissipative bracing systems for retrofitting of existing structures: Theory and Testing. Naples: University of Federico II of Naples, 316.
- D'Aniello M, Ambrosino GLM, Portioli F, et al. (2013) Modelling aspects of the seismic response of steel concentric braced frames. *Steel and Composite Structures* 15: 539-566.
- D'Aniello M, Ambrosino GLM, Portioli F, et al. (2014a) The influence of out-of-straightness imperfection in physical theory models of bracing members on seismic performance assessment of concentric braced structures. *The Structural Design of Tall Buildings*.
- D'Aniello M, Güneyisi EM, Landolfo R, et al. (2014b) Analytical prediction of available rotation capacity of cold-formed rectangular and square hollow section beams. *Thin-Walled Structures* 77: 141-152.
- D'Aniello M, Landolfo R, Piluso V, et al. (2012) Ultimate behavior of steel beams under non-uniform bending. *Journal of Constructional Steel Research* 78: 144-158.
- Dávial-Arbona F, Castro JM and Elghazouli AY. (2008) Assessment of panel zone design approaches for steel moment frames. *The 14th World Conference on Earthquake Engineering*. Beijing, China.
- Davison B and Owens GW. (2000) Steel Designers' Manual.
- Dicleli M and Mehta A. (2007) Simulation of inelastic cyclic buckling behavior of steel box sections. *Computers & Structures* 85: 446-457.
- Dubina D. (2008) Performance and benefits of using high strength steels.
- Dubina D. (2010) Dual-steel Frames for multistory buildings in seismic areas In: E. Batista PV, L. de Lima (ed) *SDSS - Stability and Ductility of Steel Structures*. Rio de Janeiro, 59-80.
- Dubina D, Dinu F, Zaharia R, et al. (2006) Opportunity and effectiveness of using high strength steel in seismic resistant building frames. In: Dubina D and Ungureanu V (eds) *Proceedings of the International Conference in Metal Structures*. Poiana Brasov, Romania, 501-510.
- Dubina D, Vulcu A, Stratan A, et al. (2014) High Strength Steel in Seismic Resistant Building Frames - HSS-SERF. European Commission - Research Programme of the Research Fund for Coal and Steel, 1-240.
- EERC. Loma Pietra Collection. Berkeley.
- Elghazouli A. (2003) Seismic design procedures for concentrically braced frames. *Proceedings of the Institution of Civil Engineers, Structures and Buildings Journal* 156(4): 381-394.
- Elghazouli A. (2005) Assessment of Capacity design approaches for steel-framed structures. *International Journal of Steel Structures* 5: 465-475.
- Elghazouli A. (2009a) *Seismic Design of Buildings to Eurocode 8*: Taylor & Francis e-Library.

- Elghazouli AY. (2009b) Assessment of European seismic design procedures for steel framed structures. *Bulletin of Earthquake Engineering*: 65-89.
- Elghazouli aY, Castro JM and Izzuddin Ba. (2008) Seismic performance of composite moment-resisting frames. *Engineering Structures* 30: 1802-1819.
- Elnashai AS. (2002) A very brief history of earthquake engineering with emphasis on developments in and from the British Isles. *Chaos, Solitons & Fractals* 13: 967-972.
- EN1990. (2002) Eurocode - Basis of structural design. European Standard.
- EN1991-1-1. (2002) Eurocode 1: Actions on structures - Part 1-1: General actions - Densities, self-weight, imposed loads for buildings. European Standard, 1-44.
- EN1992-1-1. (2004) Eurocode 2: Design of concrete structures - Part 1-1: General rules and rules for buildings. European Standard.
- EN1993-1-1. (2005) Eurocode 3: Design of steel structures - Part 1-1: General rules and rules for buildings. European Standard.
- EN1993-1-8. (2005) Eurocode 3: Design of steel structures -Part 1-8: Design of joints. European Standard.
- EN1993-1-12. (2007) Eurocode 3 - Design of steel structures - Part 1-12 : Additional rules for the extension of EN 1993 up to steel grades S 700. European Standard, 1-9.
- EN1994-1-1. (2004) Eurocode 4: Desing of composite steel and concrete structures - Part 1-1: General rules and rules for buildings. European Standard.
- EN1998-1-1. (2004) Eurocode 8: Design of structures for earthquake resistance - Part 1: General rules, seismic actions and rules for buildings. Brussels, 1-229.
- EN1998-1-3. (2005) Eurocode 8: Design of structures for earthquake resistance - Part 3: Assessment and retrofitting of buildings. Brussels: European Standard.
- Engelhardt MD and Popov EP. (1989) On Design of Eccentrically Braced Frames On Design of Eccentrically Braced Frames. *Earthquake Spectra* 5: 495-511.
- Fajfar P and Fischinger M. (1987) Non-linear seismic analysis of RC buildings - Implications of a case study. *European Earthquake Engineering* 1: 31-43.
- Fajfar P and Fischinger M. (1988) N2 – A method for non-linear seismic analysis of regular.pdf. *Proceedings of the 9th World Conference on Earthquake Engineering*. Tokyo, 11-16.
- FEMA-273. (1997) FEMA 273 - NEHRP Guidelines for the seismic rehabilitation of buildings. Washington DC.
- FEMA-350. (2000) Recommended Seismic Design Criteria for New Steel Moment-Frame Buildings. Federal Emergency Management Agency, 221.
- FEMA-356. (2000) FEMA 356 - Prestandard and commentary for the seismic rehabilitation of buildings. Washington DC, 1-54.

- FEMAE-74. (2011) Reducing the Risks of Nonstructural Earthquake Damage - A practical guide. Federal Agency Management Emergency.
- Fragiadakis M and Papadrakakis M. (2008) Modeling, analysis and reliability of seismically excited structures: Computational issues. *International Journal of Computational Methods* 5: 483-511.
- Galambos TV, Hajjar JF and Earls CJ. (1997) Required Properties of High-Performance Steels.pdf. Minneapolis.
- Geschwindner L, Disque R and Bjorhovde R. (1994) Load and Resistance Factor Design of Steel Structures. 2005: 10-11.
- Ghobarah A. (2001) Performance-based design in earthquake engineering: state of development. *Engineering Structures* 23: 878-884.
- Goggins J and Salawdeh S. (2013) Validation of nonlinear time history analysis models for single-storey concentrically braced frames using full-scale shake table tests. *Earthquake Engineering & Structural Dynamics* 42: 1151-1170.
- Goggins JM, Broderick BM, Elghazouli AY, et al. (2005) Experimental cyclic response of cold-formed hollow steel bracing members. *Engineering Structures* 27: 977-989.
- Grecea D, Dinu F and Dubină D. (2004) Performance criteria for MR steel frames in seismic zones. *Journal of Constructional Steel Research* 60: 739-749.
- Hjelmstadt K and Popov E. (1983) Seismic behavior active beam links in Eccentrically Braced Frames. Berkeley, CA, 2-3.
- Hollings JP. (1968) Reinforced concrete seismic design. *Seismic Problems in Structural Engineering*. 217-250.
- Iyama J and Kuwamura H. (1999) Probabilistic advantage of vibrational redundancy in earthquake-resistant steel frames. *Journal of Constructional Steel Research* 52: 33-46.
- Kasai K and Popov E. (1986) General Behavior of WF Steel Shear Link Beams. *Journal of Structural Engineering* 112: 362-382.
- Krawinkler H and Seneviratna GDPK. (1998) Pros and cons of a pushover analysis of seismic performance evaluation. *Engineering Structures* 20: 452-464.
- Krawinkler H, Zareian F, Medina Ra, et al. (2006) Decision support for conceptual performance-based design. *Earthquake Engineering & Structural Dynamics* 35: 115-133.
- Lestuzzi P and Badoux M. (2003) An experimental confirmation of the equal displacement rules for RC structural walls. *An experimental confirmation of the equal displacement rules for RC structural walls*. 1-10.
- Lumpkin EJ, Hsiao P-C, Roeder CW, et al. (2012) Investigation of the seismic response of three-story special concentrically braced frames. *Journal of Constructional Steel Research* 77: 131-144.
- Mander J, Priestley M and Park R. (1988) Theoretical stress-strain model for confined concrete. *Journal of Structural Engineering* 8: 1804-1826.

- Marino E and Nakashima M. (2006) Seismic performance and new design procedure for chevron-braced frames. *Earthquake Engineering & Structural Dynamics* 35: 433-452.
- Martínez-rueda E and Elnashai AS. (1997) Confined concrete model under cyclic load. 30: 139-147.
- Menegotto M and Pinto P. (1973) Method of analysis for cyclically loaded RC plane frames including changes in geometry and non-elastic behaviour of elements under combined normal force and bending. *Symposium on the Resistance and Ultimate Deformability of Structures Acted on by Well Defined Repeated Loads*.
- Miki C, Homma K and Tominaga T. (2002) High strength and high performance steels and their use in bridge structures. *Journal of Constructional Steel Research* 58: 3-20.
- Neuenhofer A and Filippou F. (1997) Evaluation of nonlinear frame finite-element models. *Journal of Structural Engineering* 123: 958-966.
- Palmer K. (2012) Seismic behavior, performance and design of steel concentrically braced framed systems. University of Washington.
- Papadimitriou I, Fragiadakis M and Papadrakakis M. (2005) Inelastic analysis of framed structures using the fiber approach. *5th Int. Cong. Computational Mechanics*.
- Paulay T. (2002) The displacement capacity of reinforced concrete coupled walls. *Engineering Structures* 24: 1165-1175.
- Popov E and Engelhardt M. (1988) Seismic Eccentrically Braced Frames. *Journal of Constructional Steel Research* 10: 321-354.
- Priestley M. (1993) Myths and fallacies in earthquake engineering - conflicts between design and reality.pdf. *Bulletin NZ National Society for Earthquake Engineering* 26: 328-341.
- Priestley M. (1998) Brief comments on elastic flexibility of reinforced concrete frames and significance to seismic design.pdf. *Bulletin of the New Zealand National Society for Earthquake Engineering* 31.
- Priestley M. (2005) Viscous Damping in Seismic Design and Analysis. 9: 229-255.
- Priestley M, Calvi GM and Kowalsky M. (2007) *Displacement-Based Seismic Design of Structures.pdf*, Pavia, Italy: IUSS Press.
- Priestley M and Kowalsky M. (1998) Aspects of drift and ductility capacity of rectangular cantilever structural walls. *Bulletin of the New Zealand National Society for Earthquake Engineering* 31.
- Priestley MJN. (2000) Performance based seismic design. *12WCEE - World Conference on Earthquake Engineering*. Auckland, New Zealand, 1-22.
- Priestley MJN. (2007) Displacement-based seismic assessment of reinforced buildings. *Journal of Earthquake Engineering* 1: 157-192.
- Priestley MJN and Grant DN. (2005) Viscous damping in seismic design and analysis. *Earthquake Engineering* 9: 229-255.

- RFSR-CT-2007-00039. (2013) Optimizing the seismic performance of steel and steel-concrete by standardizing material quality control (OPUS).
- Roeder CW, Lumpkin EJ and Lehman DE. (2011) A balanced design procedure for special concentrically braced frame connections. *Journal of Constructional Steel Research* 67: 1760-1772.
- Sabelli R, Roeder CW and Hajjar JF. (2013) Seismic Design of Steel Special Concentrically Braced Frame Systems - A Guide for Practicing Engineers. NEHRP Seismic Design Technical Brief No. 8, 36.
- Salvitti L and Elnashai AS. (1996) Evaluation of behaviour factors for RC buildings by nonlinear dynamic analysis. *Eleven World Conference on Earthquake Engineering*.
- Samuelsson A and Schroter F. (2005) High-Performance Steels in Europe - Production processes, mechanical and chemical properties, fabrication properties. *LABSE - Structural Engineering Document No 8 - Use and application of high performance steels (HPS) for steel structures*. IABSE-AIPC-IVBH, 99-109.
- Sedlacek G, Aachen R and Müller C. (2005) The use of very high strength steels in metallic construction. *Super-High Strength Steels*. Rome, Italy, 1-23.
- SeismoStruct. (2011) SeismoStruct. Seismosoft - Earthquake Engineering Software Solutions.
- SEOC-Vision-2000. (1995) SEOC Vision 2000 - Conceptual framework for Performance-based seismic design. Sacramento.
- Serra M, Rebelo C, Silva LS, et al. (2010) Study on concentrically V-braced frames under cyclic loading. *STESSA 2012: Behaviour of Steel Structures in Seismic Areas*. 123-133.
- Shibata A and Sozen M. (1976) Substitute-structure method to determine design forces in earthquake-resistant reinforced concrete frames. *Journal Structural Engineering* 102: 3548-3566.
- Sivaselvan MV and Reinhorn AM. (2000) Hysteretic models for deteriorating inelastic structures. *Journal of Engineering Mechanics* 126: 633-640.
- Song JK and Pincheira JA. (2000) Spectral displacement demands of stiffness and strength degrading systems. *Earthquake Spectra* 16: 817-851.
- Stratan A, Dubina D and Dinu F. (2003) Control of global performance of seismic resistant EBF with removable link. *STESSA 2003: Behaviour of Steel Structures in Seismic Areas*. 8.
- Sullivan TJ, Calvi GM, Priestley MJN, et al. (2003) The limitations and performances of different displacement based design methods. *Journal of Earthquake Engineering* 7: 201-241.
- Susantha KAS, Ge H and Usami T. (2001) Uniaxial stress – strain relationship of concrete confined by various shaped steel tubes. *Engineering Structures* 23: 1331-1347.
- Takanashi K, Aburakawa M and Hamaguchi H. (2005) Utilization of High Performance Steels in Urban Structures. *Advances in Steel Structures - ICASS'05*. 1827 - 1835.

- Tenchini A, Rebelo C, Lima L, et al. (2013) Avaliação sísmica de pórticos com contraventamento centrado. *IX Congresso de Construção Metálica e Mista e I Congresso Luso-Brasileiro de Construção Metálica e Sustentável*. Portugal, 1-10.
- Tremblay R. (2002) Inelastic seismic response of steel bracing members. *Journal of Constructional Steel Research* 58: 665-701.
- Uang C-m and Bertero VV. (1986) Earthquake simulation tests and associated studies of a 0.3-scale model of a six-story concentrically braced steel structure.
- Uriz P. (2005) Toward Earthquake-Resistant Design of Concentrically Braced Steel-Frame Structures. The Earthquake Engineering Online Archive.
- Vamvatsikos D and Cornell CA. (2002) Incremental dynamic analysis. *Earthquake Engineering & Structural Dynamics* 31: 491-514.
- Wakabayashi M, Matsui C, Minami K, et al. (1974) Inelastic Behaviour of Full-Scale Steel Frames with and without bracings. *Departmental Bulletin Paper*: 1-23.
- Willms R. (2009) High strength steel for steel constructions. *The Nordic Steel Construction Conference*. Malmo, Sweden, 597-604.
- Wilson E, Der Kiureghian A and Bayo E. (1981) A replacement for the SRSS method in seismic analysis. *Earthquake Engineering and Structural Dynamics* 9: 187-194.

[Digite aqui]

---

[Digite aqui]